A Design Tool for use in Simulation and Training of Sinus Surgery

By

Richard Elliott Taylor

M.Eng. (Hons)

Doctoral thesis submitted in partial fulfilment of the requirements for the award of Doctor of Philosophy of Loughborough University

November 2010

ABSTRACT

The traditional approaches to training surgeons are becoming increasingly difficult to apply to modern surgical procedures. The development of Minimally Invasive Surgery (MIS) techniques demands new and complex psychomotor skills, and means that the apprentice-based system described by "see one, do one, teach one" can no longer be expected to fully prepare surgeons for operations on real patients, placing patient safety at risk. The use of cadavers and animals in surgical training raises issues of ethics, cost and anatomical similarity to live humans. Endoscopic sinus surgery involves further risk to the patient due to the proximity of vital structures such as the brain, eyes, optic nerve and internal carotid artery. In recent years, simulation has been used to overcome these problems, exposing surgeons to complex procedures in a safe environment, similarly to its use in aviation. However, the cases simulated in this manner may not be customised by training staff to present desired pathology.

This thesis describes the design and development of a new tool for the creation of customised cases for the training of sinus surgery. Users who are inexperienced and non-skilled in the use of three-dimensional (3D) Computer Aided Design (CAD) modelling software may use the tool to implement pathology to the virtual sinus model, which was constructed from real CT data. Swelling is applied in five directions (four horizontal, one vertical) to the cavity lining of the frontal and sphenoid sinuses. Tumours are individually customised and positioned in the frontal, sphenoid and ethmoid sinuses. The customised CAD model may then be latterly manufactured using Three-Dimensional Printing (3DP) to produce the complex anatomy of the sinuses in a full colour physical part for the realistic simulation of surgical procedures. An investigation into the colouring of the physical model is also described, involving the study of endoscopic videos to ascertain realistic shades.

The program was evaluated by a group of medical professionals from a range of fields, and their feedback was taken into account in subsequent redevelopment of the program, and to suggest further work.

Keywords: Sinus Surgery, Surgical Training, Simulation, Additive Manufacturing, Rapid Prototyping, Customisable Training Models

ACKNOWLEDGEMENTS

Firstly, my sincere thanks go to Russ Harris for his supervision throughout the duration of my work, and for initially taking me on board. Darren Watts deserves great thanks for his advice and assistance with all NX-related queries, and in particular for the considerable time he gave to help to bring this thesis together. Russ and Darren have been great supervisors, and the friendly experience they passed on has helped me to avoid many stumbling blocks throughout the course of my research. Their guidance at each stage has been invaluable and helped me to change personally, from feeling unsure and overwhelmed three years ago, to confident, organised and in control at the end of this period of my life.

I have great appreciation for the time sacrificed and enthusiasm shown by our partners at QMC in Nottingham, particularly Anshul Sama and Jason Watson, who made themselves available for consultation, photo shoots, trials and observation despite a hectic work schedule and important commitments to many other projects, and their patients. Their interest and eagerness to see the development of the research kept me aware that my work would benefit real lives, and the knowledge that it had the backing of professionals in the field was of great comfort. Thanks must also be given to their colleagues, who gave any few minutes they had spare to trial my program, and tolerated my lingering around the ward and office between sessions.

I must thank Tony Sutton for his lectures, and Stu McLeod for his consultation on VB. As a programming beginner at the start of this research, their assistance was absolutely invaluable and made the rest of the work possible, allowing me to build my knowledge and skills on the base they provided.

Thanks to my friends in T.2.02B, who created an... “ideal” working environment, and made every day fun.

Thanks to the team-mates I have coached and played alongside throughout these three years. You have offered an important and thoroughly enjoyable way for me to step

away from the work, ready to return after a weekend in the rain, wind, snow and occasionally, sun.

Thanks to Jen for putting up with me while I was frustrated, lost or just plain tired. Your support every day for the last three years has kept me smiling.

Lastly, thanks to my family. You have always been proud of me and pushed me on to do the best I can, in everything I do.

This work is dedicated to Grandma, who took pride in being the proudest, Granddad and Laurie May. You are an inspiration to me and we miss you.

DECLARATION

Research Student Office, Academic Registry
Loughborough University, Leicestershire, LE11 3TU, UK
Switchboard: +44(0)1509 263171 Fax: +44(0)1509 223938

Certificate of Originality

This is to certify that I am responsible for the work submitted in this thesis, that the original work is my own except as specified in acknowledgements or in footnotes, and that neither the thesis nor the original work contained therein has been submitted to this or any other institution for a higher degree.

..... (Signed)

..... (Print)

..... (Date)

NOMENCLATURE

2D	-	Two-Dimensional
2½D	-	Two-and-a-half-Dimensional
3D	-	Three-Dimensional
3DP	-	Three-Dimensional Printing
AM	-	Additive Manufacturing
CAD	-	Computer Aided Design
CNC	-	Computer Numerically Controlled
CT	-	Computed Tomography
µ-CT	-	Microtomography
ENT	-	Ear, Nose and Throat (medical field)
GUI	-	Graphical User Interface
HSL	-	Hue, Saturation, Luminosity (or Lightness) cylindrical co-ordinate representation of RGB colour model
IGES	-	International Graphics Exchange Specification
MIS	-	Minimally Invasive Surgery
MRI	-	Magnetic Resonance Imaging
NX	-	Unigraphics NX5 (3D CAD package)
OR	-	Operating Room
QMC	-	Queen's Medical Centre (Nottingham)
RGB	-	Red, Green, Blue colour model
ROI	-	Region of Interest
SLA	-	Stereolithography Apparatus
SLS	-	Selective Laser Sintering
STL	-	*ST*ereo*L*ithography file format
RE	-	Reverse Engineering
UV	-	Ultra-Violet
VB	-	Microsoft Visual Basic®
VR	-	Virtual Reality
VRML	-	Virtual Reality Modelling Language

LIST OF PUBLICATIONS AND PRESENTATIONS

Submitted Publications

Taylor, R.E., Watts, D.M., Sama, A., Watson, J., Harris, R.A., 2010, "**Design Tool for Creating Variable Training Cases for Human Sinus Surgery**," Proceedings of the Institution of Mechanical Engineers, Part H: Journal of Engineering in Medicine.

Proposed Publications

Taylor, R.E., Sama, A., Watson, J., Harris, R.A., 2010, "**Reproducing Accurate Colours by Three-Dimensional Printing**," Rapid Prototyping Journal.

Taylor, R.E., Watts, D.M., Sama, A., Watson, J., Harris, R.A., 2010, "**Customisation of 3D Anatomical Models by Indirect, Guided Control of CAD Software**," Computers and Graphics.

Presentations Resulting from Research

Work has been presented at:
Health Technologies Knowledge Transfer Networks, Loughborough University, December 2008.

NHS Trust Patient Safety Conference, Trent Simulation Centre, Queen's Medical Centre, Nottingham, February 2009.

NHS Training for Innovation, 6th Stakeholder Workshop, York, November 2009.

CONTENTS

Abstract ..... **i**

Acknowledgements ..... **ii**

Declaration ..... **iv**

Nomenclature ..... **v**

List of Publications and Presentations ..... **vi**

Contents ..... **vii**

List of Figures and Tables ..... **xii**

1 Introduction **2**

1.1 Research Need 2

1.2 Surgery Simulation 3

1.3 Additive Manufacturing 6

1.4 Research Aims and Objectives 8

2 Additive Manufacturing **13**

2.1 Data Acquisition from Inorganic Parts 16

2.2 Medical Imaging 17

2.2.1 Magnetic Resonance Imaging 18

2.2.2 Computed Tomography 19

2.2.3 Microtomography 21

2.3 3D CAD Model to AM Machine 22

2.4 Additive Manufacturing Processes 24

2.4.1 3DP (Z Corporation) 24

3 Sinus Anatomy and Surgery **31**

3.1 Sinus Anatomy 31

3.2 Pathology in the Sinuses 36

3.3 Performance of Surgery in the Sinuses 37

4 Surgical Training Methods, Simulation and Preoperative Planning 41

4.1 Traditional Training Methods 41

4.2 Surgery Simulation and Preoperative Planning Models 45

4.2.1 Organic Surgery Simulation 47

4.2.2 Inorganic Surgery Simulation 50

4.3 Simulation for Sinus Surgery 66

5 Colouring of 3DP Parts 75

5.1 'Proximity Nesting' to Induce Internal Colouring 75

5.1.1 Aim of Experiment 75

5.1.2 Methodology 76

5.1.3 Results 77

5.2 ZEdit Benchmarking 77

5.2.1 Aim of Experiment 78

5.2.2 Methodology 78

5.2.3 Results 79

5.3 Colour of Anatomy 84

5.3.1 Results 85

5.4 Colour Reproduction Accuracy on Spectrum Z510 89

5.4.1 Colour Reproduction Accuracy – Trial 1 90

5.4.2 Colour Reproduction Accuracy – Trial 2 95

5.4.3 Anatomical Colour Reproduction – Trial 1 100

5.4.4 Anatomical Colour Reproduction – Trial 2 102

5.4.5 Anatomical Colour Reproduction – Trial 3 103

5.4.6 Anatomical Colour Reproduction – Trial 4 104

5.4.7 Anatomical Colour Reproduction – Trial 5 105

5.5 Infiltrants 106

5.5.1 Infiltrants Used in this Research 106

6 Investigating Customisable Anatomical Models 109

6.1 Selection of Medical Imaging for this Research 109

6.2 Reconstruction of CT Scan Data 110
6.2.1 Manipulating Medical Data with Materialise's Mimics® 110
6.2.2 Exporting Medical Data from Mimics 120
6.3 Customisable Models of Sinus Anatomy 125
6.3.1 Controlling NX using Visual Basic 126
6.4 Manufacture of Customised Sinus Surgery Simulation Models 130
6.5 Hypothesis 132
7 Methodology 137
8 Customisable Sinus Surgery Training Model – Swelling Application 142
8.1 Horizontal Swelling - Exploratory Work 143
8.1.1 Swelling in Simple Cylindrical Model 144
8.2 Developing Horizontal Swelling Application Method 153
8.2.1 Swelling in Anatomically Representative Geometry 154
8.2.2 Swelling in Sample of Real Anatomical Data 160
8.3 Final Horizontal Swelling Application Method 168
8.4 Three-Dimensional Swelling 172
8.4.1 Swelling in the Vertical Direction 172
8.4.2 Three-Dimensional Cavity Shrinking 179
8.4.3 Vertical Region Selection 181
8.5 Simulation of Swelling in 3D Model 182
8.5.1 Scaffold Splines 182
8.5.2 Splitting 3D model to apply swelling 184
8.5.3 Solid Modelling of Swelling 188
9 Customisable Sinus Surgery Training Model – Tumour Addition 195
9.1 Switching Tumours On and Off 196
9.2 Positioning of Tumours within Sinus Anatomy 197

9.2.1 Sliding Scale Positioning System 198
9.2.2 Mouse-Click Positioning System 204
9.3 Sizing of Tumour Body 209
9.3.1 'Three Sizes' Method 210
9.3.2 Sliding Scale Method 211
9.4 Addition of Multiple Tumours 212
9.5 Simulation of Tumour Body in NX 214
9.6 Exporting Model from NX 220
10 Design of GUI and Program Trial A 224
10.1 Development of 'Wizard' Style User Interface 224
10.2 Navigational Programming 226
10.3 Cyclical Navigation System 229
10.4 Stages of Case Creator Wizard 232
10.4.1 Home Page 232
10.4.2 Swelling Application Page 233
10.4.3 Vertical Region Selection Page 237
10.4.4 Tumour Application Page 238
10.4.5 Summary Page 239
10.4.6 End Page 240
10.5 'Save' and 'Load' Functions 243
10.5.1 Saving Case Settings 243
10.5.2 Loading Case Settings 246
10.5.3 Saving NX Part File 248
10.5.4 New Case Settings File 249
10.6 'Undo' Function 250
10.7 Program Trials 251
10.7.1 Results from Case Creator Trial A 253
11 Redevelopment of GUI and Program Trial B 274
11.1 Redeveloped Wizard Navigation System 274
11.2 Stages of Redeveloped Case Creator Wizard 282

11.2.1 Program Information Page 282
11.2.2 Settings Selection Page 283
11.2.3 Swelling Application Page 286
11.2.4 Vertical Region Selection Page 288
11.2.5 Tumour Application 289
11.2.6 Summary Page 299
11.2.7 End Page 301
11.3 Results from Case Creator Trial B 301
11.3.1 Participant Information 302
11.3.2 General Ratings 304
11.3.3 Navigation System 307
11.3.4 Inclusion of Functionalities 308
11.3.5 Swelling Application Controls 309
11.3.6 Tumour Application Controls 311
11.3.7 Results Achieved through Case Creator 312
11.3.8 Summary 316
11.4 Conclusions from Program Trials 317
12 Discussion and Conclusions 320
13 Limitations and Recommendations for Further Work 325
13.1 General Improvements to Case Creator 325
13.2 Swelling Application 325
13.3 Vertical Region Definition 327
13.4 Tumour Application 327
13.4.1 Silicone 331
References 333
Appendix
Appendix A - Case Creator Questionnaire A-1

LIST OF FIGURES AND TABLES

Figure 1: Physical model of main arteries in skull, produced by 3DP [5]..... 3
Figure 2: Karlsruhe VR endoscopic surgery trainer [6] 4
Figure 3: Examples of geometrical complexity made possible with AM, approx. size 40mm [8]..... 6
Figure 4: Physical AM model for the planning of conjoined twin separation [10]..... 7
Figure 5: Flow chart of plan for information gathering, leading to concept development..... 11
Figure 6: 3D model of skull constructed from CT data [24] 18
Figure 7: MRI slice image of human head taken in sagittal plane [25]..... 19
Figure 8: µ-CT image of human ethmoid sinus showing density definition 22
Figure 9: Exaggerated example of stair-step effect (adapted from [22])..... 23
Figure 10: Circular part manufactured on X/Y plane 23
Figure 11: 3DP process prior to printing of next layer..... 25
Figure 12: Sinus anatomy viewed from front [41] 32
Figure 13: Sinus anatomy viewed in sagittal plane [43]..... 33
Figure 14: Shoulder model, showing fragments of bone [115] 51
Figure 15: Airbus A380 VR simulator [119]..... 53
Figure 16: VOXEL-MAN VR and haptic surgery simulator system [125]..... 55
Figure 17: Laparoscopic Training Simulator (LTS) 2000 physical reality simulator [100]..... 59
Figure 18: "Model of the nasal cavity integrated in segmented MRI dataset" [162] .. 67
Figure 19: Rubber cast training model of sinuses [7]..... 70
Figure 20: Positioning of blocks in 'proximity nesting' trial (X/Z plane)..... 76
Figure 21: Positioning of blocks (subsequent build layers) in 'proximity nesting' trial (X/Y plane) 76
Figure 22: Resulting part built by 3DP machine 77
Figure 23: Image suspended over a part in ZEdit..... 79
Figure 24: Mapping image around apex of cube 80
Figure 25: Mapping image (centred) on apex of cube..... 80
Figure 26: Image wrapped around entire part..... 81
Figure 27: Square-windowed cube with image wrapped around window edge 82

Figure 28: Fins model with image wrapped around base of two fins 83
Figure 29: Colour analysis using RGB values and hue, saturation and luminosity..... 85
Figure 30: Screenshot from “Endoscopy Movie Edit 1” video 86
Figure 31: Screenshot from “Endo-Polypectomy” video 87
Figure 32: Screenshot from “Antrocoanal Polyp” video 88
Figure 33: Colour levels for benchmarking exercise on Spectrum Z510 90
Figure 34: Percentage error of green element in printed parts compared to desired level..... 93
Figure 35: Percentage error of blue element in printed parts compared to desired level 94
Figure 36: Test samples for individual colour reproduction accuracy 95
Figure 37: Images of *a)* bottom left, *b)* centre and *c)* top right of uninfiltrated red square 96
Figure 38: Colour palette A – to represent colours A4, A11, A18, A25, A31 100
Figure 39: Colour palette B – to represent colours A25 and A31 from Figure 38 103
Figure 40: Colour palette C 104
Figure 41: Colour palette D 105
Figure 42: Colour palette E..... 106
Figure 43: Images from *a)* MRI, *b)* CT scans of the same patient (axial plane, forehead level) 110
Figure 44: Mimics, showing ethmoid sinus µ-CT scan data on three planes 111
Figure 45: µ-CT sample of ethmoid sinus thresholded – lower threshold set too low 113
Figure 46: µ-CT sample of ethmoid sinus thresholded – some features lost (circled) 114
Figure 47: Erasing a layer of the data in Mimics..... 115
Figure 48: Split frontal sinus model *a)* assembled, *b)* showing internal anatomy, from Spectrum Z510 3D printer using ‘Erased Layer’ method..... 115
Figure 49: STL file of µ-CT data imported from Mimics 116
Figure 50: Region growing tool used to remove outlying pixels 117
Figure 51: Morphology operations applied – *a)* Erode, *b)* Dilate 118
Figure 52: 3D CAD model created from blue mask..... 119
Figure 53: IGES splines from CT scan data imported from Mimics into NX..... 121

Figure 54: Editing geometry of 2D splines from IGES file using nodes 122
Figure 55: Nodes controlling 2D spline geometry – 'Through Points', degree of curvature *a)* 3, *b)* 1 123
Figure 56: Nodes controlling the 2D spline geometry – 'By Poles' 123
Figure 57: IGES splines from µ-CT scan data imported from Mimics into NX 124
Figure 58: Block creation VB code 128
Figure 59: Geometry definition of block by manually altering dimensions 128
Figure 60: Geometry definition of block by using variable in dimension definition 129
Figure 61: Geometry definition of block by altering variable within dimension definition 129
Figure 62: 2D spline codename definition in VB code 130
Figure 63: Flowchart of customised anatomical model production 134
Figure 64: Gantt chart of project plan 138
Figure 65: Plan for development of swelling simulation function 142
Figure 66: Tubular cavity through a block, consisting of 21 spline layers 144
Figure 67: Circular cross-section with fifteen nodes on circumference 145
Figure 68: Circular cross-section with swelling applied 146
Figure 69: GUI for swelling application in three zones using buttons 146
Figure 70: Swelling applied to Zone 1 of tube model shown from *a)* side, *b)* top 147
Figure 71: Sample *If-Then-Else* statement 148
Figure 72: GUI for swelling application in three zones using radio buttons, four levels of severity 149
Figure 73: Three severity levels of swelling applied in separate zones of tube 150
Figure 74: Sample code extract of co-ordinate definition 151
Figure 75: GUI for swelling application in three zones using sliding scales 152
Figure 76: Sliding scale value integrated into co-ordinate definition code 152
Figure 77: Calculation of new co-ordinates using sliding scale value 153
Figure 78: Frontal sinus cavity shown in CT scan, X/Y plane 154
Figure 79: Nodes around frontal sinus cavity split into two zones, to be controlled separately 155
Figure 80: Combination of swelling and movement to apply case symptoms to simulation 155
Figure 81: Zones of frontal sinus (1 = left, 2 = anterior, 3 = posterior, 4 = right) 157

Figure 82: Movement of nodes in two zones - swelling applied to *a)* nodes 3 and 4 only, *b)* all nodes 157
Figure 83: Swelling applied to left (Zone 1) of sinus cavity – *a)* settings, *b)* result . 158
Figure 84: Thirty points around circumference of cavity wall, swelling applied 159
Figure 85: Shape of cavity perimeter in X/Z plane 159
Figure 86: µ-CT image of frontal sinus section in X/Y plane 161
Figure 87: µ-CT data imported as IGES to NX using 'By Poles' setting 162
Figure 88: Spreadsheet showing co-ordinates of spline points and automatically-calculated sliding scale multiplication factors 163
Figure 89: Movement of node by sliding scale 164
Figure 90: µ-CT data swollen – settings (*a)*) applied to the left cavity (*b)*) 165
Figure 91: µ-CT data with 100% swelling applied to the left cavity 165
Figure 92: Cavities subtracted from solid outer geometry, with modelling anomaly circled 166
Figure 93: STL file of sectioned ethmoid sinus showing complexity of cavity geometry 168
Figure 94: CAD model of skull, frontal and sphenoid sinuses, ethmoid placeholder 169
Figure 95: Cavity formation in frontal sinus at three slices on the X/Y plane, 0.5mm apart 170
Figure 96: Global positioning of swelling relative to head 171
Figure 97: Swelling applied to cavities as a whole (from the left) 171
Figure 98: Swelling in z-axis – *a)* current capability, *b)* desired capability 172
Figure 99: Swelling in z-axis achieved by moving highest layer points inwards 174
Figure 100: Trial code to alter vertical position of layers 175
Figure 101: Trial showing capability to simulate swelling in z-direction – *a)* before, *b)* after 175
Figure 102: Simulation of swelling in vertical direction 176
Figure 103: Vertical swelling direction in the frontal sinus 178
Figure 104: Vertical swelling direction in the sphenoid sinus 178
Figure 105: Error due to combination of horizontal and vertical swelling 179
Figure 106: Cavity shrinks towards centre of head 180
Figure 107: Shrunken cavities produced within original anatomy – sphenoid sinus 180
Figure 108: Selection of vertical region of swelling 181

Figure 109: Frontal sinus anatomy - cavities split, therefore single scaffold solid cannot be used 184
Figure 110: Cavities of the frontal sinus divided into six sections 185
Figure 111: Scaffold splines structure for frontal sinus – *a)* and *b)* in original state, *c)* swollen 186
Figure 112: Scaffold splines structure for sphenoid sinus – *a)* and *b)* in original state, *c)* swollen 187
Figure 113: Iterative loop forming part of swelling application subroutine 188
Figure 114: Using subtracted scaffold solids to create swollen lining 189
Figure 115: Scaffold solid strays outside cavity solid boundary causing modelling errors 189
Figure 116: Using larger interior solid to avoid modelling errors on subtraction of scaffold solid 190
Figure 117: Swelling applied to frontal sinus using final swelling method in three views (*a), b), c)*) 192
Figure 118: Swelling applied to sphenoid sinus using final swelling method in three views (*a), b), c)*) 193
Figure 119: Plan for development of tumour simulation function 195
Figure 120: User interface for tumour placement 199
Figure 121: Positioning tumour relative to different co-ordinate systems 200
Figure 122: TumourPosition() – tumour positioning subroutine 202
Figure 123: Tumour positioned within anatomy, positional feedback given 204
Figure 124: Finding the mouse position within the GUI 205
Figure 125: Finding the mouse position within the relevant groupbox 207
Figure 126: Conversion of mouse click form co-ordinates into sliding scale values 208
Figure 127: Shift applied to tumour icon to position by centre 209
Figure 128: Three sizes available for tumours 210
Figure 129: Tumour size variable values in 'three sizes' method 211
Figure 130: Resizing tumours using sliding scales 211
Figure 131: Storage of tumour positioning slider value for re-use 213
Figure 132: Scaffold solids for tumour simulation 215
Figure 133: Sizing of tumour bodies in three dimensions 217
Figure 134: Code run to apply settings to Tumour 1 in frontal sinus 218

Figure 135: Tumours applied to all sinus areas 220
Figure 136: Fully customised sinus anatomy in CAD software *a)* isometric view, *b)* from below 221
Figure 137: *a)* Model exported as STL file, *b)* part information for exterior frontal anatomy 222
Figure 138: Simplified flow chart of "Next" button process 228
Figure 139: Sinus area selection page of Case Creator wizard 229
Figure 140: Identification of sinus area change using SinusRegion 231
Figure 141: Frontal sinus settings have been applied; option to do so is disabled 232
Figure 142: Home page of Case Creator wizard 233
Figure 143: Swelling application page of Case Creator wizard 234
Figure 144: No swelling is to be applied; swelling checkbox has been unchecked 234
Figure 145: Flowchart of "Next" button actions at swelling application stage 236
Figure 146: No swelling applied - error message is prompted 237
Figure 147: Vertical region selection page of Case Creator wizard 237
Figure 148: *a)* Vertical region error; bottom layer above top layer, error message (*b)*) is prompted 238
Figure 149: Tumour application page of Case Creator wizard 239
Figure 150: Information provided before summary page is shown 239
Figure 151: Summary page of Case Creator wizard 240
Figure 152: Final options screen and confirmation of case settings application 241
Figure 153: Procedure to save CAD part file with a new filename 242
Figure 154: Save and Open functions in Case Creator wizard menu 243
Figure 155: Frontal sinus swelling settings stored in area-specific variables 244
Figure 156: Prompt to save case settings before exiting the wizard 244
Figure 157: *a)* Saved information in .txt file, *b)* explanation of information 245
Figure 158: Information provided showing which sinus area settings will be saved 245
Figure 159: Area-specific variables updated with loaded values 246
Figure 160: Code checks if case has been loaded, to apply saved values to sliders 247
Figure 161: CAD part filename entry page of Case Creator wizard 248
Figure 162: Prompt to save CAD model before exiting the wizard 249
Figure 163: UndoCount is updated on application of settings 251

Figure 164: Undo subroutine is run the required number of times by using *For-Next* loop 251
Figure 165: Average ratings for common program features – Trial A 254
Figure 166: Ratings frequency for experience level in relevant skill areas – Trial A 256
Figure 167: Ratings frequency for ease of use of 'wizard' style program – Trial A .. 257
Figure 168: Average ratings for 'wizard' style program vs. experience in relevant skill areas – Trial A 258
Figure 169: Ratings frequency for task order – Trial A 259
Figure 170: Ratings frequency for number of functions supplied – Trial A 259
Figure 171: Ratings frequency for feedback given during settings application – Trial A 260
Figure 172: Ratings frequency for instruction given during settings application – Trial A 261
Figure 173: Ratings frequency for appropriateness of cyclical navigation system – Trial A 262
Figure 174: Ratings frequency for inclusion of swelling and tumour application – Trial A 263
Figure 175: Ratings frequency for ease of use of swelling application controls – Trial A 264
Figure 176: Ratings frequency for intuitiveness of swelling application system – Trial A 265
Figure 177: Ratings frequency for ease of use of tumour application controls – Trial A 266
Figure 178: Ratings frequency for predictability of end result – Trial A 267
Figure 179: Ratings frequency for realism of wizard results – Trial A 268
Figure 180: Ratings frequency for use of program – Trial A 269
Figure 181: Average ratings for use of program vs. experience in relevant skills – Trial A 270
Figure 182: Ratings frequency for use of program in training sinus surgeons – Trial A 271
Figure 183: Settings from previous wizard page saved by determining which page is now visible 275

Figure 184: Code to determine settings page to display to user when using "Next" button 277
Figure 185: SettingNo and SettingTotal display the step being performed 278
Figure 186: Code to determine settings page to display to user when using "Previous" button 279
Figure 187: User progression through Case Creator program 281
Figure 188: Program information page of Case Creator wizard 283
Figure 189: Settings selection page of Case Creator wizard 284
Figure 190: Updating value of SettingsTotal to display at each step of wizard 285
Figure 191: Error message shown when no settings are selected 285
Figure 192: Final version of swelling application page of Case Creator wizard 286
Figure 193: Labelling of swelling directions for left sphenoid cavity 287
Figure 194: Selection of vertical region of swelling in frontal sinus 288
Figure 195: Selection of vertical region of swelling in sphenoid sinus 289
Figure 196: Tumour size sliding scales appearing on demand 291
Figure 197: Functions and positions of resize handles 292
Figure 198: Resizing handles move to match position of tumour icon 293
Figure 199: Resizing tumour icon using handles - events for programming 294
Figure 200: Mouse y-co-ordinate stored when top resizing handle is clicked 294
Figure 201: Resizing tumour icon - repositioning required 295
Figure 202: Resized tumour icon is repositioned upwards 296
Figure 203: Tumour application stage in frontal sinus 297
Figure 204: Tumour application stage in sphenoid sinus 299
Figure 205: Settings summary page of Case Creator wizard 300
Figure 206: Progress window displayed during update of CAD model 301
Figure 207: Average ratings for common program features – Trial B 302
Figure 208: Ratings frequency for experience level in relevant skill areas – Trial B 303
Figure 209: Ratings frequency for ease of use of 'wizard' style program – Trial B .. 304
Figure 210: Ratings frequency for task order – Trial B 305
Figure 211: Ratings frequency for number of functions supplied – Trial B 305
Figure 212: Ratings frequency for feedback given during settings application – Trial B 306

Figure 213: Ratings frequency for instruction given during settings application – Trial B 307
Figure 214: Ratings frequency for appropriateness of concurrent navigation system – Trial B 308
Figure 215: Ratings frequency for inclusion of swelling and tumour application – Trial B 309
Figure 216: Ratings frequency for ease of use of swelling application sliders – Trial B 310
Figure 217: Ratings frequency for intuitiveness of swelling application system – Trial B 310
Figure 218: Ratings frequency for ease of use of tumour application controls – Trial B 312
Figure 219: Ratings frequency for predictability of end result – Trial B 313
Figure 220: Ratings frequency for realism of wizard results – Trial B 314
Figure 221: Ratings frequency for use of program – Trial B 314
Figure 222: Ratings frequency for use of program in training sinus surgeons – Trial B 316
Figure 223: Organically-shaped tumours 330
Figure 224: Code used to create more ‘organic’ shapes in tumour bodies 330

Table 1: Colour level results from “Endoscopy Movie Edit 1” video 86
Table 2: Colour level results from “Endo-polypectomy” video 87
Table 3: Colour level results from “Antrocoanal Polyp” video 88
Table 4: RGB level analysis of red (255,0,0), green (0,255,0), blue (0,0,255) and yellow (255,255,0) 91
Table 5: RGB level analysis of printed colours acquired from endoscopic videos 92
Table 6: Results of colour reproduction accuracy trial 2 98
Table 7: Levels of customisability for the application of swelling 143
Table 8: Levels of customisability for the application of tumours 196
Table 9: Likert rating system for closed Case Creator trial questions 253
Table 10: Experience level of participants in three relevant skill areas – Trial A 255
Table 11: Experience level of participants in three relevant skill areas – Trial B 303

CHAPTER ONE

INTRODUCTION

1 Introduction

1.1 Research Need

"Education, training and the accurate assessment of skills and performance represent the most important challenge of the new century for medical schools, scientific societies, academic and clinical environments" [1].

The major determinants of patient safety and the outcome of surgical procedures are the skill and judgement of the surgeon [2], which must be acquired through training. The field of surgical training is under constant study and development to ensure that student surgeons acquire and continually improve the skills they need to perform to a high standard in 'real life' situations. The traditional apprenticeship approach to training surgical students involves the gradual increase in involvement of the student with live cases, as their experience and physical skills grow through the use of cadavers, animals, or live patients with direction and advice from their supervising physician. Recently, the number of hours that medical residents are permitted to work has been reduced, limiting the amount of time they may spend acquiring the skills and knowledge they need. This is criticised by some, who claim that reduced work hours actually harm the level of patient care and restrict graduate medical education [3].

The apprentice-based method has been brought into question since the release of figures in 1999 in the "To Err is Human" report [4] by the Institute of Medicine in the United Sates, regarding the level of mortality in American hospitals and their possible causes. Kohn *et al* stated that up to 98,000 deaths occur annually in the USA due to medical error. It was subsequently suggested by numerous authors (as discussed in Chapter 4) that this level of mortality was linked to the quality of training received by surgical and medical students, the subjective assessment supplied throughout their training, their involvement in live cases and the performance of qualified surgeons that have passed through the training system in the past.

By using the training method described above, students are unable to gain experience of hands-on surgery without increased risk to living patients. In the case of

endoscopic sinus surgery, the risks are amplified due to the complex and unique anatomy of each patient, the proximity of vital structures such as the brain, eyes, optic nerve and internal carotid artery and the specific psychomotor skills required to safely perform surgical procedures viewed on a monitor. The use of cadavers and animals in the simulation of surgical procedures also raises ethical, financial and practical issues, as well as causing problems with lack of availability.

1.2 Surgery Simulation

Surgery simulation techniques may be employed to overcome these problems. In the field of surgical training, simulators aim to allow the participant to acquire and develop the skills necessary to perform real surgery, without risk to a patient. While some simulators focus specifically on the acquisition of these skills, others aim to develop the surgeon's skills while exposing them to the experiential aspects of performing surgery, through the complete submersion of the participant in a realistic environment. In the last decade, surgical simulation has been developed for use in a range of medical fields.

Depending on the particular simulation model, the preoperative planning of surgical procedures, assessment of clinical competence, communication of case details to patients and colleagues and intraoperative support and reference may be made possible (Figure 1). Surgical simulation models are therefore making an impact on the entire process of patient treatment, from the training of surgeons to the performance of actual operations and subsequent treatment.

Figure 1: Physical model of main arteries in skull, produced by 3DP [5]

Cadavers are still used as a means of simulating surgical procedures, as they are considered to provide a realistic experience for the surgeon. However, as discussed earlier the cost, ethical and availability issues related to their use makes this an undesirable training method. Furthermore, the physical similarity of the cadaveric tissue to that of live patients is questionable, which gives further strength to the argument for alternative surgery simulation methods.

Virtual reality (VR) had been used extensively for many years in aviation, to train pilots in the execution of crisis procedures in a safe and controllable environment before its introduction and acceptance in surgical training. In this method, a 3D computer-generated anatomical model (and occasionally, surrounding environment) is displayed to the user. Their movements are reproduced on-screen with virtual operating instruments, as they interact with the model to perform the designated procedure (Figure 2).

Figure 2: Karlsruhe VR endoscopic surgery trainer [6]

The physical sensations experienced by the surgeon through the instruments during real surgery may be replicated through the introduction of haptic 'force feedback' technology. This is important in many types of surgery, including in the sinuses, where surgeons frequently rely on the physical feedback received through the tools to orientate themselves, navigate to the surgical site and apply appropriate force to the

anatomy. The equipment may also be set up to track the user's movements and provide objective feedback, for the surgeon to personally monitor their progress in the repeated performance of the same procedure.

However, VR equipment is expensive and can be criticised for not fully replicating the experience of performing surgery on a live patient. By creating a physical means of surgery simulation, the experiential realism of operations using cadavers may potentially be combined with the ethical, practical and educational advantages of VR simulation.

As discussed in Section 1.1, surgery in the paranasal sinuses involves great risk to the patient and requires the acquisition of complex psychomotor skills by the surgeon during training and complete knowledge of the patient's anatomy. While work has been done recently to assist in the training of paranasal sinus surgery using VR simulation, physical simulation has been slower to develop. This is largely due to the small size and high level of complexity of anatomy in this area of the body, which has made any simulation difficult to produce to an acceptable level of accuracy. Rubber cast models have been produced [7], which act as a visual aid in the teaching of sinus anatomy, but cannot assist in the simulation surgical procedures. Additive Manufacturing (AM) was identified as an appropriate and capable manufacturing process for the production of more complex anatomy for realistic simulation of surgical procedures, described in Section 1.3.

For training of surgical procedures, it is necessary to expose the student to a wide range of anatomies and pathologies, in order to fully prepare them for the cases that will arise in the performance of real surgery. By training for sinus surgery using cadavers, students are limited to operations on the case presented by the available body, which cannot be controlled. This can cause delays in acquiring samples of specific pathology in training programmes where cadavers are used, while examples of the required pathology are obtained. VR simulation cases are also, as yet, highly inflexible and must be selected from the predefined range of cases that are provided. Limited customisation may be performed on the virtual models once the model is acquired to broaden the range of cases that may be simulated.

The development of a means by which customisation of the pathology exhibited in the sinus model may be performed directly by medical or training staff, or students themselves, to simulate a specific case or developing pathology would be extremely beneficial. This would allow the training programme to be tailored to the needs of individual students, and significantly increase the number of pathological cases that may be simulated on each anatomical model, therefore increasing the total number of cases to which trainee surgeons may be exposed before operating on live patients.

1.3 Additive Manufacturing

AM (or Rapid Prototyping, RP) is a term used to describe manufacturing processes in which material is solidified or bonded together in thin layers to additively produce a 3D part directly from CAD data, avoiding the restrictions and limitations of conventional manufacturing methods (see Figure 3). The technique was initially used to aid the visualisation of design prototypes and iterations, helping designers communicate ideas more effectively than with the use of two-dimensional (2D) sketches and drawings.

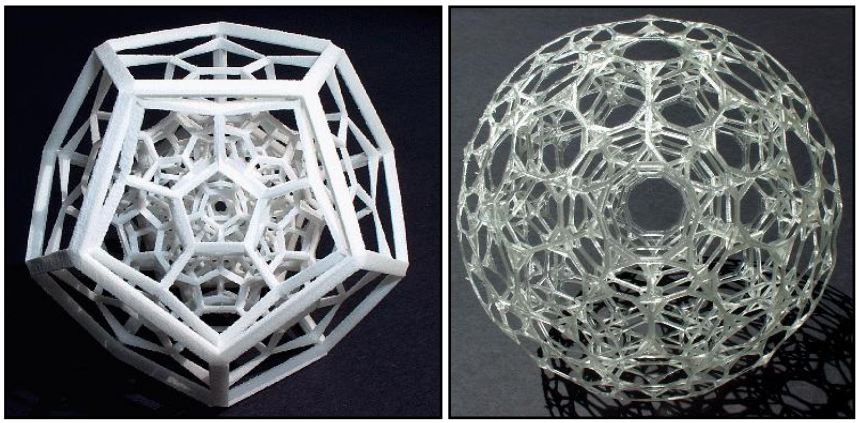

Figure 3: Examples of geometrical complexity made possible with AM, approx. size 40mm [8]

AM is now also used to produce finished products or components, and AM processes have recently been assessed and developed for use in many other areas, including the medical sector (for example in the case of conjoined twin surgery simulation and communication, see Figure 4). As AM processes produce parts directly from digital CAD data, many different parts, each potentially individually customised, may be produced simultaneously, at no extra cost and in the same time as the production of

many of the same part. The automated nature of the process also eliminates the inter-operator variation suffered by other approaches [9].

AM processes have been explored significantly in recent years in the medical sector, for the production of custom-fitted implants and prosthetics, drug delivery systems and representation of complex anatomy. The layered approach of medical imaging is ideally suited to manufacture by AM, which can reproduce the levels of intricacy and geometric complexity present in most anatomical areas. In the paranasal sinuses, the thickness of bone can be as low as 0.2mm; AM processes are able to produce parts with a resolution of 0.05-0.10mm. AM may be used in conjunction with live patient data from medical imaging sources such as Magnetic Resonance Imaging (MRI) and Computed Tomography (CT), to produce models which replicate the anatomy of a live patient awaiting surgery or to display unusual anatomy for preoperative planning and training complex surgical procedures.

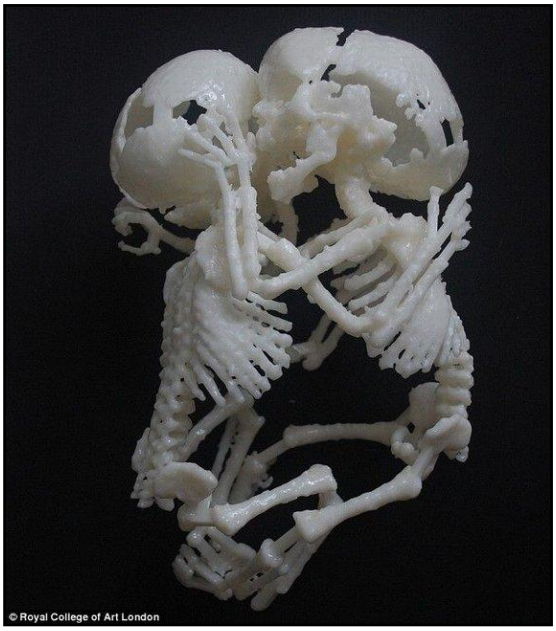

Figure 4: Physical AM model for the planning of conjoined twin separation [10]

As discussed earlier in Section 1.2, the physical experience of performing a surgical procedure is an important factor in the acquisition of the skills required for the safe performance of surgery. The bones in the sinuses have been found to be cancellous in nature, possessing a hard outer surface with less dense honeycomb-structured bone within. This structure is inherently replicated by some AM processes, which create a

solid outer perimeter of each layer of the part being produced, and a cross-hatched interior structure. One process which achieves this structure is 3DP.

Parts built with plaster-based material may be produced with 3DP, with physical properties similar to those of bone. Furthermore, 3DP also gives users the option of applying printed colour to the exterior of parts during manufacture. These properties make 3DP ideal for the production of both visually and physically realistic models of the sinuses.

1.4 Research Aims and Objectives

Surgical simulation is the clear solution to the problems met in the training of surgeons, if the safety of patients is to be prioritised. Physical simulation models offer educational benefits to the student, while avoiding the financial and ethical issues encountered through the use of organic or virtual simulation methods. To maximise the potential of the simulations, and to broaden the experience, knowledge and skills of the students, customisation of the simulated anatomy to exhibit the desired pathology is extremely desirable. This potential would be further enhanced by allowing the training staff, or the students themselves, the opportunity to directly influence the training cases being used, through a means of customising the anatomical model to exhibit the required pathology.

The research described in this thesis is a component part of a larger project. Initially, the larger project aimed to develop a means of producing a physically and visually realistic model of the sinuses, portraying real-life cases for use in training surgical procedures. This part of the larger project was focussed on achieving visual realism in the physical part, through automatic compensation of the colours of the real anatomy for accurate reproduction by 3DP (having been previously identified as the most appropriate method for the production of sinus surgery simulation models), and internal colouring of the physical part. After some investigation and clinical input, some aspects of this research were found to be unnecessary or unfeasible, as described later. The aims and scope of this part of the larger project were therefore revised after approximately 9 months, to also encompass the development of a customisation tool to enable medical staff to design training cases themselves. The aim of this tool is to

allow the user to add customised disease to sinus anatomy, at their own discretion, before manufacturing the altered model with 3DP for training purposes.

All pre-manufacturing aspects of the training tool are included in the scope of this thesis, before leading into the work performed in the accompanying research on increasing the physical realism of the 3DP model. The accompanying research project investigates the possibility of producing varying physical properties throughout the same part by 3DP; this required the file for manufacture to consist of separate bodies. Some collaboration was required to identify potential infiltration techniques for the finished physical model. Aside from these instances, the two projects were carried out separately.

The objectives of this thesis are therefore:

- Investigate colour reproduction accuracy of 3DP, and the possibility of internal colouring of physical parts
- Identify colours and textures to be used to achieve visual realism in physical parts, and a means of producing these once the colour reproduction accuracy of the manufacturing process is taken into account
- Investigate sinus anatomy, disease and surgery to identify, with clinical input, the most beneficial pathology and functions to include for customisation of the training tool
- Identify a means by which medical staff may customise anatomical data, potentially from different datasets, on a continuous scale, to display the required position, type and size of pathology, which may then be exported for production by 3DP
- Develop a concept that achieves the above
- Trial the concept with a relevant sample of users, before acting on the results obtained to refine the concept
- Re-trial the concept to assess the success of any alterations

For the purposes of this research, the term ‘customisation’ is used to describe the ability of the user to alter the case in hand by applying additional features or

pathology to the anatomy, each of which will be fully adjustable, for example in their size and position. As opposed to some other user-driven customisation tools, this tool will aim to provide complete freedom for the user, to allow them to create training models that are as close as possible to the case they require. The pathology to be simulated does not follow a discrete scale of set positions and sizes; as such, the tool must aim to provide the user with the opportunity to adjust the case along a continuous scale. The final concept will therefore avoid the use of catalogued cases, which provide limited scope for user-driven customisation.

The target users of the customisation tool are medical staff, specifically sinus surgeons, both experienced and trainee, and training co-ordinators. Maxillofacial prosthetists may potentially make use of the system in collaboration with surgeons, to produce models of the development of pathology. The success and adoption of the customised sinus surgery training model into everyday use depends largely on the level to which it may benefit both users and patients. From clinical input, the users' needs and expectations of the final model were analysed and found to understandably centre on the benefit to the surgeon who uses the model and their patients. This relies heavily on the level of realism achieved; visual and physical realism in the finished model must be based in the design stage, which forms the majority of the work described in this thesis. When considering the customisation aspect of the tool, speed and ease of use are essential, especially as the tool will be a new concept to the users. Users need to be able to repeatedly produce the same case specifications, or developments of the pathology previously produced.

Figure 5 shows the initial stages of investigation to be undertaken to define the requirements of the anatomy customisation concept, and complete the colour reproduction work. The process and capabilities of 3DP will be evaluated, before examining the anatomy present in the sinuses and the pathology that may develop therein. The most critical pathology to be simulated will be identified, aided through the involvement and consultation of clinical expert Anshul Sama and maxillofacial modelling staff at Queen's Medical Centre (QMC) in Nottingham. The knowledge gained in these first stages of research will be used to investigate the possibility of

automatically compensating colours for production and internal colouring of parts using 3DP, and to guide research into surgical training methods.

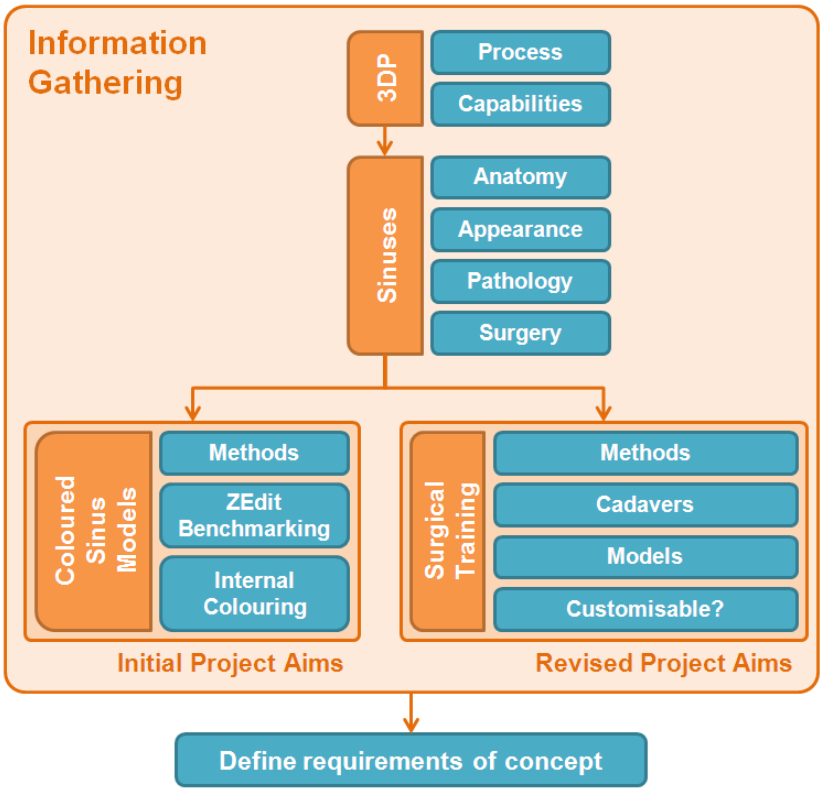

Figure 5: Flow chart of plan for information gathering, leading to concept development

As Figure 5 shows, the first line of investigation was into AM and, specifically, 3DP.

CHAPTER TWO

ADDITIVE MANUFACTURING

2 Additive Manufacturing

Additive Manufacturing is the name given to a wide range of manufacturing methods that rely on CAD data sources to automatically produce solid, physical models [11]. Complex physical structures may be produced quickly and accurately, directly from data fed by a computer to the manufacturing system [12]. This is done by employing manufacturing methods that are different to conventional and traditional manufacturing techniques; by producing parts with an *additive* approach, material is printed or deposited in layers to eventually form the finished object [13], similarly to the construction of a building exterior.

As AM parts are built in layers of as little as 0.05mm thickness, tremendous levels of flexibility are afforded and there is no limit to the complexity of geometry (internal or external) that may be built [14]. Indeed, any part that can be represented as a CAD model may be successfully manufactured. This increase in complexity comes at no extra cost to the production of very basic models, as no extra human skill is required for their manufacture.

Products or models with many components may be produced all in one build, made possible by the layer manufacturing approach, instead of the previous method of manufacturing components separately before combining them to complete the product. This reduces the need for manual labour in the production of parts and the time and financial constraints involved with manual labour. Time and money are also saved through the elimination of material waste; this is achieved due to the additive nature of the technology, meaning that no material must be discarded, as in other manufacturing methods, in order to produce the shape of the model [11].

The layer manufacturing approach of AM possesses a clear inherent link to the slice data provided by the medical imaging systems described in Section 2.2, and its value can be understood when the complexity of the anatomy of the human body is considered [15, 16].

By constructing parts in this way, the usual physical constrictions of subtractive and formative processes such as milling, moulding, casting and Computer Numerically Controlled (CNC) machining are avoided. In the past, CNC manufacturing was used to create physical models of patient's anatomy, particularly the skull, for preoperative planning and surgery simulation. A CNC milling machine fitted with a 5-axis drill was used to manufacture these models from a block of Polyurethane. The milling process is incapable of reproducing the thin, bony sections and walls of closed cavities or undercutting surfaces of the skull. For the production of patient-specific implants and prostheses, CNC cannot guarantee the reproduction of fitted surfaces or fine details over a large area. These are simply limits of the milling process, which are overcome through the wider range of capabilities and materials offered by AM techniques [17, 18]. A wide range of work has been performed which involves the production of AM surgical training and preoperative planning models (see Section 4.2.2.2); AM processes will be discussed in more detail in Section 2.4.

Chua *et al* define the main roles of AM to be:

- Experimentation and learning
- Testing and proofing
- Communication and interaction
- Synthesis and integration
- Scheduling and markers

They state that AM models can be used by product development teams to "help the thinking, planning, experimenting and learning processes whilst designing the product" [19]. The speed, low cost and flexibility of the manufacturing processes available make them ideal for quickly producing a physical representation of an idea, to allow design features to be easily communicated. AM processes are used significantly for this purpose, however now the other possibilities of their use have begun to be explored and exploited. With the advent of new materials and developments of existing rapid technologies, the processes are more commonly being implemented in different fields to their original purpose of prototyping design iterations [20, 21].

The wide range of applications for which AM processes are used today emphasise and exploit the versatility of AM processes, and how their use has expanded since the introduction of the technology. The original purpose of AM, to quickly provide a physical and visual representation of a concept or product prototype is still used, and offers as many advantages as ever. Parts may be produced in fine and complex visual and physical detail, to any scale and with full colour and livery included, in a short amount of time. These factors still assist greatly in the visualisation and presentation of concepts to groups of designers and customers. However, these advantages are now being used to create models which take on a more physical role, such as those described in Section 4.2.2.2. In physical surgery simulation, the physical characteristics of the models are of far higher importance than in the case of visual prototyping and concept communication. To be able to accurately replicate the tactile experience of performing surgical procedures whilst operating on an AM part is extremely desirable, and will be discussed further in Section 6.4.

AM techniques are beginning to be used in increasingly diverse areas, including medical applications, household furniture, Formula 1 and some types of jewellery. For these types of applications, parts are built for direct implementation into functional purposes [22, 23] instead of a prototype or visual representation of the product.

AM eliminates all tooling, as is usually required in traditional manufacturing techniques, making AM ideally suited to products that are highly customisable, or which need to be personalised for the customer to use; this applies almost universally to several areas of medical manufacture for specific patients. This is an operation that could not be performed efficiently or economically on a large scale by manual labour, which is most often the driver behind the use of additive technologies. Parts are produced repeatedly, quickly and in vast quantities, with no effect of complexity on time to manufacture; time to build depends most strongly on the number of build layers in the part. Conversely, parts may be produced as a one-off; with traditional manufacturing methods this was a costly exercise as moulds and tools would need to be made for the single part.

One example of the type of large scale customisable production for which AM is the process of choice is the manufacture of custom-fitted hearing aids. In order to create a custom-fitted hearing aid for a patient, a mould must first be taken of the space to be filled by the hearing aid, to ensure a comfortable fit. Once this mould is available, it may be digitised and produced by AM in the ways to be described in Sections 2.1 and 2.3, potentially within hours of the mould being made. Any number of the same hearing aid, or other individually customised products may be produced quickly, efficiently and simultaneously.

There are some issues which must be overcome in order for AM to be more widely used, most of which rely upon the advancement of the technologies used. One of the most significant of these issues affects all AM processes; the surface finish of the parts produced. As the parts produced by AM machines are built up in layers, a 'stair-step' effect is generally observed on the surfaces of the part. This is caused by the small vertical edges produced when layers are built not fitting, for example, a curved or angled edge of the part. This can lead to a slightly rough surface finish, depending on the layer thickness selected for the part, and may be unacceptable for some applications [22]. Work has to be done in post processing to improve the surface quality of the parts, if necessary. This will be discussed, for various AM technologies, in Section 2.4.

Sections 2.1, 2.2 and 2.3 describe the process of AM, from the acquisition and manipulation of a design or geometric data to the production of the final model. The production process has been divided into two main phases: data acquisition (from inorganic or human sources) and the production of the finished part from the CAD model.

2.1 Data Acquisition from Inorganic Parts

All AM processes require geometric part information in order to build the part in layers. This can be acquired in a number of ways, the most common of which is through design of the product, often from scratch, using CAD modelling software. It is through the production of a solid CAD model that the AM process can begin; the

CAD model allows the individual layers, cross-sections or 'slices' of the part to be defined.

Some models, however, are not the product of the designer's work. When models based on existing objects, of which no geometric data is known, are required to be built using AM techniques, their data must be acquired for the process to begin. This may be done in a range of ways, all of which fall under the term Reverse Engineering (RE).

Through RE, a part's design and geometric data may be obtained in a systematic manner and the necessary information supplied to the AM equipment. This may be done for reasons of lost information, competitor analysis, or to model items that may not be 'designed' manually; for example human body parts, implants or highly customised products that interact closely with humans.

The traditional approach to RE data collection is to directly measure the part to be modelled, using automatic contact or manual methods, and to subsequently create a CAD model from this information. This could be time consuming, inaccurate (if performed manually) and in many cases may not be an appropriate option, for example in the human-related cases described above. To automate the RE process and use a faster means of data acquisition may provide more accurate results, produce models in a shorter amount of time and allow a far greater range of items to be modelled for production.

Non-contact methods of data acquisition typically rely upon the use of light or laser beams as the main methods of deriving part information. For physical parts that may be handled, laser or light scanning techniques that record the x, y and z co-ordinates of millions of surface points on the part and directly produce a CAD surface model from the data may be used.

2.2 Medical Imaging

To acquire the geometry of bones and internal human features, it becomes necessary to draw upon the medical imaging techniques described in this section. By stacking

sequential 2D greyscale medical slice data on top of one another, a 3D model may be produced (see Figure 6) without contact to the patient. The naturally tomographic approach of AM to the production of 3D models makes it an ideal method for the manufacture of patient-specific data from medical data [16]. AM models of the region of interest (ROI) can therefore be produced which represent the patient's anatomy for the planning or teaching of surgical procedures.

Figure 6: 3D model of skull constructed from CT data [24]

2.2.1 Magnetic Resonance Imaging

MRI is used commonly for medical diagnosis of internal problems in the human body. MRI is a versatile and sensitive tool, capable of producing section images of any part of the body. Anatomy of a wide range of densities may be imaged, including organs, bones, and ligaments. The process may be performed from any angle, to provide as clear a view as possible of the ROI [15]. Subtle differences in the composition of soft tissue may be highlighted through the use of MRI (Figure 7), which can be vital in some applications.

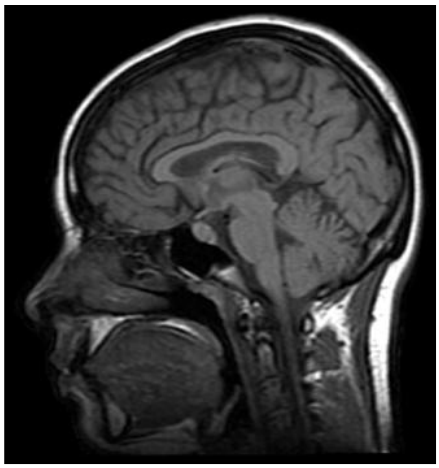

Figure 7: MRI slice image of human head taken in sagittal plane [25]

To acquire the geometry of the body parts of the patient, the sinuses for the purposes of this research, the subject must be positioned within the cylindrical magnet used in the imaging process. First, the MRI imaging equipment stimulates the body with radio waves to change the steady-state orientation of the protons (nuclei of hydrogen atoms which possess magnetic properties) in the selected area of the patient's body. By doing so and subsequently terminating the radio signal, the electromagnetic emissions from the hydrogen nuclei may be detected. The different levels of emission from each section of the scanned area are recorded on a scale of grey or colour, which permits them to be imaged against one another, providing a series of 2D images of the area concerned. The hydrogen atoms within the patient's body return to a relaxed state after the process is completed. During scanning, the patient must remain very still for the entire duration of the imaging process, to ensure clear scan results.

2.2.2 Computed Tomography

CT is similar to conventional X-ray imaging, and may be used to produce clear images of any part of the body, especially bone. These images may then be used to build a 3D model of the subject matter. CT is used to obtain clear images of dense tissue such as bone, without destructive effects to the object. Little detail is provided of the geometry and structure of soft tissues, but if used in conjunction with MRI a full impression of the object's interior may be acquired.

In conventional CT, as used for medical purposes, the patient is surrounded by the imaging machine in a similar orientation to MRI, positioned on a moving table around which the scanning equipment rotates. The equipment emits a thin X-ray beam at hundreds of different points towards the subject; the absorption rate of this beam into all areas of the scanned object is recorded by solid-state crystal or Xenon gas detectors at opposite ends of the beam. By analysing the amount of the beam that is absorbed into, or passes through each area, the density of the parts being examined may be determined. This information is subsequently used to produce a series of 2D images, showing the densities present through the use of a greyscale representation. As with conventional X-ray images, dense areas of the scanned object (hyperdense, such as bone) appear bright white, and less dense tissues (hypodense, such as muscle and tissue) appear a similar shade of grey. The slice thickness produced by the process directly influences the level of detail that may be obtained, along with the volume that may be efficiently and safely scanned; thinner slices mean that more time would be required to acquire images of a large volume, which may not be advisable for the patient due to X-ray exposure regulations [15].

The latest developments in CT technology allow many slices to be scanned simultaneously. The emergence of multi-slice scanners has improved the previous trade-offs and constraints of slice-based systems: imaging time, volume coverage and longitudinal resolution. Using the traditional method of imaging, the amount of time available for the scan was largely dependent on the length of time that the patient was able to hold their breath, thus creating a clear image free of artefacts, or the time during which an organ was enhanced through the injection of a contrast agent. Multi-slice scanners increase the volume coverage that may be achieved at any resolution, potentially allowing the scanning of dynamic processes such as the beating of a heart. The outcome of the volumetric scan is, instead of a limited range of 2D images, a 3D dataset which may be sliced or rendered in the required manner. At present, scans are available that image 256 slices simultaneously at a slice thickness of approximately 0.5-0.8mm, with less radiation suffered by the patient than with previous, less advanced machines due to the wider area exposed in each scan [26]. The ability to scan such large volumes allows images to be obtained without the need to move the patient within the machine [27].

At present, medical professionals commonly examine the 2D images obtained from CT scans in order to obtain an understanding of the geometry and anatomy of their patient. Occasionally, 3D virtual or physical models are created using the images, in order to adopt a more tactile approach to anatomical analysis. CT scans are also used in the planning and performance of reconstructive surgery, to model the shape of implants by using the mirrored or manipulated model of healthy anatomy.

In order to create a 3D representation of the patient's anatomy in the ROI, the closely spaced, axial slices of the patient's anatomy produced by CT are refined and registered against one another. This group is built up, layer by layer into a 3D simulation of the scanned volume. This process will be discussed in Section 6.2.1.

2.2.3 Microtomography

The Microtomography (µ-CT) process is performed in the same way as CT, as described in the previous section; however the scale upon which the scan takes place is far smaller. The pixel size in the cross-sectional images produced is in the micron (1/1000mm) range, achieving a higher resolution than conventional CT. The machine used is far smaller than for any medical CT applications, and cannot accommodate living human samples. Smaller objects such as small animals and, as in this case, biomedical samples have commonly been modelled through µ-CT since its conception in the early 1980's.

A sample of a human sinus from a cadaver was available to the research, and has been scanned using µ-CT for analysis and use in the development of customisation tools. An image from the dataset is shown in Figure 8, which shows the bone structure of the sample (approximately 90x60mm) in clear detail, with varied greyscale values throughout the structure. This level of detail is achievable due to the smaller pixel size offered by µ-CT, in comparison to conventional CT.

Figure 8: µ-CT image of human ethmoid sinus showing density definition

2.3 3D CAD Model to AM Machine

Once a (preferably) solid 3D CAD model has been produced from the data acquired or created during the first phase, the model must be converted into a standard format recognised by all AM machines and systems. This file format is the *St*ereo*L*ithography (STL) format, the de facto standard for the AM industry due to its ease of generation and low computing capacity requirement. The STL format represents the surfaces of the CAD model using a mesh of facets, most commonly triangular in shape [28]. It is this file, after conversion to the STL format and further manipulation, which will be inputted to the AM machine for production.

The resolution of the STL file, that is the number (and therefore size) of triangles used to approximate the surfaces of the CAD model, determines the extent to which the geometry in the CAD model will be replicated during manufacture. The tolerance of the STL file is therefore a direct determinant of end-product quality, and must be carefully defined. The tolerance of the STL file, however high, will have no effect upon the time taken to produce the part using AM, as each layer of a particular model will always take the same amount of time to build, however complex the geometry [22].

In Section 2, the effects of layer manufacturing were briefly discussed, focussing on the poor surface finish sometimes experienced due to the protrusion of layers on curved or angled surfaces of the part. This effect may be counteracted by orientating

the part within the machine build volume in such a way as to restrict this 'stair-stepping' to the non-functional or non-aesthetic surfaces of the part. For example, if a flat circular piece were to be manufactured standing upright, in the X/Z or Y/Z planes, the effect of stepping on the rounded edges of the part would be evident, as the layers would not accurately follow the profile of the part, as can be seen in Figure 9:

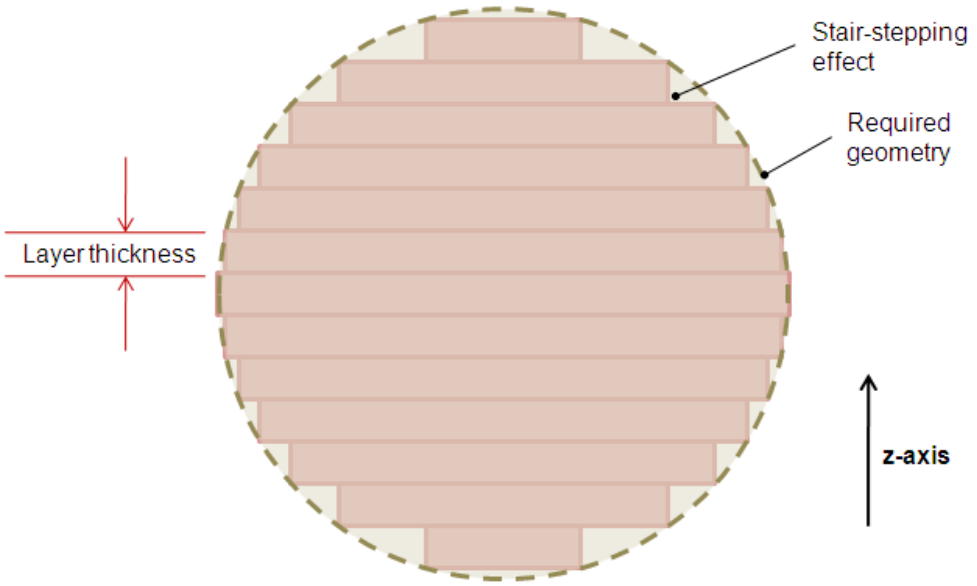

Figure 9: Exaggerated example of stair-step effect (adapted from [22]**)**

However, if the same part were manufactured lying horizontally across the X/Y plane, there would be no effect on the surface quality of the edges of the circle, as shown in Figure 10:

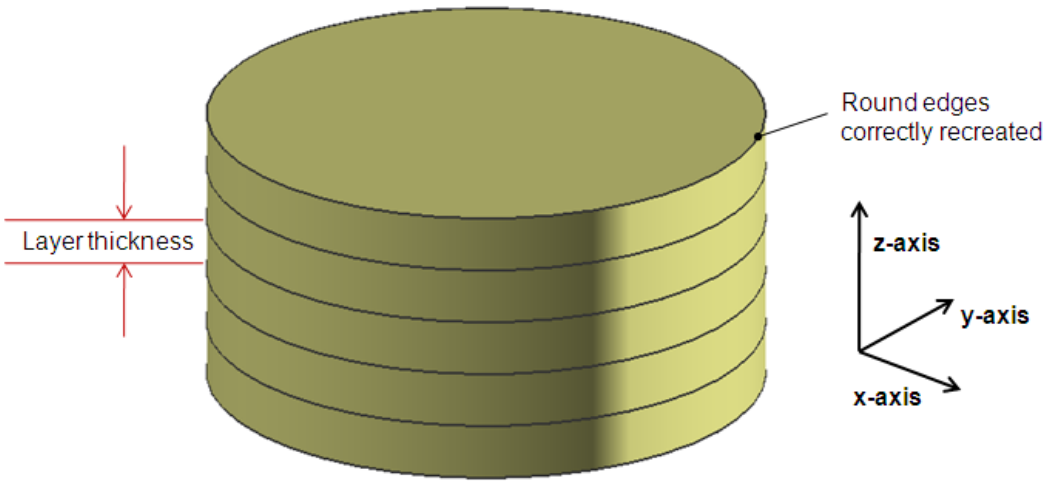

Figure 10: Circular part manufactured on X/Y plane

To build the part in the way described in Figure 9 would also take a longer amount of time, as more layers would be required to produce the complete part. The orientation of parts within the build volume is therefore an important consideration, as it may not only affect the time taken to complete the build, but the quality of the parts being built.

Depending on the AM process selected, the next stages in the production of the part may vary. In Section 2.4, the most widely used and applicable processes to this project will be described, and the steps taken to produce a part will be introduced.

2.4 Additive Manufacturing Processes

Once the procedures above have been completed, the part may be produced by a range of techniques. For the purposes of this project, 3DP has been selected for its inherent similarity to bone, the ability to print colour on the exterior of printed parts, and the variation of physical properties with changes to print strategy, build material, binder solution and methods of post-processing or infiltration.

2.4.1 3DP (Z Corporation)

3DP, developed at the Massachusetts Institute of Technology (MIT) and now commercially distributed by Z Corporation in Burlington, Massachusetts, uses powder to produce parts additively. The process is described as "a process for the manufacture of tooling and functional prototype parts directly from computer models" [29]. 3DP is an uprunner of the inkjet printing technologies commonly used in desktop printers [20]; as such the laser used in SLS is substituted for a print head, which selectively deposits an adhesive binder solution onto the top surface of a fine powder, printing out the image of that layer of the part(s) [12]. Up to four print heads may be used, with up to 1216 jets of binder being fired onto the surface of the powder [30]. The next, very thin layer of powder is then spread evenly across the build platform by a counter-rotating roller and the process is repeated until completion of the part(s) to be built (see Figure 11).

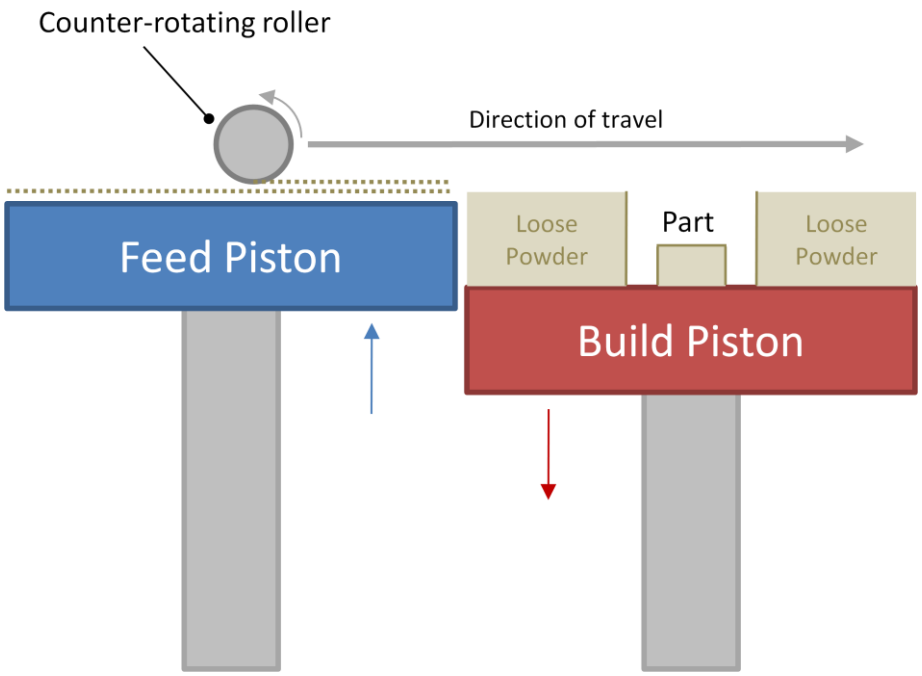

Figure 11: 3DP process prior to printing of next layer

The binder material bonds adjacent powder particles to one another, creating a solid body within the surrounding loose powder. As such, supports are not required and parts may be produced anywhere within the print volume in all three dimensions.

In recent years, 3DP has become more competitive in the field of AM, with more established processes such as Stereolithography (SLA) and Selective Laser Sintering (SLS). It has been able to compete with these technologies due to the relatively low cost and high speed of producing parts, along with a range of other unique advantages that it offers.

In their study on the achievable accuracy of the 3DP process, Dimitrov, van Wijck *et al* found that the dimensional accuracy of parts produced by 3DP are dependent on the material used, the axis on which a feature is placed and the nominal dimensions of the feature. The highest levels of accuracy achieved for small dimensions (2mm to 18mm) were with a maximum deviation of ±0.434mm. This is a suitable level of accuracy for the representation of the majority of the anatomy of the sinuses. Different methods and materials for infiltration are also available, which may also have a lesser effect on the precision of parts built [21].

The machines used in 3DP are considerably less expensive than those for other processes such as SLA and SLS, at $14,900 to $59,900. Furthermore, lower material prices mean that the machines are not only suitable for design companies, but highly viable for other institutions that wish to produce 3D printed parts. These machines are now used as commonly as a desktop inkjet printer in some companies, to produce prototypes and design iterations for communication at every stage in product development, with a machine in the design office.

A distinct advantage of 3DP over all other rapid technologies is the ability to print 24-bit colour on the exterior of parts, at a resolution of up to 600dpi. This is made possible by the use of the print head, very similar to those used in desktop inkjet printers, which applies colour to the outer perimeter of the part on each layer, creating a coloured exterior once the part is complete. The colour ink is delivered to the print head in different ways in different machine ranges from Z Corporation. The print head on the Spectrum Z510, for example, draws coloured binder solution from four reservoirs (clear, magenta, cyan, yellow) selectively using each to create the full range of colours on the exterior of the part. The latest development in the use of colour in 3DP is evident in the Spectrum Z450, where a single sealed clear binder cartridge may be slid into place at the top of the machine, removing user interaction with the liquids, and three snap-in inkjet cartridges are attached to the print head to provide colour immediately before printing through the (now) tri-colour print head.

The coloured inks combine with the clear binder to create the required shade, but also work as adhesive to bond the loose powder particles to one another on the solid exterior perimeter of the part [31]. In the interior of each part layer, the clear binder solution is used alone in a crosshatched pattern, in order to make more effective use of the colour cartridges. The option to include colour on the exterior of a physical prototype of a design adds another dimension to the understanding and communication of ideas between parties. Designers have found that to produce a 3D representation of their design concept, or even a specific section allows them to more effectively communicate the features of the design which may be unclear through the use of sketches or engineering drawings alone. The visual and tactile experience of the designers and colleagues that study the object is very similar to the way in which

surgeons can more fully understand and plan surgical procedures by considering a coloured 3D part instead of 2D greyscale medical imaging scans, as described in Section 4.2.

Colour may be applied to 3D CAD models in specialist model preparation software, in the form of coloured facets or sections of the model, or by wrapping an image around the part. The Virtual Reality Modelling Language (VRML) is a means of applying coloured surface textures to a part, by applying separate bitmap images to individual 2D facets of the part. In this way, far more complex surface textures may be applied to the part, increasing the range of use of the model and the ease of visualisation and communication between, for example designers or surgeons. This system has been used previously for the representation of virtual environments, in video games, architectural models, simulations and scientific visualisations [32] and could be a viable means of representing the internal and external appearance of the sinuses. However, VRML cannot at present achieve the representation of internal colour, which is, along with the accurate application of the external images and textures, an area for further research if parts are to be produced that are coloured throughout [31].

It is theoretically considered that any material that may be represented in powder form may be formed into a 3D part by 3DP [33]. This is exploited in many cases, for example the production of metal parts or functionally graded materials, all made through the binding of powdered material with the 3DP technique. After production, metal parts are sintered to remove the binder material and fuse the metal particles together. Depending on the level of sintering performed, the density of the part and the parent material to infiltrant ratio may be determined [23].

During the printing process, the print head forms an outer perimeter of each layer, while the internal ‘fill’ of each layer is crosshatched to reduce the amount of binder solution that is used to print large cross-sections. This gives the outer surface of the part good stability and structural integrity, and can have advantages for the use of the process in particular fields.

As will be described in Section 4.2, 3DP has been used in the medical field for the production of surgical planning aids and intraoperative reference models. Another area of use has been the production of implants and prostheses, produced directly from CT and MRI data, custom-fitted to the patient to ensure comfort. 3D printed materials such as calcium phosphates may be used as bone substitutes, implants and coatings, due to their chemical and structural similarity to the inorganic phase of bone. The simple and versatile nature of the 3DP process allows parts of a wide range of properties to be built, by varying the powder-binder system (combination of build material composition and the binder material) [34].

3D printed parts may also be manufactured with chemicals within the part, in different concentrations throughout the part. This is of great use in the field of controlled drug delivery, whereby 3DP can be used to produce drug capsules which dissolve in the human body, releasing chemicals into the bloodstream at controlled intervals and rates [31].

As with SLS, parts may be sintered to improve the bonded strength in post-processing, or infiltrated with a secondary material to impart new properties upon the part. This is often required to decrease the porosity of the produced parts, by infiltration with wax, cyanoacrylate adhesive or epoxy resin, for example. These infiltration materials are in a liquid state at room temperature and, when placed in specific conditions, harden to improve the properties of the 3D printed part. Z Corporation has developed a range of building materials that may be infiltrated with specific secondary materials to produce a selection of physical properties. For example, through the use of the company's elastomeric material, which consists of a mix of cellulose, speciality fibres and other additives, elastomers may be infiltrated into the part to give the finished article rubber-like properties [30]. Alternatively, parts may be coated, through immersion, in a secondary material to provide a hard outer shell, or to increase the vibrancy of the colours on the part surface. The material used in these cases may be a wax or PVA-type substance.

Advantages of 3DP include the opportunity to print parts with full 24-bit colour on the exterior, in a wide variety of materials which may be infiltrated in post-processing to

achieve a range of final physical properties, more quickly and cheaply than competitive processes.

Two areas of potential development of 3DP, at present, are the surface finish and achievable accuracy of the finished parts [35]. The extent of any dimensional errors is mainly dependent on the material used, but may also be determined by the axis on which a feature runs and the nominal dimensions of the feature to be printed [21]. Dimitrov *et al* (2003) suggest that through educated scaling of the CAD model, the small inaccuracies of the manufacturing process could be designed out if the errors in a specific case are found to be sufficiently significant and consistent [36].

CHAPTER THREE

SINUS ANATOMY AND SURGERY

3 Sinus Anatomy and Surgery

An area of the body in which surgery can frequently involve great risk to the patient is the paranasal sinuses. Their proximity to vital organs and the dissimilarity of anatomical geometry between patients make the surgical skills required in this area complex, and difficult to acquire without experiential training. Nevertheless, trainee sinus surgeons follow the same procedure as many other disciplines, using the traditional training methods described in Sections 4.1 and 4.2.1. This could be considered to increase the potential risk to future patients, if trainee sinus surgeons are left to acquire experience of sinus surgery in a real operation scenario.

3.1 Sinus Anatomy

The human paranasal sinuses, which form the focus of this research, are situated behind and around the nose and occupy a large area inside the head. The different areas stretch out behind the cheekbones and back approximately as far as the ear, and into the forehead above the eyebrows. There are many suggested reasons for the existence of the paranasal sinuses. It is known that the human sinuses humidify, warm, filter and help to sense what is breathed in through the nose and mouth [37]. They assist in the three main tasks of the nose (olfaction, respiration and protection) by providing a large surface area of mucus-lined cavities to filter out small particles in the air, after the coarse nasal hairs (vibrissae) have removed larger particles, and to promote turbulent airflow to assist this process [38]. This filtering of the air that is breathed in is essential in removing dust, pollen and germs from the respiratory system. It is also suggested that the sinuses help to form the sound that the human voice emits, by echoing the vibrations of the vocal chords. Vibration of sound energy through the cavities, muscles and bones of the head is affected by the resonance of the ears and sinuses, which varies between 500-3000Hz [39]. Others state that the sinus cavities also serve to simply reduce the weight of the head, to permit the turning of the head, and allow increased flexibility of the neck [40].

There are a wide range of types of anatomy, surface textures and tissues present in the sinus area, unique in geometry and physical characteristics in every human. The external nose is divided into three sections for sinal surgery; the hard upper third of

the nose is known as the nasal bone, in the middle, firm section are the upper lateral cartilages and in the lower, more flexible section are the lower lateral cartilages. The nasal bone is attached to the maxilla (the cheekbone), the upper lateral cartilages attach to the undersurface of the nasal bone and the lower lateral cartilages attach, in turn to the upper lateral cartilages. The lower part of the nose, consisting of cartilage and soft tissue, gives pliability and structural rigidity to the external nose.

The septum is situated at the bottom of the nose, and supports the lower lateral cartilages. In doing so, the septum also separates the nasal cavity into two, forming the nostrils. The back part of the septum, nearest the face is bony, with the front part constructed from cartilage, in a similar way to the nose. Figure 12 shows the human paranasal sinuses and their physical relationship with the nose.

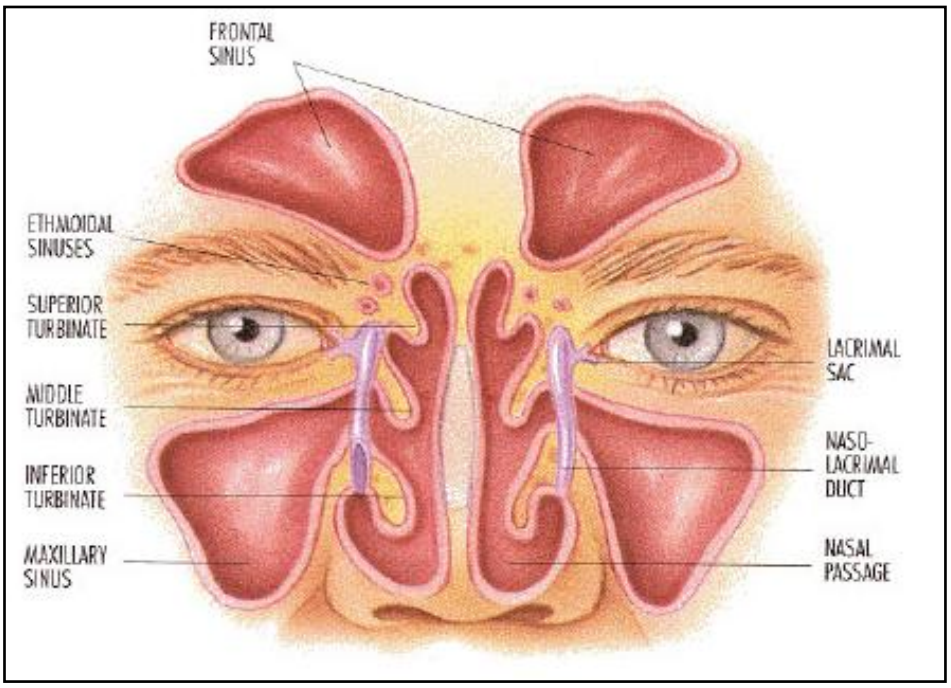

Figure 12: Sinus anatomy viewed from front [41]

Inside the lateral wall of each nostril, three turbinates are situated, each consisting of a rigid bone ‘shelf’, projecting out into the nasal cavity and a soft tissue covering [42]. The turbinates are termed superior, middle and inferior; the inferior turbinate is the largest, situated nearest the nostril. The turbinates protect the entrance to the sinuses through the nose; it is therefore by lifting the soft tissue covering of the turbinates that access is gained to the sinuses during endoscopic surgery. The air space enclosed by

the hanging tissue is known as the meatus, and these are termed by the turbinate under which they are situated, e.g. the inferior meatus (linked to the tear duct, as seen in Figure 12). It is through the middle meatus that the majority of access for sinus surgery is gained, partially due to the immediate link to the maxillary sinus, which will be discussed shortly. Figure 13 shows the sinus anatomy from the side (in the sagittal plane):

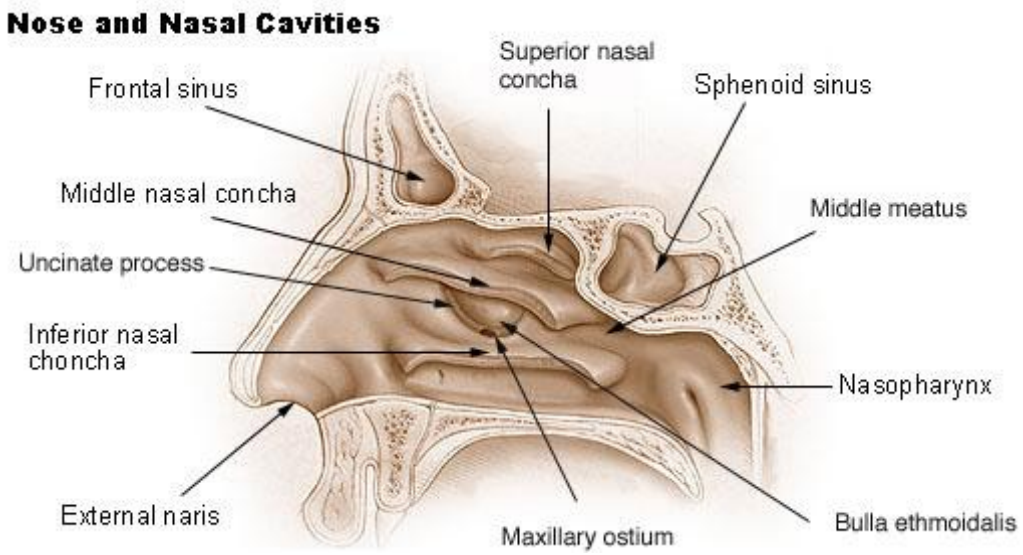

Figure 13: Sinus anatomy viewed in sagittal plane [43]

The sinuses are divided into four areas, each occupying a different space within the head, and consisting of varying sizes of air cells with different physical and anatomical properties:

- The frontal sinus, situated above the eyebrows
- The sphenoid sinus (visible in Figure 13) situated further back in the head, at the skull base
- The ethmoid sinus, situated between the eyes behind the bridge of the nose
- The maxillary sinus, situated under the maxilla bone in the cheeks

The frontal sinus drains into the nose near the top of the nasal cavity and is surrounded by very thick bone for the region, between approximately 4 and 6mm in thickness. A common procedure during surgery in the frontal sinus involves the use of a burr tool, equipped with a 3.2mm tip in order to remove bone from the frontal beak, an area of bone which may restrict access.

The sphenoid sinus also drains directly into the nose, however the location of the sphenoid means that any mistake during surgery could prove to be very damaging or fatal for the patient. The sphenoid sinus "has many important neurovascular relationships" [38] and is located near the skull base, which is very close to the middle of the brain, optic nerves and pituitary gland. The two latter features run very closely behind the bone by the sphenoid sinus, meaning that contact could be made with the optic nerve or pituitary gland if the bone were penetrated. The internal carotid artery also runs laterally to the sinus, through the cavernous areas of the anatomy. The size of the internal carotid artery varies between patients, and may only be seen as a bulge in the lateral wall of the sphenoid sinus [44]. This leaves an extremely small margin of error with severe consequences for the patient and surgeon, who operates using an endoscopic camera attached to their surgical instruments.

The ethmoid sinus is surrounded by bone which is of an entirely different structure and possesses individual physical characteristics to all other areas. This bone was described by Anshul Sama (clinical expert) as having the consistency of potato crisps; however this may vary from patient to patient. Anatomical variation of the middle meatus may lead to impeded ventilation and drainage of the ethmoid sinus, and subsequently other areas of the sinuses [44]. Surgery in this area of the head presents great risk for the patient and the surgeon, as the thin bone, known as the lateral lamella [38] separating the sinus from the brain, can be as little as 0.2mm in thickness. If a leak in cerebrospinal fluid, which supports the brain, were to be caused through damage of the thin bone, a risk of infection and potentially meningitis could be suffered.

The maxillary sinuses are accessed through a small hole in the middle meatus, although the cavity that is then revealed is large, filling almost the entire area behind the cheekbones and under the orbits, making them the largest of the paranasal sinuses [38]. It is through the blocking of the small hole to the maxillary sinuses or the drainage sites of the other sinuses that infections may occur in this area, leading to common ailments such as a cold or sinusitis, an inflammation or irritation of the sinuses [40]. More serious problems which require surgery may involve the presence

of tumours, which most often occur in the maxillary sinuses, and are routinely removed along with areas of the anatomy itself as a means of treatment.

Surgery in and around the sinus complex involves high risk for the patient, and requires a high level of specific skill on the part of the surgeon (surgical procedures in the sinuses will be described further in Section 3.3). This makes the involvement of newly-qualified surgeons in the treatment of patients undesirable, and is forcing the level to which surgeons are trained prior to operating on live patients to be raised. Safer and more efficient ways to learn than the traditional methods are therefore required [45].

The range of bones in and around the sinuses and their respective physical properties mean that surgeons must be sufficiently skilled in the use of a number of tools. For thick bone, drilling tools may be used to quickly but precisely remove bone from the area. Intermediate thicknesses of bones may be removed using a large through-cutting device or punch. Thin bones, such as those described in the ethmoidal complex, may be removed through the use of tools known as rongeurs, which use a pincer-like action to grasp the bone and allow the surgeon to move or break sections away. Not only the bones need to be dealt with during surgery, soft tissue and cartilage must be moved or removed in order to facilitate access to the problem areas; these actions also require the use of specific tools. The sinuses are lined with a thin mucous membrane; a layer of soft, moist tissue which is covered with a layer of mucus [40]. This layer is often also removed during surgery for facilitated access to other areas.

Endonasal (minimally invasive, endoscopic) surgery has become the standard means of treating diseases of the paranasal sinuses and other organs which may be accessed through the nasal cavity. The surgical procedures performed are generally to relieve pain, remove tumours or to prevent the spread of infection [46]. MIS can relieve chronic sinusitis symptoms; for example headaches which may have been present for many years [47]. Endoscopic sinus surgery is not as common as other surgical techniques, due largely to the complexity of the intranasal anatomy involved [48].

The training environment that students encounter in most cases is not sufficiently equipped to provide surgeons with the intricate and highly refined skills they need to perform well in real-life situations [49]. Only through the development of new training methods that accurately replicate the experience of endoscopic sinus surgery and that may repeat this experience readily and indefinitely can it be ensured that surgical students are acquiring the skills needed to reduce the end risk to their patients.

3.2 Pathology in the Sinuses

Pathology in the sinuses, requiring surgical intervention, arises most commonly in the forms of swelling (inflammation), polyps or tumours. All three types of disease constrict the cavities of the sinuses, restricting the access of the surgeon and increasing the difficulty of the procedure. Disease usually begins in the nose, before spreading into the ethmoid sinus, then the frontal, sphenoid and maxillary sinuses.

Swelling and inflammation in the sinuses (sinusitis) is caused by infection of the lining of the bones in the sinuses, or mucosa. This can occur in all areas of the sinuses, due to cavities becoming blocked by inflammation or mucus, meaning that nasal fluid and mucus cannot drain from the cavities. When the entries to the sinus cavities (ostia) are blocked, fluid is trapped within the cavities. Without proper drainage, the natural bacteria in the sinuses are also trapped, causing infection [50].

Polyps are a specific type of swelling that form in the mucosa. Nasal polyps are most commonly found in the ethmoid sinus, although they may occur in the maxillary sinus and may be cancerous. The cause of nasal polyps is largely unknown, however some factors are thought to contribute towards their formation. Allergies such as hayfever and asthma, along with cystic fibrosis, whereby the patient overreacts to inhaled allergens are thought to cause nasal polyps. In these cases, polyps are caused by infection of the mucosa [51]. In some institutions, swelling may be graded for communication and monitoring of the progression of pathology, using a simple scale of severity, ranging from a rating of 0 to 3.

Tumours grow within the sinuses, filling and expanding or narrowing cavities, altering the anatomy and eroding through bone. By eroding through bones in the skull and entering new cavities, a tumour may affect the patient adversely in a number of ways. Tumours entering the orbit can cause visual swelling on the face, depending on the location of the tumour within the head; vision may be impaired by the tumour entering the orbit or coming into contact with the eye; proctosis may also be experienced, whereby the eye is pushed forwards by the tumour. If the tumour enters the cranial cavity and comes into contact with the brain, the patient may experience fits, headaches or dizziness, or areas of the brain may become compressed, leading to far more serious symptoms.

Not all causes of tumours in the sinuses are known, however some are believed to be related to occupational exposure to wood dust (as well as flour and leather dust). Woodworking has been found to lead to adenocarcinoma, a cancer of the epithelial tissue in skin, glands and cavity linings throughout the body, including the sinuses. Smoking can also cause tumours to form within the sinuses, some of which are also cancerous. [52, 53]

3.3 Performance of Surgery in the Sinuses

As explained earlier, surgery is necessary due to the adverse effects of swelling and tumours within the sinuses. When tumours stray outside the sinus complex into the cranial cavity or orbit, coming into contact with the brain or eye, the dangers for the patient are greatly increased. Moreover, some tumours are cancerous, and must be removed to stop or control the spread of cancer throughout the area.

Disease usually begins in the nose (rhinogenic disease), and then spreads into the chambers of the ethmoid sinus. From here, the disease may spread into the larger sinuses (frontal, sphenoid and maxillary). Operations may therefore be based in the ethmoid sinus, treating or removing diseased compartments and clearing the pre-chambers to the frontal and maxillary sinuses of disease [54].

Previously, surgical procedures in the sinuses were performed as open surgery, similarly to procedures in many other parts of the body. The understanding of

pathology in the sinuses was not as comprehensive as it is today, and this approach was frequently fraught with failure. Patients suffered increasing discomfort and further surgical interventions were often necessary. The advent of MIS has served to greatly increase the understanding of the pathology and anatomy of the sinuses, particularly the areas in which pathology is likely to occur, and the most appropriate course of treatment [55].

Surgery in the sinuses most often involves the removal of tumours, polyps, infected mucosa or sections of the bony anatomy. The excision of tumours and polyps is limited by access to the affected region. As such, access must be gained by removing sections of the anatomy using endoscopic tools such as drills, burrs and forceps [56]. In extreme cases, an entire area of bone, such as the whole ethmoid complex, may be removed to clear all trace of disease from the region. A single tumour may grow throughout the entire sinus complex, with a presence in all four areas of the sinuses. This presents a significant challenge for the surgeon, to remove the large tumour through endoscopic procedures with limited access. Alternative procedures are extremely undesirable, as they may involve cutting the face, or removing some areas to gain access to the tumour.

In such a case, large tumours are removed in piecemeal, working through the sinus complex to remove parts of the tumour and ease access to the next part. This is a thorough and complicated procedure which requires careful planning in addition to surgical skill and experience.

The endoscopic surgery being considered in this research is less invasive and therefore far more intricate than some of the cases of conventional open surgery described earlier, requiring the surgeon to be more skilful due to the limited range of vision and lack of mobility of instruments [49]. Paranasal sinus surgery involves all the restrictions of endoscopic surgery, combined with the risks of operating on complex, varying anatomy in very close proximity to vital organs such as the brain, carotid artery, pituitary gland and optic nerve; as described in Section 4.2.1, it is only through realistic training methods that the required skills may be learnt quickly and

effectively, to reach a required standard, allowing students to then develop their skills in real-life applications.

CHAPTER FOUR

SURGICAL TRAINING METHODS, SIMULATION AND PREOPERATIVE PLANNING

4 Surgical Training Methods, Simulation and Preoperative Planning

Surgical training is necessary for medical students and residents in order for them to acquire the knowledge required to perform the tasks they will encounter on a day-to-day basis throughout their careers. This training can be designed to improve general skills, or be directed towards specific surgical procedures.

In recent years, the aptness and effectiveness of the training undergone by surgical students has been called into question. This has been caused by the release of a range of figures describing the level of mortality in hospitals due to medical error. A 1999 Institute of Medicine report estimated that between 45,000 and 98,000 deaths occur annually in the USA as a result of medical error, the vast majority of which are claimed to have been preventable [4]. It is believed by many that the cause of the high number of medical errors is the ineffective training of medical and surgical students, leading to a range of parties being held responsible: "the medical community in general has ascribed errors to the 'system'; however, during a surgical procedure, surgeons are actually the sole perpetrators of an error ... and must not shirk their accountability by blaming the error on the 'system'" [1].

As such, training methods for surgical students are under examination and new methods are being investigated, with the hope of improving the standard of training and assessment for future surgeons and reducing the level of medical errors and adverse effects of surgery. Many of these new methods involve the use of surgical training models or simulation, a concept which has been evident in a wide range of fields for many years. The use of these training methods and their effectiveness will be discussed in this chapter, along with an overview of the traditional surgical student training process.

4.1 Traditional Training Methods

The traditional means of teaching medical and surgical students may be described as "watch (or see) one, do one, teach one" [57]. By this method, a student begins to learn

how to perform procedures and the way in which to respond to particular situations by practicing on cadavers and observing those who have studied before them, dubbed by Klein as “the master”.

The student’s training is lengthy, with gradually increasing involvement in patient treatment, time observing experienced surgeons and growing responsibilities in the operating room (OR) in order for them to acquire and develop new skills [58, 59], until they are judged competent enough to perform some treatments themselves. This decision is the responsibility of the trainer; the student progresses after a primarily subjective means of assessment. In most cases, students could not be objectively assessed on operative skill, but only factual knowledge [60].

Deficiencies in a student’s performance are difficult to identify and correct without objective feedback [61]. There is no guarantee by this method that residents permitted by training to perform procedures can do them well; the passage of knowledge from senior surgeons and observation of manual tasks by trainees can therefore inherently lead to the potential transfer of poor practice and inaccurate information from one generation of trainees to the next [62-64]. Ericsson found in a 2008 study that observed performance did not correlate with greater professional experience [65].

The learning curve of surgeons is defined as the number of operations that they must perform before reaching a level of experience at which there is a low surgical complication rate, which, depending on the procedure involved, can be between 15 and 100 operations [66]. The skills the student requires take time to acquire, governed by their own learning curve until they reach a pre-defined level of proficiency. Decision making is still the responsibility of the attending physician at this point, however once training is completed, the student is often permitted to begin performing procedures on live patients themselves, drawing on what they observed in the earlier stages of their training [57]. The experiential aspect of training is emphasised by Spencer, who estimates that a skilfully performed operation consists of 75% decision-making and only 25% manual dexterity [67], and Barnes, who describes the operating room as the “ultimate arena to refine one’s technical ability” [68].

Nonetheless, this system, which relies on the performance of operations resulting in high complication rates until the student improves, is widely criticised. Sackier highlights the risks of this training method: "when calamity situations arise in the operating room, all are stressed and might not perform to the best of their abilities ... the first time that a resident deals with crisis management should not be in a situation of true crisis" [69]. Aggarwal *et al* suggest that the means by which the skill of a surgeon is measured is not accurate: "the surgeon is learning on a live patient, and the only benchmark used to qualify level of skill is 'number of procedures performed', inappropriately correlating experience with expertise" [70].

Reznick and MacRae cite "sheer volume of exposure, rather than specific curricula" as the basis of this traditional approach [71] and Torkington *et al* (2000) agree, calling for a more structured training scheme, based on "quality, not quantity" [72]. It is widely accepted that relevant experience is required to become a skilled professional, but that experience does not invariably lead people to become experts [73]. Ziv summarises this traditional training method by saying that "medical training must at some point use live patients to hone the skills of health professionals", but that "patients have the right to receive the best care that can be reasonably provided ... harm to patients as a by-product of training or lack of experience is justified only after maximising approaches that do not put patients at risk" [74].

The performance of surgery by newly qualified surgeons raises various other issues. By basing the training of students on exposure to real patients exhibiting the (potentially rare) required symptoms, the quality of training relies strongly on the competence of the trainer in the relevant procedure [62]. Students therefore do not often receive the opportunity to 'see one' or 'do one', leading to a long training period until the required number of observed or performed procedures is reached [75]. Patients are becoming increasingly concerned that students and residents are 'practicing' on them, and medicolegal pressure is mounting for hospitals to show that all efforts are made to place patient safety as the priority, or be held accountable for the consequences [60, 68, 76, 77].

The figures released by Kohn *et al* have caused the effectiveness of preoperative planning and surgical student training methods to be investigated, and given rise to the development of new teaching and planning methods. The main objective of the new methods is to remove the risk to live patients caused by the direct involvement of trainee surgeons in their treatment, and insufficient preoperative planning and communication.

With the advent of new surgical procedures comes the requirement for increasingly complex skills, in potentially higher risk situations. Surgery in the sinuses (and other areas, such as the abdomen) typically employs MIS procedures, using endoscopic techniques. This type of procedure requires the surgeon to view the surgery on a monitor, while using both hands simultaneously to position the endoscopic camera and perform the surgical tasks. MIS has been shown to dramatically reduce morbidity, recovery times and cosmetic detriment [78, 79] however the surgeon's access to the anatomy is inherently limited, affecting not only the procedures to be performed, but the physical skills required of the surgeon, and the ease with which these skills may be taught and acquired [80-83].

Typically, the view of the anatomy is distorted by the use of a wide-angle lens on the endoscope [84]. The surgeon must therefore learn psychomotor skills that are not required in conventional open surgery and develop sensitivity to new types of tactile feedback with hands-on experience [85-87]. The lack of depth perception available by viewing the procedure through a 2D video image (on the monitor) handicaps the surgeon further [88] and the translation of the 2D information into the 3D working environment demands considerable time and dedication to overcome the differences between MIS and conventional open surgery [89, 90]. The combination of these issues can lead to a significant learning curve and longer operating times during the student's training, adding to the risk to patient wellbeing [91]. This learning curve not only applies to the surgeon performing the procedure, but the multi-disciplinary support team responsible for a range of factors involved with the care of the patient [92].

Some authors maintain that in cases such as this, where difficult new skills must be learned, proper training of the technique could prove to be important in the widespread implementation of the procedure, and that surgeons should familiarise themselves with the basic principles of the technique in the surgical skills laboratory on a realistic model [93].

Munz and Almoudaris describe the difficulties in training such techniques in the traditional manner: "Teaching these novel skills was even more difficult because it appeared to be almost impossible to acquire those skills from merely seeing a procedure" [94].

For the reasons described above, new training methods that reduce the involvement of live patients in the training of new surgeons until they can be proven to be skilled and knowledgeable enough, by thorough and comparative assessment, to operate in a real-life situation are being developed. Simulatory operations are often now the preferred means of training students, rather than allowing them to hone their skills on real-life cases, as errors made in the simulated, non-threatening environment may be treated as a learning experience, do not have clinical consequences and do not result in morbidity or mortality [95, 96].

4.2 Surgery Simulation and Preoperative Planning Models

Gaba defines simulation as "a technique – not a technology – to replace or amplify real experiences with guided experiences that evoke or replicate substantial aspects of the real world in a fully interactive manner" [97]. Krummel adds that "there must be sufficient realism to suspend the belief of the participant" [98]. Simulation can be used to effectively and safely expose students to rare diseases, near misses and crises outside of the operating room, that would otherwise be impossible or dangerous to experience firsthand, while they are mentally prepared for such situations [2, 74, 99, 100].

Importantly, compared to traditional training methods, simulation may legitimately place the participant's education as the priority [64]. The students may then make the necessary adjustments to their performance through additional training. Ericsson cites

the preparation of surgeons for their first surgical procedure with an actual patient as probably the most important use of simulation [83] and observed that training students in the traditional apprentice-based manner does not ensure good performance, but instead that "superior performance requires ... representations for the execution, monitoring, planning and analyses of performance" [65].

In order to reduce the involvement of live patients in the training of surgical students, simulatory training methods have been developed which may be constructed to develop skills in a certain discipline, or based upon the actual anatomical data of a patient [84]. Surgical simulation is still not used as standard as a means of training surgical students, however Gaba argues that "no industry in which human lives depend on skilled performance has waited for unequivocal proof of the benefits of simulation before embracing it" [101].

The developing training and planning methods described in this section rely mainly on the use of 3D models, whether physical or virtual, natural or man-made. The man-made models discussed here may not only be used for the training of studying surgeons, but in 'real-life' applications such as surgery planning, prosthesis fabrication, radiation therapy planning and volumetric assessment, along with use as a communication aid to the patient.

An early reported use of a 3D model for use as a planning aid in surgery was in 1995, where a solid model of the patient's anatomy was used to assist in the preparation for a skull defect graft [102]. The representation of organs and surgical procedures in three dimensions is described by Creehan and Bidanda as "crucial to the present medical field"; with the following benefits outlined for the use of 3D models in medical industries:

- Quantitative morphological description of the patient's anatomy
- Pre-operative planning and simulation of surgical models
- Biomechanical modelling of joints
- Use in conjunction with computer-assisted surgery
- Development of a knowledge base

- Manufacture of precise physical models and implants [15]

Klein says that the general concept of surgical training is that "the experiential facets of medicine, especially procedural techniques, are non-cognitive and thus cannot be taught in a classroom but have to be learned at the bedside" [57]. This concept gives reasoning to the traditional training of surgical students by involving them with live cases from a very early stage. Now, this concept is manifested in the common usage of simulation in surgical training, with the aim of increasing patient safety.

Aggarwal and Cheshire suggest that objective measurement by a simulator could be used as a valuable tool in assessing students' performance in preparation for work in the operating theatre with real cases, as opposed to the subjective measurement provided by experts or examiners. As suggested in Section 4.1, there is no guarantee that surgeons educated in the traditional manner have obtained the skills required to perform surgery safely. The role of surgical simulators is therefore also expanding to encompass not only the education of trainees, but the assessment and assurance of clinical competence of other surgeons [64].

Many studies have been conducted into the requirement for and effectiveness of surgical simulation models (and the use of simulations in many other fields). The use and design of such surgical training and preoperative planning models are summarised in this section, to analyse the effectiveness of this training method and the opportunities to improve upon the existing procedures.

Surgical training and preoperative planning simulation models fall into two distinct groups: organic and inorganic [95]. Traditionally, organic models such as human or animal cadavers and organs have been used to train medical and surgical students.

4.2.1 Organic Surgery Simulation

Organic models may take the form of, for example organs from donors, living animals, and animal or human cadavers. The latter are often used as cadaveric surgery may provide training not only in the operation being performed, but "can provide the added dimension of learning surgical anatomy at the same time" [103].

Human cadavers have been used for hundreds of years as a means of teaching and training surgical procedures. A limit has also recently been placed on the number of hours that surgical residents are permitted to work, citing tiredness as a cause of errors. As a result, the time allotted to the study of anatomy in medical schools has been reduced. Many disagree with these legislations, which are believed to provide graduating students with less comprehensive knowledge, and experience and understanding of anatomy, pathology and their treatment [3, 104].

There are a range of issues which arise from the use of cadavers in surgical training, which in many cases exist in both the human medicine and veterinary fields. In order to give students the best chance of transferring skills from the training procedures they have performed to real-life situations, their training must mimic these situations as closely as possible. It therefore follows that the more realistic the training exercises are, the more successfully the student will transfer their knowledge to the real world. When considering the benefit of the training being undertaken, the likeness of cadaveric sample physical properties and operating and behavioural characteristics to those of living tissue is often called into question.

Rigor mortis is one such problem with the use of cadavers for surgical training, as after time, the difference between the tissue and organs being operated on to those in a living patient can become substantial enough to cause the exercise to be of no worth to the student, as exemplified by the work of Nebot-Cegarra and Macarulla-Sanz. In their paper studying new approaches to laparoscopic training, rigor mortis was concluded to be a limiting factor when attempting to simulate the creation of the pneumoperitoneum (the injection of gas into the peritoneal cavity as a diagnostic or therapeutic measure) [105]. Organs and other body parts retain their shape, however the stiffness and tactile feedback obtained from manipulation of the body differs from that of a live patient [106].

Furthermore, the use of cadavers does not allow the simulation of specific pathologic situations or anatomic variations; training must be based around available samples, which can lead to lengthy and potentially unfulfilling training programs, as described earlier in Section 4.1.

In organic training, realistic surgery commonly requires a blood flow to be present, often leading to the use of live animals for some surgical training procedures. Wolfe considers the use of animals in surgical training to be "essential", especially for the teaching of dissection [107]. The issue of representing bleeding and blood-filled areas of the body to provide realistic, situational training can be addressed by introducing an extracorporeal pump and 'blood' supply. In 2005, Emad Aboud of the Swaida National Hospital, Syria, developed a method in which the use of live animals for human surgery simulation for the above reason could be avoided, by connecting the blood vessels of the cadaver to a pump which would circulate coloured liquids throughout the system. This development successfully removed the need to use live animals in both human medicine and veterinary surgical training [108]. The use of animals can achieve a level of physical and emotional realism; students have been known to become extremely distressed at the death of the animal subject [71].

One of the most substantial issues surrounding surgery simulation using cadavers is ethics. Since the latest update to the Human Tissue Act came into enforcement in the United Kingdom in September 2006, the training of students using cadavers has recently begun to reduce and consent is required for the use of human tissue for research, transplants, education and training; cadavers may no longer simply be used as they become available. Before using the body of a newly deceased patient for training, the use of the body, type of training that will be performed, visible and physical effects of this training on the body and views of the patient's family, surgeons, residents or students must all be taken into consideration. Jones *et al* state that "It would be difficult to argue against the practice on the basis of the rights of the newly dead patient, inasmuch as the rights of patients expire when they expire ... Autonomy attaches to living persons, not cadavers" [109]. Therefore, as in the cases of autopsy and organ donation, it is common practice to pass responsibility onto those surviving the dead patient. If consent is not obtainable from the deceased, persons of an appropriate relationship may decide on the use of the tissue and organs.

The traditional educational practice of using dissection of cadavers to allow students to observe pathological conditions, anatomical abnormalities and variations that may

be present in future cases is therefore affected by the Human Tissue Act, and the regulations on the use of organs that it enforces [104].

There is a risk of infection to those using cadavers for surgical training [110]. As such, precautionary measures must be taken, which could potentially limit the effectiveness of the learning process. The availability of cadavers is also reducing, which, along with high costs for their acquisition and the educational and ethical issues discussed earlier, have caused this technique to be undesirable, and others to be sought out [87, 111].

The inorganic, man-made models being developed to simulate surgery in a safe and often repeatable environment are described in the next section.

4.2.2 Inorganic Surgery Simulation

One of the main advantages of the use of inorganic simulation models over live patients and cadavers is the possibility to physically or visually represent live patient anatomy for surgery simulation, patient communication, preoperative planning and training of students on interesting or challenging cases. Operations on these cases may be repeated as many times as is necessary through reproduction of the model, allowing comprehensive training on the same case to acquire or develop a specific skill, build experience or assess the suitability of various operative methods.

In the traditional method of diagnosis and assessment of problems, surgeons and physicians most commonly study the 2D images produced by X-ray, MRI or CT, (described in Chapter 2.2) to comprehend the patient's internal anatomy and the problems being experienced. When using this method, the surgeon must be responsible for mentally reconstructing the 2D slice images into the 3D form they describe, with no real concept of the relative size of the anatomy until the operation is performed [112]. This conceptualisation of the form of a 3D object through the study of a range of thin, 2D slices is a difficult task for a human to perform [113], and may lead to uncertainty in the mind of the surgeon, and consequently errors during surgery. According to Wei and Lal, "the loss of the third dimension is an inherent

problem with examining sectioned material when the tissue to be examined possesses a complex morphology" [16].

The sufficient interpretation of patient anatomy by studying a 2D slice image may be complicated by the presence of bone fragments or debris around the ROI or deformity of the area. However, if combined with the rest of the range of 2D slice images into a 3D virtual or physical model, the user may view the anatomy from any angle and bone fragments may be distinguished from the area on which the surgeon will operate (see Figure 14), giving a more accurate impression of the level of deformity: "even though the 3D models were derived from the same data as 2D images, 3D models display anatomical relationships in an extra dimension to enhance the quality of visual information and model utility compared to 2D images" [114].

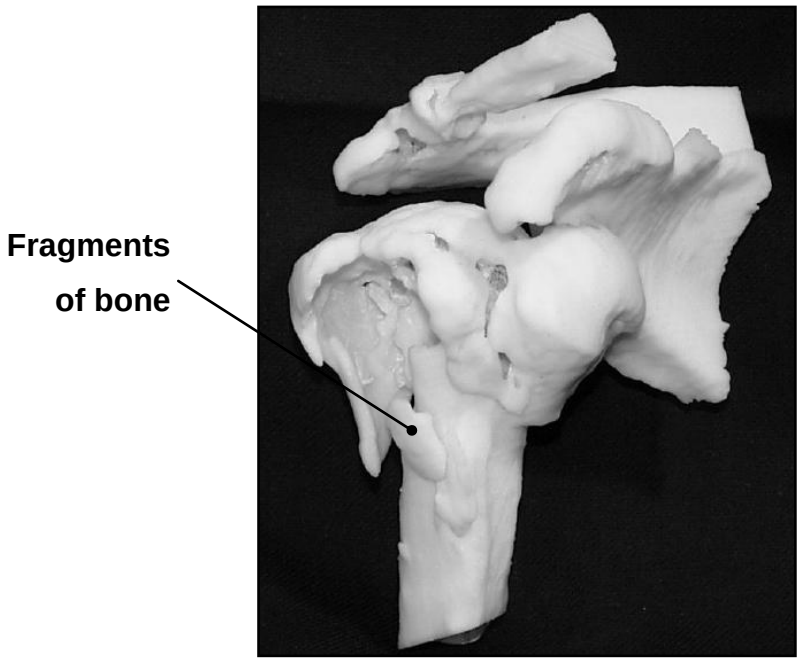

Figure 14: Shoulder model, showing fragments of bone [115]

The proper analysis of the problems to be addressed for a particular patient, and the manner in which this will be done is a vital stage in the treatment process. The increased focus on patient safety and the effect of good training on the performance of doctors and surgeons described earlier have meant that the knowledge of the exact procedures that will be performed during surgery must be very detailed, if the risk to the patient is to be fully reduced. Litigation could also be incurred if surgery is

performed with any uncertainty in mind, as may be experienced with the traditional method of studying X-ray, MRI or CT slice images only [115]. It is therefore becoming more common for medical and surgical staff to use, or require 3D representations of the patient's anatomy in the area of interest in order to safely and correctly assess the situation "at a glance" [17, 116]. Recently, these 3D representations of patient anatomy have also been used to create simulations of patient anatomy for surgical training.

4.2.2.1 VR Surgery Simulation

Coleman defines VR as a "computer-generated representation of an environment that allows sensory interaction, thus giving the impression of actually being present" [117]. Munz *et al* expand: "the rationale behind the use of [VR] simulators for training is not to exactly replicate real life but rather to provide an alternative environment that will allow users to use the same skills as in real life for training and shortening of the learning curve" [94].

VR has been used extensively and for many years in many different areas, for example in the fields of defence and aviation, for the training of combat soldiers and aeroplane pilots. The United States Department of Defence discovered that of the combat soldiers who survive their first 10 combat experiences, 95% of those will survive any further encounter. They used this knowledge in conjunction with VR simulators to train combat soldiers and in particular, to simulate those first ten combat experiences; critically, these were performed in a non-lethal environment [98].

In aviation simulations, pilots have for decades been routinely subjected to the 'worst case scenario' in order to be fully prepared in the event of an emergency in real-life [118]. The most common means of training is the flight simulator, which completely immerses the trainee in the realistic environment of the cockpit (Figure 15).

Figure 15: Airbus A380 VR simulator [119]

The simulations allow the crew to gain experience of situations that would otherwise have been too expensive, dangerous, difficult or even impossible to acquire [58]. Again, the main advantage and reasoning behind training pilots in this way is to avoid any risk to the trainee or anyone involved in the training. This method of training is expected of a pilot in control of a commercial flight by the passengers; however this expectation is not commonly held of surgeons in the field of medical training [57]. Ayache *et al* put forward that surgery simulation should become as common for surgeons as flight simulators for pilots [84].

Simulation of medical procedures is more complex to achieve than in the mechanical, physical, measurable environment of aviation, as anatomical features may be stretched, cauterised and cut, leading to an infinite number of consequences [120]. The dynamic behaviour and complex shapes of the patient's anatomy make any simulation extremely difficult to produce and run smoothly [58]. VR surgery simulators are, however, used extensively today as training and pre-operative planning tools [99] and rely on the creation of a rich and realistic experience, to be accepted by the operator as cognitively valid [78]. Simulators have had previous success in some areas of medicine including anaesthesia, intensive care and

endoscopy. Recently they have begun to be applied to the performance of surgical procedures, in order to allow trainees to co-ordinate the use of instruments, practice teamwork, and trial new instruments with no harm to live patients [1, 121]; particular use has been made in the training of laparoscopic (endoscopic surgery in the abdominal and pelvic cavities) techniques [122].

Neubauer *et al* identify preoperative planning as a key application of VR simulator training systems. In the area addressed by their paper, the authors state that the planning process is "enhanced by additionally using simulated 3D views as provided by virtual endoscopy" [123]. By studying the virtual representation of the patient to be operated upon, the surgeon may plan the exact actions that they will perform in actual surgery, observe the progress of the procedure from different angles, as well as being able to render some surfaces semitransparent in order to plan paths and openings to avoid vital areas. This clearly means that by being able to more thoroughly plan the actions to be taken in the real surgical procedure and practice these on the simulator, the surgeon can ensure that less risk is placed on the wellbeing of their patient than if preoperative planning were performed in the traditional manner.

In surgical training using VR, the physical experience of a surgical procedure, as felt through the surgeon's instruments may be replicated with the use of a haptic device. Haptic devices give the user intricate control over the virtually represented version of their tool onscreen, whilst also providing physical 'force feedback' through the device being held, as shown in Figure 16. Many consider this to provide the user with a realistic experience that, importantly, will not differ greatly from the sights and sensations involved in real-life surgery [124].

Figure 16: VOXEL-MAN VR and haptic surgery simulator system [125]

It has been found in studies on the effectiveness of haptic VR surgical training that students react well to exposure to the haptic device and transfer the skills obtained with the VR and haptic equipment to live surgery [94, 126, 127]. Inexperienced students trained by VR are also commonly shown to perform more homogeneously than those trained in the traditional manner [128]. Exceptions are most often due to students who require a longer amount of time to familiarise themselves with the VR interface.

The learning curve of students using VR training equipment has been studied in-depth, through the use of automatic objective assessment by the equipment itself. The equipment has been found to accurately distinguish between the varying experience levels of the participants, and that the learning curve of new surgeons could be followed and analysed. Again, the aim of introducing this style of teaching at such an early stage in the student's training is to remove the need for the involvement of live patients, typically 10 to 30 in traditional training programmes [129].

Kinematic data may be obtained using motion analysis of the physical tools, to determine operative movement efficiency and give students detailed and, importantly,

objective feedback to closely monitor their improvement [130]. Neequaye *et al* describe VR training as "a useful tool enabling objective demonstration of improved skills performance both in simulated performance and in subsequent in-vivo performance" [131].

This approach can facilitate the education and improvement of students' skills with additional formative and summative feedback from their supervisor. The trainee may be mentored through the case being simulated, stopping as necessary to discuss progress or to explain parts of the procedure. Alternatively training may be performed alone, as the automatic measurement of performance inherently removes the need for experienced surgeons to be present, and allows the training to be performed at any time [132]. The data provided by the equipment can also be used to create solid benchmarks of performance for advancement into the next stages of training. This, in turn, will provide insurance that students who pass through this training have reached the pre-requisite levels of skill before they are permitted to deal with live patients [70]. This ability to measure performance over a wide range of parameters, and the subsequent delivery of objective feedback is considered to have significant implications for the future assessment of dexterity and hand-eye co-ordination [86, 94].

However, some research has demonstrated the opposite results to those reported above. For example, Ahlberg *et al* showed that after a short period of training on the MIST-VR simulator to perform a laparoscopic appendectomy, the students who used the simulator had not improved significantly in skill level [118]. It has also been suggested that time must be allowed for the user to adapt to the virtual environment and successfully interface with the computer [129]. This may delay any improvements experienced by the student from using the training equipment.

The costs associated with VR equipment are significant [100] and other problems arise from the use of a virtual, computer generated model as opposed to a physical representation of the anatomy. Due to the use of the image-stacked 3D model as a virtual simulation of the ROI on a computer monitor, some users may experience difficulty in the viewing of the part on-screen, as the orientation of the model may be

ambiguous due to rotation, gaps in the surfaces and lighting anomalies. Some difficulty may also be experienced in the use of the software to manipulate the model and visualise the procedures to be performed, if the users are not skilled in the use of the software [115].

The quality of the simulation is also dependent on the performance of the hardware and software used to display the model. Real-time simulation of actions and movements is "essential" to the experience and progression of the student [133], however some models are forced to exhibit reduced realism to allow smoother animation and immediate reaction to operative procedures, including simplified anatomical geometry, surface details and reduced haptic feedback [80, 84, 120]. As VR can be said to rely on "immersion, navigation and interaction" to function as a beneficial training tool [134], such reductions in quality are unacceptable.

Some VR models have been found to allow impossible or dangerous operative techniques (for example, over-sized drills allowed to enter smaller holes in anatomy) noticeable by experienced surgeons, but which may result in incorrect techniques being learned and applied by trainee surgeons who may have no means of comparison with real situations [66, 125].

By displaying virtual open surgery on a flat screen, the model also becomes pseudo-3D, often known as 'two-and-a-half-dimensional' (2½D), leaving it difficult for the user to determine scale, distance and the relationships between structures in the anatomy of the virtual patient [135]. The representation of a 3D volume on a 2D monitor may not provide the information required to understand the 3D geometry of the part [15]. This is less of an issue when endoscopic surgery is being simulated, which itself involves the use of a 2D screen to view the concealed operational procedure.

When studying the learning outcomes of dissection of human cadavers, Lempp found that students identified a wide range of positive outcomes of the investigative work, most of which could not be replicated by a VR simulator. Students stated that their preparation for clinical work was developed, and that they experienced a clear

integration of theory and practice through the application and improvement of their practical skills. The students also listed respect for, and familiarisation with the body as two of the major learning outcomes of their work; it was put forward that it would be impossible to represent the same emotional effect of operating on a human form in a virtual environment, as the user would be continuously aware that the subject was not real [136].

The use of cadavers is, however, as described in Section 4.2.1, restricted and provides little physical similarity to live patients. A key disadvantage of the use of cadavers in training and preoperative planning exercises is the inability to simulate live cases. Virtual surgery simulation may provide a visually realistic scenario, but lacks the realism that students require to emotionally prepare themselves for surgery on live patients. These issues with cadaveric and virtual training and preparation may be overcome by the production of a physical model of the patient's anatomy in the ROI. The surgeon, surgical team and patient themselves may then view, analyse and use the model for preoperative surgical planning and training. For these reasons, significant research is being performed into the production of physical models for surgical training and pre-operative planning, and into the combination of medical technologies with engineering approaches such as AM.

4.2.2.2 Physical Surgery Simulation

A commonly used method in the training of endoscopic techniques is the box trainer, where tasks are performed using inanimate objects within a closed box to develop dexterity, while viewing the procedure on a monitor as in surgery (Figure 17). Tasks include the use of a pegboard, where pegs must be transferred from one side of the board to the other; the tying of knots in lengths of rope or string; the stacking of discs around a thin pole and suturing through a medical glove [137]. In some cases, animal or cadaveric samples may be involved in the procedure [99].

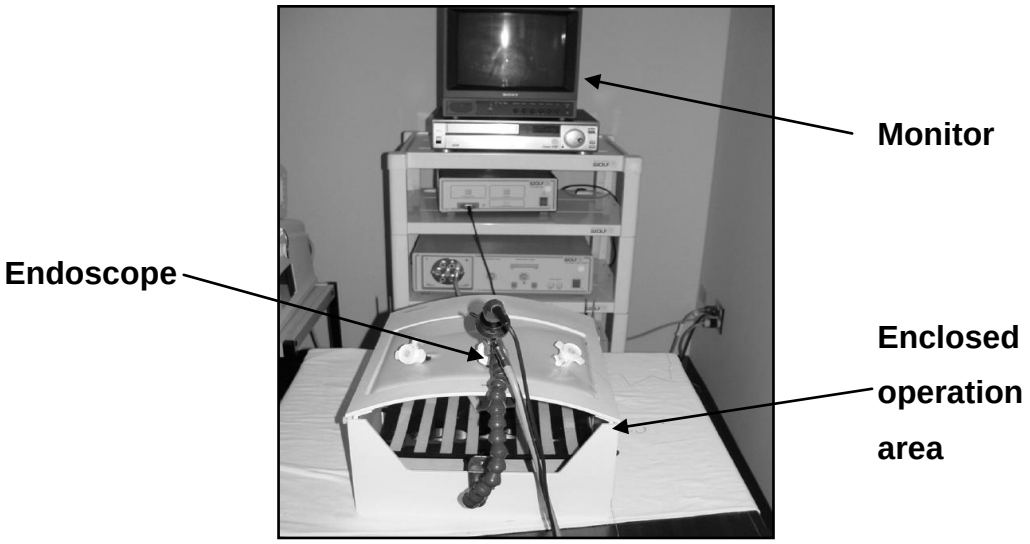

Figure 17: Laparoscopic Training Simulator (LTS) 2000 physical reality simulator [100]

The simulation of surgical procedures relies upon the suspension of belief of the surgeons involved, as stated earlier. For this to be the case, an accurate physical representation of the exterior form of the patient is often required. This may be achieved through the acquisition of a mould of the patient's anatomy and subsequent production using appropriate materials to represent tissue or flesh, which is then used as the exterior of the box trainer.

The box trainer is considered invaluable, however it cannot provide the proper education or advancement of residents to more complex procedures [88]. Although the importance of dexterity in the performance of MIS is perhaps higher than the 25% suggested by Spencer, the experiential aspect of this training method is obviously lower than the performance of actual surgery. Other inorganic physical training methods are designed to both achieve improvement in dexterity skills and add to the realistic experience of the surgeon, allowing them to progress along the learning curve defined earlier.

The main aims of the physical model may be described as simplifying an otherwise complex procedure, reducing risk to the patient, reducing costs involved with training and planning surgical procedures and easing the understanding of potentially extremely complex geometry that is in the ROI in a completely non-invasive manner [112]. By creating a physical model instead of relying on the traditional use of

cadaveric samples, specific (or current) cases may be created or replicated repeatedly for training purposes when needed.

In most cases, the representation of the interior anatomy of the patient is the most important feature of the training or surgical planning model. Accurate representation of this anatomy may be achieved through the direct use of medical imaging techniques such as MRI and CT, as described in Section 2.2 and the manufacturing methods described in Section 2.4. AM processes share an inherent similarity with the slice format of medical imaging techniques, and work has therefore recently been performed involving the production of AM surgical training and preoperative planning simulation models. The production of a physical part to represent the anatomy shown in the 2D slice images from MRI and CT (sometimes known as a biomodel) can offer a wide range of possibilities to the surgeon. The model will provide the surgeon with an immediate, intuitive and user-friendly understanding of the problems being exhibited by the patient [138].

AM processes may be used indirectly to produce moulds for parts constructed from a more flexible, lifelike material. In 1999, Lermusiaux *et al* presented their work on the production of moulds for the subsequent manufacture of abdominal aortic aneurysms for the testing, design and selection of stent grafts for live patients. SLA was used to produce a casting mould for silicone rubber to be formed into the shape of the aneurysm of a living patient, with data acquired from a CT scan. They state in their report that "rapid prototyping can be considered a new imaging technique in medicine" [139].

Alternatively, AM processes may be used to produce the biomodel itself. Figure 14 shows a shoulder joint biomodel for planning of surgical procedures; the surgeon may inspect the model from all angles to gain a thorough understanding of the problems that may be experienced during surgery and the best approach to resolving the issue. The surgical procedures to be performed on the live patient may also be physically rehearsed on the exact model of the ROI before surgery begins, if implanted into a representation of the body. The model will be produced to very closely mimic the

qualities and properties of the human form, effectively replacing the human form for the practice of surgery [140].

This "much needed dry run of the surgical procedure" [141] provides more tactile feedback to the surgeons than if a virtual model were used, which may be transferred directly to the performance of the procedure in a real situation. This new approach, switching from a purely visual to a visual/tactile means of representing the patient for diagnosis, planning and treatment is a new kind of interaction, known by some as 'touch to comprehend' [142]. By using models in this way, the needs and skills of both visual and tactile learners are taken into account [114].

D'Urso *et al* found in their study on the effectiveness of biomodels in the training of medical students that, when used in conjunction with medical images, the models improved the planning and diagnosis performed by the students. Operating time was also reduced, and informed consent levels were much higher when the model was used compared to the 2D images alone, due to improved communication between colleagues and patients [138]. AM models are commonly used in this way, to rehearse and assess the use of treatments without harm to the patient, followed by the creation of surgical guides to ensure the accurate transfer of the planned procedures to the patient during the real operation [143].

Physical models of the patient's anatomy allow enhanced communication in pre-operative planning and diagnosis amongst all involved, marking out of vital areas to avoid and possible entry points, and moulding of more successful, custom-fitted implants [116, 141]. Anatomical data may be viewed without causing discomfort to the patients themselves through extensive travel, by sending physical models of the ROI to all parties [135]. Physical models are also said to have "an enormous value as an educational teaching and patient information tool for obtaining the consent for surgery" [102]. This is essential as parties from many different disciplines may be involved with the operation, such as surgeons, imaging experts, materials scientists, engineers and the patient and their family [144], who may view a realistic representation of the anatomy that is more portable and easier to handle than a computer-generated model [145, 146]. 3D analysis of the problem and planning of the

procedure both before entering the theatre and during the operation can lead to shortened operating times and reduced complications arising from surgery [147, 148].

When used to provide a reference model to the surgeon during surgery, AM models may be used as a reminder of scale, or as a navigation aid [149]. It has been shown that AM models are well suited to use in the diagnosis and preoperative planning of skeleton-modifying operations [142]. AM technologies are ideal for the production of skeletal elements, as they are often morphologically complex and possess many canals and other structures that are only reproducible by layer manufacturing [150]. Potamianos *et al* described the use of an AM shoulder model before and during surgery as providing an "intuitive physical relationship between patient and model" and a "definitive interpretation of joint pathology", enabling the surgeon to perform a full assessment of the degree of injury before starting to operate [146].

SLA models have been used extensively as preoperative planning aids in the field of neurosurgery and cranio/maxillofacial reconstruction. The models were reported to provide better understanding of the anatomy to be operated upon, simulation of the surgical procedures to be performed, assistance in the accurate location of problem areas and lesions through their use during surgery, the possibility of producing custom-fitted implants or prostheses and improved methods of training and teaching trainees [151]. The possibility to colour a specific area of the SLA model allows surgeons to illustrate the presence and location of vital areas or problems, for example a brain tumour, with blood vessels and parts of the brain which may be at risk highlighted for visual assistance in planning the procedure. The transparency of SLA parts allows this volume of colour to be seen suspended within the model, allowing surgeons to plan procedures in three dimensions [152].

Physical surgical simulation has been used extensively in the training and preoperative planning of craniofacial and maxillofacial surgical procedures, as for these complex operations involving intricate and delicate structures, detailed preoperative planning is essential [17, 114, 153-155]. In these cases, 3D models are used to diagnose facial fractures and other problems such as impacted teeth. The

models may also be used to prepare equipment for the successful completion of the operation, such as reconstructive plates and joint prostheses [102].

Alternatively, the fit of prostheses or implants may be assessed, or casting moulds made for the production of custom-fitting implants [156]. This offers the advantage of potentially reducing the overall cost of patient treatment, as ill-fitting implants can cause the patient discomfort and may require replacement more frequently than custom-fitted designs [115]. Implants tailored to an individual patient provide a far better treatment than 'off the shelf' parts and, as a result reduce the patient's further involvement with the hospital, saving money, time and improving the quality of life for the patient [157].

In maxillofacial surgery and other similar areas, it is always important for surgeons to achieve the best possible cosmetic appearance for the patient; as such, any reduction in the level of complexity of the surgery, amount of invasive work to be done or the number of unknown problems to be overcome during surgery are welcomed. Gibson *et al* (2006) describe the case of a patient with a section of jawbone missing from one side of their face, which was to be reconstructed during a complex operation.

By comparing a physical model produced from a CT scan of the patient's skull with one showing the ideal result, produced by mirroring the unaffected side of the anatomy, an understanding was gained about the amount of work to be performed. The second model was used as a template for the preparation of the Titanium mesh that was then implanted into the patient to reconstruct the missing jawbone. This approach allowed the surgeon to make adjustments to the implant prior to surgery, reducing the potential complications in the operating room and ensuring a good result for the patient [154].

AM models of patient anatomies have been used effectively in recent cases of the separation of conjoined twins. The separation of conjoined twins is regarded as one of the most complex, intricate medical procedures that may be undertaken, potentially lasting days, requiring a team of surgeons, nurses, anaesthesiologists and care givers. With such a large number of people directly involved in the success of the operation,

communication is vital. Physical models of the way in which the patients are joined and which elements of the anatomy are shared form a vital part of the preoperative planning and surgical simulation/rehearsal process, and may be used during the operation as reference tools.

It is possible to use the colour capabilities and translucent properties of SLA to show the severely abnormal anatomy precisely, in order for surgeons to better understand the intricate anatomical relationships that exist between the patients. 3D printed models may be used to show external detail clearly in full colour, and have also been used to create full bodies of conjoined twins to assist in surgery rehearsal and the production of custom operating tables for use in the real surgical procedure. AM models may aid in diagnosis by showing the growth of twins through sequential models [135].

Often, it is required for the surgical training models to give realistic physical feedback when used for surgical simulation, as the surgeon cuts into the model in the same way as in the final operation [153]. Physical training models offer significant advantages over the use of virtual models in terms of the force feedback experienced through the surgical instruments. Reduced costs are accrued, and the instruments being used by the trainee may be left unaltered, enhancing the realism of the user's experience [158].

This can be done by producing the model from a material similar in physical properties to that of the material it represents; the use of SLS-manufactured surgical simulation parts is described by Suzuki *et al* in their study on the training of surgeons in the field of ear surgery. They state that the skills of ear surgery are most effectively learnt and developed through the dissection of the temporal bone, however few students may practice this technique traditionally through the dissection of real bones, due to the scarcity of samples. The SLS model was found to possess similar properties of hardness to real bone, and the surface structures were accurately reproduced for simulation of the procedure with real, unaltered surgical instruments [159].

This type of training, where the physical model not only provides a realistic visual and tactile experience for the users, but offers the same physical properties as the

anatomy of the live patient for the planning or practicing of surgery, could be considered invaluable for the training of surgeons in complex, intricate procedures in the future [93].

AM models may be produced in any size to assist students who are unfamiliar with certain aspects of surgery. Through the modelling of micro-scale structures, perhaps from data acquired through µ-CT (see Section 2.2.3), information on the interior structure of trabecular bones may be clearly visualised by scaling the model as required [160].

It has been shown that the use of AM models for surgical planning and simulation can also: facilitate the diagnosis of the situation; allow the prediction and solution of potential problems prior to operation; make the production of custom-fitting implants or transplants far more accurate and time-effective; provide the surgeon with an immediate and intuitive understanding of the patient's anatomy; permit the selection of the correct approach to surgery through easier discussion with peers and subsequently reduce operation time [17, 114, 140, 141, 151, 155].

AM surgical simulation models may be reproduced for practice of the procedure many times, to assess the suitability of a range of approaches [112], or to teach procedures to student surgeons over a period of repeated practice, in a way that feels physically real [161]. In this way, the surgeon can ensure the success of the operation if the optimal technique is selected, reducing operation time and the risk of the procedure for the patient [153].

It is thought that in the future, full procedure simulation, fully immersing the student in a realistic environment to develop and refine skills but where errors can be made without consequence, will "bridge the gap to the operating room" [99]. Lieu *et al* state that there is no substitute for the practice of a complex surgical procedure on a reasonably precise model to educate inexperienced surgeons, or to determine the course of action in the live operation [112]. Gaba and Okuda *et al* conclude: "the future of simulation in healthcare depends on the commitment and ingenuity of the

healthcare simulation community to see that improved patient safety using this tool becomes a reality" [97]; "simulation in medical training is here to stay" [76].

4.3 Simulation for Sinus Surgery

It is the wide range of physical characteristics in the paranasal sinuses, unique to every human, which presents the difficulty in accurately simulating sinus surgery for student training, preoperative planning or intraoperative reference. Another major factor which increases the difficulty in simulating the paranasal sinuses is the geometric complexity of the region, making it practically impossible to manufacture parts using conventional techniques to replicate the shapes and anatomical features accurately enough for the purpose [48]. The tactile experience that the surgeon has during surgery cannot easily be replicated with common manufacturing materials and as such, man-made physical sinus surgery training models have not been developed as fully as in other fields such as cranio-facial surgery, as discussed earlier.

The most regular course of training for a sinus surgeon still remains the use and study of cadavers and MRI or CT scan images, as described in Section 4.1, or the use of box trainers, as described in Section 4.2.2.2. Once a student has performed a pre-requisite number of procedures or is considered to have reached a required level of performance upon cadaveric samples, they may progress onto the treatment of live patients in order to gain actual clinical experience, under the supervision of an experienced physician. This method of training puts the patient at great risk, due to the complexity of the procedures being performed.

As stated earlier, the use of cadavers for surgical training gives rise to a range of difficulties and disadvantages over inorganic physical training methods and models. These include the acquisition of samples, ethical issues and whether the physical condition of the cadaveric samples replicates that of a live patient. Furthermore, it is clear that when using cadavers, the case of a live patient may not be reproduced for repeated training, diagnosis, patient communication, preoperative planning, surgery rehearsal or intraoperative support. In order to ensure that surgical students receive full and effective training in the performance of sinal surgery procedures, simulation must be used.

VR training methods have been developed for use in the training of student sinus surgeons over the last decade [46, 132]. In these systems, repeatable, safe surgery may be performed which mimics the situations and experiences of performing an endonasal procedure. In their study "A virtual training system in endoscopic sinus surgery", Pößneck *et al* set out to study the effectiveness of their endoscopic sinus surgery VR simulator. They were prompted to study the possibility of training students in this way by the high risks to patient safety involved in the procedure, particularly concerning the proximity of work to the orbita and skull base, along with the costs associated with training students in the traditional manner using human cadavers and anatomical studies. Although the procedure is extremely high risk, it is carried out on a daily basis by otolaryngology surgeons and, for example, approximately 600 times at the University of Leipzig in 2005 [162].

A virtual model of a patient's paranasal sinuses was produced using the KisMo© system which allows deformable objects to be modelled digitally. Using this software, every point on the model may be supplied with physical characteristics concerning elasticity, stiffness and relation to one another. Original in-vivo captured images were used to texture map the inner nose and other features in the model. These images were then allowed to be realistically affected by the virtual camera, for example by reflecting some light (Figure 18), or becoming partially transparent.

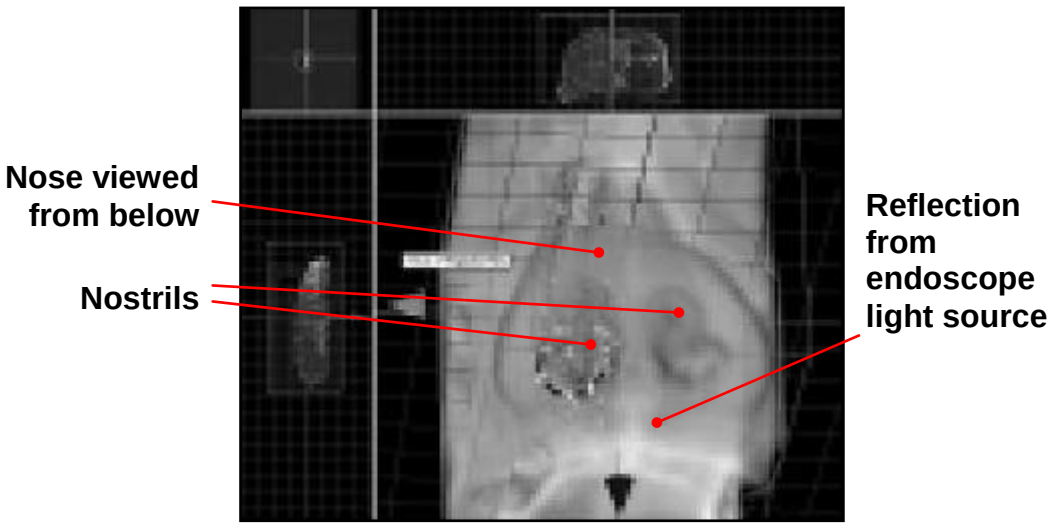

Figure 18: "Model of the nasal cavity integrated in segmented MRI dataset" [162]

The realism of the system was scored on average 4 out of 5, showing that the system was well accepted by the users, but that some aspect of reality was not yet totally represented. Users' performance was shown to improve with each training procedure performed on the simulator. Also highlighted was the importance of the haptic interface to replicate the tactile experience of performing the procedures [162].

The impact of training surgical residents with VR simulators has been investigated, showing in the vast majority of cases that the surgical simulator equipment provides the students with the skills and experience needed to perform to the required level in the operating room. Students that are trained using the simulator are commonly found to have a higher level of skill in the performance of advanced surgical procedures in the sinus region than those who did not use the equipment [163]. The devices have been shown to be valid for training junior otolaryngology residents and avoid the involvement of patients or cadavers in this process.

By training the treatment of real cases, using the medical imaging data of actual patients to produce training models, the severe complications that occur frequently during surgery due to the complex and variable anatomy and proximity to vital structures and organs may be replicated and overcome in a safe and repeatable environment [46]. This adds to the experience that a student surgeon accumulates before performing their first operation on a live patient.

However, some reservations remain about the ability of virtual simulations to replicate the physical and visual limitations, and emotional experience of performing sinus surgery. Difficulties can arise from the ability of the users to adapt to the interface with the simulator, potentially requiring time to become accustomed to its use, unlike a physical training aid. It may take experienced users a similar amount of time to become accomplished in the orientation and re-sizing of the object on-screen as it does inexperienced surgeons, as described by the work of Grantcharov *et al* in Section 4.2.2.1.

In most cases, the sense of touch is essential to provide a realistic interaction between the model and the surgeon, and allows them to "simultaneously explore and interact"

with their environment [125]. This physical feedback is essential for the surgeons involved to gain a full and intuitive understanding of the case. Some criticism of the haptic approach to physical feedback in VR simulations was described in Section 4.2.2.1.

A physical simulation may be able to avoid the shortcomings of VR, providing the physical characteristics, limitations and essence of realism required for students to effectively train for sinus surgery, and for surgeons to plan and communicate surgical procedures. The only physical models that have been typically produced displaying the anatomy of the sinuses are purely designed for observation or reference. The models are 'off-the-shelf' moulded items, not produced to represent the anatomy of a specific patient for use in that case, and are too expensive to consider operating on for practice or rehearsal of techniques [48]. The geometrical accuracy of these models is also questionable, due to the use of casting and impression-and-mould techniques to produce the shapes involved. Any complex geometry has to be removed, as the mould itself would need to be extremely complex to produce the required anatomical geometry, and the parts produced would be fragile and risk damage on removal from the mould. By producing the models from one material, no tactile feedback or education is available from the various areas represented.

Figure 19 shows a typical physical model used in the education and simulation of sinus anatomy. The model was produced from CT scan data from a cadaver head, but can be seen to be presented in thick slices, manufactured from the same rubber material throughout. However, the slices used are too thick to gain any advanced understanding of the geometry and interrelationship of the sinuses or observe the intricate, complex and individually unique anatomical geometry that exists in the area, due to the casting and moulding techniques used to manufacture the model. The face, septum, maxillary sinuses, ethmoid cells and sphenoid sinuses are represented in the model, shown respectively in Figure 19 from left to right.

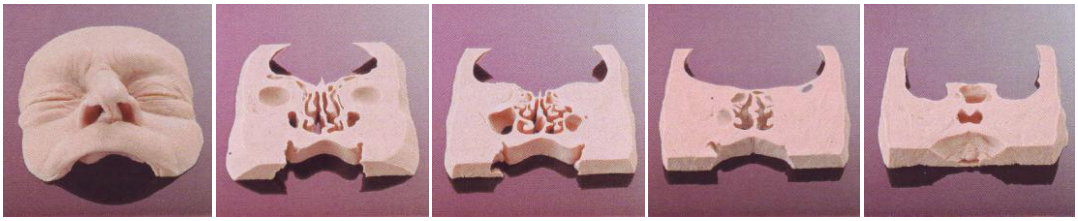

Figure 19: Rubber cast training model of sinuses [7]

In 1992, McDonnell *et al* produced a teaching model to communicate the shape of the maxillary sinus from stone. This was done by injecting dental impression material into a cadaveric sample and dissecting the mould part out of the body. This shape was subsequently used to create a replica of the maxillary sinus cavity in stone, after a number of steps of impression and mould making [164].

Yamashita and colleagues have performed extensive work into the production of physical sinus training models, claiming to have constructed the world's first precise model of the human paranasal sinus [48]. The model allows student and practicing surgeons alike to use the model to learn and rehearse endoscopic sinus surgery in a more effective manner than through the usual use of cadaveric training programmes.

The model itself is comprised of a silicone exterior, manufactured to represent the external appearance and the surgeon's view of the patient during surgery. This also ensures that the same restrictions experienced in real surgery are replicated, such as the lack of mobility of instruments when placed in the nostril. The materials and structures produced are claimed to accurately replicate the tactile experiences of operating on a real human body through the representation of the shapes, colours, textures and varying levels of hardness present in the sinuses [110]. The bone structures present were created using data from CT scans and the assistance of a skilled surgeon to analyse and select the required data, before being manufactured by SLA to achieve the level of geometrical complexity that traditional manufacturing methods could not provide [48]. It was found that in order to reproduce the tactile responses of the live tissue present in the sinuses, the plastic used in the SLA process should be coated in resin. The exterior of the model is reusable, with a replaceable internal sinus structure allowing the user to practice operating on any case, any number of times.

The group have also defined a means of objectively measuring the performance of the student surgeons that use the model, by automatically measuring the forces applied to the model during practice procedures. The forces and torques used during surgery were measured using force sensors placed within the physical model at points of risk or importance to the progress of the operation. A link was formed between the physical force applied by the student through the operating tool to perform the task, and the quality of their work. By comparing the forces used by expert surgeons to those employed by students, a relationship between operative force and performance could be established. By then identifying any unnecessary or injurious force that the student used to perform the task, the student's work could be quantitatively measured and assessed, then compared to their performance in subsequent procedures or repeated tasks. This then leads to more effective and efficient training for the students, and less risk to the life and wellbeing of their future patients [165].

However, the model cannot truly be considered a "precise" representation of the sinus structures and operative experience. This is due to the appearance of the interior of the model and the subjective manner in which the forces needed to operate on the model were compared to real life.

In the creation of the 3D CAD model from stacked 2D medical imaging slices for Yamashita's training device, some areas of the model remained undefined or not adequately filled to produce a good representation of the anatomy. In most cases, this was due to the ability of the medical imaging system to define very thin areas of bone, down to a thickness of approximately 0.1mm in some places. As the resolution of most CT imaging systems is around 0.4mm, these features may not be defined as clearly as is necessary for the production of an accurate model. In order to complete the model, experienced surgeons or engineers were asked to manually draw the outline shape of the region on the CT scan image, before reconstructing the shape in CAD and thinning the section further to close to 0.1mm.

The appearance of the bony structures in the interior of the model may also be criticised for not accurately representing the appearance of living bone. In this model, the resin used to coat the plastic features may be coloured to represent the general

appearance of the interior walls of the paranasal sinuses. The surfaces of the structures in real life show the presence of blood vessels, and other important information to the surgeon, along with providing a realistic experience during training exercises. Development could be considered for the inclusion of surface images on the actual plastic structures to accurately represent the appearance of the interior walls of the sinus region.

When analysing the comparative strengths and forces required to operate upon the plastic anatomical structures, the group chose to do so through the involvement and questioning of surgeons in sensory tests. The surgeons were asked to perform common surgical procedures on the model, in order to assess the similarity between the physical characteristics of the plastic parts and living bone.

The group took a qualitative approach to the analysis of the physical properties of the plastic, relying on the assessment and perception of the model that the surgeons were able to detect and describe. This could be susceptible to human error, or a difference in the way in which two surgeons analyse the same model. By assessing the physical characteristics of the plastic structures in this subjective manner, there is no way that the group could ensure that the model exactly replicated the structures in a live patient. In order to avoid this, a more quantitative method should be devised for the measurement and comparison of the physical properties of the model, and of the living structures. This has been undertaken by the accompanying research project.

Lastly, the model presents no means of customising the anatomy to present cases specially designed for teaching or training purposes. Users must operate on the pre-defined pathology included in the model, with no means of creating a tailored teaching program for specific students or classes. This development is the most important of all, if students of sinus surgery are to be provided with the wide range of skills and experience they require for the safe performance of operations on live patients, in a safe, realistic and repeatable environment.

The next stage of research was to investigate and define a means of creating a visually realistic manufactured customised model of the sinuses. This will accompany the

work being conducted in the accompanying research project to achieve a physically realistic model. The possibility of internal colouring of the part was also investigated. This would present a further benefit to the user, allowing internal features (such as the internal carotid artery) to be highlighted for training purposes. This work is described in the following chapter.

CHAPTER FIVE

COLOURING OF 3DP PARTS

5 Colouring of 3DP Parts

Once the simulation model has been designed, it must be manufactured in a manner that maintains the required level of visual realism. This involves the use and representation of realistic colours and shading on the surface and potentially within the solid AM part, to signify areas of importance for training purposes.

This chapter provides a description of the work carried out to ensure the realistic final appearance of the sinus model, to complement the work on reproducing the physical properties of the sinuses being carried out in the accompanying research. This is a very important factor, as the maintenance of a sense of reality adds value to the training process, and moves the performance and planning of surgical procedures using the model closer to the real operation. Prior to the definition of the shades to be used in the colouring of the final model, described in Section 5.3, benchmarking investigations were performed into the possibility of internal colouring of parts during manufacture and quality of mapped textures to the exterior of parts to be built.

5.1 'Proximity Nesting' to Induce Internal Colouring

Clinicians identified that colouring on the interior of the physical part could be beneficial in the teaching of anatomy and surgical procedures to trainee sinus surgeons. An experiment was therefore devised to ascertain the possibility of achieving this.

5.1.1 Aim of Experiment

In this experiment, the aim was to ascertain the possibility of induced internal colouring of parts on the 3D printer. At present, the 3D printer may produce coloured parts, however the colour is only applied to the exterior of the model. This is done during the printing process; as each layer is produced the colour is applied to the outer perimeter of each cross-section within the adhesive. The rest of the interior of the model is produced using clear adhesive arranged in a wider crosshatch design, instead of the cyan, magenta and yellow adhesives combined to colour the exterior.

In previous studies, it was found that any internal colour applied to a 3D model is ignored once the part is exported from the software used before printing (ZPrint) to the printer. It is possible that the software or machinery may be re-programmed to achieve this aim; however less intensive methods are to be explored first as more preferable options. This trial is designed to investigate the possibility of inducing internal colouration of parts through their strategic positioning on the print bed.

5.1.2 Methodology

The experiment will investigate the effect of positioning two externally coloured parts on two adjacent layers in the build volume, as shown in Figure 20:

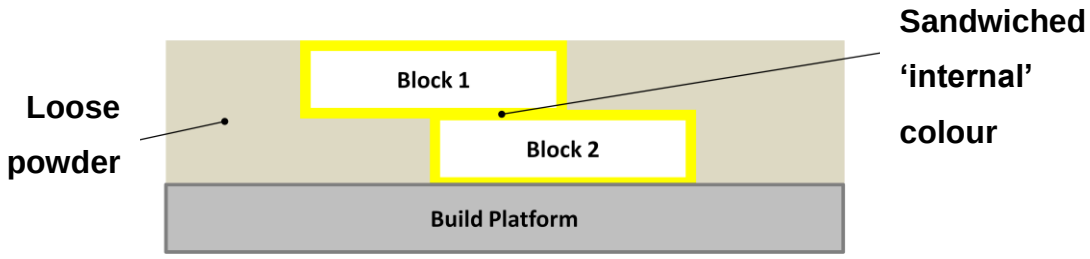

Figure 20: Positioning of blocks in 'proximity nesting' trial (X/Z plane)

By positioning the parts on adjacent layers, it is hoped that the extent to which the machine neglects internal colouring, even on separate parts will become clearer. It is possible that as the parts are separate, the machine may build them as such but also bond the two adjacent layers between the parts, creating a sandwiched layer of coloured powder and successfully inducing internal colouring. The layout of the blocks is shown from above in Figure 21, moving upwards through the build area.

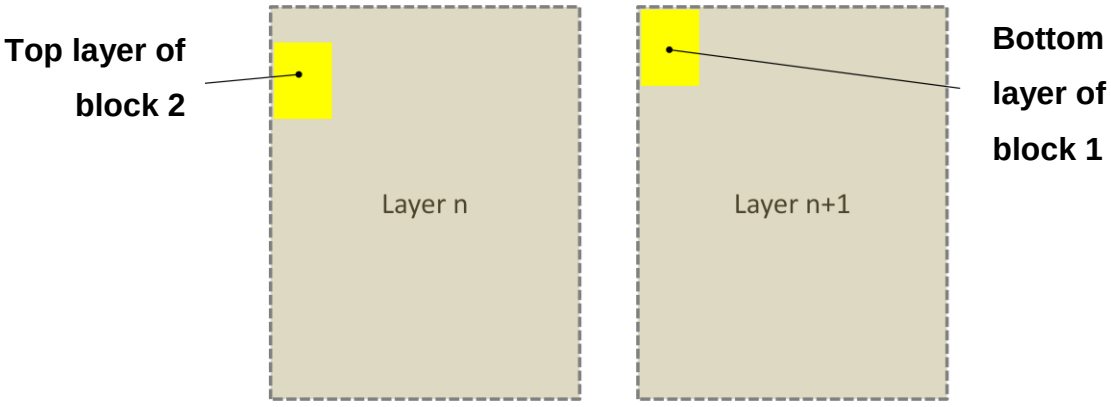

Figure 21: Positioning of blocks (subsequent build layers) in 'proximity nesting' trial (X/Y plane)

5.1.3 Results

The build process was closely observed as the machine reached the intersection between the two parts, as this would provide insight into the programming of the machinery, approach to internal colouring and the result of positioning two parts so close to one another.

It was observed that as the machine finished printing the final layer of the Block 1, three blank layers of powder were spread across the build platform before building of Block 2 was started, as shown in Figure 22. This was assumed to be an automatic function to avoid allowing separate parts to be placed, or built in such close proximity to one another, which could potentially produce an unwanted bond between the two parts as the binder fluid is deposited on the first few layers of the Block 2.

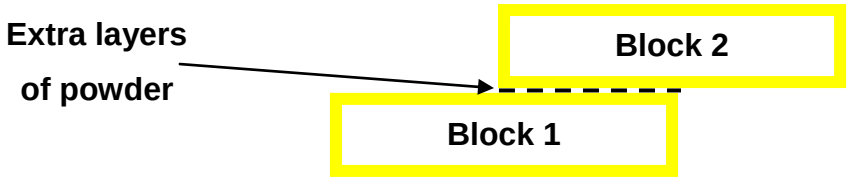

Figure 22: Resulting part built by 3DP machine

The resulting parts were, however, still bound together regardless of the extra layers of powder which had been spread between them. This meant that the final part was as designed, two blocks attached with colour sandwiched between them, except with a white area separating the two coloured faces between the blocks.

This shows that there is certainly some programming to be overcome or manipulated if the internal colouring of parts is to be achieved. The alteration of software and machine programming will be investigated as part of the accompanying research project, in order to potentially manipulate internal printing strategies. This information may then be used to implement internal colouring in the finished model.

5.2 ZEdit Benchmarking

ZEdit, the modelling software provided with the 3D printer (Spectrum Z510) in use for this research, has the capability to wrap images around 3D parts, giving a sense that, for example the part is manufactured from an particular material, or to apply a

company logo to a product before printing. Although relatively basic, compared to the CAD software used for the modelling aspects of the research, the link between ZEdit and the AM machine is key. The possibility of using ZEdit to produce anatomical models with real, in-vivo surface images from endoscopic surgery videos wrapped around the exterior (with little or no distortion to the image) will be investigated.

5.2.1 Aim of Experiment

The aim of the experiment is to attempt to wrap an image around the range of geometry, and assess the level of distortion to the image and determine the possibility of using this method for the use of in-vivo surface images on models of the sinuses.

5.2.2 Methodology

The complexity of the models involved in this research is, naturally, very high; as such the capabilities of the software will be benchmarked, by firstly using very simple models, and systematically increasing the model complexity if the first stage is successful and suitable.

Initial geometry was modelled using NX software, the first group of which were considered to be 'basic'. A cube, sphere and cone were modelled, to firstly test the software's capability in wrapping images around flat and round surfaces, and a combination of the two. Files were exported in STL format from NX to ZEdit, with the settings left as default:

- Output type: binary
- Triangle tolerance: 0.08
- Adjacency tolerance: 0.08
- Automatic Normal Generation: ON

A JPG file of a brick wall was used as the example texture to be mapped, as the straight lines in the image would provide clear definition of the amount of distortion experienced in the wrapping process.

5.2.3 Results

The means by which a texture is mapped onto the surface of a model in ZEdit was found to be inaccurate. There was no discernible way of placing an image in a precise position on the model, or of defining the size of the image in relation to the model. Instead, the image is shown suspended over the model, which must itself be rotated until the desired surface or part is underneath the image. It was found that the model must also be positioned behind the image so that the edges of the image are completely within the bounds of the visible parts of the model, as shown in Figure 23:

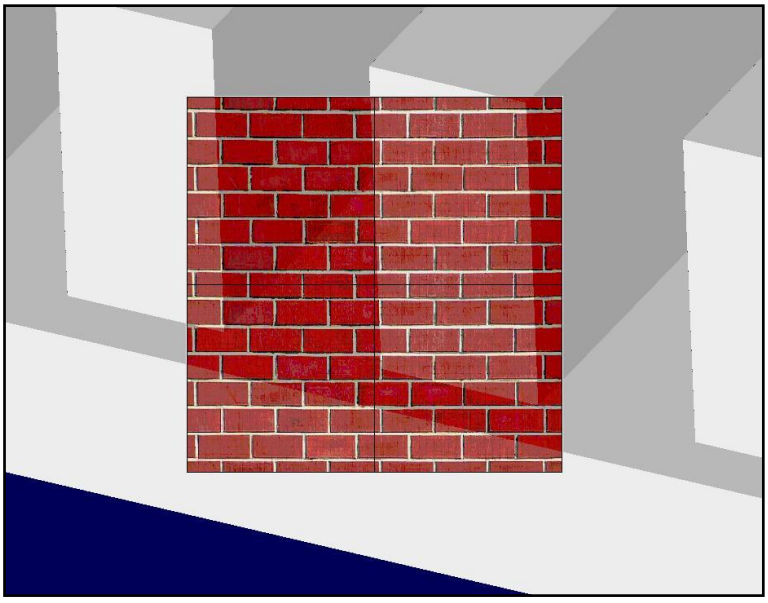

Figure 23: Image suspended over a part in ZEdit

Any attempts to position the texture so that only some areas of the image covered the model were therefore unsuccessful. In Figure 23, the image is suspended completely over the part; as such the mapping process is allowed to continue.

The first texture map was applied to the cube model, to detect whether the mapping of the image around the apex of the cube would cause distortion to the image. The resulting map is shown in Figure 24:

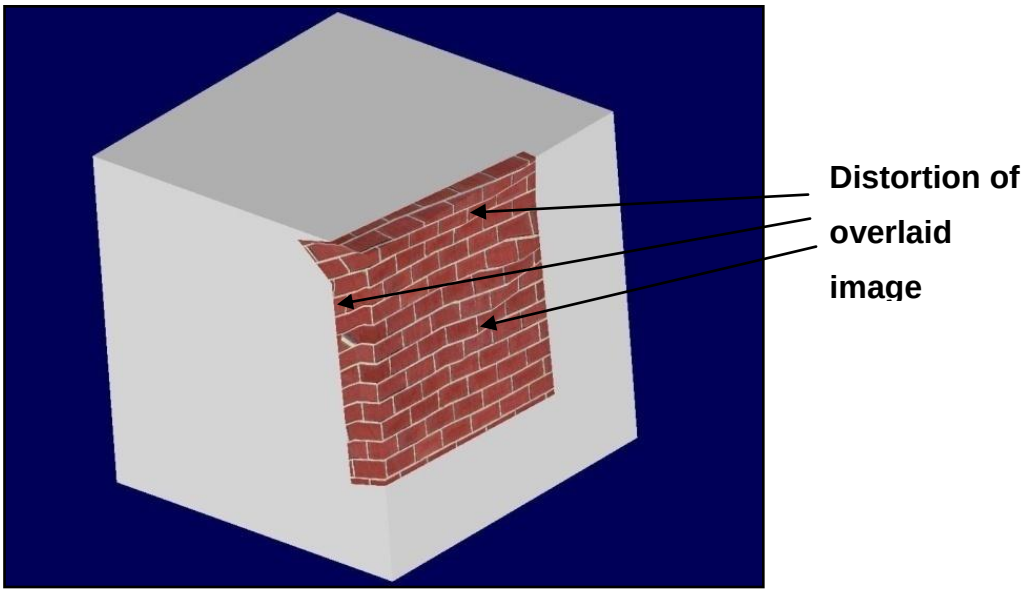

Figure 24: Mapping image around apex of cube

It is evident in Figure 24 that the image has not retained its original boundary shape, and that some distortion has occurred to the image itself.

The same experiment was performed with the centre of the image positioned roughly over the apex of the cube, as shown in Figure 25:

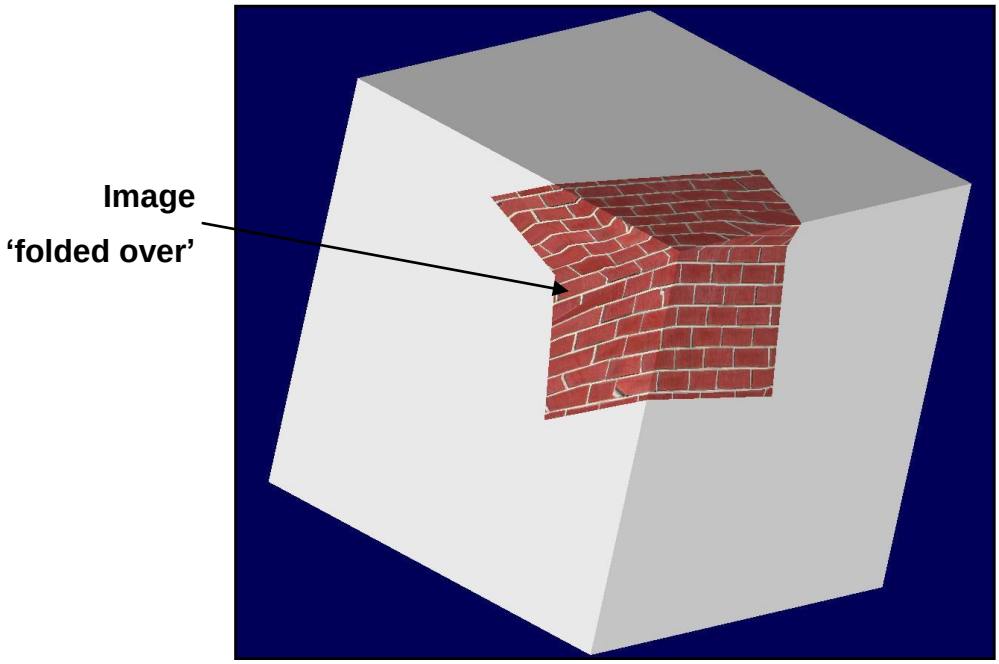

Figure 25: Mapping image (centred) on apex of cube

This shows even more distortion to the image boundary, consistent with the way a cloth would fall over the corner of the same cube. The image itself is distorted, with some parts 'folded over' one another, covering the original area of the image.

Using the 'wrap the picture around the part' function, the image may be made to completely cover all faces of the part. This is shown in Figure 26, where the image was projected straight onto the front face of the cube.

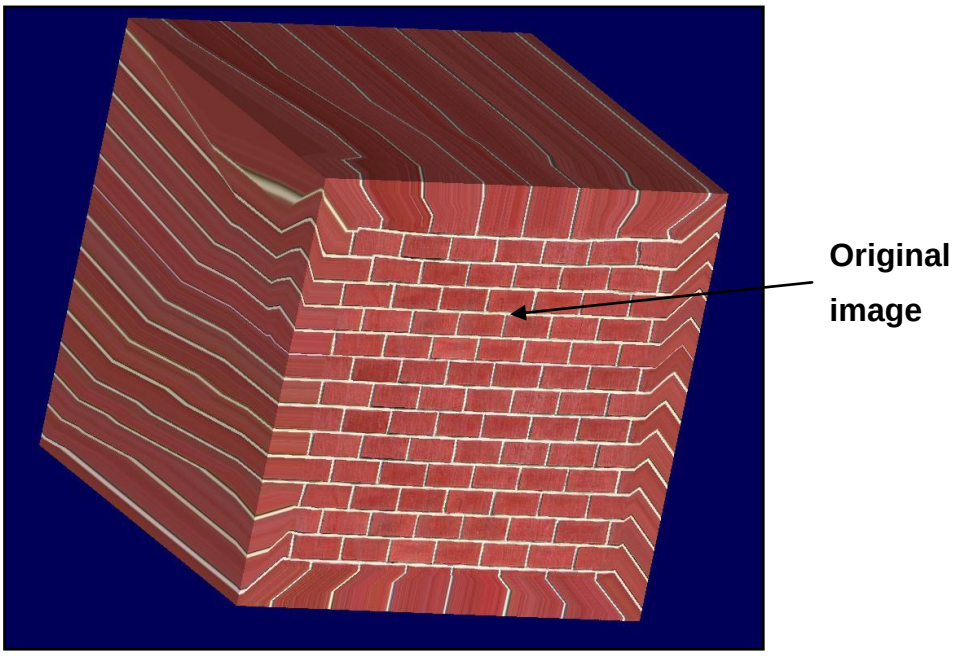

Figure 26: Image wrapped around entire part

In this case, the image remained undistorted in the original area, however the edges were stretched out to cover the sides of the cube. The back face shows the same result as the front, with an unaffected image area in the middle of the face. With these results, it does not seem that the image wrapping capabilities of the software would be suitable for the tasks within this research, whereby highly complex geometry may be covered with texture maps. The next two stages of the experiment were designed to confirm this.

When attempting to wrap the image around the sphere and cone, it was found that the image would not appear on the part surface. The outline of the part would be visible as a red line, however the image itself was not shown, even when projected onto the

flat base of the cone. This was also the case when the 'wrap the picture around the part' function was enabled.

As such, new models were created in NX with square edges, to further investigate the mapping procedure and to potentially find a way of successfully wrapping the image with a low level of distortion. The models created were:

- 'Windowed cube', with a square hole cut through the centre
- Set of 'fins', with a base and five blocks standing upright on the base
- 'Windowed cube', with a round hole cut through the centre
- Cube with a round recess going back halfway through the cube
- Cube with a protruding feature with both round and sharp edges
- Cube with a blended edge, merging two faces into one another

The square-windowed cube, shown in Figure 27 experienced the same problems as the other square-sided models, distorting the edges of the image fairly radically in their wrapping around the model:

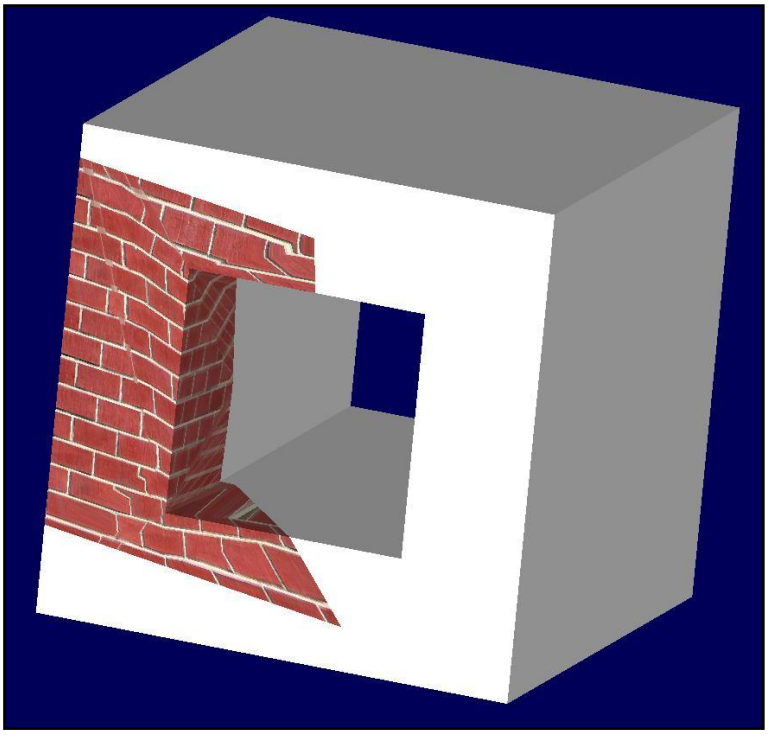

Figure 27: Square-windowed cube with image wrapped around window edge

This issue was also experienced when the image was mapped onto the fins model, as shown in Figure 28:

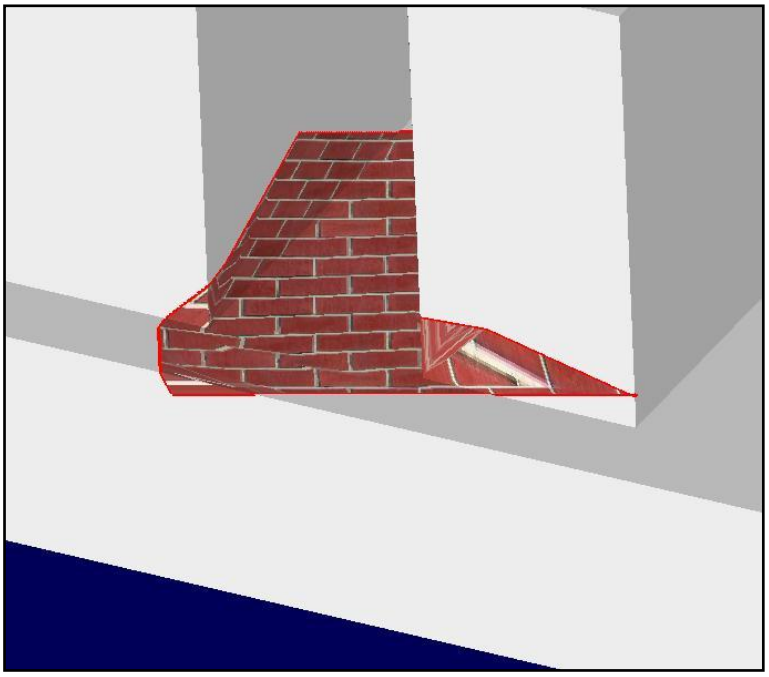

Figure 28: Fins model with image wrapped around base of two fins

It can be seen that distortion still occurs in these models. The lack of control over image positioning that is afforded by the software is demonstrated by the position of the final mapped image in comparison to the initial position of the texture shown in Figure 23.

The other models, which include some curved features, were investigated in the same way as those described above, with little success. The software was unable to display the texture map on any of the models, which suggests that the presence of curved features in models prevents the successful wrapping of images onto a model, as this occurred on the sphere, cone, round-windowed cube, cube with a recessed feature, cube with a protruding feature and the cube with a blended edge.

As this method of image wrapping was deemed unsuccessful and unsuitable for use in the research, investigation began into the possibility of alternative options. At this point, consultants from QMC were asked to offer their opinions on the appearance of the human sinuses during surgery. Using the information they provided, it was

concluded that the model could be manufactured in uniform colour, and that the wrapping of realistic images onto the exterior of the model was not necessary, as there is little detail on the surfaces of the anatomical features involved. This was met with approval from the medical consultants, who felt that this would not undermine the realism of the model in use. In order to determine which colours should be used on the model in this new design, an average colour acquisition task was set up and performed, as described in Section 5.3.

5.3 Colour of Anatomy

In order to study the accurate depiction of the appearance of the sinuses through colour on their exterior surface, endoscopic videos of live surgery were studied. From these videos, the colour levels present at points in the video where the sinus cavity wall lining was illuminated by the endoscopic light were recorded and the average colour level calculated. When physical models of the sinus anatomy are produced, they may then be coloured with the average colour calculated.

When colour is shown on a monitor, it is split into its red, green and blue (RGB) components, which are then shown simultaneously to create the correct appearance to the human eye. Every colour may be represented by the combination of the elements red, green and blue at individual levels from 0 to 255; black has a RGB value of 0,0,0; white, a RGB value of 255,255,255. It can be seen in Figure 29 that the level of blue in the colour selected is high (238), with a small amount of red (68) and green (81) altering the shade. The hue, saturation and luminosity (HSL) of colours may also be recorded; hue is described as the shade of colour being represented, luminosity as the lightness of the colour and saturation as the strength or purity of the colour in a specified hue. HSL levels change in relation to RGB. HSL may not be used alone to create a colour, but to provide a description and alter the shade of the colour. All three elements are measured on a scale of 0 to 240.

To measure the colour levels of areas of the in-vivo videos, a screen capture was taken at the required point, and imported into Microsoft Paint. Once present in the image software, the ‘pick colour’ tool was used to select the pixel of the image for analysis. The colour editing screen in Figure 29 was accessed to view the RGB levels

present in the selected colour, and the levels were recorded. This method was preferred to the use of average colour finding software due to the large areas of white or silver in the in-vivo video images, which would cause the average colour of the screenshot to be skewed and inaccurate.

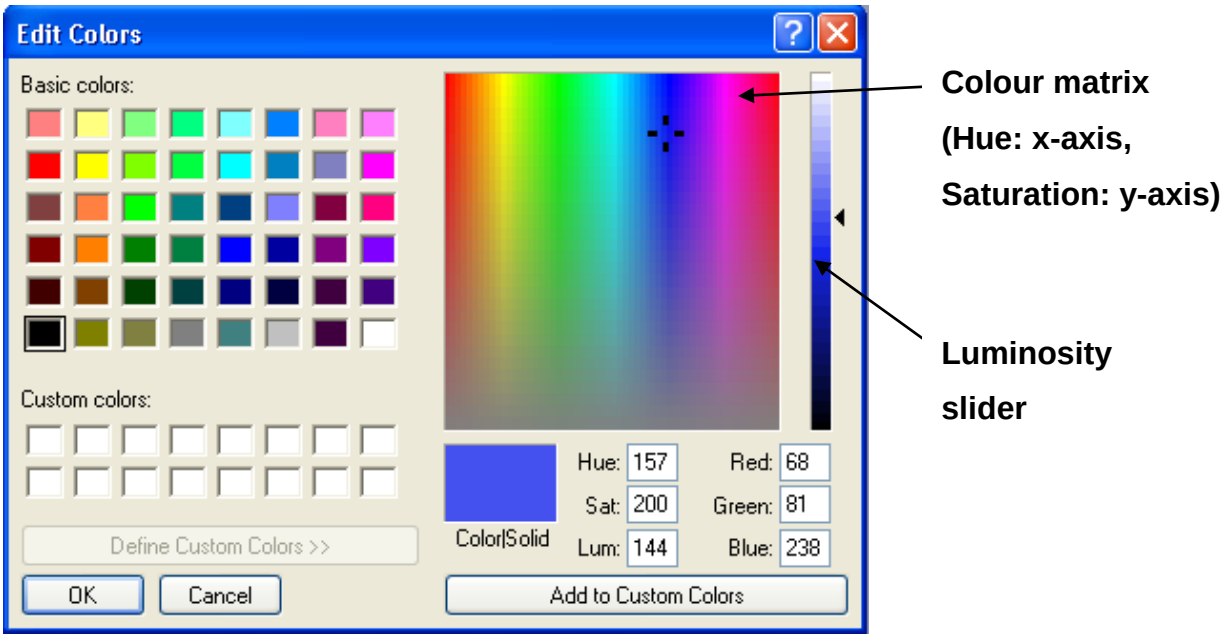

Figure 29: Colour analysis using RGB values and hue, saturation and luminosity

5.3.1 Results

The RGB levels recorded from each screenshot of the three separate endoscopic videos are shown in this section. Locations for the acquisition of colours were selected to represent the entire range of light that was reflected back to the camera from the cavity lining; colours from both well-lit and dark areas of the image were measured to produce the average colour. Points were selected throughout the screenshot, and the RGB value at each was recorded. This process was repeated until no further distinct colour levels could be found. Figure 30 shows the screenshot taken from the first endoscopic in-vivo video, and the nine points at which colour readings were taken.

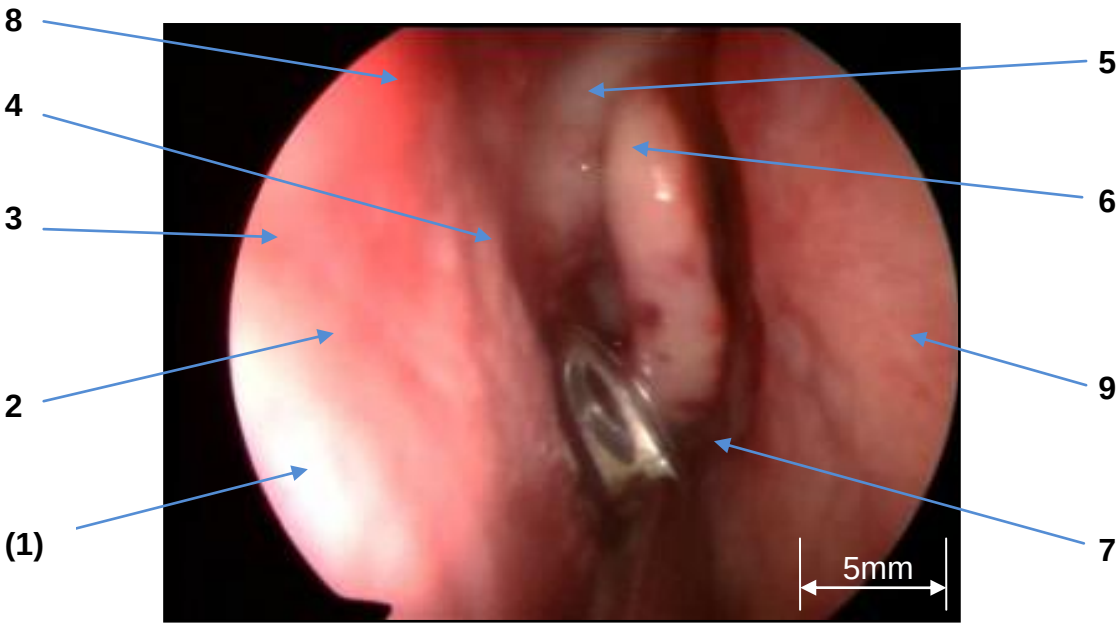

Figure 30: Screenshot from "Endoscopy Movie Edit 1" video

Table 1 shows the RGB values at the points shown in Figure 30:

No.	Hue	Saturation	Luminosity	Red	Green	Blue
2	4	230	195	253	170	162
3	1	228	182	252	139	135
4	4	117	144	203	113	104
5	8	56	112	146	102	91
6	9	102	150	200	137	119
7	2	171	46	83	18	14
8	0	235	157	253	81	81
9	7	109	138	196	115	98
Avg.	**4**	**156**	**141**	**198**	**109**	**101**

Table 1: Colour level results from "Endoscopy Movie Edit 1" video

In the case shown above, a measurement was taken of the lightest area of the image (point 1) in order to record the appearance of the reflection of the light. This range of values was not, however, included in the calculation of the average colour level so that a more realistic result for the natural appearance of the surface could be achieved.

Figure 31 shows the screenshot used for the calculation of the average RGB value in the second endoscopic video. Seven points were analysed in this case.

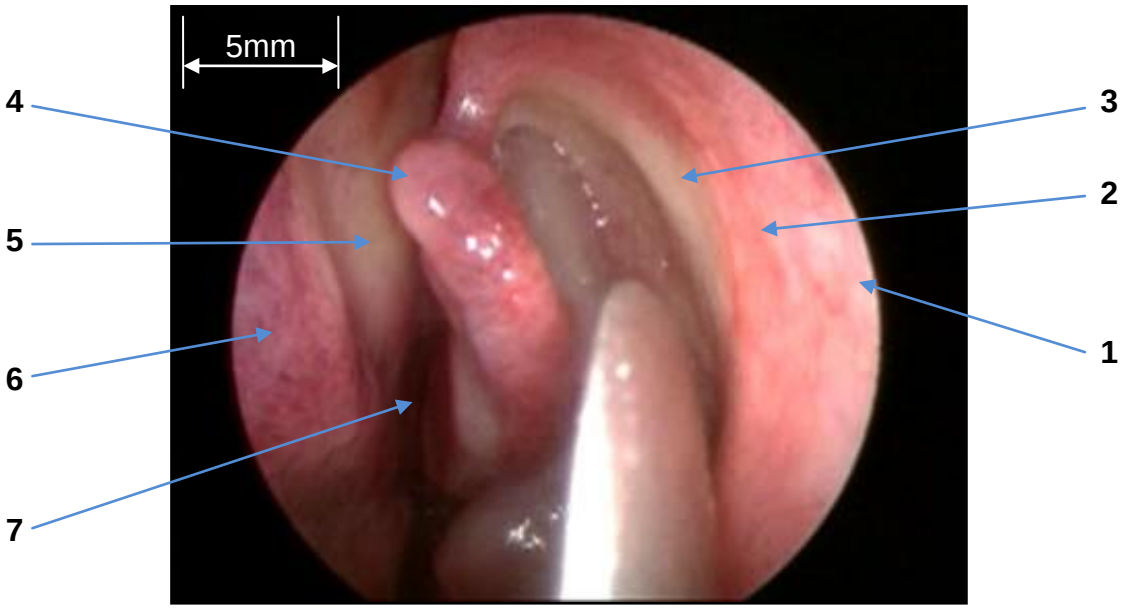

Figure 31: Screenshot from "Endo-Polypectomy" video

The RGB values at the points shown in Figure 31 are shown in Table 2:

No.	Hue	Saturation	Luminosity	Red	Green	Blue
1	0	232	211	254	194	194
2	2	236	189	254	152	147
3	12	90	160	202	157	138
4	239	102	156	204	128	130
5	10	67	137	176	130	115
6	229	68	129	171	104	122
7	238	145	40	69	17	19
Avg.	**104**	**134**	**146**	**190**	**126**	**124**

Table 2: Colour level results from "Endo-polypectomy" video

Figure 32 shows the screenshot taken from the third endoscopic video, and the eight points at which the RGB value was found:

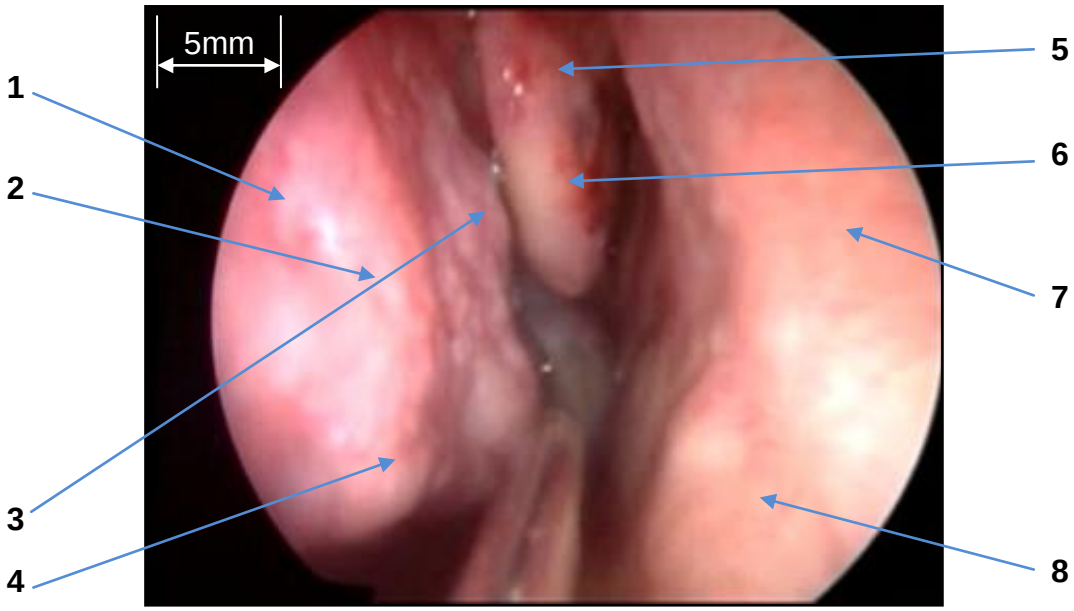

Figure 32: Screenshot from "Antrocoanal Polyp" video

Table 3 shows the RGB values recorded at each point in Figure 32:

No.	Hue	Saturation	Luminosity	Red	Green	Blue
1	234	189	177	241	136	153
2	230	233	209	254	190	206
3	235	124	174	221	148	157
4	236	226	224	254	222	225
5	0	118	110	174	60	59
6	6	134	176	225	161	149
7	4	236	181	254	146	133
8	7	240	198	255	181	165
Avg.	**119**	**188**	**181**	**235**	**156**	**156**

Table 3: Colour level results from "Antrocoanal Polyp" video

The average calculated RGB levels are shown below.

Video screenshot 1 (Figure 30) - Average RGB = **198,109,101**:

Video screenshot 2 (Figure 31) - Average RGB = **190,126,124**:

Video screenshot 3 (Figure 32) - Average RGB = **235,156,156**:

By comparing the average colours found from the first two video screenshots to the images themselves (Figure 30 and Figure 31), it was concluded in consultation with

Anshul Sama that the colours appeared too dark to completely represent the anatomy. The two screenshots were re-analysed and two further, lighter colour averages were sourced from eight points each. The new average values appeared to more closely match the colour of the anatomy when studied by eye. The colours obtained are shown below:

Video screenshot 1 (Figure 30) – Second average RGB = **243,124,148**:

Video screenshot 2 (Figure 31) – Second average RGB = **255,155,148**:

A sufficient range of colours has now been recorded (40) that may be used with the average levels to accurately represent the exterior surfaces of the sinus anatomy. However, the accuracy of the reproduction of these colours by the 3D printer must be assessed. This investigation is described in Section 5.4.

The reflective properties of the surfaces in each image are clear, as the reflection of the light source is visible on the walls as a white area. The reproduction of this wetness and reflection will be an issue to address when the coloured models of the sinuses are successfully produced, and may be achieved through the use of silicone infiltration (see Section 13.4.1).

5.4 Colour Reproduction Accuracy on Spectrum Z510

Once the colours required for accurate representation of the human sinuses had been found, it was necessary to investigate the way in which these colours appeared when produced by the 3D printer. The aim of this study was to account for any discrepancy between the colour to be produced, and the way this colour appears once printed. By analysing the appearance of a range of colours once produced by the 3D printer, and comparing these colours to the required colours, it was hoped that a rule would be identified, allowing the accurate production of the required, anatomically realistic shades. In order to ascertain the accuracy of colour reproduction on the 3D printer from the 3D computer model, a benchmarking exercise was devised.

5.4.1 Colour Reproduction Accuracy – Trial 1

This exercise involves the production of a part that includes a range of colours, and examples of the shades found in the exercise described in Section 5.3. Figure 33 shows the range of colours that were produced:

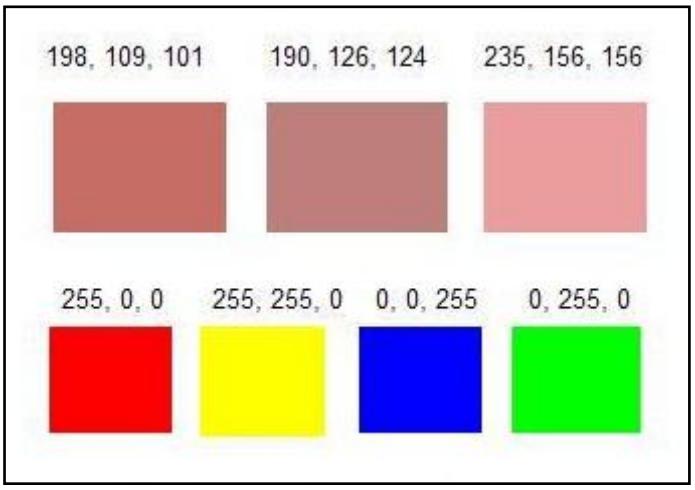

Figure 33: Colour levels for benchmarking exercise on Spectrum Z510

The colours along the top row are those initially found to be the average colours in the colour level study of the in-vivo endoscopy videos in Section 5.3. The aim of the study was to find a pattern that governed the generation of colour by the machine, in comparison to the colour it was instructed to produce. The sample was manufactured by 3DP and subsequently examined, allowing the accuracy of colour reproduction to be determined.

Once printed by the Spectrum Z510, the sample was examined under the SmartScope microscope at 17.9x and 34x zoom. This microscope, connected to a PC, allows the user to view the sample placed on the microscope table on the PC monitor, move the sample beneath the lens automatically and accurately, and export the images being viewed. The microscope also ensures that a constant level of light is present for all images. Images were saved in order for the colour levels to be analysed using graphics software. The results were tabulated and the accuracy of colour representation from the machine was ascertained.

5.4.1.1 Results

The colour levels found to have been produced by the 3D Printer were obtained through analysis in graphics software of the saved microscope images, and subsequently compared to one another in order to investigate the possible existence of a pattern. Table 4 shows the printing accuracy of four set colours (red, green, blue, yellow). The average RGB value, from analysis of microscopic images in average colour finding software is compared to the required value, giving a final percentage error where applicable.

RED	255	0	0
Zoom	Red	Green	Blue
17.9x	214	147	125
	198	137	115
34x	212	145	124
	195	135	114
Average	204.75	141	119.5
Error	-19.71%	141	119.5
Infiltrant	Red	Green	Blue
Cyanoacrylate	181	95	83
	163	87	75
Average	172	91	79
Error	-32.55%	-	-

BLUE	0	0	255
Zoom	Red	Green	Blue
17.9x	153	151	165
	139	137	149
34x	148	146	150
	135	134	147
Average	143.75	142	152.75
Error	-	-	-40.10%
Infiltrant	Red	Green	Blue
Cyanoacrylate	109	108	126
	98	96	113
Average	103.5	102	119.5
Error	-	-	-53.14%

YELLOW	255	255	0
Zoom	Red	Green	Blue
17.9x	224	222	139
	212	205	125
34x	221	218	136
	211	202	124
Average	217	211.75	131
Error	-14.90%	-16.96%	-
Infiltrant	Red	Green	Blue
Cyanoacrylate	204	190	100
	189	173	93
Average	196.5	181.5	96.5
Error	-22.94%	-28.82%	-

GREEN	0	255	0
Zoom	Red	Green	Blue
17.9x	180	208	133
	167	193	125
34x	174	204	129
	161	188	120
Average	170.5	198.25	126.75
Error	-	-22.25%	-
Infiltrant	Red	Green	Blue
Cyanoacrylate	141	178	105
	127	158	92
Average	134	168	98.5
Error	-	-34.12%	-

Table 4: RGB level analysis of red (255,0,0), green (0,255,0), blue (0,0,255) and yellow (255,255,0)

It can be seen that no colours were reproduced with the required RGB values on the printed parts. Uninfiltrated colour elements were all at least 14% away from the required value of 255, with a minimum average value of 119.5 when the required value was 0. No infiltrated element reached within 20% of the required value of 255, and the lowest value achieved was 79 when 0 was required.

The average colours acquired from inspection of the first three in-vivo endoscopic videos analysed in Section 5.3 were then printed. Table 5 shows the accuracy achieved by printing these more anatomically realistic colours.

VIDEO 1	198	109	101
Zoom	Red	Green	Blue
17.9x	211	164	137
	207	159	133
34x	195	151	127
	189	146	122
Average	200.5	155	129.75
Error	1.26%	42.20%	28.47%
Infiltrant	Red	Green	Blue
Cyanoacrylate	173	114	95
	155	102	84
Average	164	108	89.5
Error	-17.17%	-0.92%	-11.39%

VIDEO 2	190	126	124
Zoom	Red	Green	Blue
17.9x	212	178	151
	196	163	139
34x	207	171	145
	190	158	135
Average	201.25	167.5	142.5
Error	5.92%	32.94%	14.92%
Infiltrant	Red	Green	Blue
Cyanoacrylate	173	130	110
	155	116	98
Average	164	123	104
Error	-13.68%	-2.38%	-16.13%

VIDEO 3	235	156	156
Zoom	Red	Green	Blue
17.9x	225	192	164
	215	178	152
34x	224	186	159
	210	172	147
Average	218.5	182	155.5
Error	-7.02%	16.67%	-0.32%
Infiltrant	Red	Green	Blue
Cyanoacrylate	209	155	133
	186	135	116
Average	197.5	145	124.5
Error	-15.96%	-7.05%	-20.19%

Table 5: RGB level analysis of printed colours acquired from endoscopic videos

Again, no colours were exactly replicated on the printed part. However, with the reduced RGB values required, the magnitude of errors also reduced. The uninfiltrated red element values were all within 7.02% of the required value. Interestingly, the uninfiltrated red values achieved were higher than the required value, except where a relatively high value of 235 was needed. This seems to suggest that there is a range within which colours may be printed on the Spectrum Z510, hindering the ability of the process to mimic the whole range of required RGB values. Having gathered these results, the two further average colours acquired from the endoscopic videos were not analysed in this manner, and a system of compensation by eye was investigated.

A possible pattern was observed between the levels of green and blue in the uninfiltrated sample and the colour accuracy of each. A roughly linear relationship

was found to exist between the level of green and blue present in the in-vivo colours printed by the sample and the accuracy of their representation. This is shown in Figure 34 and Figure 35, produced by taking the average colour measured between the 17.9x and 34x zoom images.

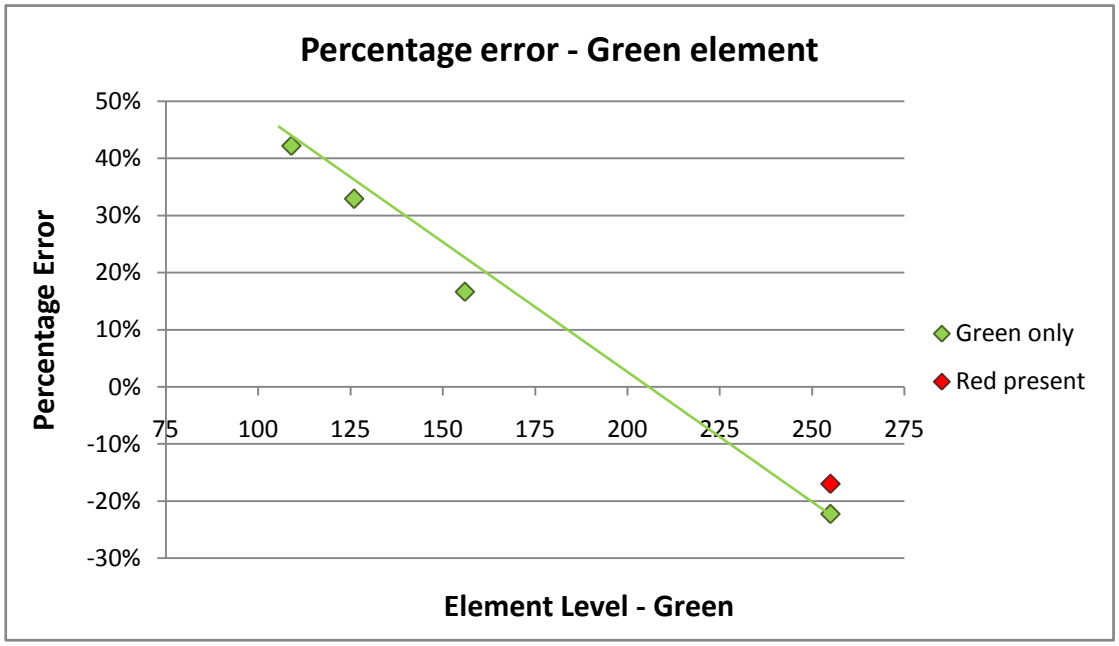

Figure 34: Percentage error of green element in printed parts compared to desired level

The red point in Figure 34 signifies the production of 255-point green in the presence of 255-point red (in the production of pure yellow 255,255,0), compared to the nearby point for 255-point green alone. In the case of these shades, the green element level was more accurately reproduced in the presence of red.

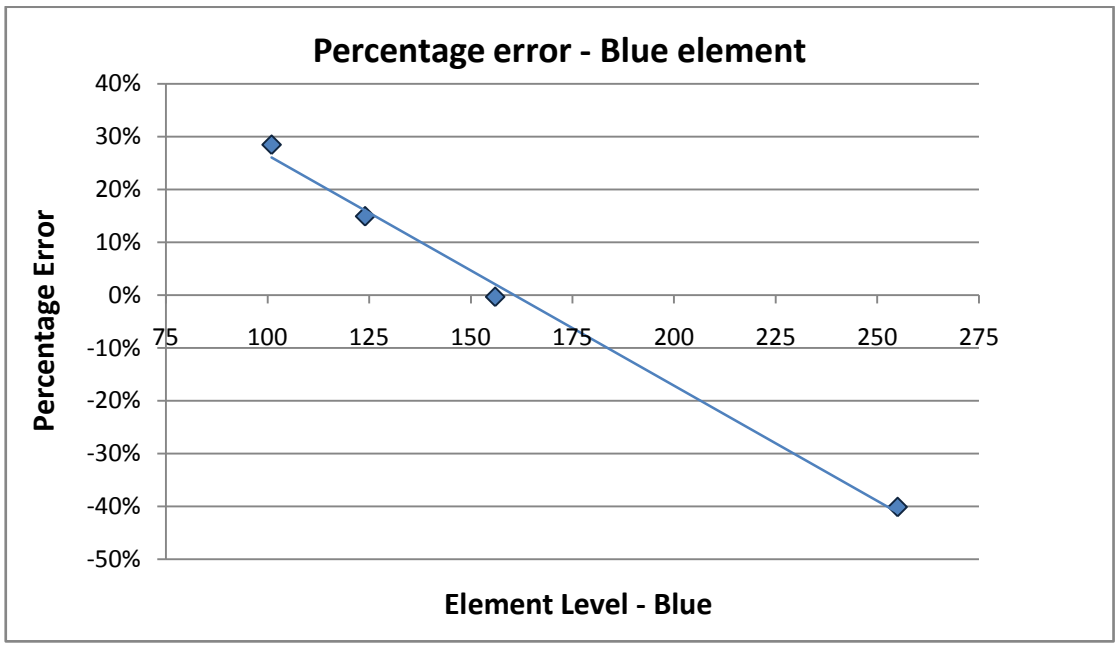

Figure 35: Percentage error of blue element in printed parts compared to desired level

However, the results shown above bore little relevance to the accuracy of the colour as a whole, as the red element did not display this behaviour. This means that no rule could be created from this observation. Indeed, on investigation of multiple samples produced from the same design as shown above, the accuracy of colour reproduction was not constant, even for the same original colour.

In each case, the overall RBG value of the colour produced was different to the required shade. Furthermore, this difference was not constant across all the required colours, or all the colour elements: the levels of red, green and blue in all the colours on the sample varied from the required level by different amounts in each case. As such, no broad pattern was found to exist between the levels of each colour element across every shade produced.

As no pattern had been observed using this sample, a further stage of investigation was performed, involving the analysis of a greater number of samples and the use of infiltrants.

5.4.2 Colour Reproduction Accuracy – Trial 2

The next trial investigated the extent to which the 3D printer could produce consistent results. The trials made use of wax and cyanoacrylate infiltrants, to examine the effect on the RGB values of the printed parts once infiltration had taken place. Infiltrants are commonly used in conjunction with 3DP, to strengthen parts, or improve the vibrancy and clarity of colours. Infiltrants are added to the parts after printing, while the model is porous and will take in the infiltrating liquid. The wax infiltrant must be heated prior to use, in order for the part to be fully immersed and left to absorb the liquid. Cyanoacrylate was applied by hand to the surface of the part.

Samples were produced, featuring blocks of standard red, yellow, blue and green, similarly to the test sample in Figure 33. In this case, each part was designed to include only one colour, to avoid the potential contamination of colours by the presence of others. The test samples are shown in Figure 36:

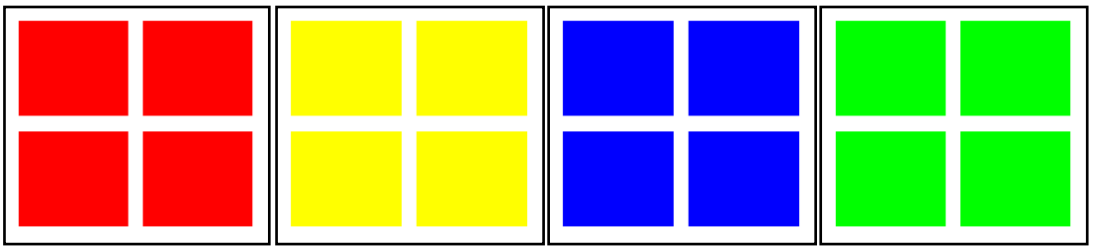

Figure 36: Test samples for individual colour reproduction accuracy

Each colour sample was produced eight times, to be analysed under the Smartscope microscope and find the average colour produced in each square. For each colour, four samples were left uninfiltrated, two were infiltrated with cyanoacrylate, and two with wax. The uninfiltrated samples were manufactured and analysed in two sets, to examine the potential difference in results arising from the use of two separate builds, three weeks apart.

Three images were taken of each square on the test samples, at the minimum (17.9x) zoom on the microscope. This was to gain an overall impression of the colour of the entire square, which could not be fully captured in one image from the microscope at the level of zoom available, by calculating the average of the RGB values shown in

each area of the square. An example set of three images taken from the analysis of one square on an uninfiltrated red sample is shown in Figure 37:

Figure 37: Images of *a)* bottom left, *b)* centre and *c)* top right of uninfiltrated red square

The average and range of RGB values found in the uninfiltrated, cyanoacrylate-infiltrated and wax-infiltrated printed colour squares was measured (the results from the two builds were measured separately for the uninfiltrated samples).

5.4.2.1 Results

The full data obtained from the analysis of the 32 printed colour samples is provided in Table 6.

		R	G	B
Average	Uninfiltrated 1	198	157	104
	Uninfiltrated 2	199	165	106
	Cyanoacrylate	152	93	61
	Wax	140	84	58
Range	Uninfiltrated 1	4	8	8
	Uninfiltrated 2	3	9	10
	Cyanoacrylate	18	27	16
	Wax	26	41	34
Error from 255	Uninfiltrated 1	-57	-	-
	Uninfiltrated 2	-56	-	-
	Cyanoacrylate	-103	-	-
	Wax	-115	-	-

RED

		R	G	B
Average	Uninfiltrated 1	137	155	150
	Uninfiltrated 2	138	159	151
	Cyanoacrylate	80	91	100
	Wax	79	87	95
Range	Uninfiltrated 1	8	7	6
	Uninfiltrated 2	6	5	3
	Cyanoacrylate	22	23	15
	Wax	64	62	48
Error from 255	Uninfiltrated 1	-	-	-105
	Uninfiltrated 2	-	-	-104
	Cyanoacrylate	-	-	-155
	Wax	-	-	-160

BLUE

		R	G	B	
Average	Uninfiltrated 1	208	200	109	YELLOW
	Uninfiltrated 2	206	198	111	
	Cyanoacrylate	173	154	75	
	Wax	178	163	89	
		R	G	B	
Range	Uninfiltrated 1	2	3	3	
	Uninfiltrated 2	2	3	5	
	Cyanoacrylate	12	11	7	
	Wax	26	30	43	
		R	G	B	
Error from 255	Uninfiltrated 1	-47	-55	-	
	Uninfiltrated 2	-49	-57	-	
	Cyanoacrylate	-82	-101	-	
	Wax	-77	-92	-	

		R	G	B	
Average	Uninfiltrated 1	168	188	120	GREEN
	Uninfiltrated 2	167	187	121	
	Cyanoacrylate	100	128	71	
	Wax	113	138	82	
		R	G	B	
Range	Uninfiltrated 1	10	8	9	
	Uninfiltrated 2	5	3	5	
	Cyanoacrylate	17	17	12	
	Wax	36	30	32	
		R	G	B	
Error from 255	Uninfiltrated 1	-	-67	-	
	Uninfiltrated 2	-	-68	-	
	Cyanoacrylate	-	-127	-	
	Wax	-	-117	-	

Table 6: Results of colour reproduction accuracy trial 2

The range of RGB values exhibited on all uninfiltrated parts was good, with a maximum range of 10 points between the maximum and minimum values recorded for each colour. It was found that after infiltration with cyanoacrylate, the range of RGB values exhibited was greater, with a maximum range of 27 (green element level on red sample). The infiltration of wax created an even higher range of RGB values, reaching 64 (red element level on blue sample). This increase in the range of RGB values measured could be due to the increased reflectivity of the parts after infiltration, particularly with wax, leading to lighter shades being recorded.

There was a good level of consistency of average RGB values within each colour on uninfiltrated parts, as suggested by the small range described above. This consistency was present between the average RGB values of squares within each part, from the same build, and between the two builds. In the case of every colour, the infiltrated parts returned lower (darker) average RGB values. Wax appeared to make red and blue colours darker than cyanoacrylate, while the opposite was true of yellow and green colours.

No uninfiltrated colour element reached within 47 points (18.4%) of the required 255 for any colour, and infiltration, as discussed above, took the average RGB values further from their required value. The most accurate infiltrated colour element was 77 points (30.2%) from the required 255, for the wax-infiltrated red element of yellow samples. Blue was the least well reproduced colour; the closest reproductions of the shade were the uninfiltrated samples, 104 points (40.8%) away from 255. Yellow was the most closely reproduced colour on average between all samples. Just as was shown in Figure 34, the green element level (in yellow and green samples) was again more accurately reproduced in the presence of red (when printing yellow samples).

While the results of this trial show consistency in the production of uninfiltrated colour, the colours produced are still dissimilar to those they attempt to represent. As suggested after the last trial, there appears to be a limit to which colour elements may be reproduced; the 3D printer is not capable of printing each element to the required limit of 255. With this in mind, it would be impossible to apply a rule of compensation to the colours for printing.

The next series of trials attempted to find the colours that should be applied to the virtual model of the sinuses, in order to successfully replicate the average RGB values found in the analysis of the in-vivo endoscopic videos in Section 5.3.1 and achieve a visually realistic result once the part is manufactured by 3DP.

5.4.3 Anatomical Colour Reproduction – Trial 1

The first colour sample was designed with the trends found through the previous trials in mind; that most colours appear lighter once printed, and are subsequently darkened through the infiltration of wax. By creating a colour chart (Figure 38) with the intended colours at the centre, and lighter and darker shades above and below, a direct comparison would be possible through visual assessment for further, more focussed investigation. The columns of the colour chart each represent one of the average RGB values found in the in-vivo endoscopic videos. For ease of reference, the colours have been numbered A1 to A35, so that column one contains colours A1 to A7, and so on. The target colours that the printed shades will be compared to are colours A4, A11, A18, A25 and A31, in the lined box.

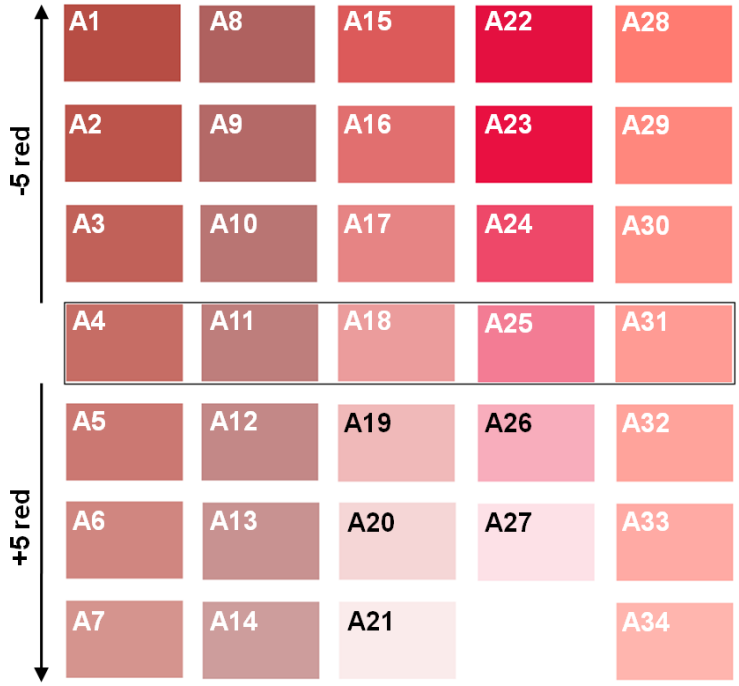

Figure 38: Colour palette A – to represent colours A4, A11, A18, A25, A31

The shades of each colour sample were produced by reducing (moving upwards away from the centre line) or increasing (moving downwards away from the centre line) the

level of red by 5 points, and allowing the other colour elements to follow naturally. This produced grades of darker and lighter colours, above and below the centre line respectively, allowing the analysis of the production of these different grades by the 3D printer. In the fifth column, where the red element value is at 255, the other two elements were both adjusted by 10 points in both directions.

Cyanoacrylate (superglue) will also be used as an infiltrant in this, and the following trials, in order to compare its effects to those of wax. The cyanoacrylate will be applied manually in these trials, which can lead to a less uniform covering of the parts' surfaces than wax, and some difficulties in handling the part during coating. Comparison of the appearance of infiltrated and uninfiltrated samples will provide insight into the way in which the infiltrants affect the perceived colour of the samples, and may suggest which, if any, will be the most suitable for use in the final model. This decision rested upon the visual quality of the models, and the ease of application of the infiltrant to a complex anatomical model.

The results of this trial were then used to create further test pieces, to narrow down the range of colours that may be used to accurately represent any of the five required shades.

5.4.3.1 Results

Some banding was evident on the printed samples, however this was not severe enough to affect the value of the colour analysis. The untreated sample exhibited colours that were, as expected, far lighter than those required. The different grades of each colour group appeared very similar to one another, and did not accurately represent the required shade.

Cyanoacrylate was used to coat one of the samples, and the effects on the colours of the blocks were recorded. All colours appeared far darker than the uninfiltrated sample, although the banding that was originally evident remained, and was heightened by the darkening of the colours. In general, however, the colours were more representative of the shades they were aiming to reproduce. All shades in column five appeared very similar, most likely due to the equal level of red in each

block. It was found that in this sample, colour A26 (248,173,188 – 5th in column four) could potentially be used to represent colour A31, the fifth target colour (255,155,148).

In the wax-infiltrated sample, the banding experienced with no, or cyanoacrylate infiltration was eliminated. The colours appeared smoother and, due to the application method, there is a more consistent, thorough and all-over coating of the infiltrant. Colours in column five were similar to one another and to the target; with a lower level of red this target could be achieved. For colour A25, the fourth target colour, the same colour element levels could be used, but dulled down to achieve the correct shade.

5.4.4 Anatomical Colour Reproduction – Trial 2

Colours A25 and A31 were chosen for use as the target colours in the next stage of colour development, due to the already apparent similarity of the colours printed in columns four and five of Colour Palette A to the target colours A25 and A31, meaning that a result could be achieved more efficiently. Changes were made to the colour chart for Trial B in accordance with the observations made about the previous sample. The colours included were chosen by slightly altering the colour levels of the closest matching shades from the last trial. Colours B1-B6 are designed to match colour A25 from Trial A; colours B7-B12, to match colour A31. The new sample for testing in Trial B is shown in Figure 39:

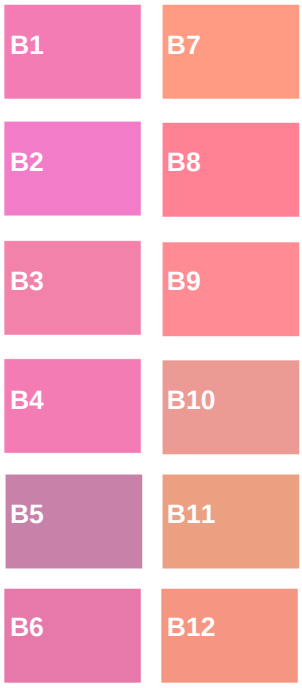

Figure 39: Colour palette B – to represent colours A25 and A31 from Figure 38

5.4.4.1 Results

In the untreated sample, colours were once again far lighter than required with not enough vibrancy. When infiltrated with cyanoacrylate, colours B3 and B6 represented colour A25 well. Colours B7 to B12 needed to be made duller in order to achieve a good representation of colour A31.

By using wax to infiltrate the part, colour B3 was once again found to be very similar to A25, but colour B6 was less similar than with cyanoacrylate. Colour B4 also became similar to A25, and for the next trial a combination of colours B3 and B4 would be tested. Further shades will be created using these colours as a base, whilst attempting to apply the necessary changes.

5.4.5 Anatomical Colour Reproduction – Trial 3

It can be seen that the colours in the palette for trial C (Figure 40) are duller than the last, and that the shade of colours C7-C12 has been lightened. This should produce the required results once the sample has been printed, and infiltrants added.

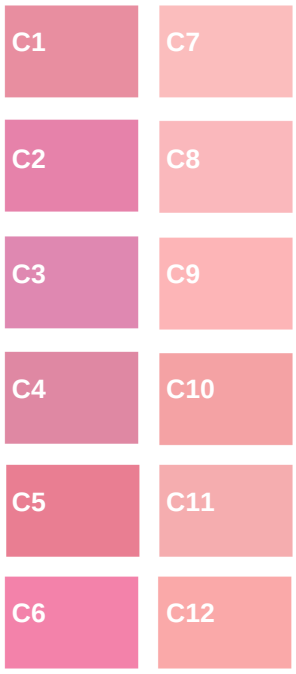

Figure 40: Colour palette C

5.4.5.1 Results

The colours of the cyanoacrylate-infiltrated sample appear brighter and more vibrant than those in the wax sample, however this is not required. In many cases, the colours needed to appear duller. In both the cyanoacrylate and wax infiltrated samples, colour C4 is very close to target colour A25, however to fully recreate the colour the blue element level may need to be reduced. C8 and C11 are also very similar to their target (A31) but must appear slightly duller.

5.4.6 Anatomical Colour Reproduction – Trial 4

Now that the colours being produced were far closer to the required shades, the final stages of the selection process could be undertaken. The colour palette for trial D is shown in Figure 41:

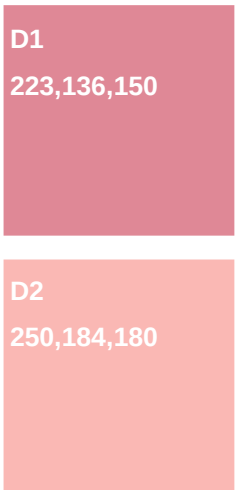

Figure 41: Colour palette D

This sample contains two colours: D1 (based on colour C4) attempts to recreate colour A25, D2 (based on colour C8) aims for colour A31. Colours C4 and C8 were altered slightly to attempt to get nearer to the desired colours; the blue element was reduced in both cases, to make C4 appear less purple and C8 appear more red.

5.4.6.1 Results

On the printed sample, colour D1 was again very similar to the required colour, but one further experiment was carried out to examine the possibility of achieving a better result. In the next trial, the blue element would be placed between the values used for C4 and D1, at 170.

Colour D2 was considered a very good match, and for trial purposes only, in the next experiment the blue element value would increase to 190.

5.4.7 Anatomical Colour Reproduction – Trial 5

For the final trial, very slight adjustments were made to the colour levels, to examine whether any further improvements could be made. The palette for trial E is shown in Figure 42:

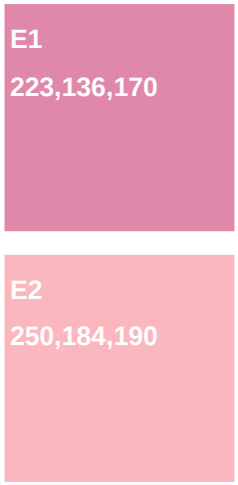

Figure 42: Colour palette E

5.4.7.1 Results

Once printed, colour E1 appeared far more magenta than the last sample, with an increase of only 20 points to the blue element. An average of D1 and E1 produce a valid result with 223,136,160 (almost exactly the same as colour C4) being used to recreate 243,124,148.

Colour E2 appears very similar to D2, although slightly more pink. Again, an average taken between this and the previous sample, giving 250,184,185 (very similar to C8) successfully reproduces 255,155,148.

5.5 Infiltrants

Work is in progress on the related research project to determine the most appropriate infiltrant for use on the final model for the replication of the physical characteristics of the sinuses.

5.5.1 Infiltrants Used in this Research

The infiltrants used in this research demonstrate similar visual characteristics, and altered the printed colour of the test parts by almost the same amount. With wax, the colours appear slightly duller, and the surface of the part has a matte finish; with cyanoacrylate, the colours are brighter and more vibrant, with a glossy finish to the surface.

From the two infiltrants used in these trials, wax appears to be the most suitable for use on the final model, mainly due to the application method employed. The immersion of the part in hot wax is simple to perform, in comparison to the manual application of cyanoacrylate, which can lead to uneven and incomplete coverage of the part. In addition, the final anatomical geometry would be extremely difficult to coat to the required standard manually, whereas full part immersion can be carried out on parts that exhibit complex geometry. Some issues may arise from the trapping of molten wax in cavities or small openings in the model, or the pressure exerted on small, thin sections of the anatomy, but this will be investigated as work continues on the accompanying research project.

CHAPTER SIX

INVESTIGATING CUSTOMISABLE ANATOMICAL MODELS

6 Investigating Customisable Anatomical Models

In order to investigate the possibility of customising medical data to show user-defined pathology, the data must be converted from 2D greyscale pixel images into a more malleable format; the slice data may not be directly altered. The first technique to be investigated will involve the use of 3D CAD modelling software to alter a 3D reconstructed model of the anatomy.

6.1 Selection of Medical Imaging for this Research

As described in Section 2.2, the layered nature of medical data is ideal for physical reproduction using AM techniques. CT and μ-CT are used primarily to define the geometry of dense tissue; in the sinuses, CT is used to determine the geometry of bony structures (constituting the majority of the anatomy in the sinuses). CT imaging is also employed to investigate simple inflammatory disease [166] or pertinent and chronic sinus disease [167], whereas MRI is used solely for the detailed analysis of softer tissues.

Figure 43 shows the same anatomical data, acquired from MRI and CT scans respectively; the front of the skull is shown at the top of the images, with the brain visible. In the top section of each image, the frontal sinus shows up as the dark air cavities within the thickness of the forehead. The MRI scan (*a)*) shows soft tissue densities on a greyscale, with harder areas in black, while the CT scan (*b)*) shows the hard, dense structures (such as bone) clearly as white areas of the image. As such, the CT scan is the best means to obtain anatomical geometry of the sinuses. It is also worth noting that in Figure 43, some swelling is visible in the patient's right side of the frontal sinus as soft tissue, and the cranial cavity bone separating the sinus from the brain has been eroded away, leaving the pathology in contact with the brain.

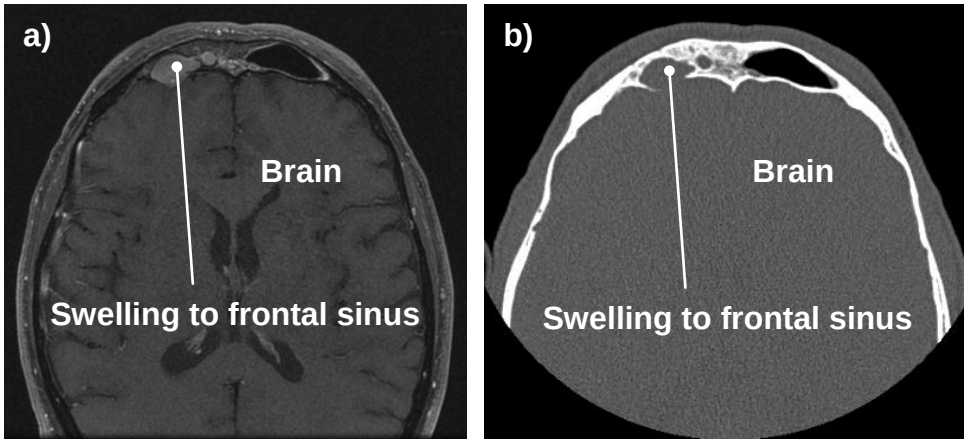

Figure 43: Images from *a)* MRI, *b)* CT scans of the same patient (axial plane, forehead level)

For these reasons, CT and µ-CT scan data of the sinuses will be used as the principle sources of data for use in this research. Where more anatomical detail is required for the development of the customisation tool in a clearly-defined environment, the available µ-CT data will be used.

6.2 Reconstruction of CT Scan Data

Once CT or µ-CT scan data has been obtained, it must be manipulated to remove any unwanted data, and display the remainder as clearly as possible for the creation of a 3D CAD model.

6.2.1 Manipulating Medical Data with Materialise's Mimics®

When obtained, data from medical scans such as MRI or CT is in slice format, which provides a layer-by-layer, 2D greyscale representation of the anatomy. Software packages such as Materialise's Mimics® allow the user to segment medical greyscale pixel images, to reveal the anatomy in the ROI and convert the images to a mesh-based surface representation of the 3D volume [115]. To do so, the series of images must be registered against one another correctly, positioned in a stack orientation and manipulated by the user to show the required data as a 3D model. The manual processing and manipulation of the images directly influences the modelling and design accuracy of the finished part [168]; therefore the procedure must usually be

performed by or with the assistance of someone with advanced knowledge of the anatomy being modelled.

At the import stage, the user may refine the part of the scan data that is required; for example if scan data of a human head is imported, the user may immediately refine the ROI to the sinus region of the head by selecting the appropriate range of scan images. This reduces processing time, and ease of use when dealing with the data in more detail.

Mimics automatically registers the images into a stack and, once positional and process information is provided by the user to define the scan properties, and front, back, left, right, top and bottom of the anatomy, it can be displayed on-screen. In this section, µ-CT data of the ethmoid sinus has been used to illustrate the functions of Mimics. The raw µ-CT data is first displayed to the user as seen in Figure 44:

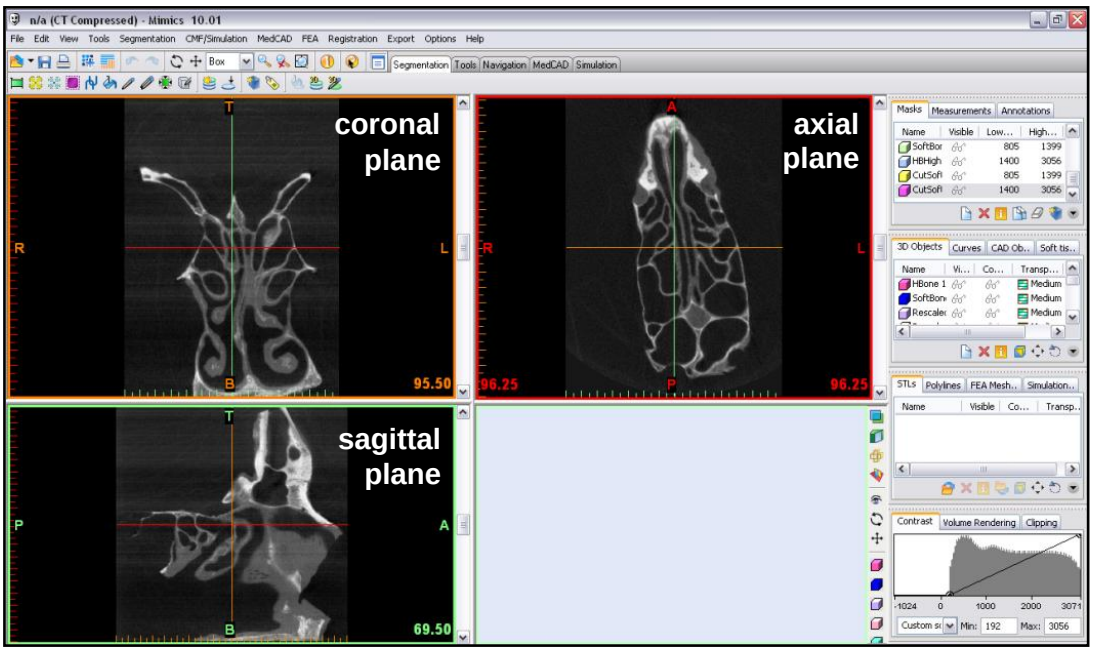

Figure 44: Mimics, showing ethmoid sinus µ-CT scan data on three planes

The software is then able to display the data from the ROI in three planes: coronal (X/Z), sagittal (Y/Z) and axial (X/Y). It is also possible to move through the scan

viewing the cross-sectional image data at each point, as is done by medical professionals during analysis of the images in their line of work.

The CT data, in the case of this research, displayed on the screen contains both hard and soft tissue data. These different tissues are displayed in terms of their density (which affects the amount of radiation returned to the equipment during the scan) as a greyscale image. Hard tissues, such as bone will appear white, and softer tissue such as the brain appears as darker shades of grey, as can be seen in Figure 8. By using this greyscale definition of tissue density, the user may identify the range that is to be included in the 3D model. The method by which this is done is known as 'thresholding', and is performed through a direct interface with the user.

During thresholding, a mask is placed over the images, and can be altered to contain the range of greyscale values that are required in the 3D model. In this way, the 3D model can be refined to contain only the bony structures of the CT scan data. In the segmentation of CT images, soft tissue is most often removed from the image; whereas in the manipulation of MRI slices, several structures of different densities must often be removed from view as the imaging technique produces images of a wider range of densities [140]. The user may move a sliding scale to capture the required data within the required upper and lower limits, and monitor the data that is included in this range as the mask updates in real time (Figure 45). This mask is applied to the whole dataset, and may be analysed in the three dimensions that are displayed on the screen, as described earlier.

Figure 45: µ-CT sample of ethmoid sinus thresholded – lower threshold set too low

When attempting, for example, to threshold the data to extract the geometry of the bony structures, the upper limit of the mask will be placed at the maximum, to include all white areas. The lower limit is then altered, while monitoring the changing mask over the images to ensure that only the correct data is included. Difficulties may arise with issues such as the separation of the inner and outer contours of bone displayed in the image, and may cause the segmentation process to take some time [156]. It can be seen in Figure 45 that although all the bony tissue is contained in the purple mask, the lower threshold level has been set too low, allowing some artefacts within the rest of the image to also be included. This can be avoided by increasing the lower threshold level, as shown in Figure 46. It is also clear, however, that once the lower threshold is increased, some features may be lost. This can be seen in the circled area of Figure 46, where a part of low-density tissue has not been included in the mask.

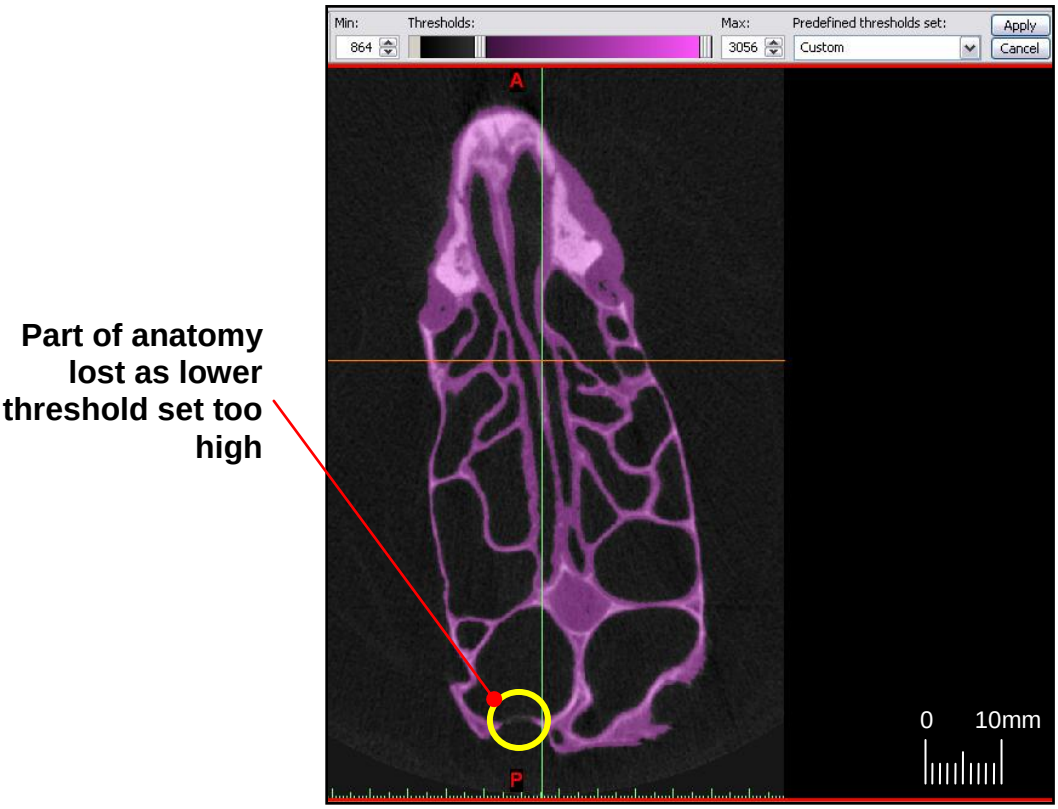

Figure 46: µ-CT sample of ethmoid sinus thresholded – some features lost (circled)

During thresholding, the user may focus in further detail on the ROI by manually 'painting' masks onto the dataset. By doing this, a small section of the tissue pictured in the scan images may be thresholded or manipulated separately to the rest of the scan. This mask may then be included with other data, or produced as a model of its own. In a similar way, some parts of the scan data may be removed from the model by manually erasing the mask in those areas. Erasing the same area of the scan on many consecutive layers can allow an opening to be created in the 3D model, to allow viewing into the interior.

By erasing a whole layer, or layers of the source mask, as shown in Figure 47, and subsequently creating a threshold mask either side of the erased layer(s), the range of scan images included in the 3D model may be reduced further. Alternatively, the model may be created with a split at the designated place. This technique may be used to apply different threshold levels either side of the split, in order to include parts that

were excluded by the original threshold level, as shown in the lower section of Figure 47.

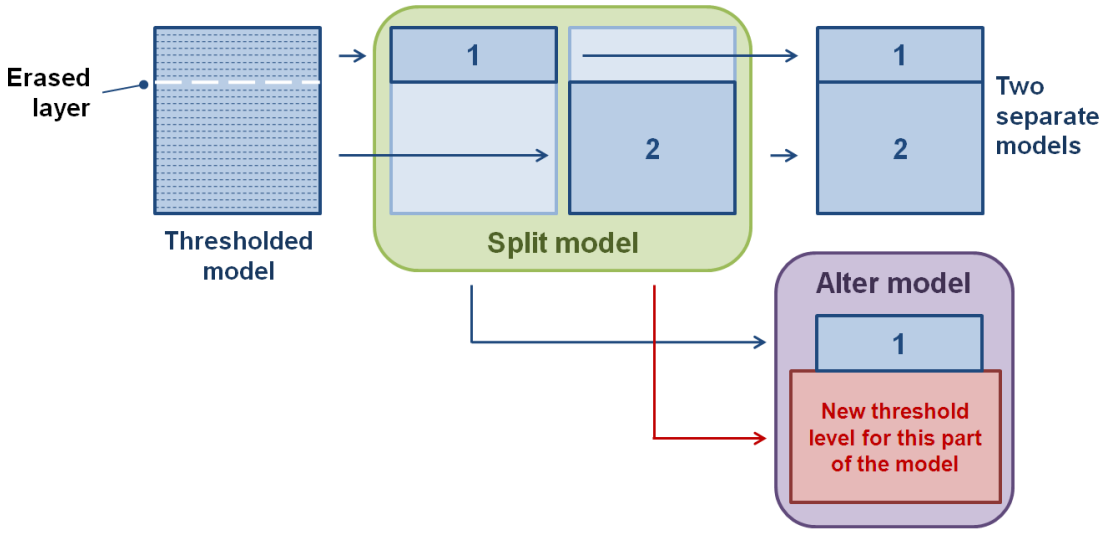

Figure 47: Erasing a layer of the data in Mimics

By creating a model with a division, by erasing one or more layers of the mask and producing a 3D model in Mimics, AM parts may be produced that allow interior inspection, which is useful for training models, prototypes and display items, as shown in Figure 48*b)*. The model shown was produced in blue due to problems being experienced with the clear binder liquid of the 3D printer at the time of production.

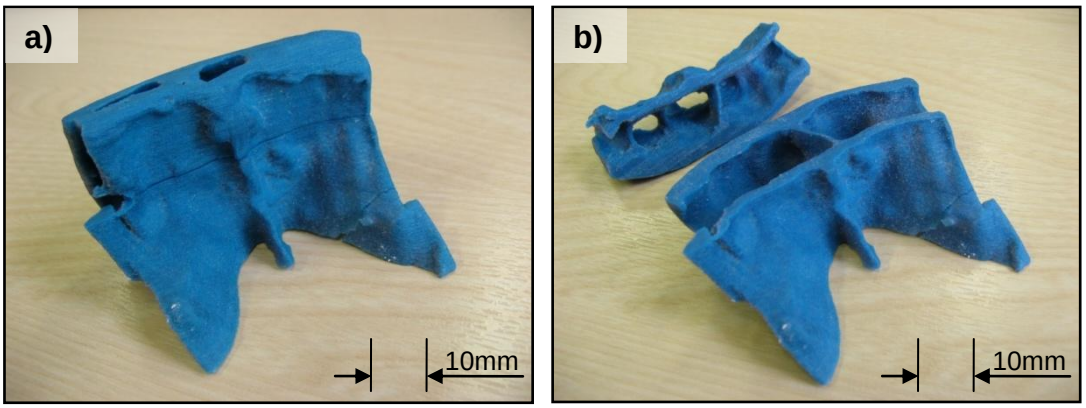

Figure 48: Split frontal sinus model *a)* assembled, *b)* showing internal anatomy, from Spectrum Z510 3D printer using 'Erased Layer' method

The physical model pictured in Figure 48*a)* and *b)* was produced from µ-CT data using the STL file shown in Figure 49. Both figures above are viewed from behind the forehead (inside the skull) and show the central region of the forehead (frontal bone), with a horizontal split line through the centre of the part. The two protruding sides of the model extend to form the sides and then the base of the cranium in a complete dataset. When split, as in Figure 48*b)* and Figure 49, the model gives a view into the central cavities of the frontal sinus.

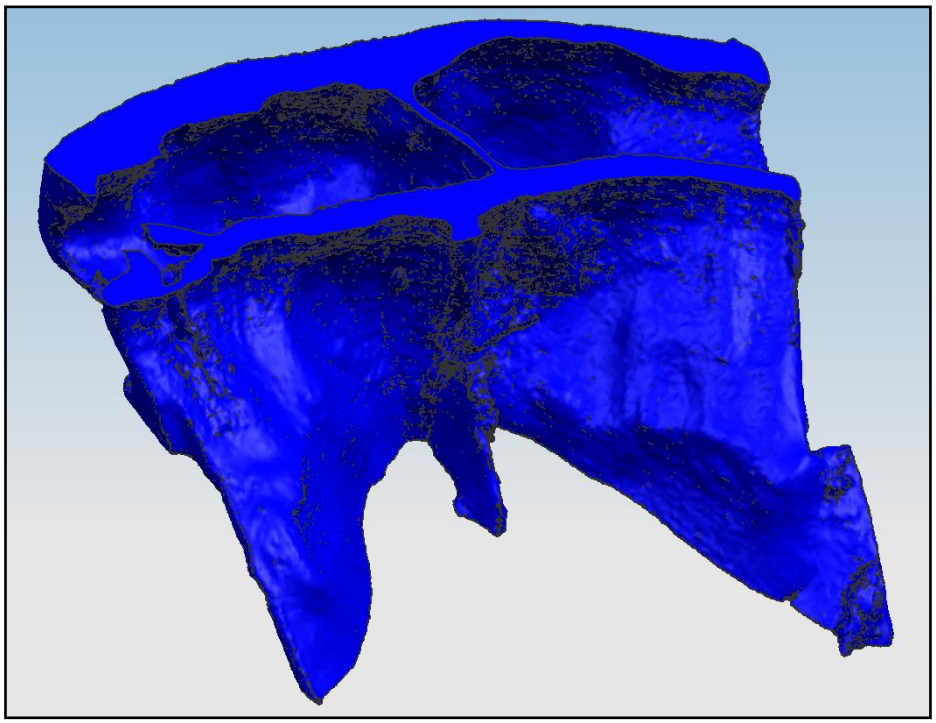

Figure 49: STL file of µ-CT data imported from Mimics

The creation of the STL file pictured in Figure 49 is described in Section 6.2.2.

Often, a compromise must be met in thresholding, whereby the mask cannot be made to completely define and separate the required data; other data is also included in the threshold, as it falls within the set greyscale range. In this case, further steps must be taken to separate out the geometry that is needed to form the 3D model. The first of these steps is known as 'Region Growing', a process that removes outlying features from the dataset. This is done by applying the user-set level of connectivity, which

filters out those areas of the threshold mask (source mask) containing pixels without the required number of adjacent pixels. This level may be set to 4 or 8 pixels on one layer, and 6 or 26 on multiple layers. Areas with less than this number of connecting pixels are removed from the mask; therefore the higher the setting for level of connectivity, the more the source mask is reduced in size to form the new, 'target' mask.

Small outlying points with very few connecting pixels will be removed from the mask, leaving only large, completely connected features, which are in most cases the required geometry. In Figure 50, for example, the unconnected artefacts included in the purple source mask can be seen to be excluded from the new, light brown target mask.

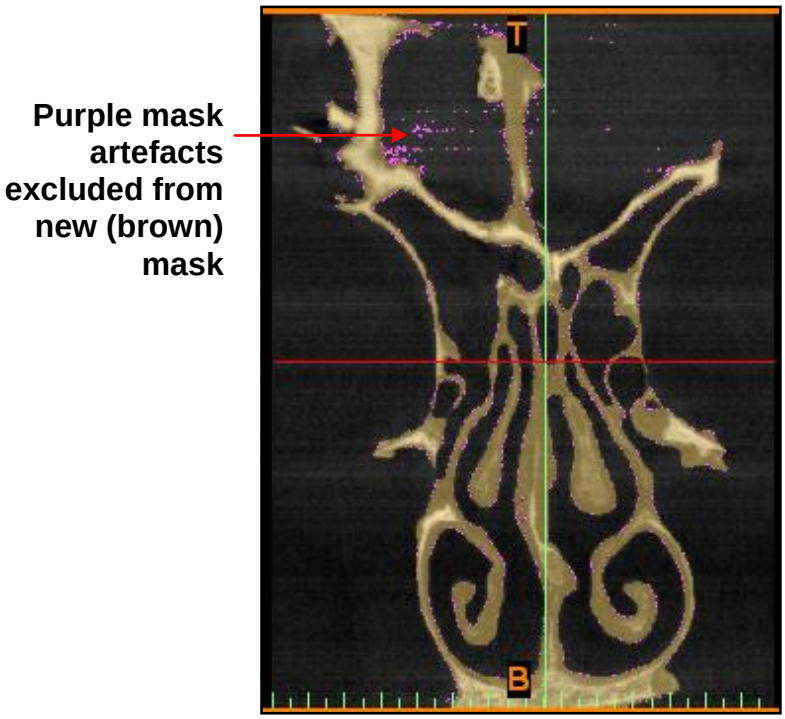

Figure 50: Region growing tool used to remove outlying pixels

The next stage, if required, involves the employment of morphology operations to further refine the data to be included in the 3D model, and provide the user with more

control over the accuracy of its final geometry. These operations include Erode, Dilate, Open and Close.

The Erode and Dilate functions are used to increase the smoothness on the exterior of the model, by removing any irregularity around the surface. With Erode, this is done by removing pixels around the perimeter of the source mask (Figure 51*a)*); with Dilate, the source mask is expanded to achieve the same smooth effect (Figure 51*b)*).

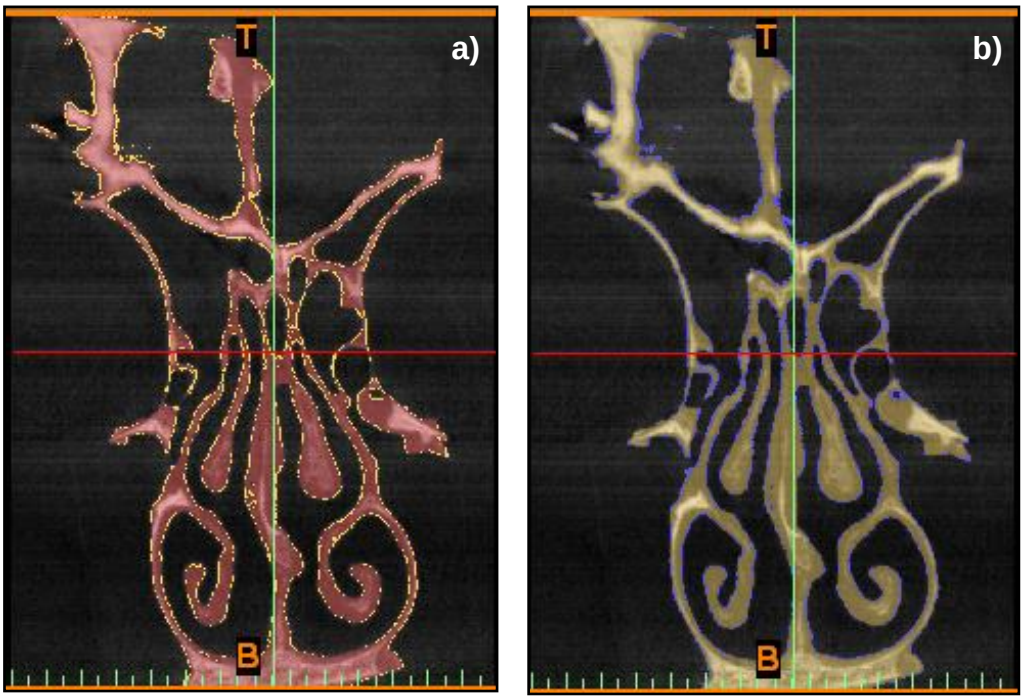

Figure 51: Morphology operations applied – *a)* Erode, *b)* Dilate

In Figure 51*a)*, the light brown source mask can just be seen around the perimeter, as it has been eroded back to achieve a smooth outer surface with no outlying pixels, shown by the target red mask. In Figure 51*b)*, the same light brown source mask has been dilated to achieve an equally smooth surface, as can be seen by the larger blue target mask behind.

By using the Open and Close functions, the same operations are run on holes or spaces within the masked area. In a similar way to the Erode function, Open increases the size of holes within the source mask to achieve a smoother perimeter, whereas the

Close function, as with Dilate, does this in the opposite manner. By this stage, the target mask, which now only includes the parts of the original data that have passed through the thresholding, region growing and morphology operations stages should now closely represent the required data.

The processes described in this section may be repeated as many times as is necessary. Once the mask suitably represents the areas of the anatomy that are needed, a 3D CAD model is created, using the MedCAD module of Mimics. The mask layers are stacked to create the 3D CAD model, which may be viewed on-screen, and rotated to gain a full understanding of the geometry in three dimensions. The model may be sliced, to view the cross-sectional geometry at any point, in any of the three dimensions that were originally scanned.

The resulting 3D CAD model shown in Figure 52 was subsequently used to produce the STL file in Figure 49.

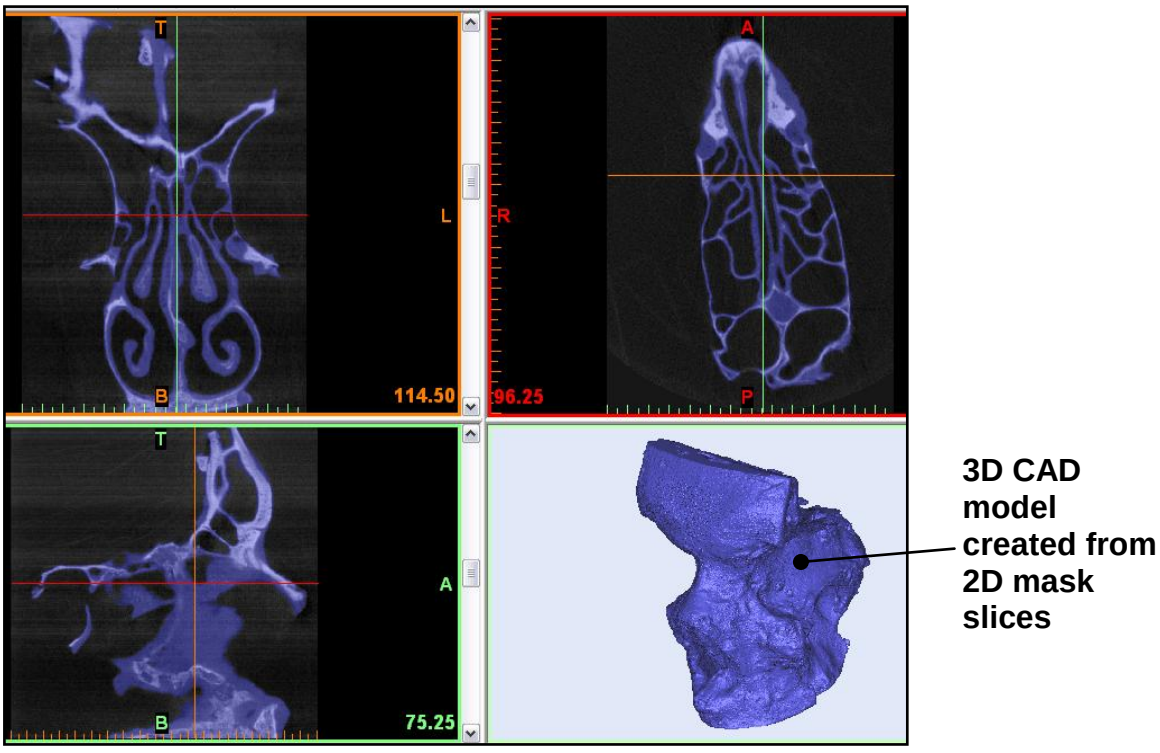

Figure 52: 3D CAD model created from blue mask

Once the user is satisfied with the resulting 3D CAD model, it may be exported to other software for AM, visual analysis, investigation or further manipulation. In the case of this research, the model was exported to other software and the anatomical data manipulated. The means by which this is done, however, must first be defined through the analysis of the suitability of different alternatives.

6.2.2 Exporting Medical Data from Mimics

One of the key factors in the use of real medical data in this research is the ability to customise the anatomy for the simulation of specific cases. In order to do this, the data will need to be exported from Mimics into another software package, as customisation in Mimics is limited to the application of threshold levels and morphology operations.

A program that has the capability to alter medical data directly from Mimics after manipulation is required; 3D CAD modelling software which can manipulate models, and subsequently produce the STL files required for AM production is the most suitable option. A potentially suitable 3D CAD modelling software package is UGS NX5 (NX), but its capacity for use with medical data had to be verified.

The capability of NX to import and manipulate medical data in different formats was assessed by analysing the quality of imported medical image slice data and attempting to alter some features of the geometry. It is known that NX cannot manipulate the raw 2D medical images taken from, for example, CT scans. NX must be provided with a 3D model, from which further steps may be taken. An investigation was launched to find a file transfer type that permits the user to alter the geometry of the medical data contained. Two standard file types were used and compared for their suitability: STL and Initial Graphics Exchange Specification (IGES).

The STL file format approximates 3D models as surfaces comprising a large number of triangular facets. The larger the number of facets (known as triangle density) the closer the approximation of the model is to reality. When imported into NX, the STL

file of the split model in Figure 48 appeared as a surface representation of a 3D model with faceted surfaces (Figure 49), as expected.

This type of model is completely non-editable in NX, as the model is represented as surfaces only; a hollow shell. This option was therefore determined unsuitable for use in the anatomy customisation aspect of this research.

The IGES file format was used to export the 3D model as a stack of separate layers. The layers are 2D slices through the model, although not necessarily the original medical data slices; the space between each IGES layer may be defined by the user as a means of controlling the resolution of the new model. Each feature on a layer is defined as an outline, represented by a 2D spline (line) in the CAD software (Figure 53). A 30mm vertical section of a skull was imported from Mimics into NX in IGES format, with layers spread 0.2mm apart. The resulting CAD model is shown in Figure 53:

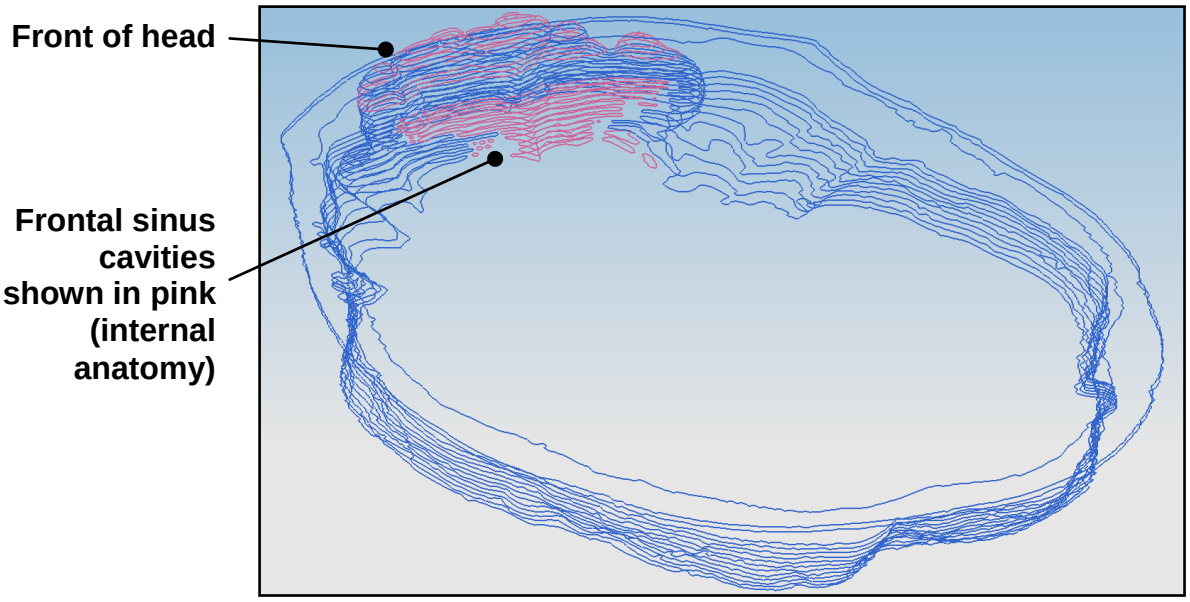

Figure 53: IGES splines from CT scan data imported from Mimics into NX

External and internal geometry are clearly defined, if the original medical data is of adequate resolution and quality. The shape of the 3D model first seen in Mimics may

be subsequently reproduced in NX by creating a solid that passes through all the splines.

The geometry of the splines is defined by nodes along their length, which may be individually moved to alter the geometry of that layer; this meant that the IGES format could be suitable for use in the customisation aspect of the research.

Figure 54 shows an enlarged view of the front of the head and frontal sinus cavities as seen in Figure 53. Each node in Figure 54 may be manually dragged, or automatically moved to a user-defined location, changing the geometry of the spline. The splines shown in Figure 54 map out the internal shape of the frontal sinus cavities layer by layer, as defined by CT image data.

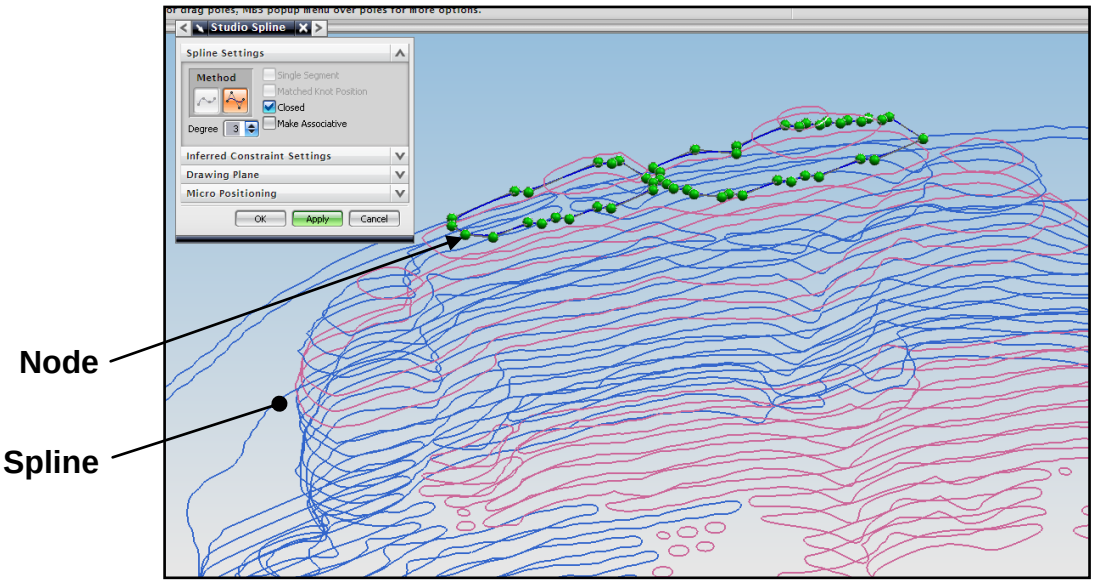

Figure 54: Editing geometry of 2D splines from IGES file using nodes

In NX, there are alternative methods of defining spline geometry, as illustrated below. In the 'Through Points' method, the spline passes directly through all the nodes. The curvature of the line may be defined by the user in 'degrees' of one or more, to alter the interpolation of the spline between each node. Increasing this degree of curvature will make the line smoother (as shown in Figure 55*a)*) or, with a degree of 1, jagged (as shown in Figure 55*b)*):

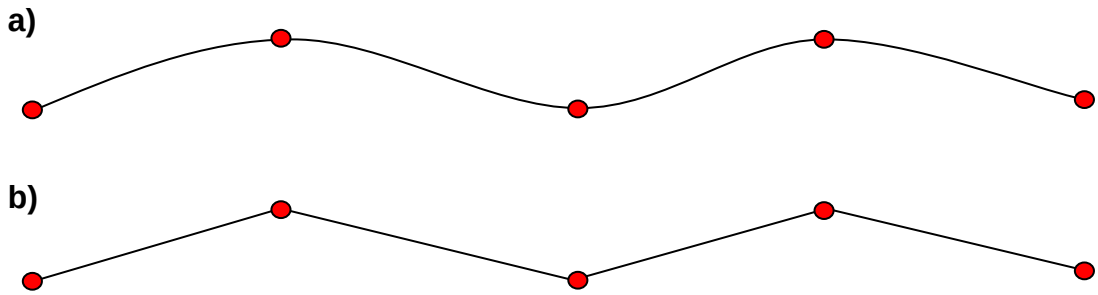

Figure 55: Nodes controlling 2D spline geometry – 'Through Points', degree of curvature *a)* 3, *b)* 1

In the 'By Poles' method, the nodes do not sit directly on the spline, but instead 'pull' the spline towards them as it passes around the series of nodes. This is shown in Figure 56, with the five nodes in the same positions as above. Alteration of the degree of curvature increases or decreases the influence of the nodes on the geometry of the spline.

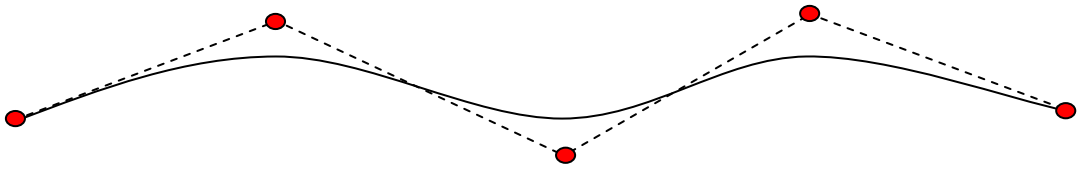

Figure 56: Nodes controlling the 2D spline geometry – 'By Poles'

These two possibilities will be compared for their suitability and ease of use for creating a realistic anatomical model from the IGES splines in NX. This took place once it became possible to manipulate real medical data in NX, and is described in Section 8.2.2.

When investigating the suitability of the IGES file format for use in NX, it was found that the spline layer model produced from conventional CT scan data, as used by surgeons and medical staff to assess the geometry and formation of bone and pathology within the sinuses, was not a clear representation of the anatomy. This was due to the thresholding stage, which takes place during the manipulation of the medical image set in Mimics, not having adequately defined the anatomical geometry clearly enough for use.

As conventional medical CT scans operate at a safe level for the patient, the clarity of the results is not as high as, for example, µ-CT, which is not used on living subjects. Medical CT scans produce a typical resolution of 0.5-1.0mm at a layer thickness of 1mm, whereas µ-CT images have a resolution of 0.005-0.100mm, at a layer thickness of 0.1mm. Due to this lower level of resolution, when thresholding the medical CT image slices, more data is lost at the very boundary of the threshold level selected, as the difference in density between some areas is not as clearly defined. This results in an IGES file that contains outlying features and falsely adjoining cavities.

µ-CT data of a cadaveric sample will therefore be used at first in this research to investigate and develop customisability, for the improved clarity of the results and ease of identification of specific features. This data was taken from a cadaver head, which had been sectioned to leave the majority of the sinus region intact. If the process of customising the medical data is verified with µ-CT data, a clearer and more representative 3D model will be produced from CT scan data for the remainder of the research. The 20-spline layer section of the µ-CT data imported into NX in IGES format, with layer thickness 0.1mm and degree of curvature 3 is shown in Figure 57.

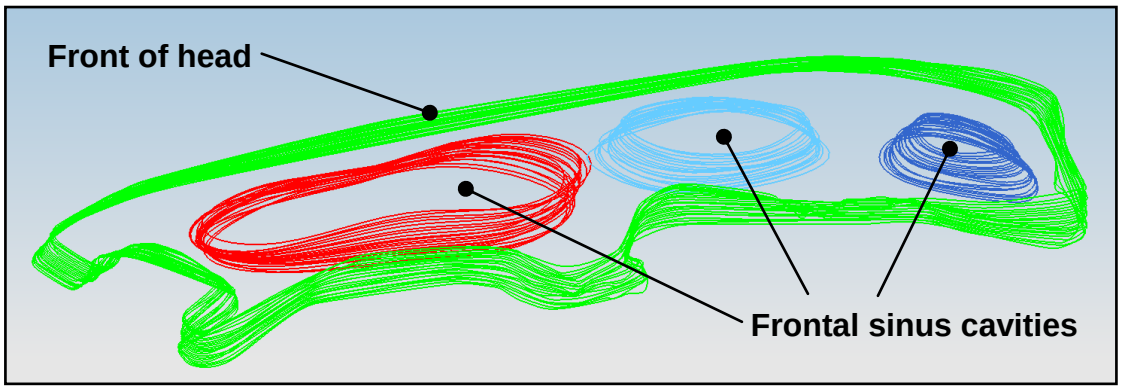

Figure 57: IGES splines from µ-CT scan data imported from Mimics into NX

The settings available to the user were also studied, to ascertain their effect on the resulting IGES model in NX and to identify the most suitable model for use in the research. When creating the IGES file in Mimics, the user is offered the following customisation options:

- Minimal segment length
- Out-of-line distance
- Hatching space and colour hatching space (X and Y)
- Minimal contour length: all contours/inner contours
- Layer thickness
- First layer height
- Scale factor

The last three options should be inputted to match the details of the imaging scan that was performed. Initial trials yielded files that contained splines consisting of hundreds of nodes each. This was unsuitable for efficient customisation of the model, and a means of reducing the number of nodes per spline before exporting the file from Mimics was explored. By increasing the minimal segment length, the spaces between nodes is increased, reducing the total number of nodes; the same effect is achieved through the increase of the out-of-line distance, with negligible effect on the geometry represented.

As the anatomical geometry of the 3D CAD model is fully customisable by altering the position of 2D spline nodes, the IGES file format, with NX, were deemed suitable for use in the anatomy customisation aspect of the research. NX links with Mimics, to successfully alter the geometry of files exported in IGES spline format. Visual Basic links with NX to control most functions of the CAD software, the details of which will be described in Section 6.3.1. In addition, NX is readily available to the research, and the software has been used extensively in the past. The combination of these software therefore offers the required functionalities for this research.

6.3 Customisable Models of Sinus Anatomy

As described in Section 6.2.2, the method to produce a customisable anatomical model found most suitable for implementation in this research was to use Mimics to handle the raw medical imaging data, before exporting a 3D model in IGES format to NX for further manipulation. This method was selected due to the ease with which the

IGES file could be altered in NX, albeit by skilled users of the software, using the 2D closed-loop splines that form the 3D model.

However, it is likely that most medical staff will not possess the skills required to perform this work, making them unable to directly customise the model. Medical staff must be given the opportunity to work on the model themselves, through a method that does not require expert knowledge of CAD systems or Mimics, to represent the pathology they wish to exhibit on the model. This section describes the investigation of the most suitable means by which users from a medical background could customise the 3D CAD model of the sinus anatomy.

6.3.1 Controlling NX using Visual Basic

If the customisation stage described above is to be introduced into the production process of customised models, it must be suitable for use by surgeons and other medical staff. This, at present, is not the case, as the software requires a large amount of training to use in an efficient and accurate manner. As this software is the most suitable way of altering the sinus models, and training on the software is not viable for all users, a way for the user to apply customisation without directly interacting with the CAD software must be devised.

A feature of NX is 'NX Open', which provides the ability to use programs written in, among other formats, Microsoft Visual Basic (VB) to control the modelling software, making it possible to execute almost all tasks that may be performed directly in NX through an interface designed in VB. The advantage of this is that only the relevant tasks and tools need to be included on the VB-designed interface window, drastically reducing the amount of knowledge of NX required by the user. This type of interface presents a very clear opportunity for the control of NX by users who have no knowledge of 3D modelling in CAD software. Nonetheless, the interface must still be simple, easy-to-use and intuitive, to allow these inexperienced users to control and apply changes to medical data. The stages of investigation of this possibility are described in this section.

Firstly, the specific requirements of the final customisable model were determined. These were set after consultation with partners at Queen's Medical Centre (QMC), who stated the features of the virtual and resulting physical model that they felt would be beneficial. These features were defined as:

- Ability to simulate swelling, tumours and resulting constriction/expansion of separate areas of the physical geometry (as described in Section 3.2)
- Clear definition of original and diseased/problematic anatomy (e.g. different colours)

The first requirement would involve direct alteration of the medical data by the user, ideally through an intuitive interface with the software. The second requirement would be an inherent feature of the finished model, which would not necessarily need to be controlled or altered by the user.

In order to create an interface through which medical staff could simulate swelling of the sinuses and tumours within the sinuses, the interaction between VB and NX was examined and an understanding of the programming that would be required was gained.

6.3.1.1 Examining the VB Code Created by NX

The principle method of doing this was through using the 'journaling' function in NX. This function works in the same way as a macro, by recording a range of actions performed by the user in the CAD software, to be automatically replayed later. NX has the capability to record these actions and represent them as VB code, which may subsequently be implemented into a VB form script to be used when required.

In order to investigate the way in which common tasks are represented in VB script, some simple examples were trialled, the first of which involved the creation of a block of dimensions 100x100x100mm. The code shown in Figure 58 is unique to the block creation program:

```
markId2 = theSession.SetUndoMark(Session.MarkVisibility.Visible, "Block")
...
Dim originPoint1 As Point3d = New Point3d(0.0, 0.0, 0.0)
blockFeatureBuilder1.SetOriginAndLengths(originPoint1,"100","100","100")
...
End Sub
End Module
```

Figure 58: Block creation VB code

These lines of code start the block creation tool in NX and then describe the properties of the block, so that these properties are recreated and the block is produced when the code is run in NX Open. Figure 58 can be seen to contain the start point co-ordinates of the block in (x, y, z) format `(0.0, 0.0, 0.0)`, named "`originPoint1`". The dimensions of the block in relation to the start point are then defined `(originPoint1,"100","100","100")`. By examining the code created by creating blocks of different sizes, the way in which the new dimensions are represented in VB was determined and understood. The next, vital stage of investigation was built around determining whether the code could be manually altered to achieve different results. This would be necessary to fulfil the criteria of the final interface and customisable model.

6.3.1.2 Altering the VB Code Created by NX

The possibility of changing the code manually was first tested by attempting to alter the x-dimension of the created block. The line:

```
blockFeatureBuilder1.SetOriginAndLengths(originPoint1,"100","100","100")
```

was altered as shown in Figure 59 to read:

```
blockFeatureBuilder1.SetOriginAndLengths(originPoint1,"50","100","100")
```

Figure 59: Geometry definition of block by manually altering dimensions

The code automatically produced a new block, with dimensions of 50x100x100mm as expected. The next stage of the investigation assessed the possibility of using variables within co-ordinate sets, for example "(x, y, z)", where the variable values have been defined earlier in the code. This was fundamental for the production of shapes and bodies whose sizes are not fixed, or depend on other user actions (such as size selection). This was again tested using the block example, as shown in Figure 60:

```
Dim x As Integer = 30
blockFeatureBuilder1.SetOriginAndLengths(originPoint1,x,"100","100")
```

Figure 60: Geometry definition of block by using variable in dimension definition

The first line uses "`Dim`" to define the variable "`x`" as an integer, and supplies it with the value 30. When `x` is entered as part of the co-ordinate set, the value of 30 is returned and used as the size in the x-dimension. This code functioned correctly, creating a new block with dimensions 30x100x100mm.

Next, the investigation determined whether variables may be altered within the co-ordinate set. In Figure 61, the x-dimension of the block was defined using the variable "`x`" as above, then adjusted within the dimension definition:

```
Dim x As Integer = 30
blockFeatureBuilder1.SetOriginAndLengths(originPoint1,x+10,"100","100")
```

Figure 61: Geometry definition of block by altering variable within dimension definition

This would make the alteration of co-ordinate values with other variables possible, such as user-selected size multiplication or translation factors. This example produced the block of required dimensions 40x100x100mm, and showed that variables may be used and altered within the co-ordinate set. The ability to create code in this manner proved to be vital for the tasks that were to be performed later.

Now that an understanding of the coding used to control simple tasks in NX had been gained, the next step was to assess the ability and effectiveness of VB to control the

shape of splines, the importance of which was described in Section 6.3. By creating and altering simple 2D splines, and examining the VB code produced when these actions were recorded, it was found that every spline has an automatically provided 'codename'. This codename appears in VB code as shown in Figure 62:

```
Dim spline1 As Spline = CType(workPart.Splines.FindObject
      ("HANDLE R-1525"), Spline)
```

Figure 62: 2D spline codename definition in VB code

On this line of the code, the spline with the codename `"HANDLE R-1525"` is to be found in the CAD model and renamed "`spline1`" for use within the rest of the code. What follows Figure 62 is a description of the properties of `spline1`; it is here that any changes may be made. The spline properties described include the co-ordinates of the nodes, line type ('Through Points' or 'By Poles') and the degree of curvature. Firstly, the co-ordinates of the original spline are defined; after this, the co-ordinates may be redefined, to alter the appearance and geometry of the spline. All changes made to the redefined co-ordinates and line properties will be applied to `spline1`, until the next spline is ordered to be 'found' in the CAD model using its automatically assigned codename, and the properties of `spline2` are described. So, for example, in a model of stacked 2D splines, code written in VB can automatically apply changes to a specific layer of the model by finding the spline with the appropriate codename, then altering the co-ordinates of the spline nodes to match those described in the code.

6.4 Manufacture of Customised Sinus Surgery Simulation Models

White bone structures are cancellous, possessing a hard outer surface with a more porous internal honeycomb structure; this may be mimicked by 3D printed parts [169] simply through the automatic print strategy of the machine (see Section 2.4.1).

The intricacy afforded by 3DP is a definite requirement for the physical replication of the bones and structures involved in sinus surgery. 3DP, as described in Section 2.4 is

able to achieve higher accuracy than clinical CT scanning, as used for imaging of the sinuses in live patients [170]. At present, 3DP is able to produce parts to a resolution of approximately 0.1mm, whereas CT has a maximum resolution of around 0.4mm owing to the large field of view and pixel size, and voluntary or involuntary muscular motion [171].

As imaging and AM develops, the achievable accuracy in both processes will no doubt improve, allowing more precise and true-to-life models to be constructed. It is felt, however, that as long as the surgeons and other parties involved with the use of the biomodel are aware and understand the extent of the inaccuracy, assist in their production and design, and know of any physical attributes of AM parts that may affect the model's quality, the effectiveness of their use and the possibility for improved patient treatment should not be compromised [172].

The 3DP process also has the capability to produce parts that are externally printed in 24-bit colour [30], a great advantage over other AM processes. The use of colour in surgical training and preoperative planning for surgeons is vital; to accurately represent the situation of live surgery without risk to patients will contribute greatly to the understanding of the case and subsequently the quality of the skills acquired or operation performed. Lim and Zein state that the use of colour in AM models in this area will "contribute endlessly to the simulation of surgical treatment, technical training and medical education" [173].

The capability to produce coloured anatomical models would allow the visual characteristics of the sinuses to be represented for students during practice surgery, along with vital organs or hazardous areas. Training models for various levels of skill may be produced, to cater for the learning curves of different students, whereby vital features and organs are, at first made more obvious to the user, before the colouring of these areas is gradually reduced to a more realistic level.

6.5 Hypothesis

As discussed earlier, the possibility of operating on an anatomically accurate, visually and physically realistic manufactured model of the sinuses of a specific patient would be extremely beneficial for both trainee and working surgeons.

When considering the training of surgeons, the provision of the opportunity to create models for a certain purpose, that exhibit specific pathology for focussed or tailored training and assessment is extremely valuable. This requires a level of customisability to be presented to the medical staff, whilst maintaining the anatomical and physical accuracy and realism, and subsequent validity of the model at its highest.

By allowing the model to be customised to present pathology, as designed by the surgeons involved, the users would be able to practice and improve their performance of a specific procedure, with defined restrictions as many times as was necessary. This case could provide a regular training exercise, represent the worst case scenario, or show the predicted progressive stages of disease. This customisation could occur using a set of specific patient data (for planning purposes) or a base model that, at first, exhibits no problems but may be made to simulate any issue for teaching, training or communication purposes.

As discussed in Section 3.1, the paranasal sinuses and surrounding anatomy display a wide range of physical properties and characteristics during surgery. It is believed that the versatility of 3DP can be used to simulate these physical properties, through variation of print strategy, build material, binder solution and methods of post-processing or infiltration, to create a physical operation simulation model for training purposes. This will help to avoid the use of cadavers in surgical training, and the associated ethical, financial and educational issues. The involvement of surgical students with live patients will also be postponed to reduce risk to the patients' wellbeing, until a required level of skill can be shown to have been reached.

As described in Section 6.3, there is a significant challenge associated with the production of customised training models for the training and rehearsal of sinus surgery; the people customising the cases will be likely to have a low level of experience in the design and production of AM models. Customisation of the physical model must take place prior to manufacture, as any later alterations would require skilled manual interaction with the model. Customisation must therefore be performed in 3D CAD software, as the 3D CAD model is used to produce the input to the 3D printer, through export in STL format. However, the medical staff that are required to customise the model will also be likely to have no experience of using such software.
If 3D CAD software is to be used to customise the model, medical staff must be made able to use the software. This will be achieved through the development of a Graphical User Interface (GUI) in VB, which will allow the user to control elements of the CAD software remotely. With a GUI, the user may perform set tasks with some input, to affect changes on the model and produce the desired result, removing the need to fully understand and have comprehensive experience of using the CAD software. This will be implemented to place the user in control of the application of swelling and tumours, as described in Section 3.2, to a 3D CAD model of sinus anatomy.

The GUI, to be named “Case Creator”, is designed to fit into the process of physical case simulation model production as shown in the flowchart in Figure 63:

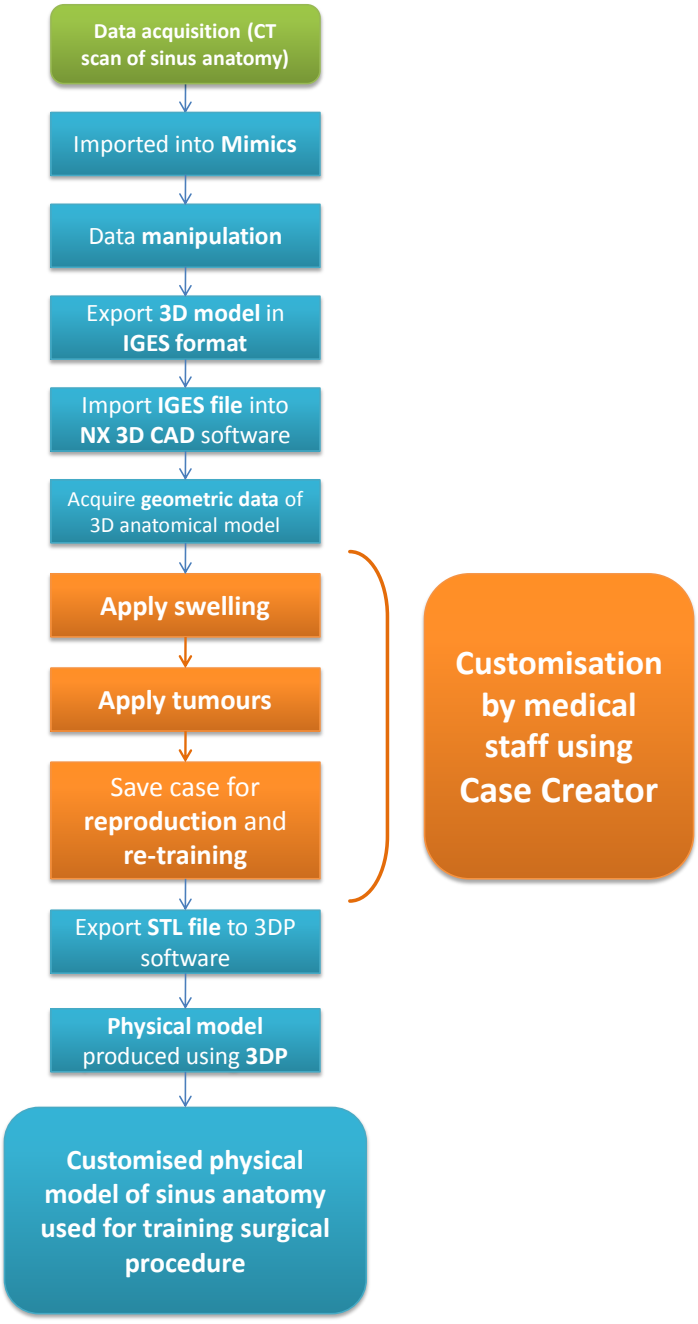

Figure 63: Flowchart of customised anatomical model production

As shown, CT medical imaging data is acquired (as described in Section 2.2) and imported into data manipulation software such as Mimics. From this software, a 3D model may be exported in IGES format (which may be manipulated using 3D CAD software, as discussed in Section 6.2.2).

The knowledge gained about the way in which NX and VB interact in Section 6.3.1 will be used to allow the user to alter the geometry of splines in NX. This will be done by the user only interacting with the CAD software through the GUI built with VB. At all times, the focus will be firmly placed upon ease of use, applicability to patient anatomical data and realism of applied pathology. Several functionalities were defined for the interface through the investigations described earlier:

- Use real patient data
- Application of swelling to sinus cavities
- Application of tumours/polyps to sinus cavities
- Simple and fast recreation of previous cases

Case Creator will fit into the latter part of the model production process, taking the imported data from the medical imaging manipulation software and allowing the user to apply anatomical changes, prior to the model's manufacture using 3DP. Without the need to interact directly with the complex CAD modelling software, a user from a medical, surgical or training background will be made able to design physical simulation models that exhibit the pathology they have defined.

The next chapter defines the methodology of the project, leading on from the initial investigations described in chapters 2 to 6.

CHAPTER SEVEN

METHODOLOGY

7 Methodology

This chapter defines the methodology employed in creating the customisation tool, in order to meet the aims and objectives of this part of the larger project.

The work performed in this research was focussed on the end use of the customisation tool by medical staff, to lead to the production of a visually realistic model by 3DP; as such, the project was redirected and evaluated at regular intervals by clinicians. This process ensured that the work being performed never strayed from the requirements or expectations of the end users, and problems with customisation, ease of use and realism were dealt with promptly under the supervision of the clinicians.

The design of the customisation tool was undertaken with an iterative approach. The design task was complex, and relied upon the assessment of the tool's ability to perform the required customisation as each function is added. Once the methods by which customisation, ease of use and realism were achieved had been set, the methods were developed to enhance each of these features further, aiming to achieve the optimum solution. This had to be performed in an iterative manner, to provide a robust base on which to develop each function. As greater understanding was acquired of the software and methods being used to create the tool, further development took place to increase the capabilities of the tool. The iterative design of the tool also allowed the clinicians involved in the project to view a working version of the customisation tool in order to use the tool, form opinions and make suggestions for development.

The project plan is illustrated in Figure 64, and addresses each of the objectives set out in Section 1.4. Following on from the definition in the last chapter of the most suitable approach to enabling unskilled CAD users to customise medical data, the next step of the project plan was to begin work on the development of methods to achieve this (at approximately one year into project plan).

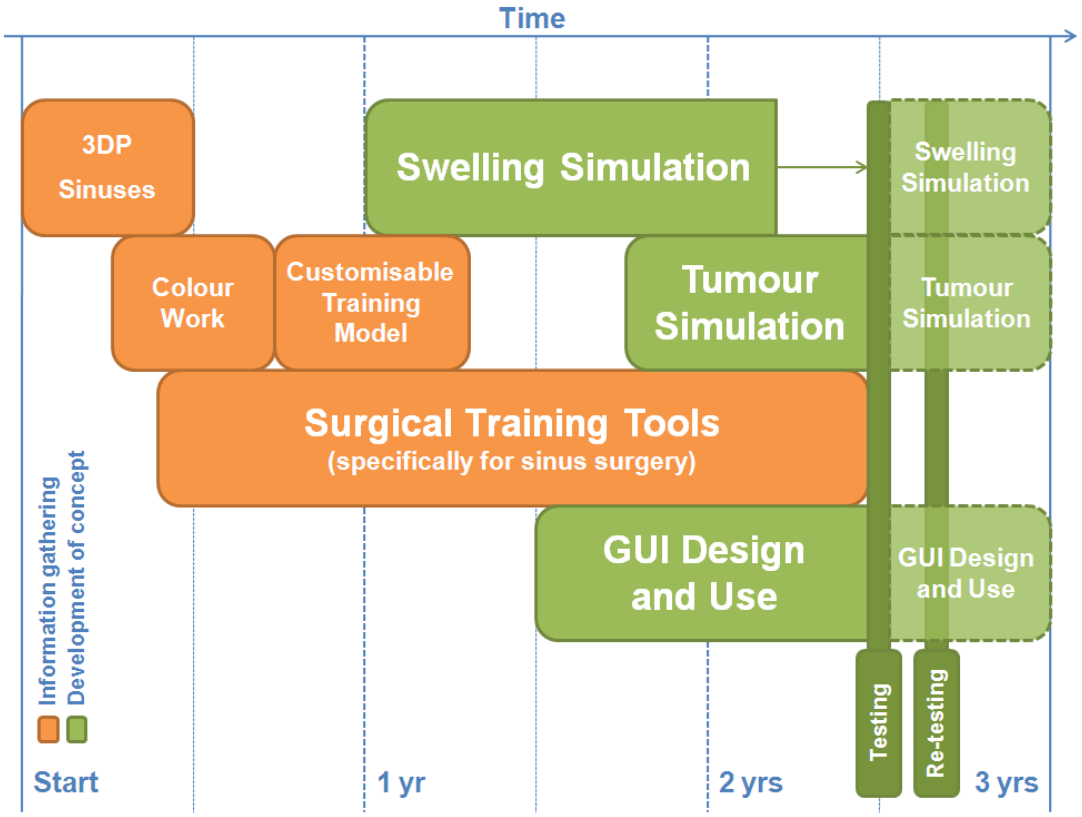

Figure 64: Gantt chart of project plan

As Figure 64 shows, the first program function to be developed was the application of swelling to the 3D CAD model in NX; this work lead into and formed the basis of the simulation of tumours in the model. Investigations into customisation techniques continued for approximately three months while the swelling simulation method was developed, to develop more suitable methods. The iterative design approach, in which versions of the program were created, then updated as new concepts were developed, meant that the methods used to achieve any customisation could be changed as new options were discovered and greater understanding was gained about the programming used. The adoption of this approach also meant that the simulation of the two types of pathology could influence each other, and the technique chosen for the application of swelling could be altered once the development of the tumour application system was started. This happened after approximately nine months of

work focussed on the application of swelling to the model, and initially drew heavily on the swelling application method that had been developed.

Developments in the application of swelling to the 3D CAD model allowed the requirements of the GUI to be defined, and the inclusion of the necessary controls formed an integral part of the swelling simulation method design. The optimum design of the GUI was considered, and a range of designs were created using VB throughout the process of developing the swelling and tumour simulation functions. These were viewed by clinicians to gain an understanding of the suitability of each design, before the undertaking of two product trials with users from the target audience. Testing only took place once a robust design that met all the project objectives had been developed. After the first trial, user responses and suggestions were taken into account to allow some development to take place between the two trials, and the altered aspects of the program to be compared to their predecessors. Final alterations and recommendations for further work were made before the end of this part of the larger project.

The program trials aimed to generate the maximum amount of feedback from users, in order to make structured and reasoned improvements to the program before re-testing. To this end, the trials were opinion-based to assess the fulfilment of the project objectives: ease of use, suitability of controls, types of customisation, realism of results and benefit to the end user with a questionnaire to be completed by participants. Qualitative and quantitative questions were used, to allow responses to be grouped and directly compared against one another, whilst providing the opportunity for users to elaborate on their opinions of the program.

It was the aim of this project to provide customisation on as close to a continuous scale as possible, to closely mimic real life. This allows the users of the program to design their own training models, as opposed to selecting from a pre-defined list of models defined by an outsider. The type of customisation ideally required by this research could therefore be termed “full customisation”, whereby the user is given the

opportunity to alter any aspect of the pathology in the model to any degree, offering a limitless source of practice and experience for trainee surgeons.

For this research, NX is used by medical staff, through the guidance of the GUI. NX provides the user with a 3D view of the anatomy both before and after application of pathology, which offers an advantage over the 2D medical imaging data currently used in the training and diagnosis of disease and surgery planning, and the static images that are used in some user-customised design tasks (such as web-based clothing design).

A method for the medical staff to customise a set of medical data to exhibit the effects of swelling in the sinus cavities, prior to producing the physical model, was the first to be investigated and is described in Chapter 8.

CHAPTER EIGHT

CUSTOMISABLE SINUS SURGERY TRAINING MODEL – SWELLING APPLICATION

8 Customisable Sinus Surgery Training Model – Swelling Application

This chapter describes the work undertaken to develop the methods to allow the user to implement cavity swelling to the model, as shown in the project Gantt chart in Figure 64. Figure 65 shows a detailed plan for the development of the swelling simulation function of the program.

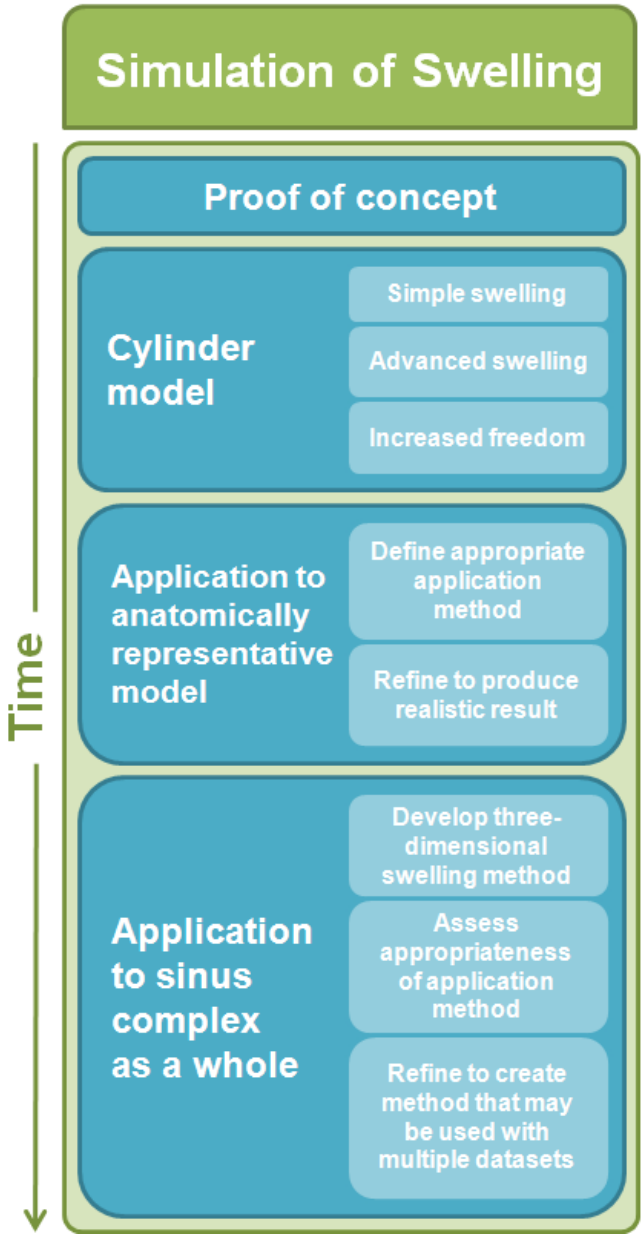

Figure 65: Plan for development of swelling simulation function

The proof of concept was achieved in Section 6.3.1, where VB code was altered and re-used to control NX modelling tools. The next stage of investigation was the application of this knowledge to the simulation of swelling in a simple model.

8.1 Horizontal Swelling - Exploratory Work

The first functionality to be programmed for use in Case Creator was the application of swelling to sinus cavities; this could be simulated through the alteration of individual splines throughout the model. It was the aim of this functionality to be able to accurately and simply simulate swelling in a completely customisable manner. In order to monitor the development of Case Creator and compare the capabilities of different versions of the program, a scale of customisability was devised. The scale is described in Table 7:

Customisability	Action
Level 0	Swelling automatically applied, same position/severity every time
Level 1	Option given to apply swelling, automatic position
Level 2	Option to apply, catalogue offers selection of severities, auto position
Level 3	Option to apply, catalogue of severities, different positions available
Level 4	Option to apply, different positions, severity altered manually
Level 4+	Option to apply, different positions, severity altered manually (finer scale)

Table 7: Levels of customisability for the application of swelling

In traditional training methods, using live patients or cadavers, specific cases can be chosen that exhibit swelling; however this clearly could not be altered at the will of the trainer, roughly equating the use of human bodies in the training of sinus surgery to a customisability of Level 1. The ideal level of customisability in the application of swelling using Case Creator is Level 4+, which provides the user with a large amount of design freedom to create a wide range of simulation models.

8.1.1 Swelling in Simple Cylindrical Model

The first model that attempted to realistically simulate clinical cases had to use geometry that may be clearly constricted or expanded. This was achieved in the form of a cylindrical tube through a rectangular block, as shown in Figure 66:

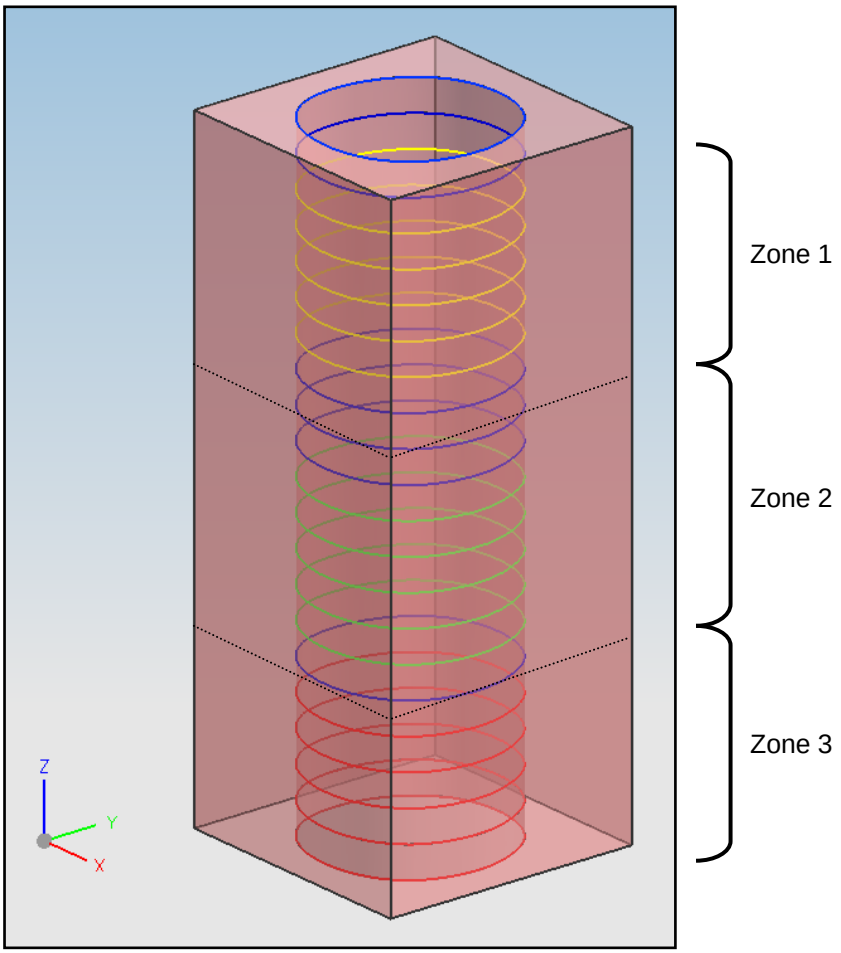

Figure 66: Tubular cavity through a block, consisting of 21 spline layers

The tube was formed by creating a cylindrical solid which passed through 21 identical, roughly circular 2D splines, and subtracting it from a block to represent a sinus cavity on the layers of a CT scan. The aim of this exercise was to create a VB interface that would allow the user to easily alter the tube's geometry as required.

At first, the level of customisation was restricted to a set case which could be applied, in order to ascertain the success and applicability of this approach to guided geometry

alteration. The circular layers were controlled by fifteen nodes around their circumference, to represent the way in which IGES files are embodied in the modelling software. Fifteen was chosen as an arbitrary number of nodes, but allows an adequate level of detail to be simulated by each spline, to assess the performance of the geometry alteration system. The nodes were positioned evenly around the circumference of each layer, as shown in Figure 67:

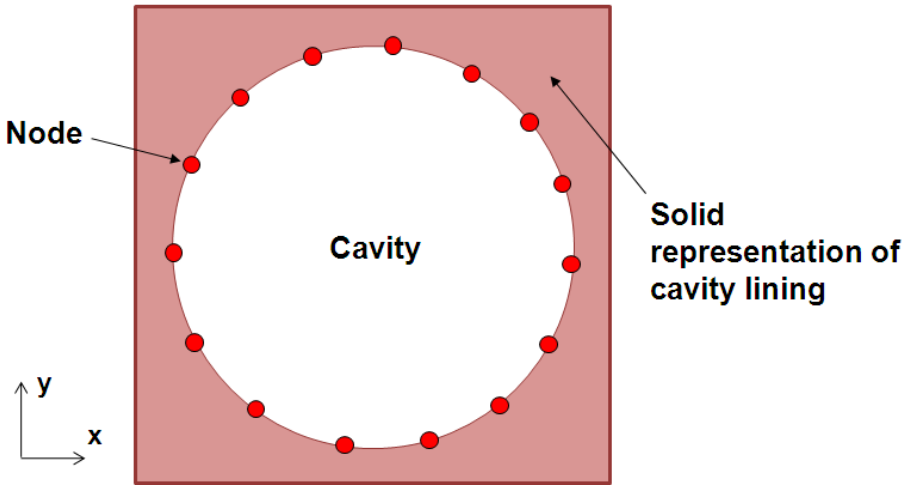

Figure 67: Circular cross-section with fifteen nodes on circumference

The first stage in this part of the exercise was to manually apply new co-ordinates to some of the points on the circular layers, in order to simulate constriction of a certain area of the tube. Nodes were moved inwards to simulate swelling in that area of the cavity wall, as shown in Figure 68. The new co-ordinates were recorded and entered into the VB code as described in Section 6.3.1.2, replacing the original x- and y-co-ordinates in the definition of each point. The tube (Figure 66) was divided vertically into 3 zones as shown, to allow different conditions to be simulated in different areas of the tube. In zone 1, the end of the tube became narrowed, with all-around constriction; in zone 2 one side of the tubular cavity became constricted due to swelling of the cavity wall (as in Figure 68); and in zone 3 the opposite wall moved further into the centre of the cavity.

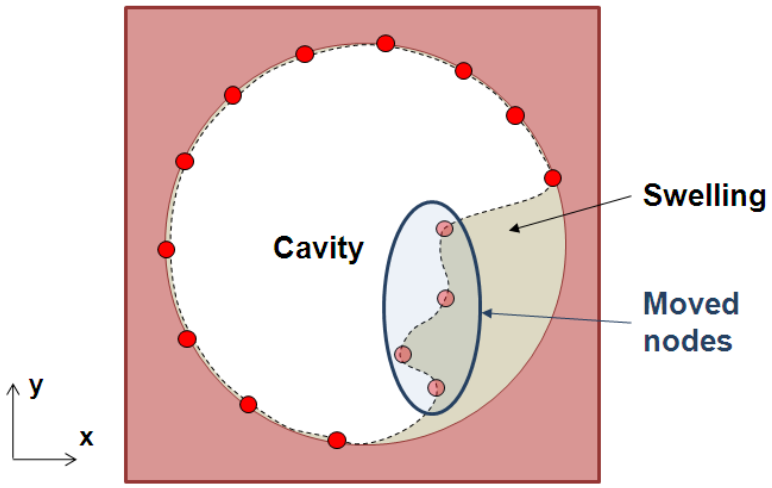

Figure 68: Circular cross-section with swelling applied

The GUI was designed to allow the user to select which of the three vertical regions of the tube they wished to apply swelling to, by dividing the program into three corresponding sections. Three buttons were supplied on-screen for the user to apply changes to zones one, two and/or three, respectively, as shown in Figure 69. The coding for each button was identical, except that the splines controlled by each button were only those included in the appropriate zone, and the new co-ordinates for the nodes on each layer were those that had been manually applied, recorded and inputted earlier.

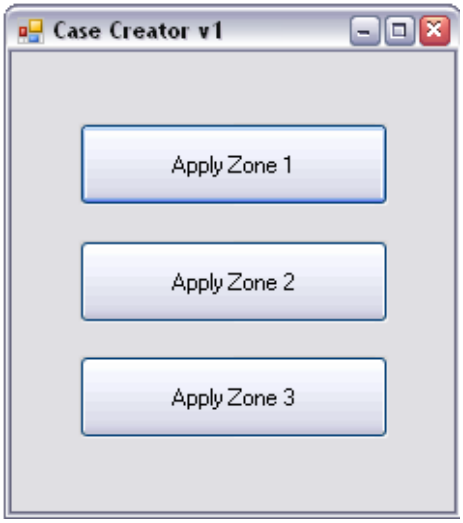

Figure 69: GUI for swelling application in three zones using buttons

When a button is pressed, the section of code for that button is run, affecting only the desired zone of the tube. Each spline (layer) is found by its `"HANDLE R-XXX"` value as described in Section 6.3.1.2, and the co-ordinates of the nodes around that layer are changed to those defined in the code. This produced the result of applying swelling to a certain region of the tube. This achieved Level 1 customisability as described in Table 7, allowing the user to choose whether to apply swelling (discrete variability – swelling is "on" or "off"), but with no input into positioning or severity. Figure 70 shows the effects of swelling in zone 1 of the tubular cavity, where the cavity perimeter has moved inwards towards the centre of the cavity:

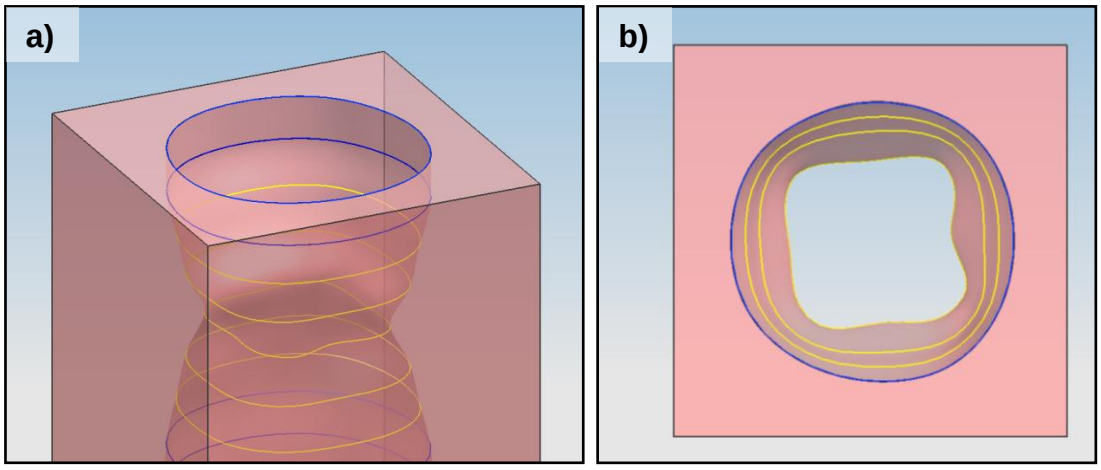

Figure 70: Swelling applied to Zone 1 of tube model shown from *a)* side, *b)* top

In order to provide the user with Level 2 customisability, a choice of different levels of severity was to be made available. A method was developed in which the user is asked to select from a pre-defined list of cases in each of the three zones: None, Low, Medium or High severity of swelling, forming a link to the severity rating system described in Section 3.2 to involve concepts that are familiar to the users of the program from a medical field. Each case, at each level of severity, was positioned and simulated manually, then recorded as a journal and the new co-ordinates entered into the code. The type and position of swelling simulated in each zone remained the same as in the previous version of the program, but the user was permitted to select the extent to which this swelling affected the anatomy. This was done by using conditional operators *If*, *ElseIf* and *Else*.

If-Then-Else statements form the root of conditional programming. This function runs sections of VB code depending on the satisfaction of an initial statement (*If-Then*). Should no statements be found to be true, the section of code is ignored and reading continues at the discovery of an *End If* line. Contingency statements may be included with code to be run should the initial statement be false (*Else)*. Other sections of code may be run in a prioritised order should a series of different actions be required (*ElseIf*). This is illustrated in the example code shown in Figure 71:

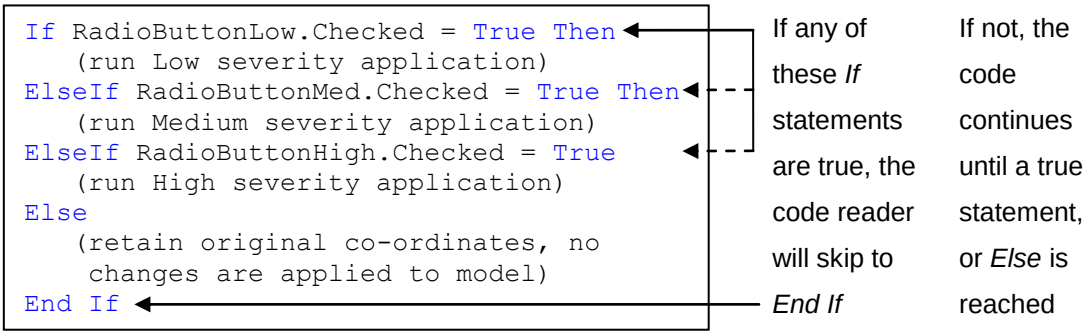

Figure 71: Sample *If-Then-Else* statement

Any number of *If-Then-Else* statements may be nested within each other, to perform further tests and perform the appropriate action. The GUI was altered to show a group of four radio buttons for each zone, from which the swelling severity would be selected. The changes to each vertical zone of the anatomy are then applied individually, and coloured feedback is given to signify the severity of swelling in each zone, as shown in Figure 72:

Figure 72: GUI for swelling application in three zones using radio buttons, four levels of severity

Changes were applied to the circumference of each layer cross-section, and the walls of the solid body smoothly integrated between each layer. This system allowed the user to apply four different cases, in all three zones on this model, equating to Level 2 customisability on the scale defined earlier in Table 7. Figure 73 shows the resulting case as set in Figure 72, with medium severity swelling applied to zone one, low to zone two and high severity swelling in zone 3.

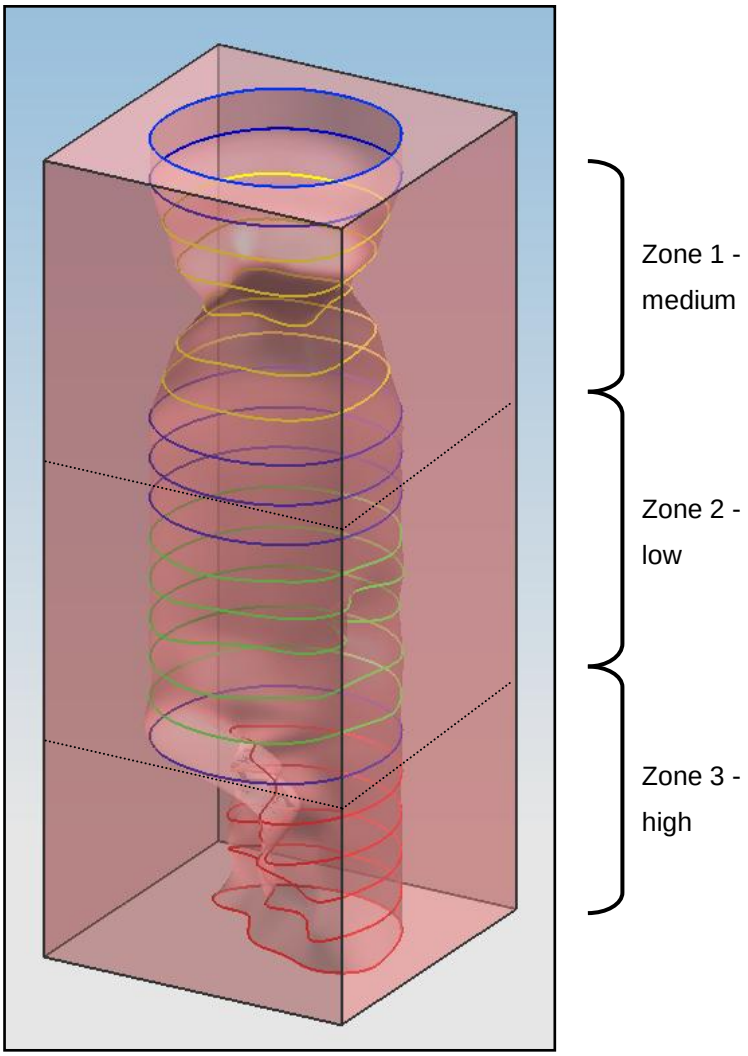

Figure 73: Three severity levels of swelling applied in separate zones of tube

However, more freedom is required in the alteration of the model, as the provision of four levels of severity in each zone was considered, by clinicians in collaboration with the project, to be too restrictive. Even so, the development of this feature required a large amount of new coding, as the set of co-ordinates for each case of swelling had to be entered into the code. This required four sections of code for each zone of the tube, to give instructions for None, Low, Medium and High severity cases, allowing $4^3 = 64$ possible cases.

The next versions of the program were focussed on the opportunity for further customisation, whilst reducing the amount of code used, consequently making the

program more easily altered. The user was given further design freedom in the form of sliding scales (known in VB as 'TrackBars'), allowing the co-ordinates of the layers' nodes in each zone to be changed in relation to the value selected on the scale (0-20). The use of the sliders instead of radio buttons meant that no conditional programming was necessary, as there are no discrete cases being created. This was done in a similar way to the investigative work done in the latter part of Section 6.3.1.2, using variables within the co-ordinate set that had been defined earlier in the code. The co-ordinates for each node around the layer circumference were listed as variables prior to the co-ordinates being altered, as shown in the example in Figure 74:

```
Dim x1 As Double = 36.784364092
Dim y1 As Double = 24.409309475
Dim z As Double = 15
```

Figure 74: Sample code extract of co-ordinate definition

These three lines define three variables (`x1`, `y1` and `z`) as numbers, and supply them with the values listed. The values `x1` and `y1` are used to represent the x- and y-co-ordinates of node 1 on the layer. The z-co-ordinate of the layer is constant for every node; as such it is used as "`z`" in every co-ordinate set. The use of `x1`, `y1` and `z` in the co-ordinate sets made it easier to make mass alterations to the code.

To allow the user to change these co-ordinates, the window displayed sliding scales, which were linked to each zone. The coloured feedback, signifying the severity of the swelling in each zone was retained, to maintain the link with the clinical severity rating system (Section 3.2). The GUI for customising the model using sliders is shown in Figure 75.

Figure 75: GUI for swelling application in three zones using sliding scales

In the code, the value shown on the sliding scale was integrated into the co-ordinates of the layers in the appropriate zone as shown in Figure 76:

```
Dim coordinates107 As Point3d = (x1 + TrackBarZone1.Value * 0.1, y1, z)
```

Figure 76: Sliding scale value integrated into co-ordinate definition code

In this line, "`TrackBarZone1.Value`" represents the value shown on the sliding scale for zone 1; it is used to increase the x-co-ordinate of this node by (0.1 x [sliding scale value]). The multiplication factor for the sliding scale value, 0.1 in this case, was tested and chosen in order to alter the model whilst retaining its integrity. If this value were too high, the points would move too far with each step on the sliding scale, causing modelling errors as nodes moved outside the surrounding block.

So in the case of this node, with a severity of 13 out of 20 selected on the slider, the new co-ordinates of the node are calculated as shown in Figure 77:

```
Dim x1 As Double = 36.784364092
Dim y1 As Double = 24.409309475
Dim z As Double = 15
```

Original co-ordinates:

```
   (36.784364092, 24.409309475, 15)
```

New co-ordinates:

```
   (x1 + TrackBarZone1.Value * 0.1, y1, z)
= (36.784364092 + (13 x 0.1), 24.409309475, 15)
= (38.084364092, 24.409309475, 15)
```

Figure 77: Calculation of new co-ordinates using sliding scale value

This method was used throughout the code, applying changes to both the x- and y-co-ordinates of the layers, to reproduce the swelling described earlier in a more gradual and controllable fashion.

The introduction of the sliding scales increased the number of possible cases that may be simulated to 21 in each zone of the tube; $21^3 = 9{,}261$ cases in total. This makes use of the manual alteration of the severity of the case, as listed in customisability Level 4, however the position of the swelling around each layer is still automatic. The ability to define the direction from which swelling occurs was considered to be an important function for Case Creator; this was to be addressed in the next versions of the program.

8.2 Developing Horizontal Swelling Application Method

The proof of concept was shown in Section 8.1. Progress was then made in developing the swelling simulation system with increasingly complex 3D CAD models.

8.2.1 Swelling in Anatomically Representative Geometry

As planned in Figure 65, the program was further developed through the creation of a more realistic model of the geometry of the frontal sinus. This shape was taken from CT and MRI images of patients, most of which displayed similarly shaped cavities in this area. In the example shown in Figure 78, the frontal cavity is visible on the right hand side, whilst the left side is swollen in this region and cannot be seen as clearly. The shape used in these trials was that of the swollen left hand cavity. This presented a challenge due to the increased level of complexity of the shape of the cavity. In order to accurately simulate swelling in the cavity, the points around the layers of the model would need to be treated and programmed individually; no two points would behave in the same manner once swelling was applied. Moving vertically through the whole model, the two separate cavities visible on this slice image may combine, or split into additional cavities.

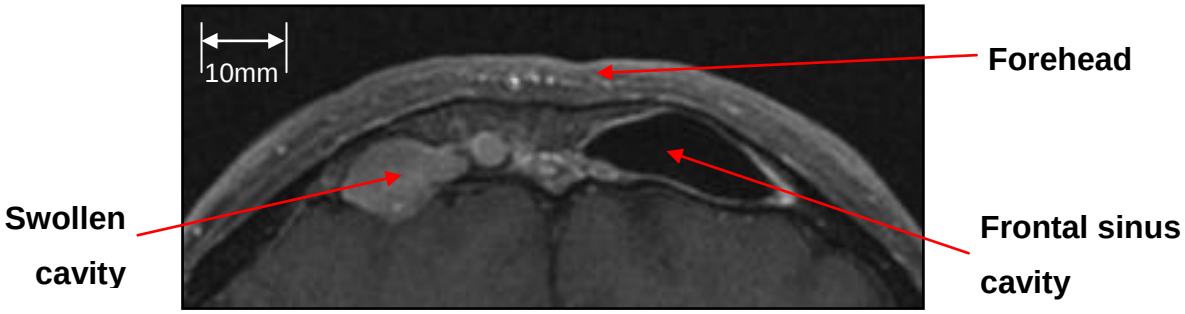

Figure 78: Frontal sinus cavity shown in CT scan, X/Y plane

As discussed in a meeting with Anshul Sama (clinical expert) at QMC, the problems affecting the frontal sinus are mainly based around the swelling of the lining of the cavity, and occasionally the alteration or creation of bony structures. This swelling may begin at any point around the cavity wall, and does not grow in a uniform fashion. In this model, a stack of nine 2D splines were created above one another, 1mm apart, to represent CT scan images. The same geometry was produced on each layer, for simplicity, again using 15 points.

The sliding scale method was used again, however the ‘zones’ from the previous versions of the interface were altered to be more applicable to the more realistic

geometry. Zones were added within each layer, therefore permitting the user to alter the swelling of the model on the left, right, or both sides of the cavity through the use of sliding scales. This was done by dividing the 15 points around the circumference of the cavity into two groups as shown in Figure 79, which were subsequently assigned to one of two sliding scales.

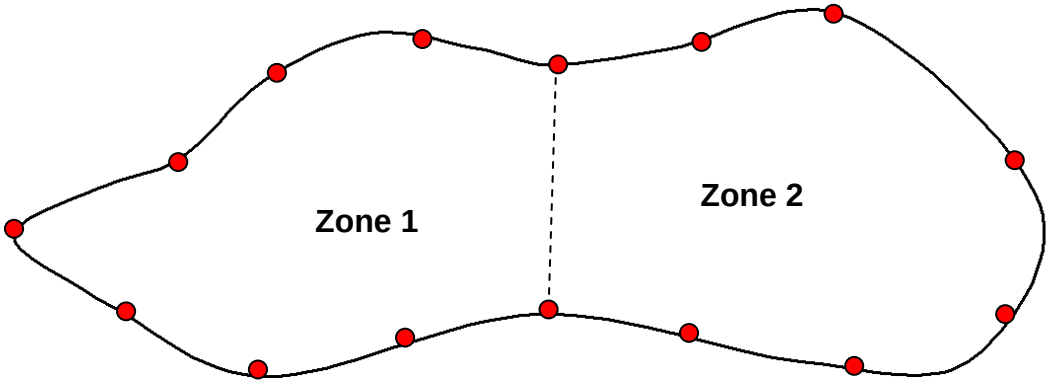

Figure 79: Nodes around frontal sinus cavity split into two zones, to be controlled separately

A new means of customisation was trialled, whereby swelling could be applied to the cavity prior to moving the sinus cavity wall inwards. This means that the user could apply swelling to the side of the cavity, constricting that end of the sinus, then move the whole side inwards, simulating further swelling (Figure 80 – left). Alternatively, the user may decide that no prior swelling is to be applied and that the end of the cavity should simply be moved inwards, as on the right of Figure 80:

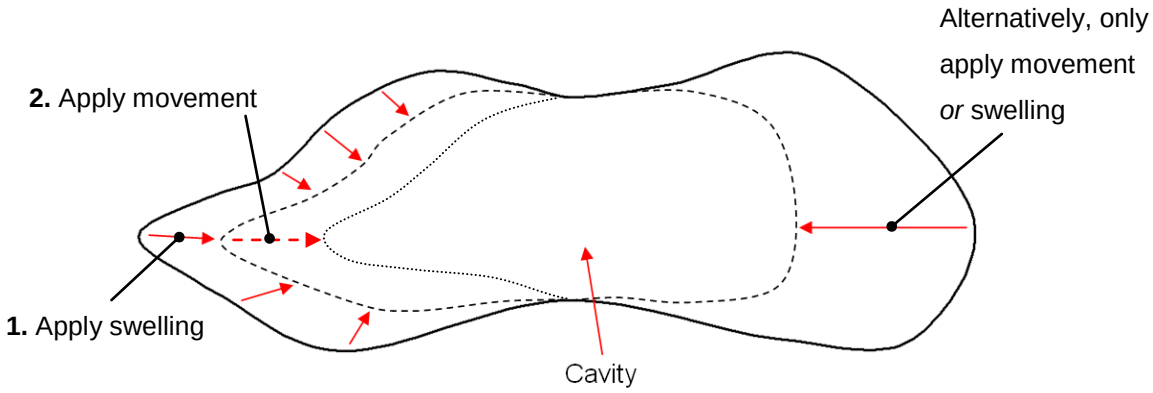

Figure 80: Combination of swelling and movement to apply case symptoms to simulation

This customisation was included by programming the second set of sliding scales to change only the x-co-ordinates of the points around the circumference, to move the entire side of the cavity inwards. The factors by which the sliding scale value was multiplied for each node was set individually, so that the sides would move in to eventually reach the midline of the cavity, closing either zone 1 or 2 as defined in Figure 79.

The changes to the model and programming that have been described so far greatly increased the cases that the user can simulate. Initially, the user could simulate only one case, as the layer points would always move to the same position, as described in Section 8.1.1. By allowing the user to choose the severity of the case in two different areas of the sinus and then apply a second degree of alteration in these areas, they have the opportunity to model up to 21^4 = 194,481 possible cases (21 divisions on four sliding scales, defining swelling and movement in two zones).

Even though the approach of applying swelling, then shifting the wall of the cavity inwards had dramatically increased the number of cases the user could create, the application of horizontal movement to swelling in the sinus cavity was not considered to be intuitive and would not be suitable for use on a sample of more than one layer, where vertical variation may be required. The results were also achievable through the original swelling system, so the next developments of this method of swelling application were begun.

An alternative was implemented by giving the user two further zones in which to apply swelling to the cavity lining. The user was no longer asked to apply movement to the swelling, but instead to apply it in one, or a combination of zones until the required case was simulated. This version also trialled the use of 30 points around the circumference of the cavity as shown in Figure 81, which meant that the interpolation between points was shorter, decreasing its effect on the shape of the new cavity. The effect of the increase in the number of nodes would be monitored and a decision made as to the number to include in future versions.

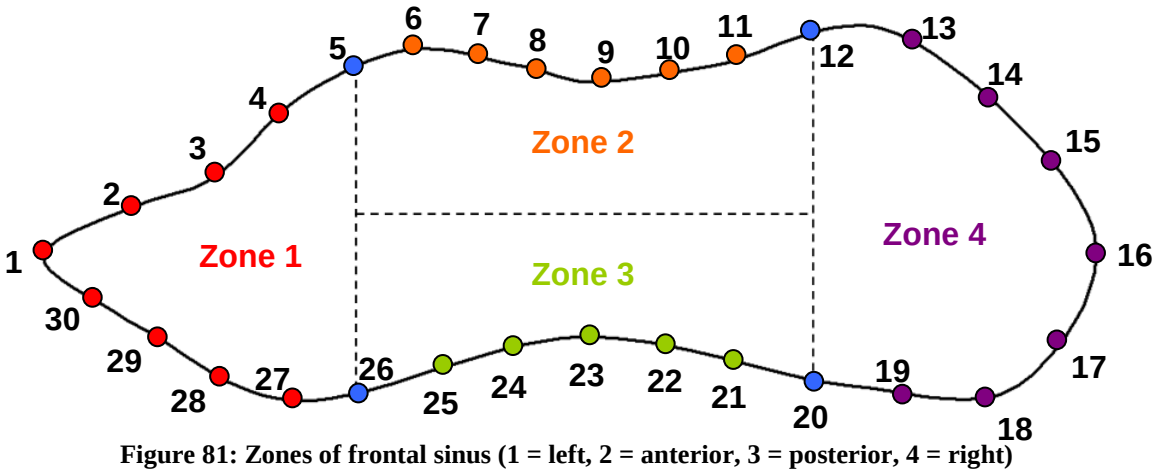

Figure 81: Zones of frontal sinus (1 = left, 2 = anterior, 3 = posterior, 4 = right)

The points within each zone are controlled, as before, by the relevant sliding scale for that zone. The user may now apply swelling to the left, right, anterior or posterior sections of the frontal sinus, and any combination of all four, at varying levels of severity. The shape of each zone's swollen geometry at 100% severity (closest to centre of cavity) is designed to simulate the worst case in each of those areas. Some points, on the border between two zones (points 5, 12, 20 and 26 in Figure 81) have been programmed to move with respect to both zones' sliding scales, to maintain a realistic shape.

This was done by incorporating both of the relevant sliding scales into the co-ordinate definition for the point in question, each sharing half of the influence upon that point, as demonstrated by point 5 in Figure 82:

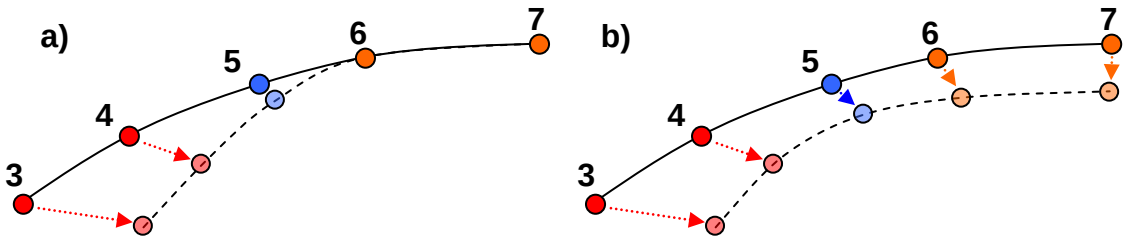

Figure 82: Movement of nodes in two zones - swelling applied to *a)* nodes 3 and 4 only, *b)* all nodes

It can be seen that when there is no swelling applied in Zone 2 (nodes 6 & 7, Figure 82*a)*) the border node between the two zones (node 5) only moves with the swelling applied in Zone 1 (nodes 3 & 4). Once swelling is also applied in Zone 2 (nodes 6 &

7, Figure 82*b)*) the border point moves to incorporate the level of swelling applied in both zones.

It was found that the shapes created through the use of this simulator, with 30 points around the cavity circumference, were more detailed in shape, as edges were less smoothed and smaller areas were achievable. The way in which settings are now applied is shown in Figure 83*a)*. The solid body created by the lofted 2D splines is subtracted from another solid, to simulate the swollen cavity lining. In Figure 83*b)*, the pink areas of the model are the normal anatomy, with the cream coloured parts representing abnormal growth.

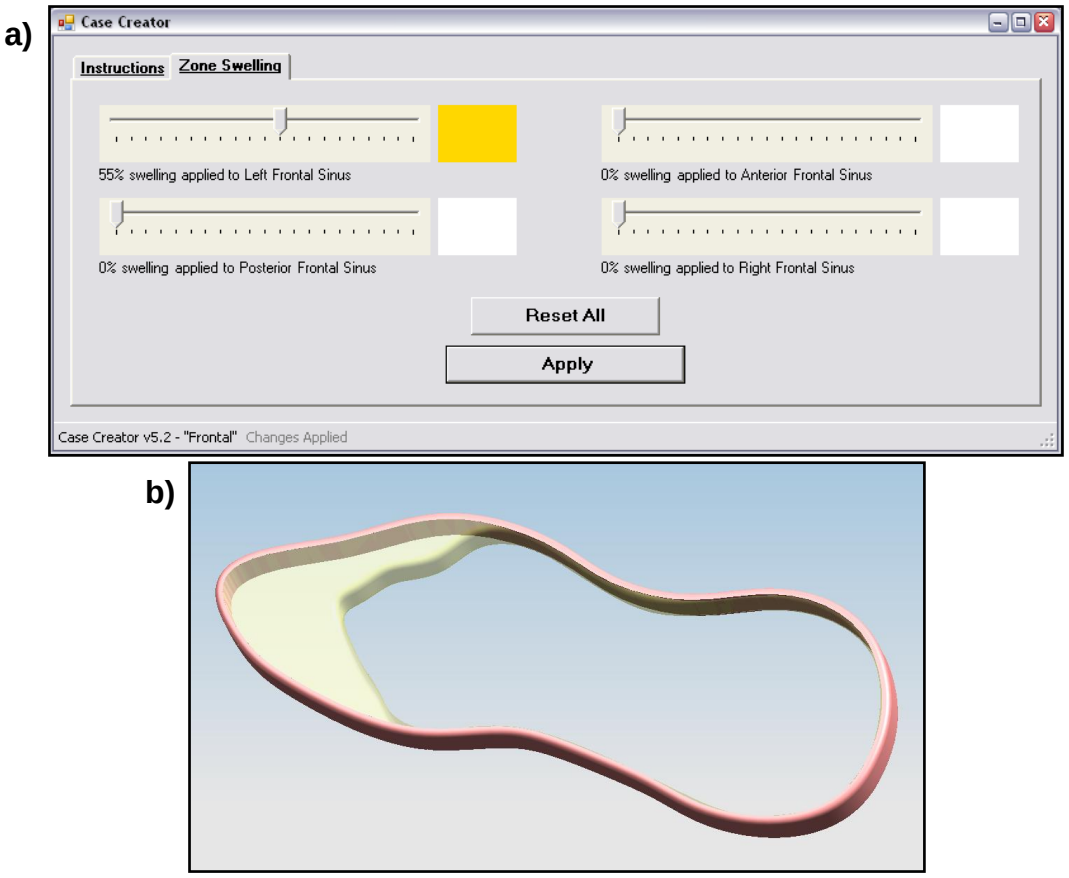

Figure 83: Swelling applied to left (Zone 1) of sinus cavity – *a)* settings, *b)* result

In Figure 84, the nodes around the circumference of the swollen cavity wall are shown, with swelling applied in all directions (55% left, 20% anterior, 25% posterior, 30% right):

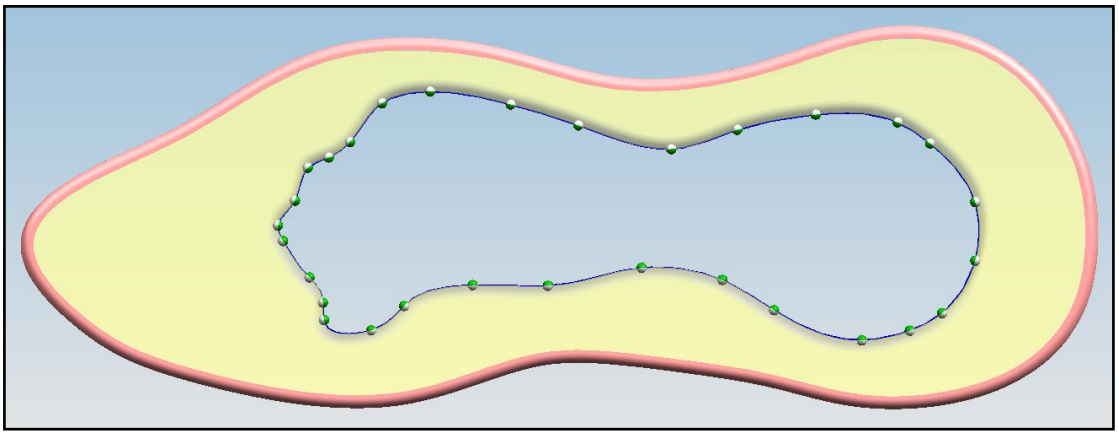

Figure 84: Thirty points around circumference of cavity wall, swelling applied

Feedback is now supplied both in the forms of coloured panels, linking to the clinical swelling severity rating system (Section 3.2) and percentages for more detailed information.

The anatomical geometry used in this version of the program was made more applicable through the introduction of shape variation between layers, down the sides of the cavity. This was the next step towards representing the anatomical geometry with greater realism than before. The cavities were drawn manually to represent the original frontal sinus geometry over the nine layers, to examine the ability of the software and VB interface to apply individual changes to each layer and retain the required realistic wall shape, as shown in Figure 85:

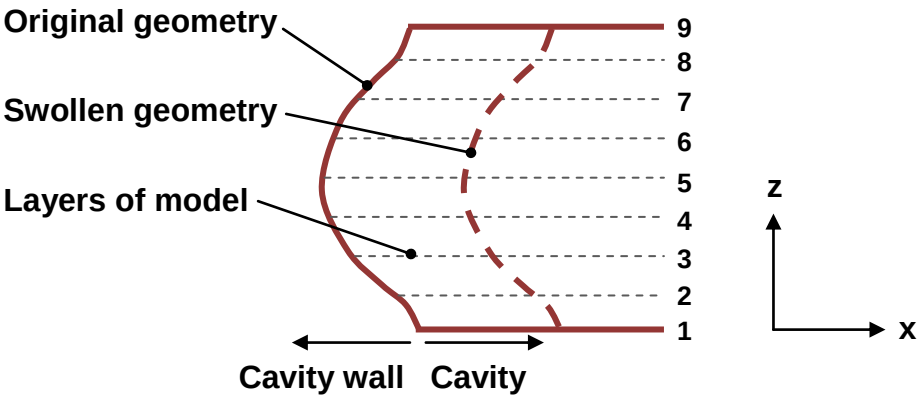

Figure 85: Shape of cavity perimeter in X/Z plane

In this version of the program, the number of points around each layer's perimeter was returned to 15, to reduce the amount of work required to enter each set of co-ordinates for all nine layers into the code. Some difficulty was encountered when the modelling software attempted to integrate between the layers; at times the cavity would protrude through the sides of the cavity walls.

It was decided that the next version of the program should investigate the direct use of real medical data imported from Mimics, to achieve further realism, avoid the modelling errors experienced with the created geometry and enable the assessment of the concept in an applicable environment. The capture and use of the original and new co-ordinates would also be made more intelligent, aiming to improve and accelerate the programming process.

8.2.2 Swelling in Sample of Real Anatomical Data

The development of the program to meet these objectives began with the selection of a suitable area of µ-CT scan data. As described in Section 6.2.2, µ-CT data was used due to the superior clarity and resolution achieved in comparison with medical CT. This meant that cavities could be clearly identified and used to develop the anatomy customisation tool. The frontal sinus was chosen for use as the sample exhibited clear boundaries between dense bone and air cavities.

An issue was encountered with the µ-CT data; due to the limited area shown in the scan, some cavities were not wholly contained by the sample, and did not form a complete cavity perimeter. A section of twenty layers was identified within this scanned data that was suitable for trialling the program. These twenty layers exhibited three separate cavities, wholly contained within the sample, which presented the opportunity for separate manipulation using the program. One layer of the chosen region, 0.1mm in thickness, is shown in Figure 86.

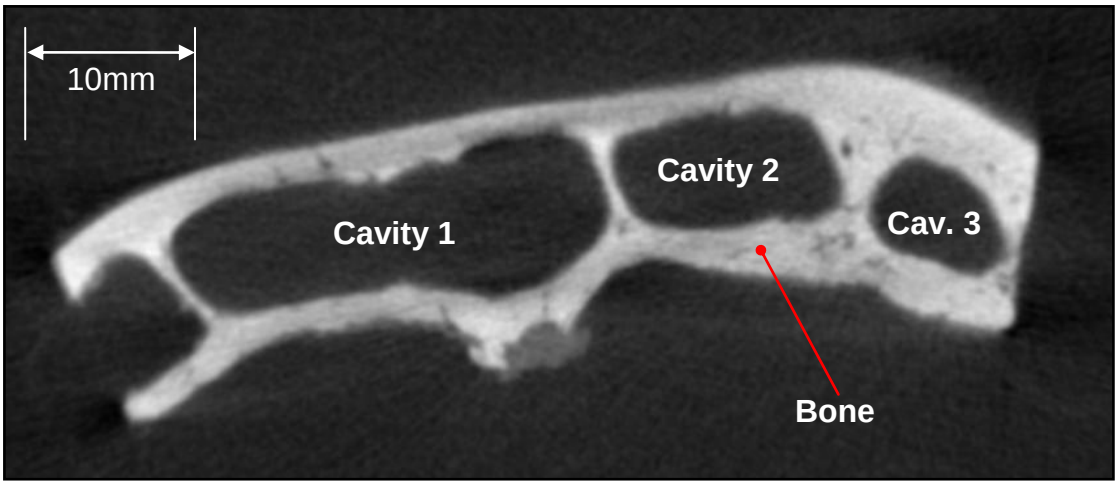

Figure 86: µ-CT image of frontal sinus section in X/Y plane

The µ-CT scan was manipulated in Mimics, through thresholding and region growing, refining the original scan to only the data required for this purpose. Once the model was considered to be sufficiently representative of the bone geometry of the frontal sinus, a 3D model was created. The model was exported to the CAD system in IGES format, ready for manipulation.

The file appeared as shown in Figure 87, with the outer geometry of the bone defined with separate splines. As expected, these splines were found to be identified by `"HANDLE R-XXX"` codenames, in the same way as the splines used in the previous development work, meaning that they may be altered under the control of VB code. This further justified the selection of IGES as the optimum import file type for Case Creator.

However, because NX uses these tags to identify each spline, and there is no discernible pattern in the numbers used in each tag, at present there is no way to equip the program for immediate use with any newly imported CT scan model. With the current level of knowledge, the program is suitable for use with the specific set of data with which it is associated. This is acceptable, if the program is to be used as a swelling simulation tool on a base model for training purposes (see Hypothesis, Section 6.5). If the program were required to be used with any possible set of data, for

example for patient-specific simulation, further understanding of the way in which the splines are numbered would need to be gained, or a new method of simulating swelling developed (see Section 8.5.1).

The 'By Poles' spline setting (see Figure 56) was used, allowing a more aggregated curve to be created, using a closed loop with degree of curvature of 3. This produces a smoother curve once changes have been applied, making any solids created through the curves far easier to compute and use in the model. This in turn reduces the model's similarity to the dataset, however this is acceptable for the initial development of the program, which may be used in the future to customise more anatomically representative geometry. In Figure 87, the 20-layer section of µ-CT data to be used is shown from above, as imported into NX in the IGES format.

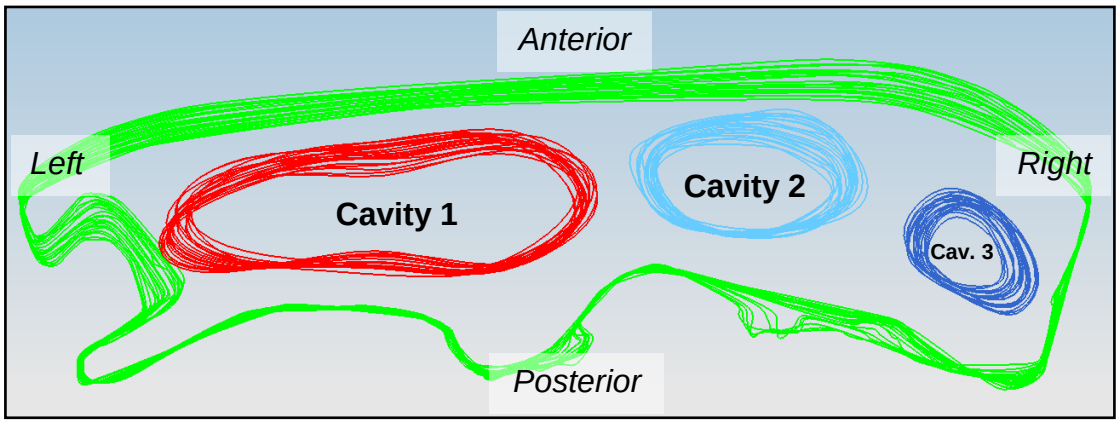

Figure 87: µ-CT data imported as IGES to NX using 'By Poles' setting

In Figure 87, the green splines represent the outer geometry of the bone in the sample, while the other groups of splines (red and two shades of blue) represent the interior cavity geometries of the frontal sinus. When imported, each area of the model, and each layer in those areas consisted of a different number of nodes; in order to simplify the programming of the alterations to the internal cavity geometry, each spline was reduced to eight nodes. This was done by selecting eight points manually which could accurately represent the geometry of the cavity. It was found that similar results could be achieved with this number of points to the previous trials with fifteen and thirty nodes, while this complete process is much faster than the method used earlier in the

research. This is due to the greatly reduced number of node co-ordinates that must be recorded for each cavity and layer of the model, and subsequently entered into the code. Previously, up to 30 x 3 x 20 = 1800 co-ordinates would have had to be entered; this has now been reduced to 8 x 3 x 20 = 480.

Previously, each node of every layer was manually recorded and then entered into the code at the appropriate point. The VB script also had to be tailored for the number of points on each layer of the model, making it impossible to repeat sections of code. For these reasons, the programming involved took an unacceptable amount of time, and was not viable for any more complex models. By keeping the number of points at a constant value of eight, the code is far more repeatable and requires less alteration. The selection method of the points was also changed; by consulting experts in the use of NX, it was discovered that it is possible to record the co-ordinates of spline points far more quickly and with less manual work. The co-ordinates are automatically exported to an Excel spreadsheet once selected, ready for manipulation.

This stage of programming is far more accurate and produces faster results than the previous techniques. Once the original co-ordinates of the spline points are recorded in the Excel spreadsheet (Figure 88), the splines are all moved into their "100% swollen" positions, and the new co-ordinates are recorded. The difference between the original and new co-ordinates is returned, and divided by the number of divisions on the sliding scales used in the interface (**n**).

		x	dx		y	dy		z
LAYER 1	x1=	28.70332	0.00275	y1=	15.26439	-0.09243	z=	4.000008
	x2=	36.85742	-0.31522	y2=	19.50008	-0.27606		4.000008
	x3=	47.69833	-0.78689	y3=	14.73457	-0.0589		4.000008
	x4=	36.43850	-0.25029	y4=	7.54198	0.247946		4.000008
	x5=	28.69143	0.01742	y5=	11.96235	0.033965		4.000008
	x6=	15.33899	0.59004	y6=	7.69613	0.224403		4.000008
	x7=	9.16540	0.83890	y7=	12.41631	0.014786		4.000008
	x8=	19.71259	0.38543	y8=	17.41885	-0.18256		4.000008

Figure 88: Spreadsheet showing co-ordinates of spline points and automatically-calculated sliding scale multiplication factors

This value (*dx*, *dy*) is therefore the step change, in co-ordinate terms, between each point on the sliding scale (0-20, when **n**=20). *dx* and *dy* are used as the multiplication factors in the co-ordinate manipulation section of the code to achieve an accurate representation of swelling from 0-100%. By recording the original and 100% case co-ordinates in this way, and calculating very accurate step changes (*dx*, *dy*), each node on the anatomical geometry will move along a set path towards its 100% position, as depicted in Figure 89:

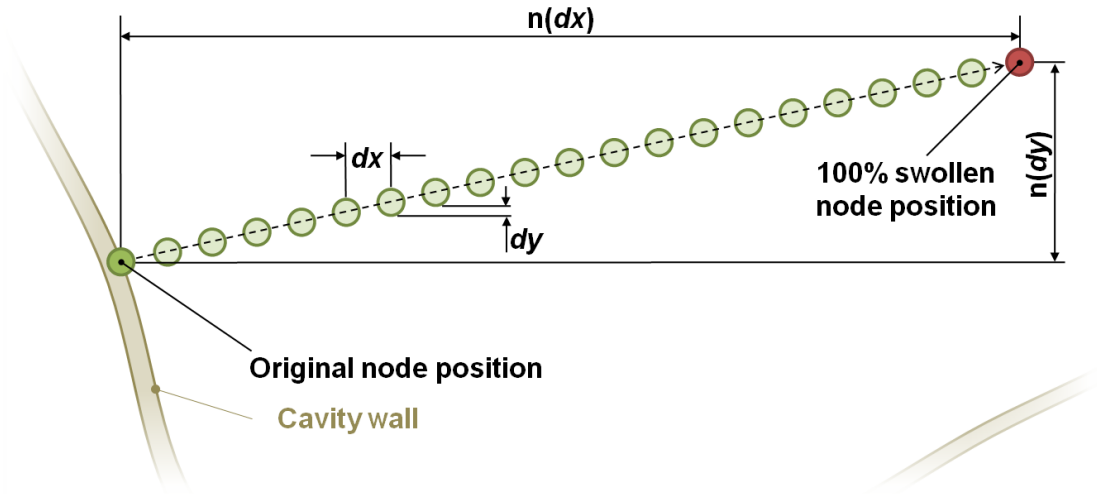

Figure 89: Movement of node by sliding scale

After programming the swelling simulation code for cavity one, the other cavities could be included with repeated code, due to all splines being made to use only eight nodes. The only changes to be made were alterations to the slider value multiplication factors as calculated in Excel. The entire programming process was greatly accelerated in comparison to the earlier versions, mainly due to the repeatability of the code and the more automated manner in which the co-ordinates of the spline nodes were gathered.

The GUI for application of swelling to the µ-CT sample, and resulting case are shown in Figure 90*a)* and *b)* respectively. The user may apply changes to any combination of the three cavities in this case using one window:

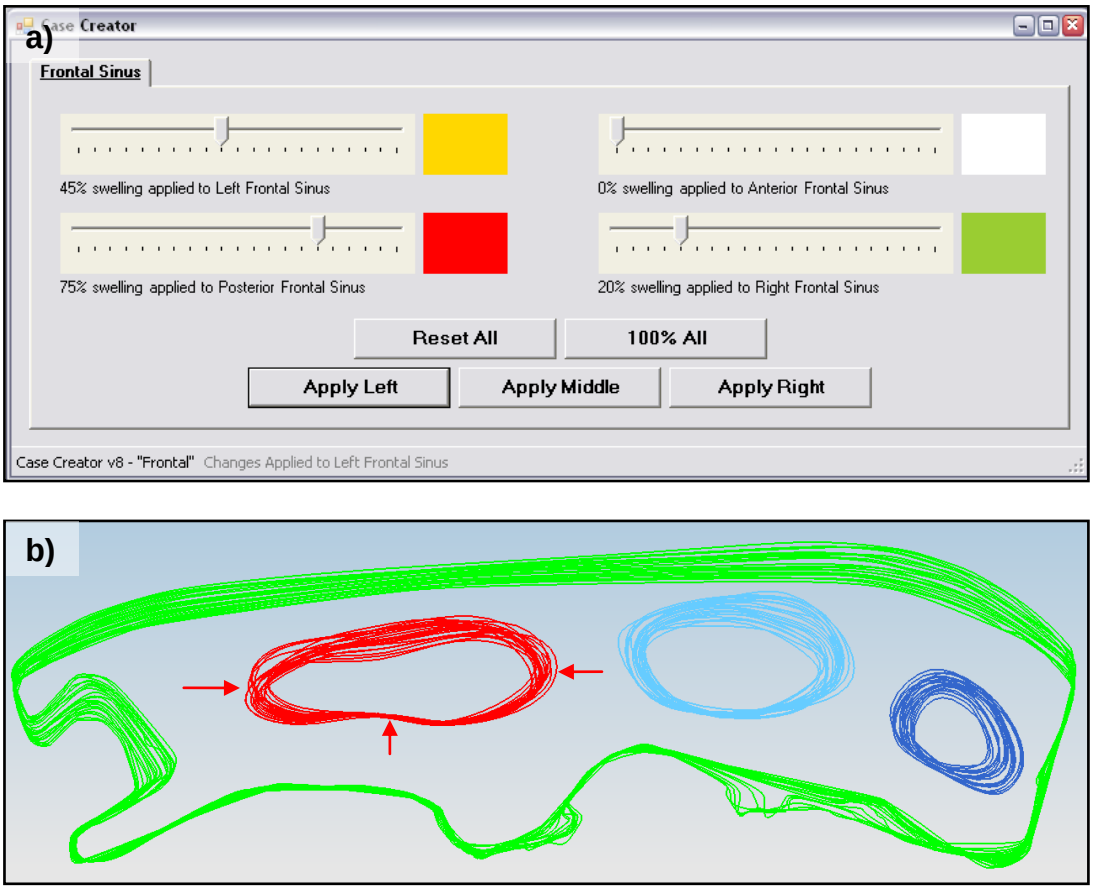

Figure 90: µ-CT data swollen – settings (*a)*) applied to the left cavity (*b)*)

When compared to the original geometry of the cavities (see Figure 87) it can be seen in Figure 90*a)* that the cavity one has been swollen on the left, posterior and right hand sides. In Figure 91, all nodes around cavity one have been moved to their '100% swollen' position, as defined during co-ordinate collection.

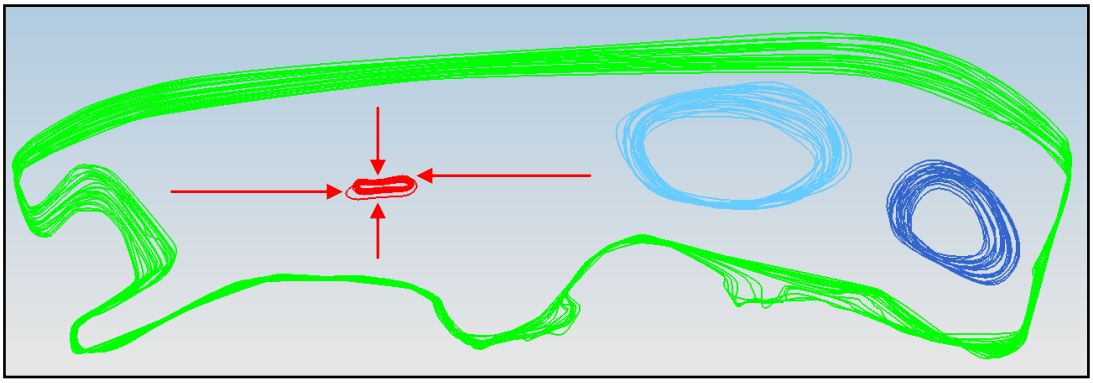

Figure 91: µ-CT data with 100% swelling applied to the left cavity

It is worth noting that even with nodes in the "100% swollen" positions, the cavity is not completely closed. This is due to the modelling capabilities of NX, where nodes around a spline may not occupy the same 3D space. The nodes are therefore positioned as closely to one another as possible, leaving a cavity of approximately 2 x 1mm, in this case. This remaining cavity was reduced in size in subsequent versions of the program.

Further developmental steps were then defined for the program, as outlined below. Most importantly, the program had to be developed to automatically simulate both the original geometry (bone) and separate solids representing the swollen cavity lining, positioned within each cavity. It was proposed that this would be done by creating two instances of each cavity's geometry (red, dark blue and light blue splines in Figure 87). The first instance of the cavity wall splines (bone spline set) would represent the original anatomical geometry, with the swelling spline set representing the swollen geometry. The proposed steps to accurately simulate the different parts of the model are outlined below:

1. Outer geometry solidified using 'Through Curves' operation in NX
2. Same operation used to create solid parts from bone spline set
3. These parts are then subtracted from the solid outer geometry, forming cavities, as shown in Figure 92:

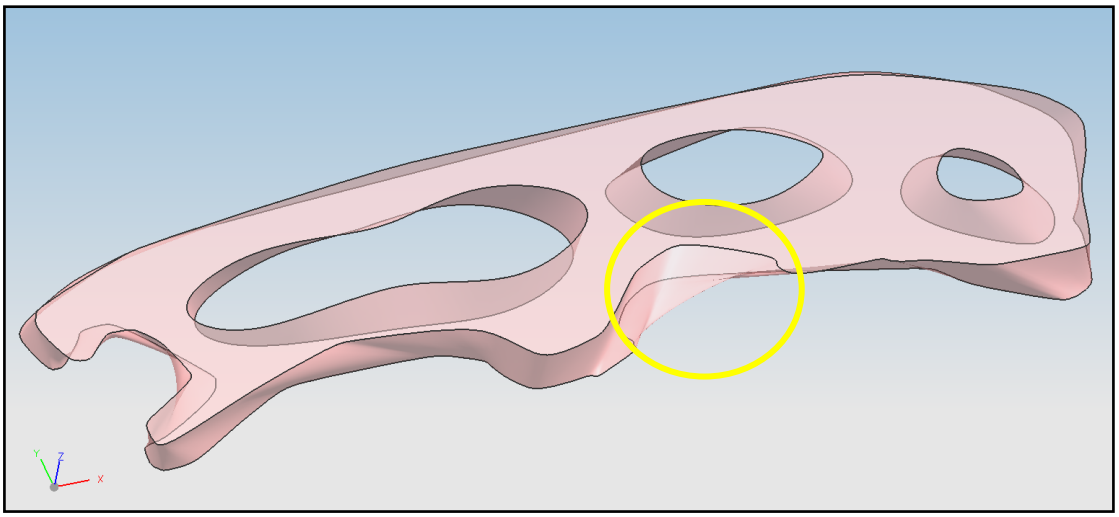

Figure 92: Cavities subtracted from solid outer geometry, with modelling anomaly circled

When trialling this method of solidifying the model, it became apparent that the capabilities of NX to accurately represent the 3D body as a stack of 2D curves were somewhat limited. As circled in Figure 92, there are some areas which do not follow the outside line defined by the 2D splines, but which are skewed, often incorrectly adding a large area of solid to the body. This effect can be overcome through manual manipulation of the model once solidified, but an automatic solution would be preferable. Further development of the solidification method to be used is described in Section 8.5. The second part of the process, in steps 4 to 6 listed below, will need to be simplified, as the model becomes too complex to manipulate efficiently.

4. Bone spline set formed as solid bodies again, within the cavity spaces
5. Swelling spline set, lying within the cavities, formed as solid bodies
6. Swelling spline set subtracted from bone spline set to leave solid bodies where swelling has occurred

Until this point, the development of Case Creator has been based upon data acquired from µ-CT due to the higher levels of achievable resolution. Higher resolution allowed the anatomical geometry and node co-ordinates of the sinus cavities to be clearly defined. These nodes were then needed to move the anatomical geometry to different locations, simulating the effect of swelling in the sinus cavities.

In future applications of the program, if more models are to be used as the basis for case simulation, µ-CT will not be able to be used, as described in Section 2.2.3. It was therefore necessary to enable the program to be used with conventional clinical CT data. Along with the developments noted here, further work was performed on the means of simulating swelling using CAD splines, to achieve easier integration of the program with new anatomical models. This work is described in Section 8.5.

In addition, any inert parts of the model – that is, any bodies that were not needed for geometrical data extraction or modification – would be imported from Mimics in STL format, to reduce any inaccuracy in the generation of solid bodies from IGES files as

shown in Figure 92. The most significant inert body to be imported in STL format was the skull, which gave scale and realism to the model. This is of great benefit to the user, as they may contextualise the anatomy, and the changes to be made to the model.

The next version of the program was implemented on a fuller dataset, as planned in Figure 65, acquired from CT scan data of a cadaveric head. The quality of the data imported from Mimics was optimised for this application; a good quality IGES file was essential for accurate geometrical data to be gathered.

8.3 Final Horizontal Swelling Application Method

In consultations with Anshul Sama, it was concluded that the simulation of swelling to the cavity lining of the ethmoid sinus would not be included in the program at this developmental stage, due to the anatomical complexity of the area and number of small, interconnecting cavities to be altered, as shown in Figure 93. Once the method for applying swelling to the sinus cavities is finalised, the ethmoid sinus may be included in the system. This is discussed in the recommendations for further work (Section 13.2).

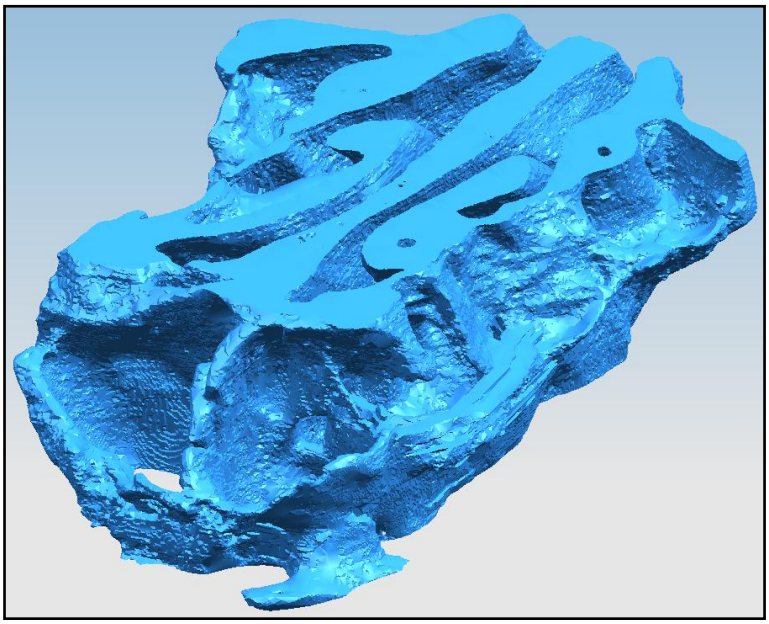

Figure 93: STL file of sectioned ethmoid sinus showing complexity of cavity geometry

Figure 94 shows the new CAD model to which swelling to the cavity lining is applied.

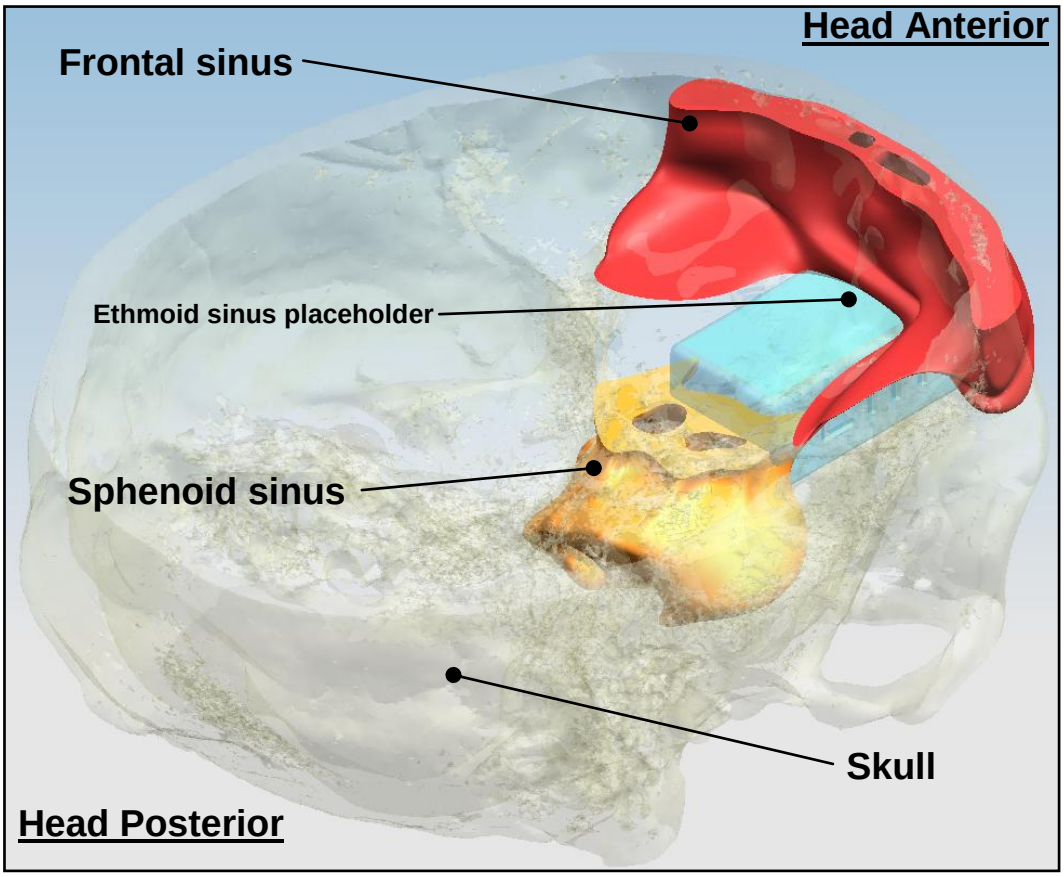

Figure 94: CAD model of skull, frontal and sphenoid sinuses, ethmoid placeholder

The individual frontal and sphenoid sinus models can be seen within a section of the skull model, along with a rectangular marker for the ethmoid sinus. The skull model section is between the cheekbone and the upper levels of the forehead. The ethmoid sinus is represented by a placeholder block in the CAD model, as no swelling is to be applied within the cavities of this area. As no medical data was available for the maxillary sinus, two markers either side of the ethmoid sinus were used to assist in visualising the space inhabited; these are not shown in Figure 94 for clarity.

At this stage, further thought was given to the use of the program on models of the whole head, involving entire sinus regions. The impact of this expanded model on the design of the program to date is that cavities may no longer be treated as separate entities, due to the complex manner in which they combine, split, open up and close

off throughout the model. In the sequential µ-CT images of the frontal sinus in Figure 95, taken less than one millimetre apart, cavities form and combine when moving downwards (from image 1 to image 3) through the head.

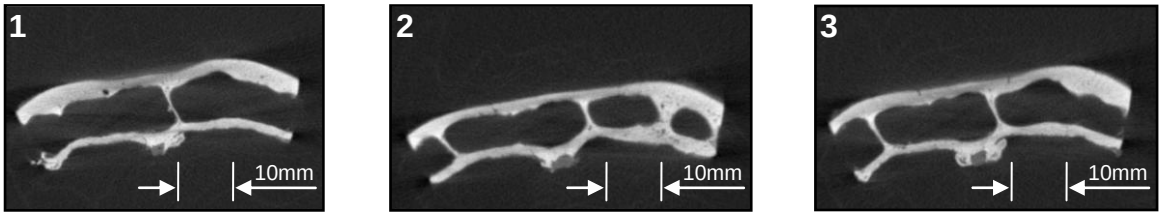

Figure 95: Cavity formation in frontal sinus at three slices on the X/Y plane, 0.5mm apart

To treat each cavity separately, and ask the user to apply individual case properties to each, would not be a viable or realistic approach to swelling application. The alternative approach that has been taken involves less input from the user, and more substantial automation of case property application to the model. The model is always treated as a whole, instead of segregating the treatment of the cavities. Furthermore, alteration work on the model is divided into the four distinct areas of the paranasal sinuses, namely the frontal, sphenoid, ethmoid and maxillary sinuses, each of which may be selected separately for use in the wizard (see Chapter 10 for more detail).

In order to apply swelling to the chosen sinus area, while treating the area as a part of the whole head, changes had to be made to the spline co-ordinate alteration code. Changes were made so that swelling applied to the "left", "right", "anterior" and "posterior" (L, R, A, P) were no longer in relation to the sinus area, but in relation to the head as a whole (see Figure 96). This more closely mirrored the effects of pathology on the sinuses that had been observed in MRI and CT scans.

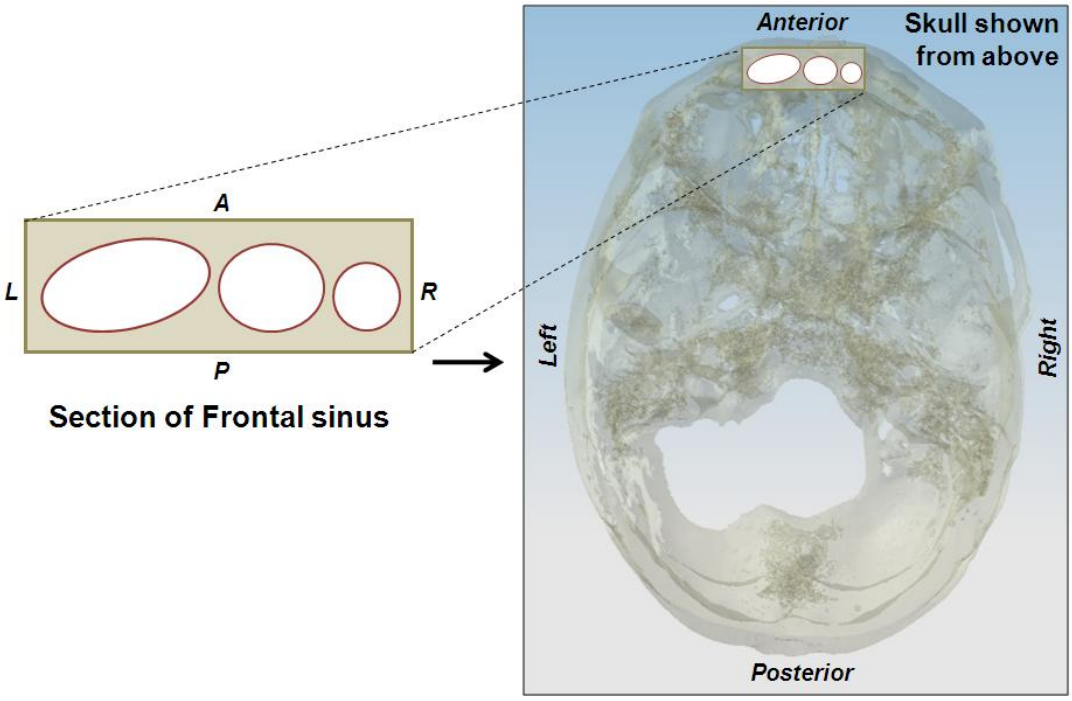

Figure 96: Global positioning of swelling relative to head

Therefore, swelling would not be visible in some cavities, depending on their position within the head. In the example in Figure 97, swelling has been applied on the left side of the head in the frontal sinus; previously this would have affected the left side of each cavity as shown, but now only affects those cavities on the left of the model.

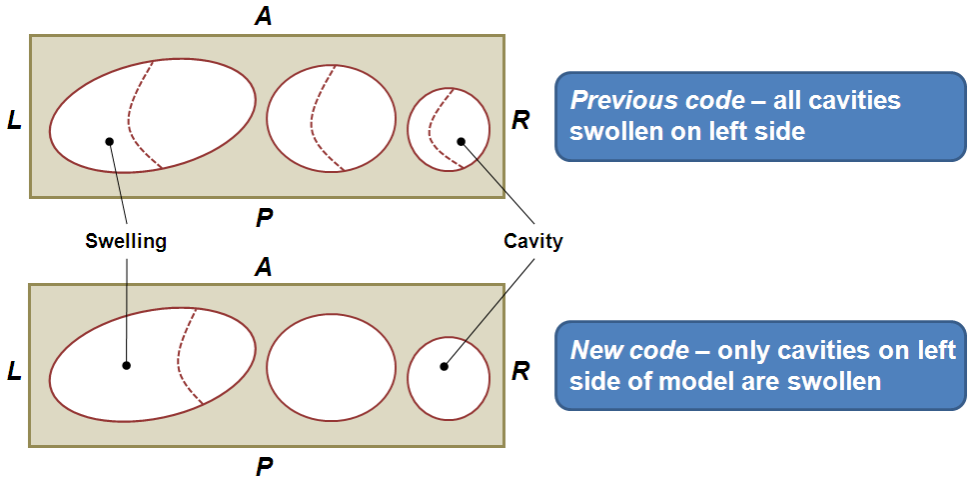

Figure 97: Swelling applied to cavities as a whole (from the left)

The cavity spline nodes have been reprogrammed to be affected only by the sliders controlling swelling on the appropriate side of the head. This manual programming process is considered acceptable for the purposes of the first complete model. As the cavities combine and split, moving downwards through the model, swelling will be applied in the same way.

Of course, in reality, swelling will occur in three dimensions throughout the sinus region in question. This was the next factor to be addressed, and is described in Section 8.4.

8.4 Three-Dimensional Swelling

Further capability and customisability was then added. In doing so, it was hoped that the realism of the finished product would also be improved.

8.4.1 Swelling in the Vertical Direction

It was noted that with the current model, no swelling is simulated in the z-axis, due to the movement of all nodes inwards or outwards along the X/Y plane (Figure 98*a)*). This is anatomically inaccurate, as swelling will most likely occur in all directions, all around the interior of the cavity, which is three-dimensional (Figure 98*b)*).

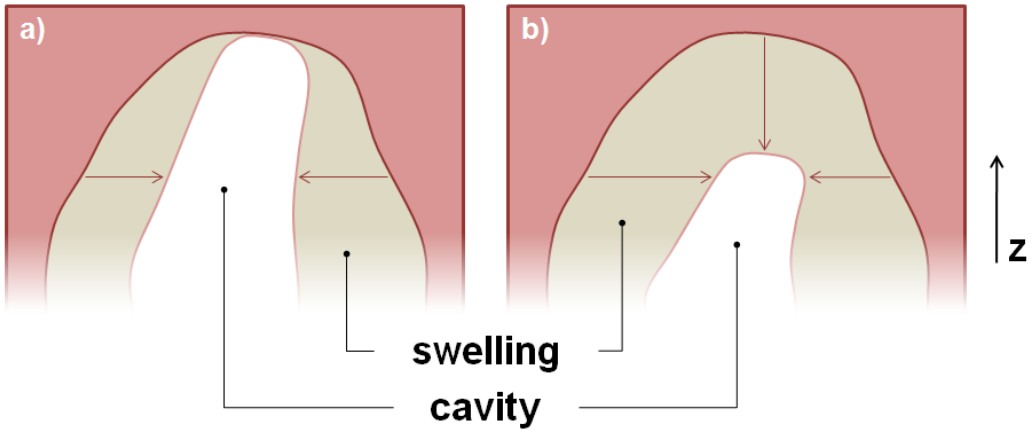

Figure 98: Swelling in z-axis – *a)* current capability, *b)* desired capability

With clinical consultation, it was decided that this feature should be included in the program, in order to maintain the required level of realism. However, some problems were faced with the programming and modelling of such a feature.

The difficulty in simulating swelling in the z-direction is rooted in the use of 2D splines to form the layers of the 3D model. As swelling is applied in the z-direction, it would appear (as in the red area in Figure 98*b)*) that the splines defining the top of the cavity in Figure 98*a)* are made to disappear to simulate the swelling. For the model to retain integrity and customisability, this cannot occur; errors would be faced upon the deletion of layers when NX modelled the case, and the regeneration of the layers, should changes need to be undone, would also be problematic.

The first attempt at avoiding this problem made use of the previous work on node movement in the X/Y plane. The concept of this first trial was to 'negate' some layers; to move nodes around a layer inwards to the exact same central point, effectively removing the layer concerned from the model. The layer would remain in the same place on the vertical axis, but no cavity would be perceived.

In trials using NX with a simple VB interface and code set to move all four points around one spline to the same central co-ordinates, the software was unable to calculate the new solid shape. Modelling errors were caused when the solid attempted to pass through the spline where the points inhabited the same space. This was anticipated, as described in reference to Figure 91, but assisted in documenting the limitations of the software. An alternative method was formulated to simulate the swelling of cavities in the z-direction.

The second concept adopted a similar approach to the first, but instead moved the points around the layer to points close to one another (similarly to if 100% swelling were applied to the layers in question). Some issues were experienced in this case with the integration between each layer of the model, however the modelling succeeded. Consequently, a gap of negligible size would be formed through the build

material of the final physical model (formed by the layers where points have been moved within close proximity of each other as shown in Figure 99). With a sufficiently small gap left in the material, this would not be detectable in the solid model owing to the maximum printing resolution of the 3DP process.

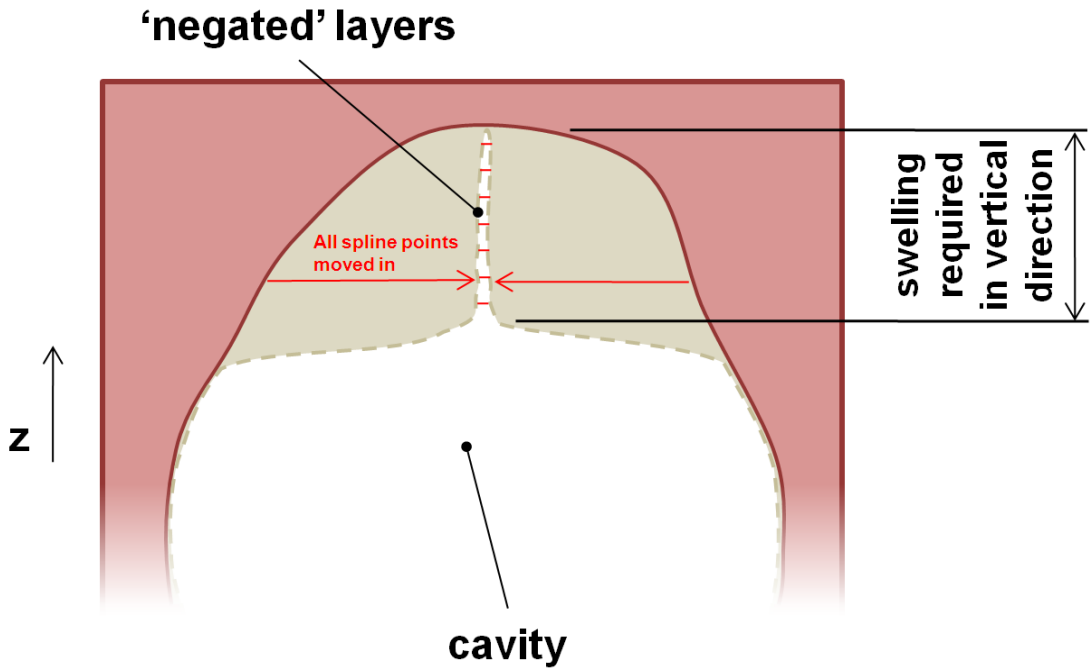

Figure 99: Swelling in z-axis achieved by moving highest layer points inwards

While this method simulates swelling in the vertical direction by appearing to bring the majority of the cavity roof/floor down/upwards, a method by which no small cavity remained in the model was investigated, to achieve clearer inspection of the CAD model and more robust physical model production.

The next trial proved to be more successful, realistic and viable than the last. Instead of 'negating' layers to give the appearance of swelling downwards or upwards in a cavity, the layers themselves would be moved. This method works in the same way as the horizontal swelling system, translated into the vertical direction. In horizontal swelling, the nodes around the splines are moved in the X and Y dimensions by amounts determined by the user's selection. In the new vertical swelling system, the layers will be retained, but moved upwards and downwards in the same fashion.

Code was written to allow the user to apply varying levels of vertical swelling to the cavity using a sliding scale, in the same way as the horizontal swelling system (see Figure 100).

```
Dim coordinates1 As Point3d = (x1, y1, z + TrackBarVert.Value * 0.1)
```

Figure 100: Trial code to alter vertical position of layers

A simple trial of this method was carried out with a five-layer cavity within a block (Figure 101*a)*). For this simple model, the top and bottom layers were programmed to move simultaneously inwards towards the centre of the cavity by the amount specified by the user on a sliding scale. The middle layer was programmed to remain in position for this trial. The layers moved as required, applying swelling to the top and bottom of the cavity as shown in Figure 101*b)*.

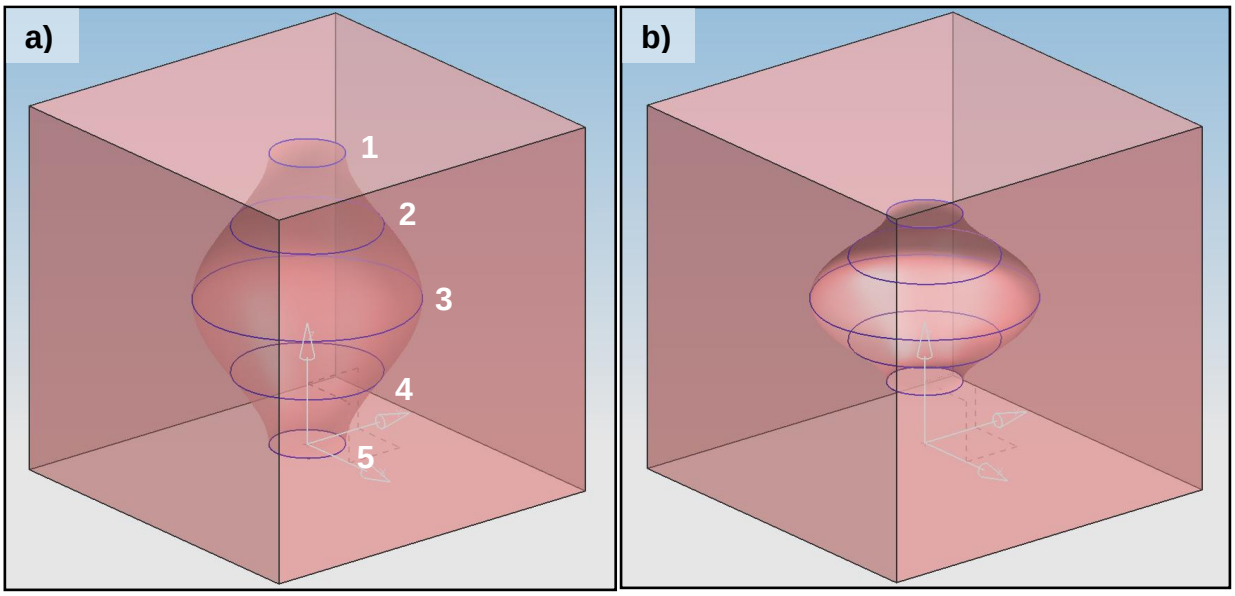

Figure 101: Trial showing capability to simulate swelling in z-direction – *a)* before, *b)* after

This trial succeeded in simulating swelling in the vertical direction towards the centre of the cavity by moving all layers inwards by the same amount. This method did not maintain an equal distance between layers, nor was a great range of swelling achievable as the maximum movement applicable to all layers was the distance between the centreline and nearest layer (spline 2 or 4 in this case). An improved

method was therefore created, where splines move by amounts relative to their distance from the centreline, as shown in Figure 102.

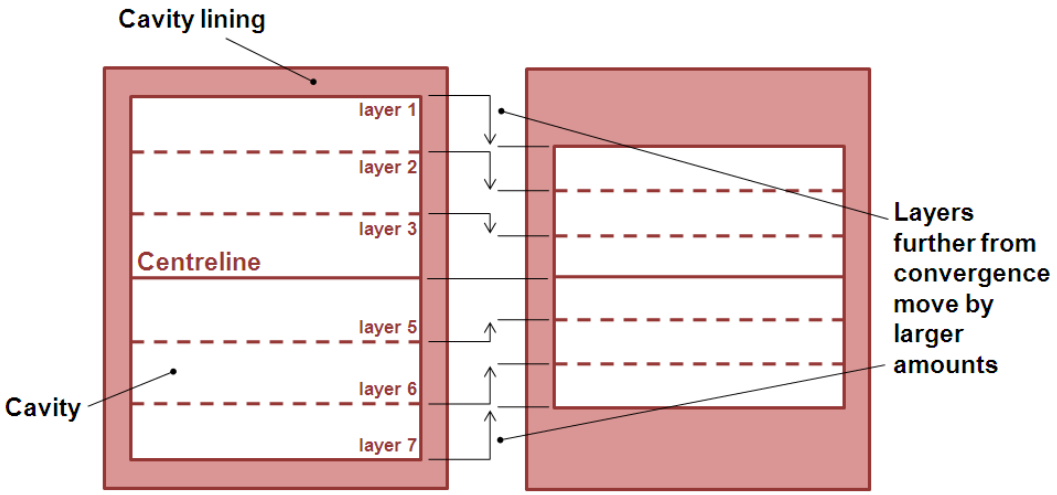

Figure 102: Simulation of swelling in vertical direction

In Figure 102, the distance between the layers has been scaled down; a greater range of vertical swelling may be simulated, allowing the overall height of the cavity to be reduced by a larger amount. This is done by varying the amount each layer moves in relation to the amount of vertical swelling applied and the layer's distance from the centreline (or layer of convergence) – layers near to the convergence are moved a shorter distance than those further away.

The next stage of work was to implement this z-swelling system into the program, giving the user the ability to alter the original co-ordinates of the medical data in the x, y and now z-directions as a result. A separate, vertically orientated sliding scale was used to apply varying severities of swelling to the cavities in the z-direction at the same stage as the horizontal swelling. The program was then used to alter the vertical swelling of a 20-layer model where each layer was 0.1mm in thickness.

During development of the swelling application system, the swelling sliders were altered to offer a maximum value of 50 and are used as such in this example. This value was chosen arbitrarily, but offers a large range of customisation to the user. In

order to achieve maximum swelling inwards towards the centreline, the outer layers must move by 1mm; the multiplication factor to convert the z-swelling slider value into a co-ordinate change is therefore set at:

$$\frac{\text{Distance from layer to convergence}}{\text{Maximum value of z-swelling slider}}$$

The factor reduces by 0.02 per layer in this case, which effectively 'squashes' the layers together. Therefore, when set to maximum swelling, the outer layers move inwards by (50 x 0.02)mm = 1mm, and the nearest layers to the centre move inwards by (50 x 0.002)mm = 0.1mm.

It was subsequently decided that separate, manual application of swelling in the z-direction was not an intuitive method of simulating vertical swelling in the sinus cavities. This conclusion was drawn through use of the program and consideration of the users' experience with 3D CAD software. The effect of the slider upon the swelling applied was rarely predictable and its function was considered to be too rooted in CAD modelling to be completely understood by clinicians. Instead, a method was developed by which swelling in the z-direction was automatically applied at the same time as horizontal swelling. This was done by altering the z-co-ordinates of all nodes around each layer on the application of horizontal swelling, using the average of the horizontal swelling values.

Vertical swelling is simulated in different ways depending on the area of the sinuses being affected. The frontal sinus is closed at the cranial (top) end and opens caudally (downwards) into the ethmoid sinus. Vertical swelling was therefore simulated from the roof of the sinus downwards, leaving the bottom layer of the frontal sinus model unmoved, as shown in Figure 103.

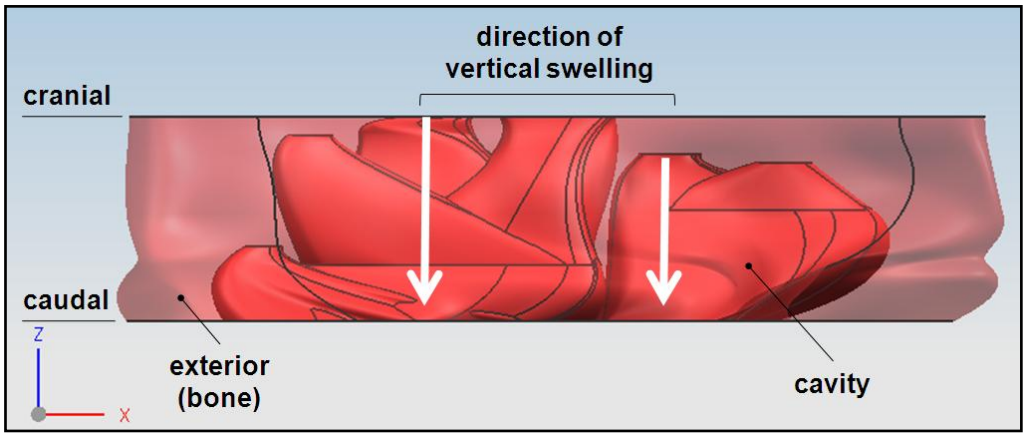

Figure 103: Vertical swelling direction in the frontal sinus

The sphenoid sinus is open at its cranial extent to join with the ethmoid sinus, and closed at the caudal end. The opposite effect was applied to this area, leaving the top layer unmoved and the floor of both cavities movable in an upwards direction, shown in Figure 104. This achieves swelling, on the whole, towards the centre of the entire sinus complex.

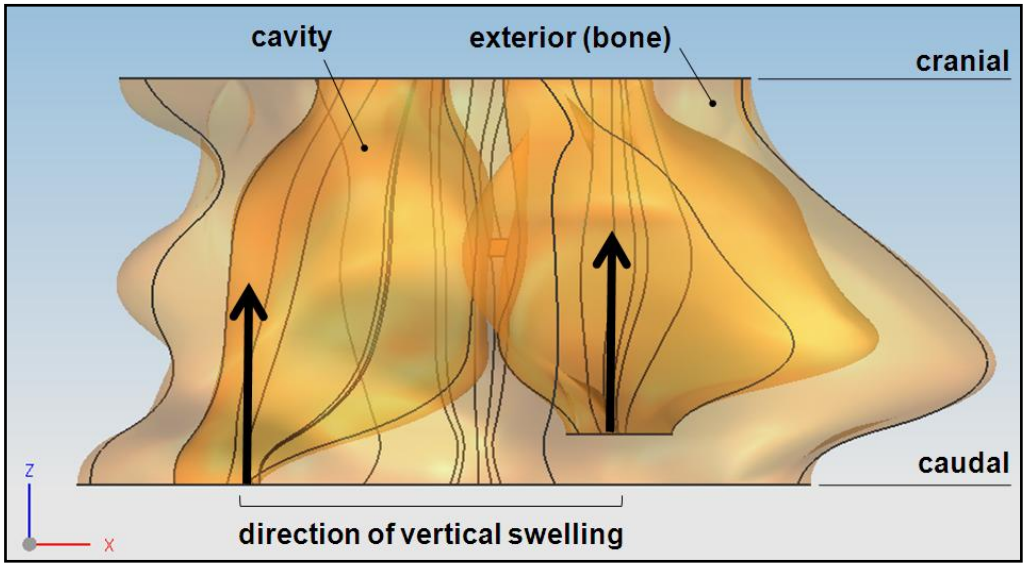

Figure 104: Vertical swelling direction in the sphenoid sinus

The combination of horizontal swelling applied in four directions, at a severity level selected by the user, and vertical swelling, successfully achieves Level 4 customisability on the scale devised in Table 7.

8.4.2 Three-Dimensional Cavity Shrinking

The application of horizontal and vertical swelling together to the original co-ordinates of the anatomy occasionally produces undesirable results in the CAD model, as the alteration made to the splines does not result in 'shrinkage' of the cavities. Figure 105 shows the problem in more detail:

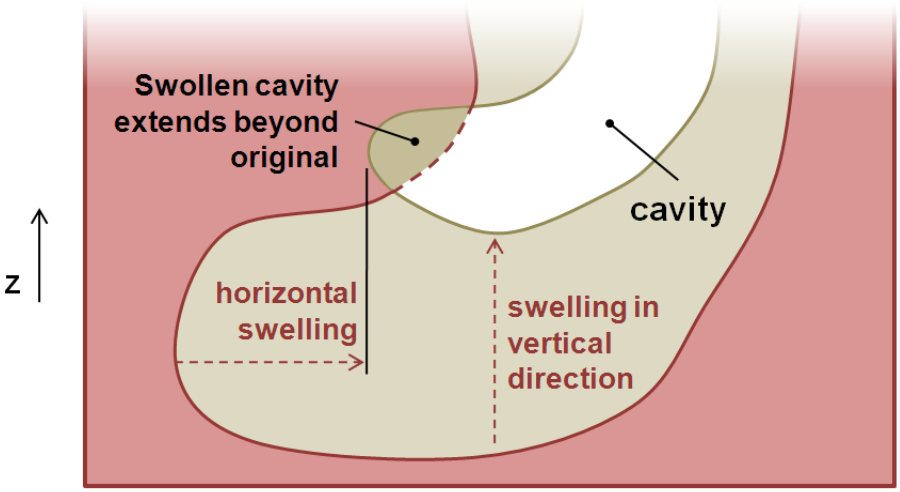

Figure 105: Error due to combination of horizontal and vertical swelling

As the horizontal swelling system was designed before the development of the vertical swelling system, this error can occur. Horizontal swelling is applied, then the cavity is reduced in vertical size towards the centre of the head; depending on the original cavity geometry and the level of swelling applied, the new cavity may stray outside the original cavity. This may lead to modelling errors when the CAD model is updated (see Section 8.5.3). To combat this, the horizontal swelling system was updated to behave in the same way as the vertical system, shrinking the cavities towards the centre of the head. This will achieve the required result, as shown in Figure 106:

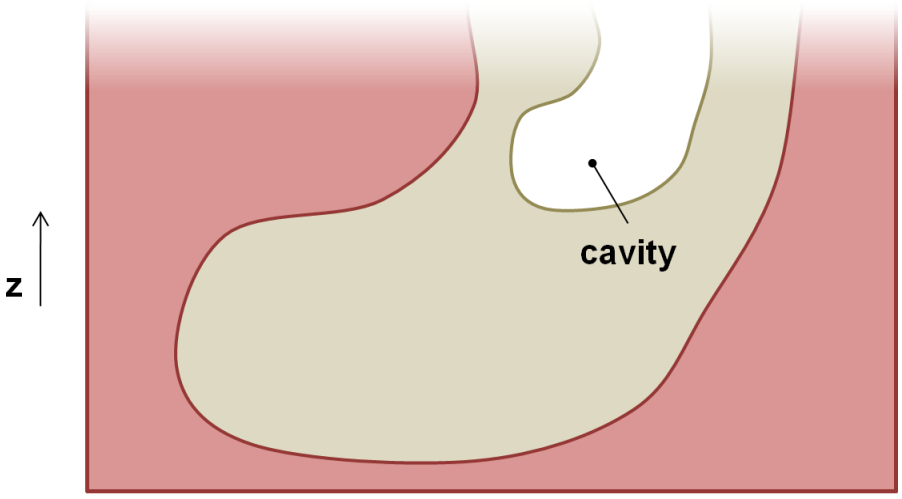

Figure 106: Cavity shrinks towards centre of head

To develop the final swelling system, shrunken copies of each of the original frontal and sphenoid cavities were first created, at half the original size. The node co-ordinates on the splines of the copied cavities were then recorded and entered into the Excel spreadsheet, replacing the data used previously. The copied cavities of the sphenoid sinus are visible in Figure 107 in green, within the original, larger cavities:

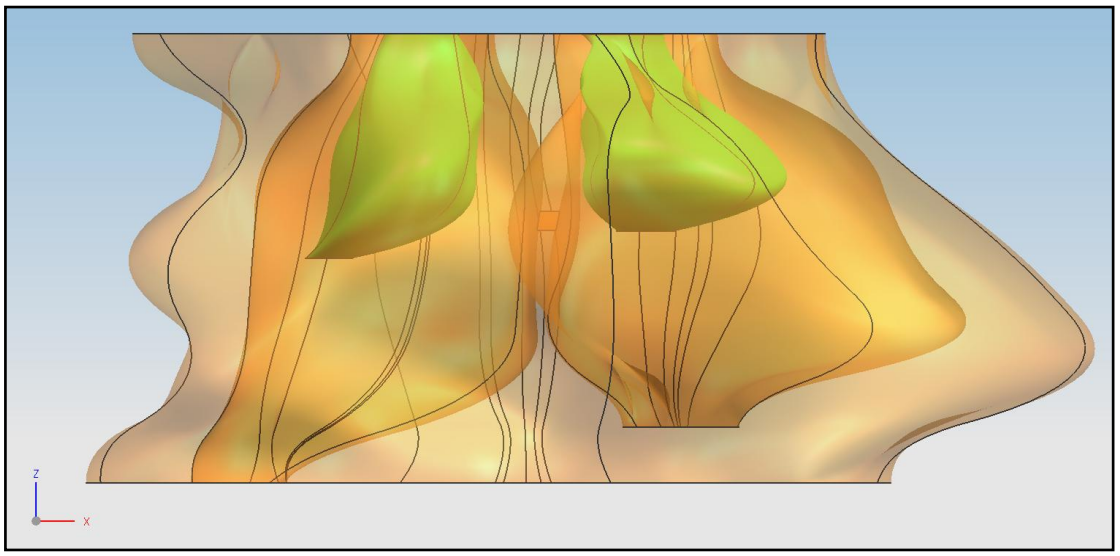

Figure 107: Shrunken cavities produced within original anatomy – sphenoid sinus

To apply swelling, the eight nodes around each scaffold spline move gradually towards the co-ordinates of its equivalent point on the shrunken copy of the sinus

cavity. Values of `dx`, `dy` and `dz` were calculated for each point around the scaffold splines, by dividing the distance in each dimension by the number of slider ticks in use. This value is 100 in the final version of the program, again selected arbitrarily but to ensure that a large range of customisability is provided to the user. These factors are then used to multiply the slider values (and swelling average for vertical swelling) as explained before, and produce the nodes' new positions.

8.4.3 Vertical Region Selection

A further level of user control over the swelling of the sinus cavities was incorporated in later versions of the program, by allowing the selection of the vertical region of the model to alter. This allows the user to apply swelling to only part of a sinus area, leaving the remainder of the area unaffected and is performed in a similar way to the application of swelling, using sliders to define the region. The user makes their selection by defining the top and bottom levels of the required region with the sliding scales. The definition stage of the program is shown and described in more detail in Section 10.4.3.

The selection of the vertical region in which to apply swelling affects the model in the manner shown in Figure 108, using the sphenoid sinus as an example.

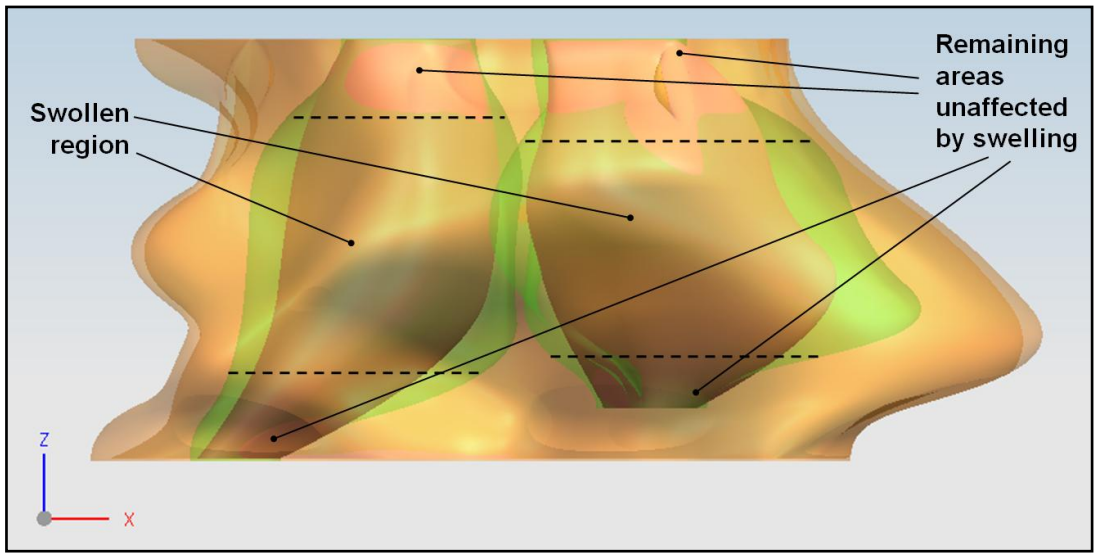

Figure 108: Selection of vertical region of swelling

In this case, the user has selected an area from the centre of the sinus to be affected, leaving sections at the top and bottom of the cavities unaffected. This method of vertical region selection must be tailored to the sinus region that is being altered; the frontal sinus requires only one selection to be made, as the cavities continually split and combine, making them impossible to treat separately. The sphenoid sinus, however, always exhibits two distinct cavities that may be altered individually, as shown in Figure 108. As such, two separate sets of sliding scales are provided for the user to make region selections for the left and right cavities of the sphenoid sinus (see Section 10.4.3).

This stage of the wizard is integrated into the application of the swelling through the use of *If* and *Else* functions in VB, to apply a comparison between the layer number being affected and the vertical layer region selected by the user. If the layer is found to be within the selected range, the swelling application code is run; if not, the code is skipped and the next layer is tested for inclusion.

8.5 Simulation of Swelling in 3D Model

The best method by which swelling would be applied to the 3D CAD model then had to be determined. This section describes the steps taken to develop the swelling simulation process, and the way swelling is eventually simulated in the model of the sinuses.

8.5.1 Scaffold Splines

An investigation was undertaken to determine whether a simpler means of simulating the swelling applied to the 3D anatomical geometry model existed than those already used. Until now, two methods of swelling simulation had been employed. Both methods simulate the shape of the swelling required as a solid body before subtracting this from another solid body within the CAD system, using a Boolean operation to achieve the final result. The two methods are summarised below:

1. The actual anatomical geometry is changed; this creates the need to copy the original splines, if they are to be used in the subtraction of swollen solid

bodies. To do so, the codenames of the newly created splines must also be known, in order for the effects of swelling to be applied or for alterations to be made later.

2. New splines are created from scratch; these new splines are immediately supplied with the swollen geometry, however their codenames are not known and their shape can therefore not be altered.

The ability to alter the model after the first application of pathology is absolutely vital to the success of the program, especially in the early stages of its use when inexperienced users may not initially achieve the required results. Using method 2, above, meant in practice that to make changes to case settings the code would have to be run again, creating a new set of splines within the model, leaving two sets of splines on each layer. It was therefore decided that these methods were unsuitable for use in the final version of the program, primarily due to the inability to alter new splines once they have been created, as their codenames are unknown. The subtraction of a manipulated solid from part of the CAD model was considered to be a good way to differentiate between the original bone anatomy and the newly formed swollen cavity lining, and was kept for use in the new method.

'New' splines must therefore be used to take on the geometry of the pathology being applied, but if created by the code, their codenames would be unknown. The original splines cannot be used as they form part of the model themselves, to change their geometry would disrupt the anatomy to which the pathology is applied – but their codenames would be known. What was therefore created was a method involving a combination of both options, where 'new' splines would be created and left within the model, awaiting the application of swelling to their area of the model. The codenames of these pre-existing new splines, or 'scaffold splines' are therefore known and can be used in the VB code as shown in Section 8.3 and 8.4.

In this new method, the original anatomical geometry remains unchanged and the imported splines are used only to acquire the initial co-ordinates from which swelling

will occur. The scaffold splines are then manipulated separately, but interact with the original model to create the final result.

By using this method, which manipulates the shape of pre-existing splines, the alteration of previously saved cases is made possible, as described in Section 10.5.2. Changes may also be undone (see Section 10.6) or alterations may be made to the settings after application. If the user decides to move back through the wizard after applying case settings, the new settings are still applied to the same splines, achieving alteration of the pre-existing case.

The solidification of the scaffold splines, in order to be subtracted from other parts of the model and leave a simulated affected cavity was the next part of the swelling application method to be developed.

8.5.2 Splitting 3D model to apply swelling

Due to the complex, branching structure of the cavities in the frontal sinus, it was impossible to use a single series of scaffold splines to create a solid for manipulation and swelling simulation. Figure 109 shows the divisions that occur in the cavities of the frontal sinus:

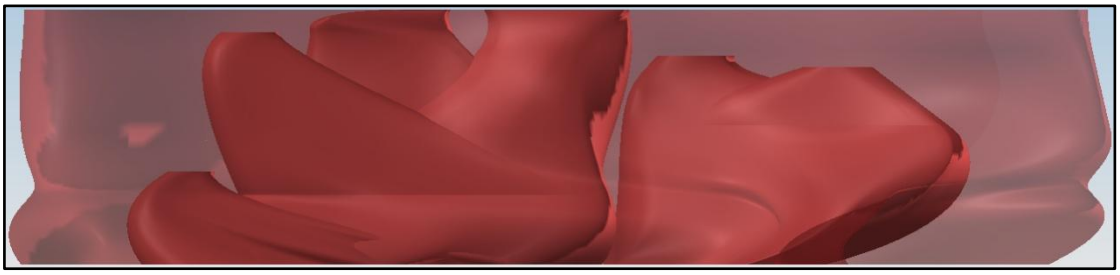

Figure 109: Frontal sinus anatomy - cavities split, therefore single scaffold solid cannot be used

Instead, the cavities of the frontal sinus were divided into six sections, each represented by a scaffold solid to fill that area. The solids are named Left 1-4 and Right 1 and 2, as illustrated in Figure 110 and consist of differing numbers of scaffold splines, depending on the size of the cavity in question:

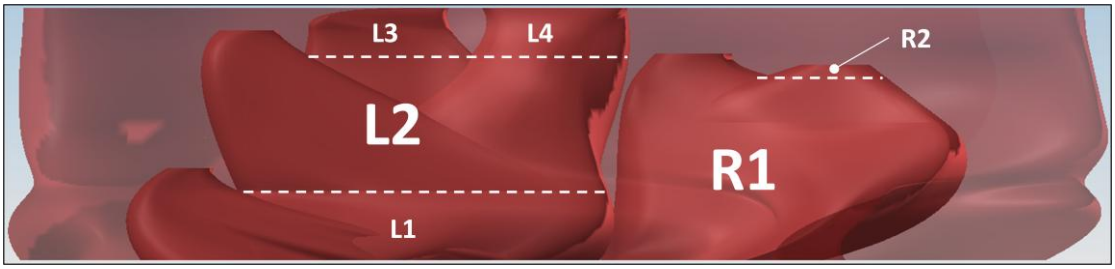

Figure 110: Cavities of the frontal sinus divided into six sections

It can be seen in Figure 110 that sections L1, L2 and R1 are used in the main body of the left and right cavities respectively, while sections L3, L4 and R2 are used in small sub-cavities that branch off from the main cavities. Moving downwards through the left side, sections L2, L3 and L4 share a common layer, shown by the uppermost white line, at which point their division ends. After this layer section L2 may be used alone to subtract from the main body of the left cavity, until it too joins with section L1. Section L1 may then be used for the remainder of the frontal sinus. The same is true in the right side, where section R2 covers a small vertical region until joining with section R1, which may be used for the rest of the cavity. The groups of scaffold splines are joined by a through curves operation prior to the model being used. The codename of the solid produced through the splines is therefore known and may be used in the subtraction code to simulate the swollen cavity.

In order to give a smoother result, avoid causing modelling errors and simplify the modelling procedure, the number of layers included in the model was reduced from 23 (one layer per mm) to a number for each section to maintain sufficient realism. Sections L1, L4 and R2 consist of two layers; L2 and L3 have three layers; section R1 consists of five, which help to maintain the shape of the right cavity. The realism achieved by this method is verified by the users of the program in Section 10.7.1.7.

To simplify the sets of scaffold splines and geometry alteration system further, the scaffold solids were made to share the spline at convergence points. This avoided the existence of repeated splines at these points and created a tree structure (shown in Figure 111*a)* and *b)*) which more closely matched the anatomy shown in Figure 110.

The scaffold splines are shown in their swollen state in Figure 111*c)*, ready to be subtracted from the solid representing the cavity lining.

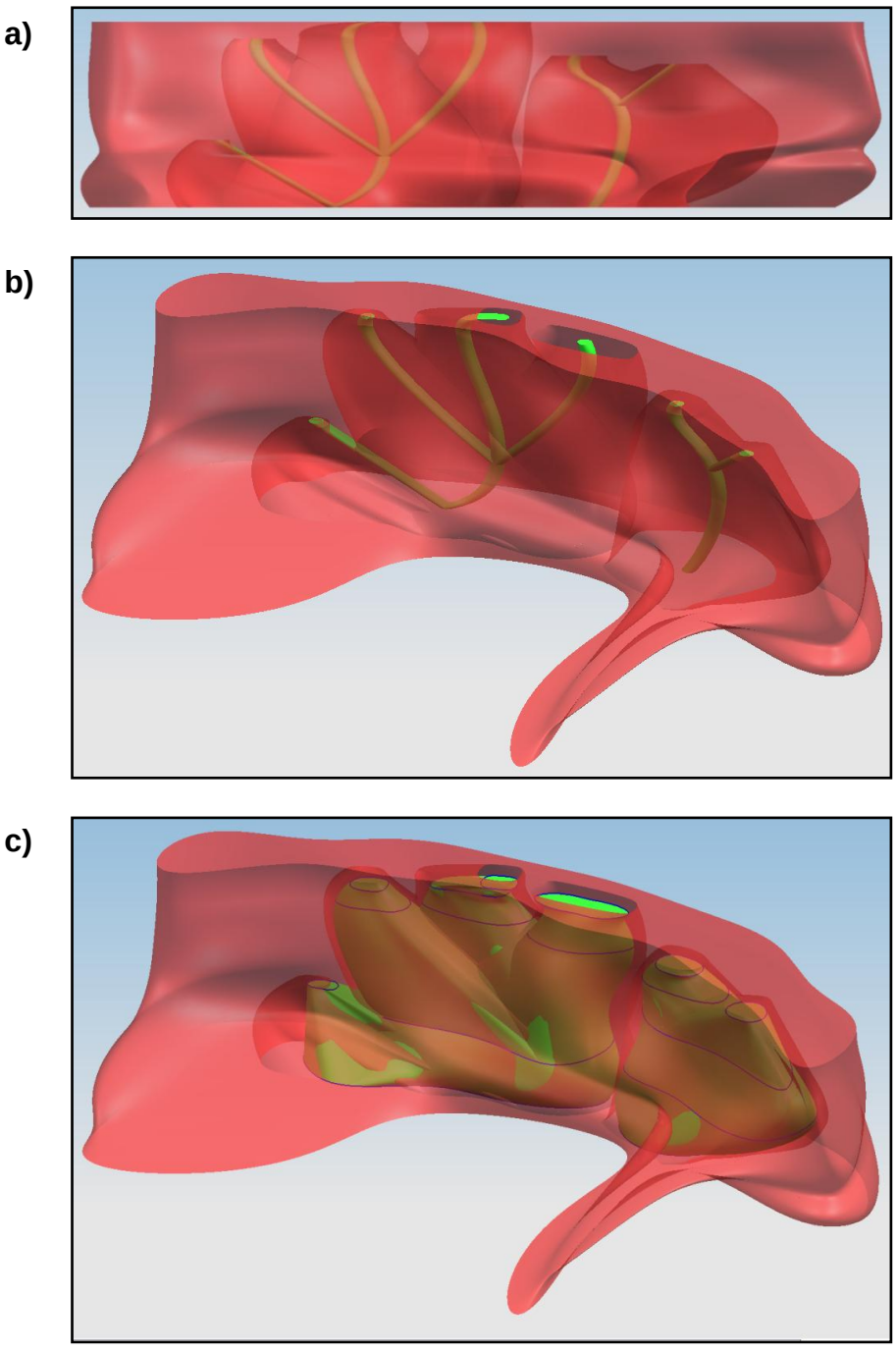

Figure 111: Scaffold splines structure for frontal sinus – *a)* and *b)* in original state, *c)* swollen

The scaffold solids for the sphenoid sinus are simpler than for the frontal; one solid is used for each of the two separate cavities, as shown in Figure 104. The scaffold

splines are shown in their original states in Figure 112*a)* and *b)* and swollen in Figure 112*c)*.

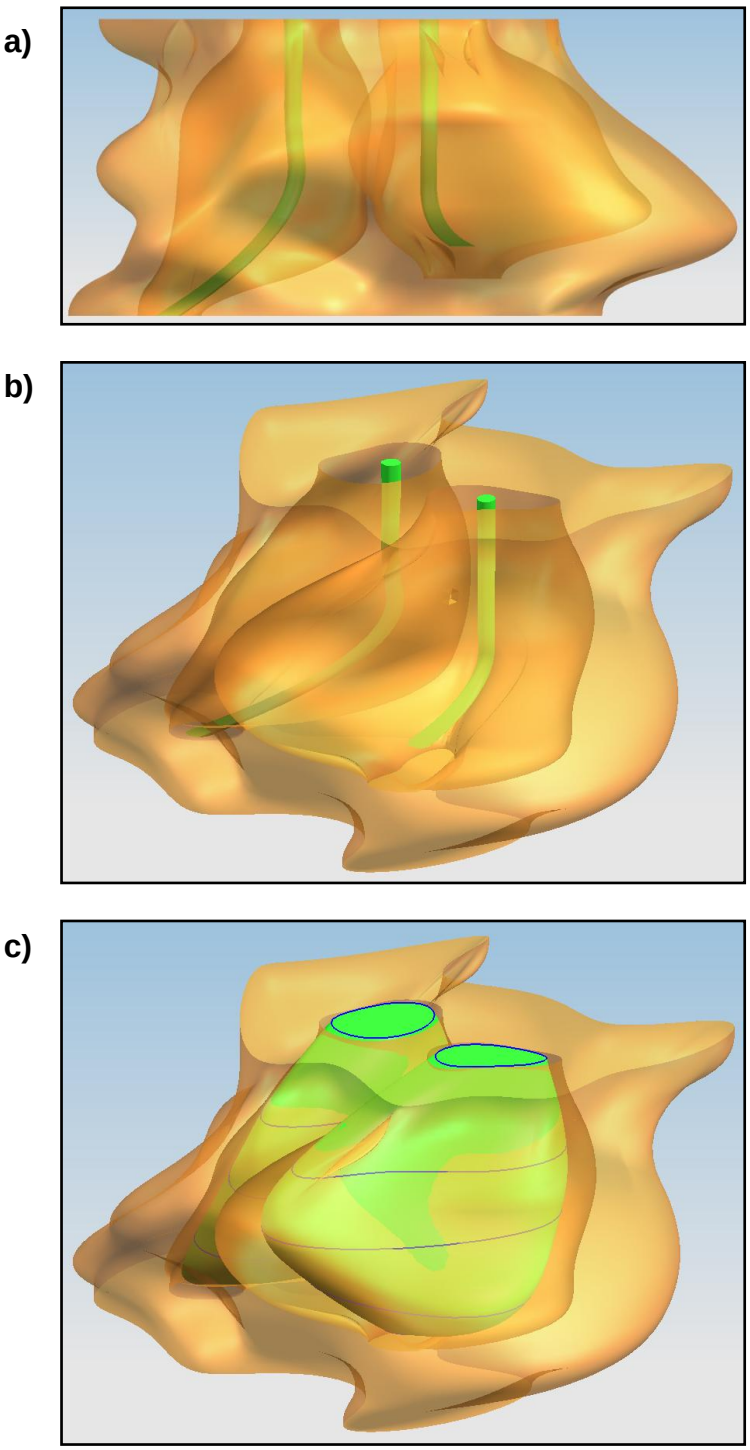

Figure 112: Scaffold splines structure for sphenoid sinus – *a)* and *b)* in original state, *c)* swollen

The code required to apply the swelling settings individually to every spline of each section of the frontal or sphenoid sinus would be of considerable length. Instead of doing this, an iterative loop of spline alteration code was used within a swelling application subroutine.

The code in Figure 113 shows one of the iterative loops used to apply changes to the splines in the frontal sinus; in this case, to alter the geometry of section L1 (layers 15 and 23). This loop is run with increasing values of `LayerNoFrontal`, from 15 to the final layer number (`Layers`). Each time the value of `LayerNoFrontal` satisfies the conditions shown, i.e. when the value matches 15 or 23, the spline alteration code held in the subroutine for section L1 is run with the appropriate variable values.

```
For LayerNoFrontal = 15 To Layers
    If LayerNoFrontal = 15 Then
       SplineName = "HANDLE R-228004"
       FrontalSplinesL1()
    ElseIf LayerNoFrontal = 23 Then
       SplineName = "HANDLE R-228007"
       FrontalSplinesL1()
    End If
Next
```

Figure 113: Iterative loop forming part of swelling application subroutine

This is repeated throughout the spline application subroutine for all sections of the frontal sinus, and a similar method is used for the sphenoid sinus.

8.5.3 Solid Modelling of Swelling

The first method used to simulate the swollen lining of the sinus cavities with scaffold splines involved the use of a second set of solid bodies, the same size as the original cavities. The geometry created by the scaffold splines would be subtracted from the cavity bodies to leave the swollen cavity lining, as shown in Figure 114:

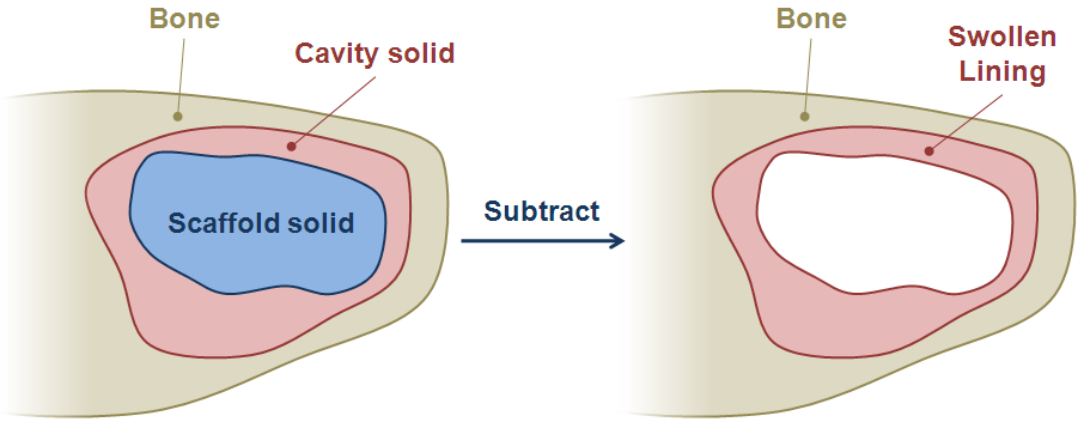

Figure 114: Using subtracted scaffold solids to create swollen lining

This method encountered modelling errors when the geometry of the scaffold splines was not entirely enclosed by the cavity solid. This is undesirable, as errors in NX halt the running of Case Creator, ending the ability of the user to work on the model. Errors can occur if the interpolation between two nodes of any of the scaffold splines is not direct, such as between nodes C and D in Figure 115:

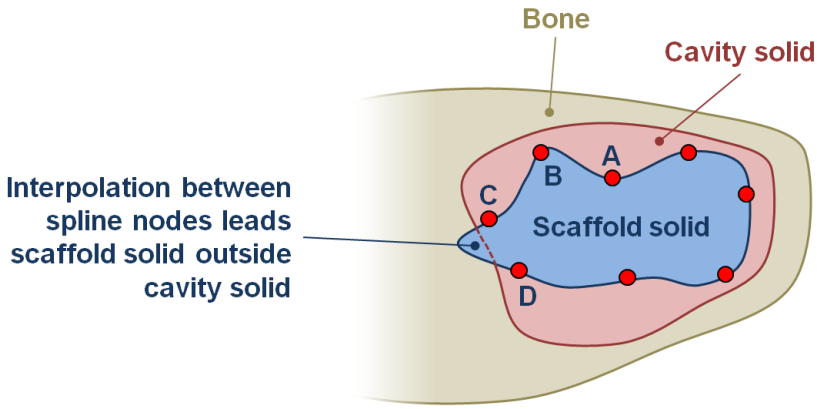

Figure 115: Scaffold solid strays outside cavity solid boundary causing modelling errors

In the example in Figure 115, the interpolation between scaffold spline nodes C and D is forced outside the perimeter of the cavity solid. Node A is further towards the centre of the cavity than node B, which causes the spline between nodes B and C to bend concavely. This in turn leads to the spline between nodes C and D bending convexly, taking it outside the cavity solid perimeter. This, of course is the case between most nodes to some extent, but some combinations of node positions (set by

the user's swelling settings) will inevitably lead to this undesirable situation, which causes modelling errors to occur.

The problem was combated by using far larger cavity solids throughout the CAD model. Only one cavity solid was used in each sinus area, which instead of only filling the cavities of the sinus area, were created as a near-identical copy of the exterior anatomy. The cavity (now termed 'interior') solid is created to fit inside the exterior anatomy with a tolerance of 0.5mm, occupying the same 3D space and filling all the cavities therein. The scaffold solids are then subtracted from the interior solid; as this is now far larger, the scaffold solids will never protrude through the outer face. As a result, no errors are encountered should the scaffold solid stray outside a cavity boundary. In the same case as described previously, now shown using the new system in Figure 116, the left wall of the cavity will exhibit an area of bone with no lining:

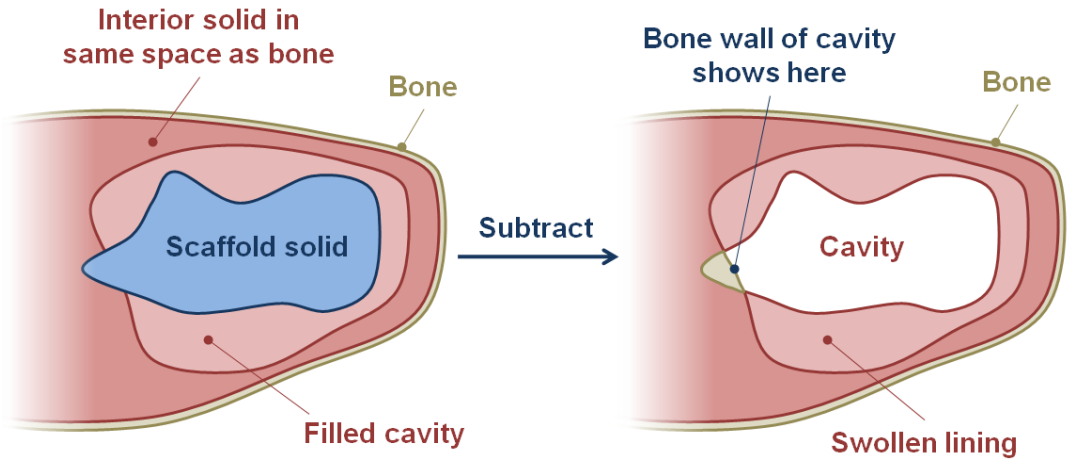

Figure 116: Using larger interior solid to avoid modelling errors on subtraction of scaffold solid

By using this method, no CAD errors are produced, enabling the user to continue to work with Case Creator to adjust their settings, or accept the result.

To speed up the case application process and display a clearer and more accurate result, visibility settings were incorporated into the swelling application code. Should the user select not to apply swelling to the frontal sinus, the interior solid will not be displayed, leaving the original anatomy visible as the result. If the selection is

changed, the geometry of the scaffold splines is altered, subtracted from the interior solid and the result is made visible within the cavities of the anatomy.

In the sphenoid sinus, where the two cavities are treated separately, the user may select to apply swelling to only one side. If this is the case, the interior solid (which covers both cavities) must be made visible. Therefore the cavity that has no swelling applied must be created in the normal way, but with swelling values of 0%.

The final results of swelling applied to the frontal sinus are shown in Figure 117 (red body represents original bony anatomy, pink represents swollen cavity lining) using the final swelling method. Red is used in this area of the model, and gold in the sphenoid sinus, to allow colour co-ordination to be used at all stages of the wizard, making it clear which area of the sinuses is being worked on. Figure 117*a)* shows the sinus area from above and behind, where the pink cavity lining can be seen. Figure 117*b)* shows the sinus area from below and in front, allowing the swelling within the cavities to be seen. In Figure 117*c)*, taken from directly below the sinus, with the anterior at the top of the image, the swelling from each side of the head can be seen, up into the roofs of the cavities.

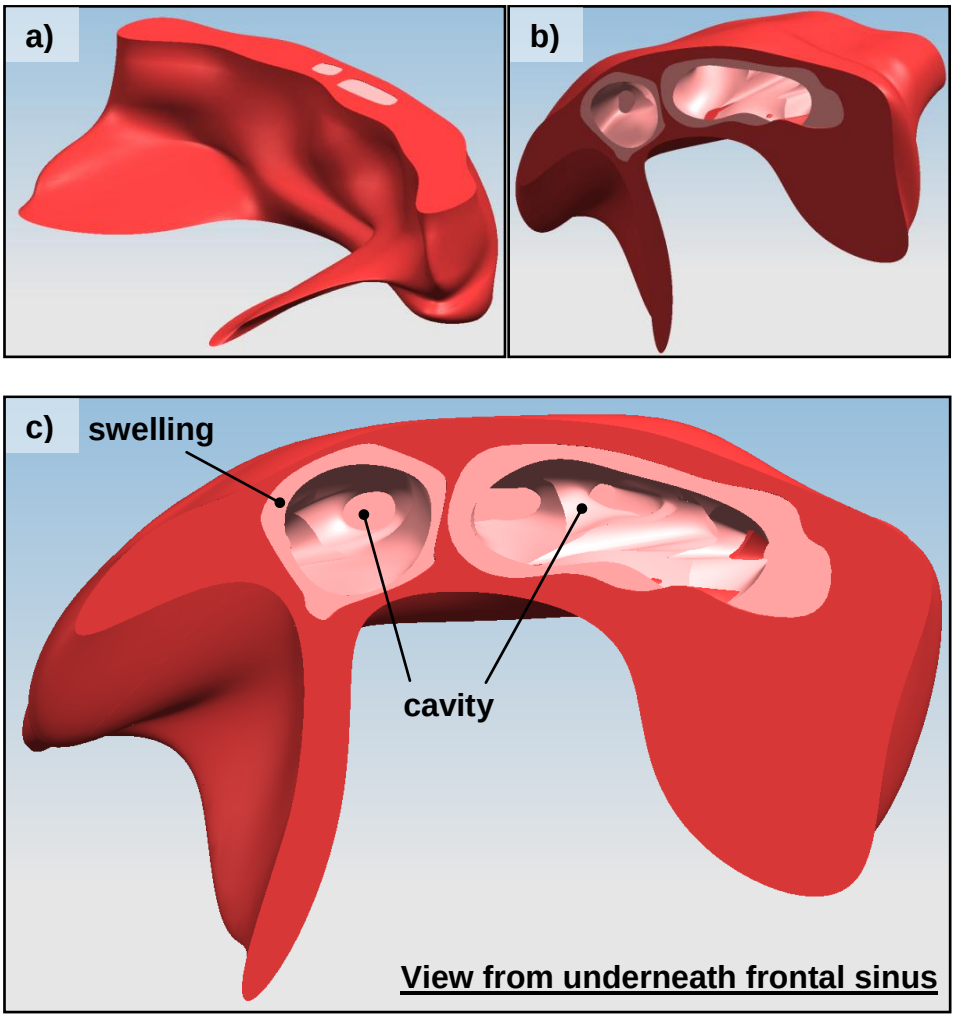

Figure 117: Swelling applied to frontal sinus using final swelling method in three views (*a), b), c)*)

The results of swelling applied to the sphenoid sinus are shown in Figure 118. In Figure 118*a)*, the sphenoid sinus is shown from behind and above, with the pink swollen cavity lining visible at the top of both cavities. Figure 118*c)* shows the swelling within the cavities from the same direction; the sinus area is sectioned at the line shown in Figure 118*b)* (showing the sinus from the back). The marbling visible in the bottom image is due to the bony anatomy (gold) and swollen cavity lining body (pink) occupying the same 3D space. The bottoms of both cavities are visible, having been swollen upwards from their original position.

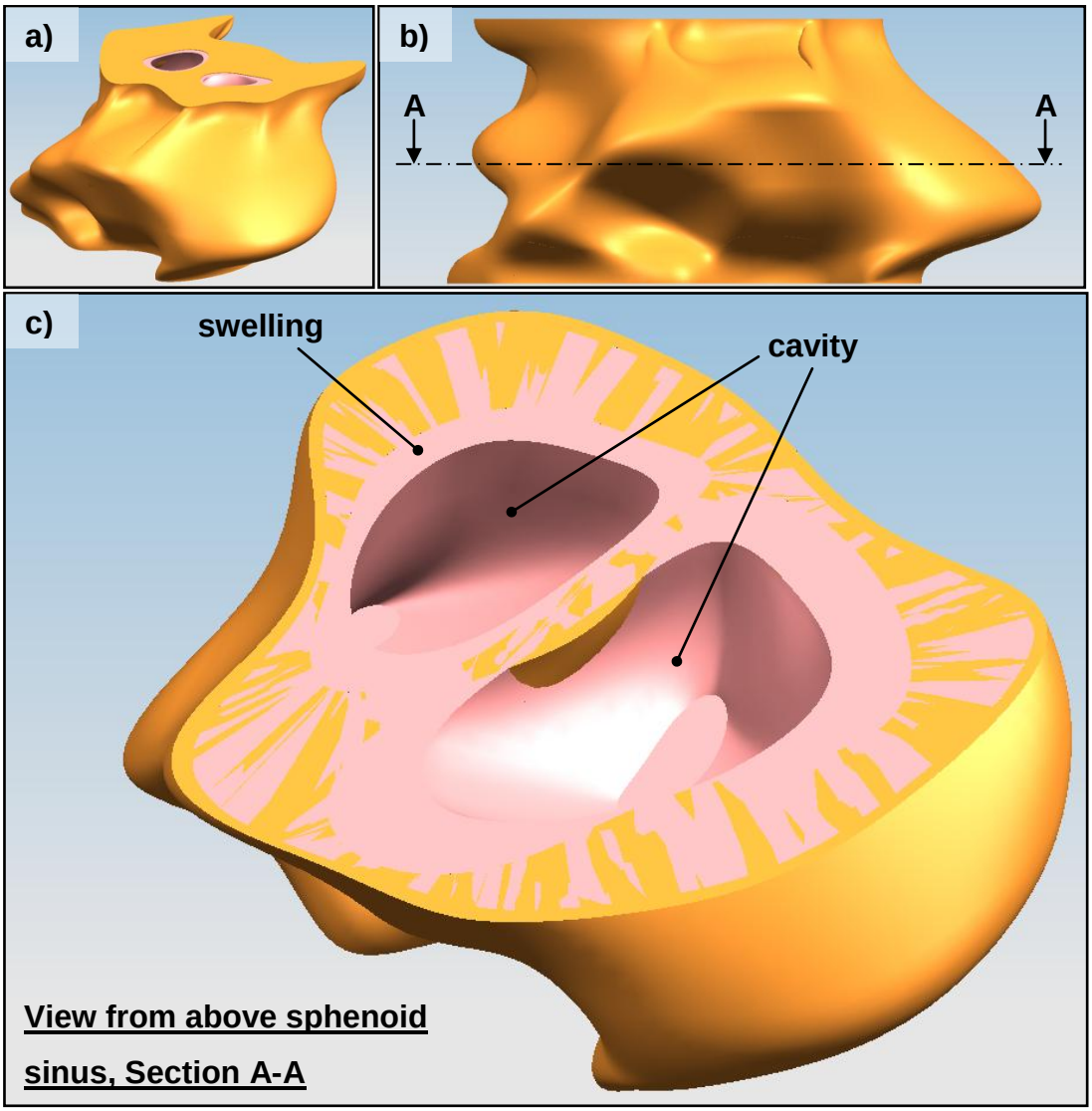

Figure 118: Swelling applied to sphenoid sinus using final swelling method in three views (*a), b), c)*)

CHAPTER NINE

CUSTOMISABLE SINUS SURGERY TRAINING MODEL – TUMOUR ADDITION

9 Customisable Sinus Surgery Training Model – Tumour Addition

An important feature to include in the program was the addition, sizing and placement of tumours in the sinuses. As Figure 64 shows, this work began in order to coincide with the development of the swelling application method, and draws from the discoveries made in that investigation. The work to be done to achieve this is set out in the flow chart in Figure 119:

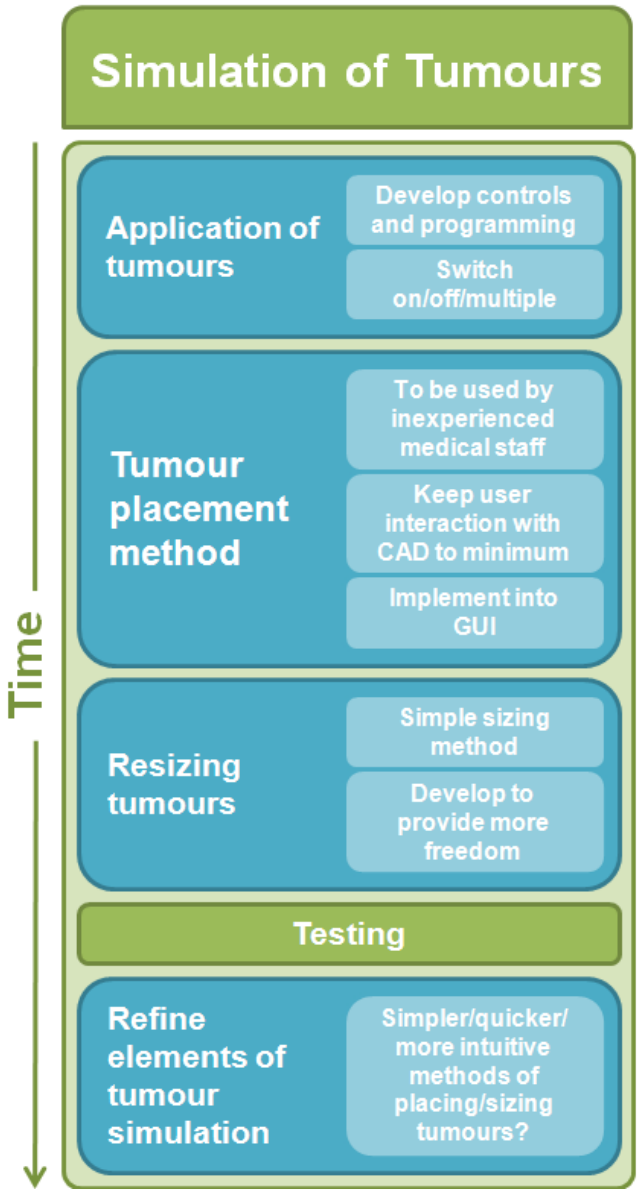

Figure 119: Plan for development of tumour simulation function

As with all previous functions, the GUI had to be designed to allow the user to perform the operation with no direct interaction with the CAD software, to ensure that the simplicity of the task was maintained. As with the application of swelling, the application of tumours could be performed on a range of levels of customisability, as shown in Table 8:

Customisability	Action
Level 0	Tumours automatically placed, same position every time
Level 1	Option given to apply tumours, automatically positioned
Level 2	Option to apply, catalogue offers selection of placement positions
Level 3	Option to apply, catalogue of positions, multiple tumours available
Level 4	Option to apply, multiple tumours positioned manually
Level 5	Option to apply, multiple tumours positioned and sized manually
Level 5+	Option to apply, multiple tumours positioned and sized manually on a finer scale

Table 8: Levels of customisability for the application of tumours

The aim of this project is to provide the user with customisability at Level 5+, whereby tumours may be resized and positioned manually, if required.

9.1 Switching Tumours On and Off

As shown in Figure 119, the first task was to provide the user with the option to apply a tumour to the anatomy. This was done through the use of a checkbox, and Figure 120 in Section 9.2.1 shows the option to apply the tumours at the top right of the Case Creator window. The system was later expanded to allow more than one tumour to be added or removed from the anatomy during customisation (see Section 9.4).

When the checkbox is clicked, code is run to perform actions dependent on whether the user has selected, or deselected the tumour. If the tumour has been switched off, the tumour icon on the form is made invisible, and the positioning sliders and sizing controls (to be described in Sections 9.2.1 and 9.3) are disabled. Also, if the user reaches the final stage of the wizard and applies the settings to the model in NX, the

code used to finalise the tumour body in NX is ignored and the pre-existing tumour body is made invisible (see Section 9.5) making the overall process quicker. If the property of the checkbox is changed back to checked, the icon is made visible, in the last location it was placed, the sliders are enabled, the tumour creation code will be run and the tumour body is made visible on application of the case settings. This achieved at least level 1 on the scale of customisability shown in Table 8.

9.2 Positioning of Tumours within Sinus Anatomy

Once the initial choice of applying tumours to the anatomy had been provided, the way in which the user would define their position within the sinus complex was developed. One possible method considered for the positioning of tumours within the sinus anatomy was to provide the user with a catalogue of tumour sizes and positions, to select as they wished. While this would reach customisability level 2 or 3 in the scale described in Table 8, this method has several drawbacks. The range of cases that may be produced using this method is limited to the number of catalogue entries provided. Secondly, the application of catalogued options to different patient anatomy could lead to errors in modelling, as all anatomy will be unique in geometry. Tumours may accidentally be placed outside the anatomy; indeed, the user may not gain any understanding of where the tumours were to be placed until the process was complete.

This meant that for this program, the positioning of tumours could not be limited to a set of choices, or performed automatically. For the user to position the tumour within the anatomy themselves, some knowledge, whether geometrical or visual, of the anatomy involved is required. A method by which the user enters the co-ordinate position of the tumour to be created in the CAD model is unsuitable, as the geometrical knowledge required is too precise and would involve some interaction with the CAD software to ascertain the 3D co-ordinates they required. Such a method would therefore be unlikely to reliably produce the expected results.

A visual positioning approach was therefore deemed more suitable, still with the aim of doing so without interaction with the CAD modelling software. With user

interaction limited to actions within the Case Creator GUI, positioning of the tumours within a 3D workspace was ruled out. It was decided that the simplest, most user-friendly way of giving the user a clear impression of the tumour position in three dimensions was to show the sinus region in two planes, and move the tumour(s) in two dimensions at a time. The sinus anatomy is shown in two simulatory images; from the back and above (coronal and transverse planes), allowing movement of the tumour in the X/Z plane and X/Y plane respectively. This method was judged to be more suitable due to surgeons' experience of studying 2D MRI and CT images in these planes. Using the two images, tumours would be placed by eye (with co-ordinate feedback) and the CAD model automatically updated once their position was finalised.

The user is therefore presented with a clear placement window, offering a preview of the positioning of the tumour in relation to the real anatomical geometry, prior to applying the case. The preview also updates to give an impression of the size of tumour selected and its relation to the surrounding anatomy. The tumour positioning system is described in the following section.

9.2.1 Sliding Scale Positioning System

Figure 120 shows the controls for positioning and sizing a tumour within images of the frontal sinus region initially obtained from µ-CT data.

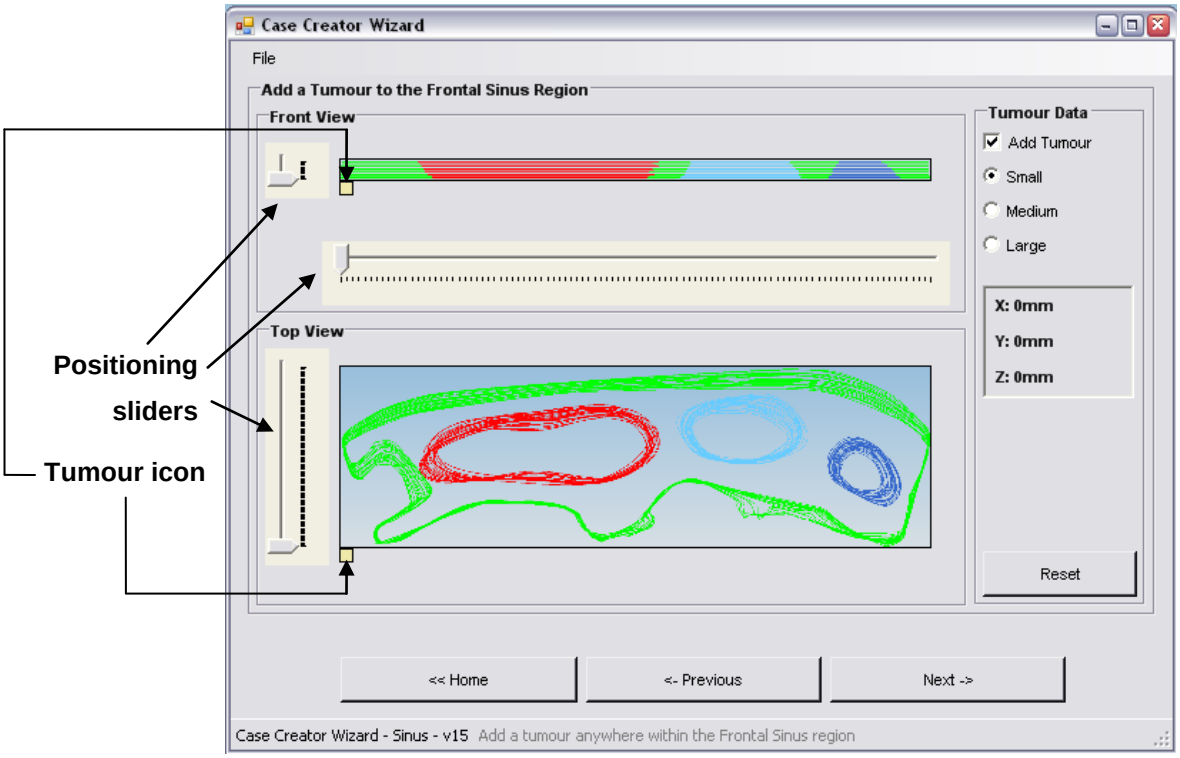

Figure 120: User interface for tumour placement

Shown in Figure 120 is the pair of medical images, showing the anatomy from the back (top image in Figure 120 – until later versions of the program were developed, this view was incorrectly labelled as "Front View"; this error is corrected in Section 11.2.5.2) and the top (lower image in Figure 120). The small square shown in the bottom left corner of each anatomical image represents the tumour to be sized and positioned. A square is used as only rectangular shapes may be placed within the VB window. With the image of the back view of the sinus anatomy, there are two sliding scales for applying movement in the x- and z-directions in the 3D CAD model. One sliding scale is positioned with the top view of the anatomy, which controls movement in the y-direction. The x-direction slider alters the position of the tumour in both the top and back views.

The user will move the tumour over the anatomical images, inwards from the images' bottom left, as shown in Figure 121*a)*. This is done to simulate movement in the positive x-, y- and z-directions from an origin in the CAD model, as in Figure 121*c)*.

However in VB, the co-ordinates of objects within the 'form' (the program window) are set from the top left corner of the containing 'groupbox' (in this case the "Front View" and "Top View" containing boxes) to the top left corner of the object (shown in Figure 121*b)*); as such, the start point of the squares is with their top-left corners at the bottom-left corner of the relevant anatomical image. Figure 121 summarises the two different co-ordinate systems, using the anatomical data from the CT scan:

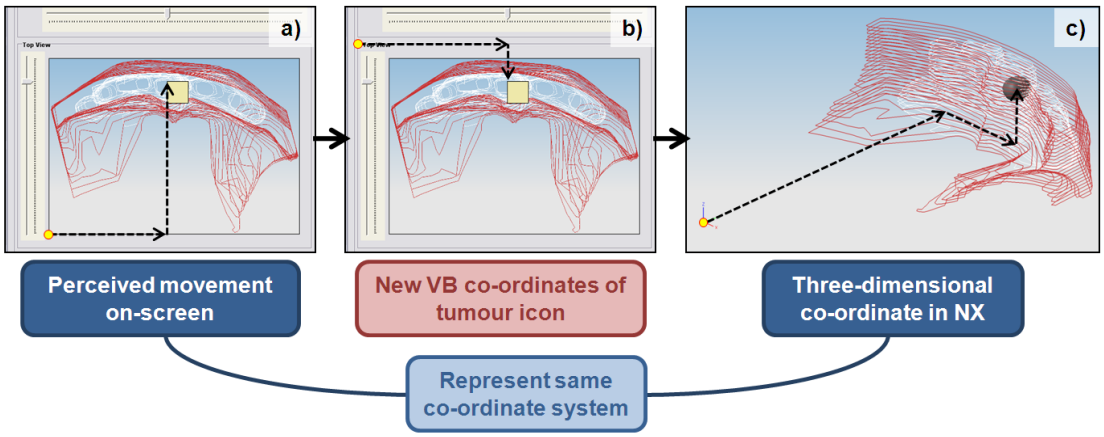

Figure 121: Positioning tumour relative to different co-ordinate systems

The tumour is positioned using the sliding scales in the X, Y and Z dimensions while studying the visual preview of the tumour's position and size in relation to the sinus anatomy. Each time the sliding scale value is altered, the effect that is required is to make it appear as if the tumour icon is matching the position of the slider handle (Figure 121*a)*). In reality, the value of the slider is converted into pixels depending on the size of the anatomical image, and then used in the calculation of the new icon co-ordinates. The co-ordinates of the tumour square within the form are adjusted accordingly (Figure 121*b)*), in a similar manner to the application of swelling described in Chapter 8.

The sliding scales consist of a different number of divisions to the on-screen size of the anatomical images in pixels. As such, the positioning of tumours within the form requires the sliding scales' divisions to move the tumour icons by differing amounts, depending on the size of the image in question. This is done by altering the

conversion from sliding scale to form co-ordinate value, to maintain the correct, consistent positioning method. For example, the x-position sliding scale shown in Figure 121 consists of 100 divisions, while the image of the frontal sinus is 465 pixels wide. This means that in order for the scale to move the tumour square from one side of the anatomy to the other, the sliding scale value must be multiplied by 4.65 before being used in the tumour squares' form x-co-ordinate calculation.

The form x-co-ordinate is calculated by adding the converted sliding scale value to the original tumour square x-co-ordinate. This process is repeated, with the appropriate adjustments, for the form y-co-ordinates of both tumour squares. As y-co-ordinates are measured downwards from the top left corner of the containing groupbox in VB, the converted sliding scale value must be subtracted from the original tumour square co-ordinate to obtain its new position.

The positions of the tumour icons on-screen must be transformed into 3D co-ordinates for the single tumour in NX (Figure 121*c)*). This was initially done by comparing the size of the anatomical images in VB to the CAD model, and converting the form co-ordinates to NX co-ordinates. This however was a fairly complex process, which had some inherent flaws. The two stages of conversion meant that the final position of the tumour body in the CAD software would sometimes be different to the simulated tumour position in the GUI. A new method was therefore developed, which calculated the NX co-ordinates in the same way as the tumour icons' form co-ordinates.

A tumour positioning subroutine (named `TumourPosition`) is run every time the x, y or z-position sliding scales are changed, which sets all positions related to the tumour, in whichever sinus area is being addressed. A range of non-area-specific variables is used in the subroutine, to allow it to be repeatedly used for each sinus area, and to ease the addition or alteration of code. The code for positioning a tumour on the form and in the CAD model is as shown in Figure 122:

```
TumourPosition()

1   dxTum = SinusSizeX / TrackBarXTum.Maximum
    dyTum = SinusSizeY / TrackBarYTum.Maximum
    dzTum = SinusSizeZ / TrackBarZTum.Maximum

2   xCoordTumOnForm = TumOriginX + (TrackBarXTum.Value *
          TBXTumFactorPixels)
    yCoordTumOnForm = TumOriginY - (TrackBarYTum.Value *
          TBYTumFactorPixels)
    zCoordTumOnForm = TumOriginZ - (TrackBarZTum.Value *
          TBZTumFactorPixels)

3   PanelTumFront.Location = New System.Drawing.Point
          (xCoordTumOnForm, zCoordTumOnForm)
    PanelTumTop.Location = New System.Drawing.Point
          (xCoordTumOnForm, yCoordTumOnForm)

4   xCoordNX = SinusXPos + (TrackBarXTum.Value * dxTum)
    yCoordNX = SinusYPos + (TrackBarYTum.Value * dyTum)
    zCoordNX = SinusZPos + (TrackBarZTum.Value * dzTum)

5   LabelTumX.Text = "X: " & xCoordNX & "mm"
    LabelTumY.Text = "Y: " & yCoordNX & "mm"
    LabelTumZ.Text = "Z: " & zCoordNX & "mm"
    LabelTumCoords.Text = "(" & xCoordNX & ", " &
          yCoordNX & ", " & zCoordNX & ")"
```

Figure 122: TumourPosition() – tumour positioning subroutine

The tumour positioning subroutine consists of five parts, each run every time the sliding scales are altered. The variables used in the code (listed below) are supplied with the appropriate values when the user selects which sinus area they wish to alter:

- `xCoordTumOnForm`/`yCoordTumOnForm`/`zCoordTumOnForm` (form co-ordinate of the tumour icon in VB, measured from the top left corner of the containing groupbox)
- `TumOriginX`/`Y`/`Z` (starting position of the tumour icon on the form, bottom left corner of the sinus image)
- `TBXTumFactorPixels`/`TBYTumFactorPixels`/`TBZTumFactorPixels` (conversion factor from sliding scale value to form co-ordinate)
- `SinusSizeX`/`Y`/`Z` (dimensions of the sinus area in NX)

- `SinusXPos`/`SinusYPos`/`SinusZPos` (co-ordinates of relevant area of sinus model in the CAD model)

Part 1

The first part of the tumour positioning subroutine sets the value of `dxTum`, `dyTum` and `dzTum`, which are used to position the tumour in NX. These variables work in the same way as `dx`, `dy` and `dz` in the application of swelling; they are set as the amount of movement applied by each division on the sliding scales. This is done by dividing the overall sinus area size by the number of divisions on the scale (the maximum value of the scale).

Part 2

Here, the x- and y-co-ordinates of the tumour icon positions are set as variables named `xCoordTumOnForm`, `yCoordTumOnForm` and `zCoordTumOnForm`. The form co-ordinates are set as described earlier, by adding or subtracting the converted sliding scale value to the starting point of the tumour icon. Subtraction is used for `yCoordTumOnForm` and `zCoordTumOnForm` as they are measured downwards from the top left of the groupbox. So for the form y-co-ordinates of the two tumour icons, the higher the value on the sliding scales, the more is subtracted from the form co-ordinate, moving the tumour icon closer to the origin (upwards).

Part 3

In this part of the subroutine, the form position of the two tumour icons is set to the values above.

Part 4

To set the 3D position of the tumour in the CAD software, the amount of movement applied in each direction (slider value multiplied by `dxTum`/`dyTum`/`dzTum`) is added to the CAD x-, y- and z-co-ordinate of the sinus area model in use.

Part 5

Feedback is provided for the user by updating labels on the form showing the co-ordinates of the tumour in NX. These are displayed on the tumour positioning page, as shown in Figure 123**,** and again at the end of the wizard on the case summary page (described in Section 11.2.6).

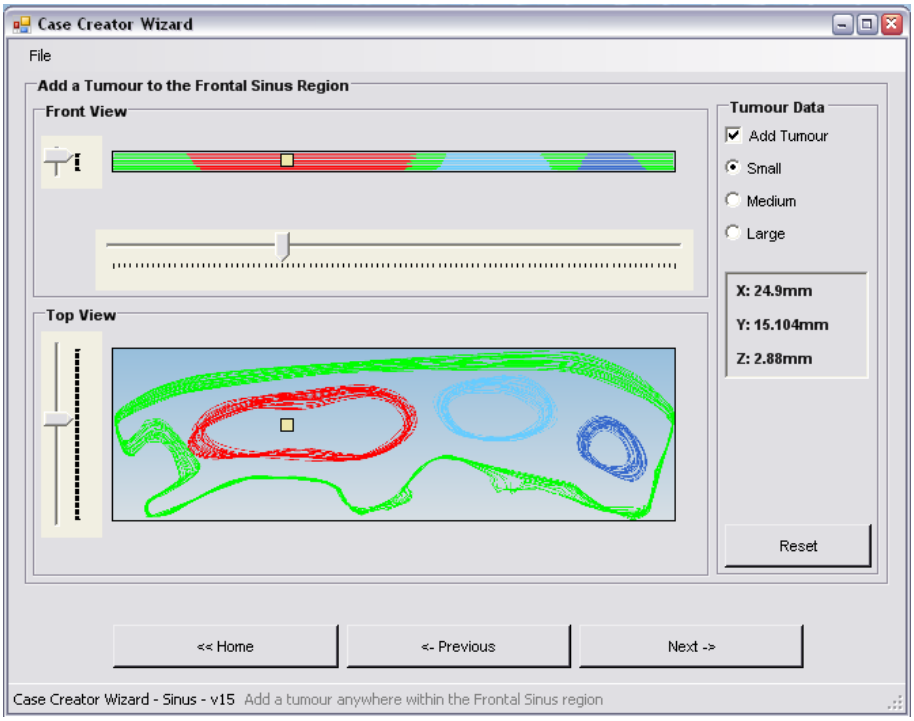

Figure 123: Tumour positioned within anatomy, positional feedback given

9.2.2 Mouse-Click Positioning System

After finalising the sliding scale tumour positioning system, a quicker, more intuitive system was developed. This system would allow the user to also position tumours within the anatomy by simply clicking on the anatomical images at the position they wished to create a tumour. With the two systems working in tandem, the user can choose which to use according to preference, or use the sliders for a more precise approach after having positioned the tumour quickly with a mouse click.

The implementation of this system was far more complex than originally perceived, and required much more intricate programming than the sliding scale system used previously. The aim was to develop a method to position the tumours with a mouse

click, using the same tumour positioning subroutine as shown in Figure 122. By bringing the two tumour icon positioning methods together at this point, the position of the icon in the form and tumour model in the CAD software would be updated in the same way as previously, requiring the minimum amount of new code. In order to make use of the pre-existent subroutine, it had to be provided with the sliding scale values needed to calculate the tumour position (Figure 122, Part 2). Focus was therefore placed on the conversion of the position of the user's mouse click (when clicked within either anatomical image) to the sliding scale values for use in the tumour positioning subroutine.

Investigations were first undertaken into the way in which mouse click positions are recorded, and the amount of information that could be obtained about the location of the mouse pointer, as illustrated in Figure 124.

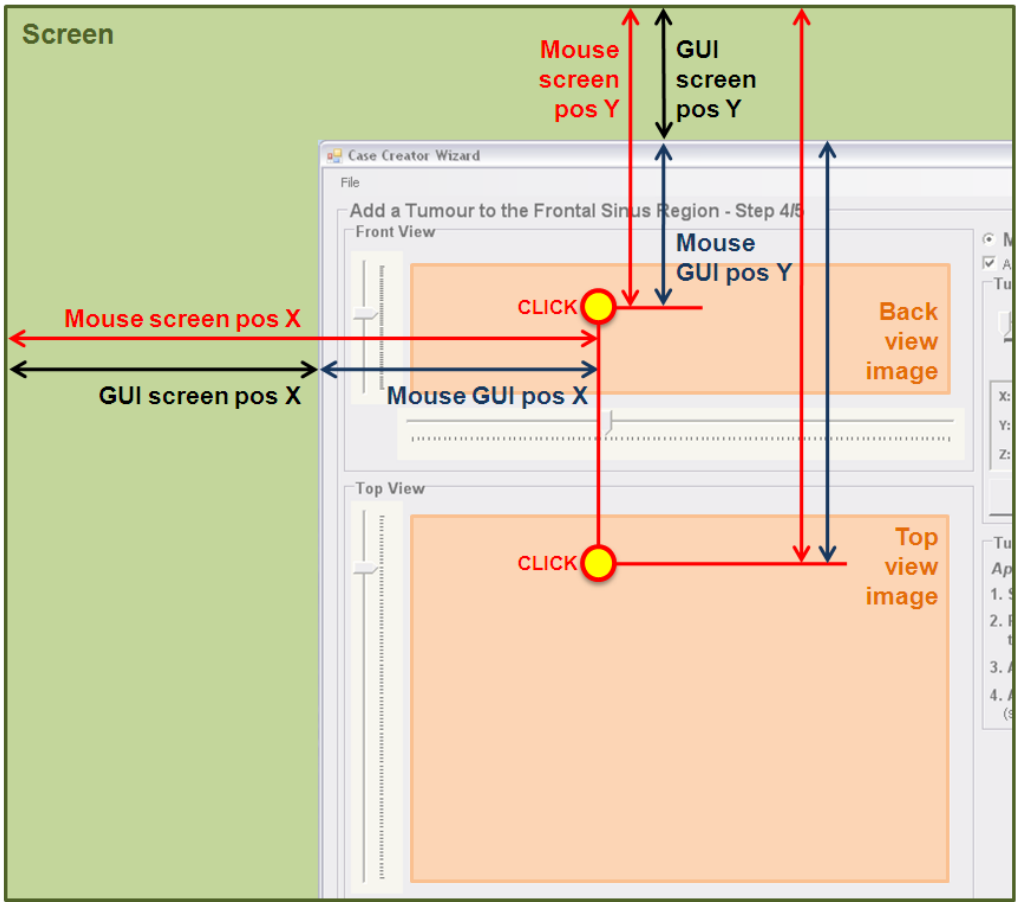

Figure 124: Finding the mouse position within the GUI

Through investigations into available functions in VB, it was found that the location of a mouse pointer could be found, and linked to a mouse click event in VB; the co-ordinates of the mouse at the time of the button being clicked could therefore be recorded. However, the co-ordinates of the pointer could only be recorded with reference to the whole screen (measured downwards from the top left, "Mouse screen pos X/Y" in Figure 124). A more local mouse position was required; as such, the next step was to find a way to detect the mouse position within the GUI. Due to the functions available in VB, the only way in which this could be done was to compare the on-screen positions of the mouse and window at the time the mouse button was clicked. By subtracting the on-screen window co-ordinates from the mouse co-ordinates, the position of the mouse within the window was found ("Mouse GUI pos X/Y" in Figure 124).

As stated earlier, the co-ordinates of items on the form in VB are calculated downwards from the top left, and the origin of any form object co-ordinates is set at the top left corner of the groupbox containing the item on the form, such as the "Front View" groupbox in Figure 124. To position the tumour icon on the form, the position of the mouse click in relation to the top left corner of the relevant groupbox must therefore be found. This value will then be used in the conversion back into slider values before running the tumour positioning subroutine.

The work described above was developed to find the position of the mouse within the groupbox containing the anatomical image over which the mouse was clicked, to determine the final tumour position required by the user. Firstly, the co-ordinates of the mouse click relative to the top left hand corner of the groupbox containing the sinus image (such as the "Front View" groupbox) are calculated.

This is done by finding the position of the mouse within the Case Creator window, as described above, coupled with further calculation to find the position of the mouse within the "Front View" groupbox. As shown in Figure 125, the "Front View" groupbox is located 23 pixels inside the left edge of the Case Creator window. By

subtracting 23 from the x-position of the mouse within the window, the x-position of the mouse within the "Front View" groupbox is found ("xCoordTumClick" in Figure 125).

The process is repeated to find the y-co-ordinates of the mouse click over the image, as shown by "zCoordTumClick" in Figure 125 (to find the z-co-ordinate of the tumour in the CAD model). The groupbox is located 72 pixels from the top of the window, so 72 pixels are subtracted from the co-ordinates of the mouse within the window. The position of the "Top View" groupbox changes depending on the size of the "Front View" groupbox, and the calculations to find the y-co-ordinate of the tumour in the CAD model are adjusted accordingly.

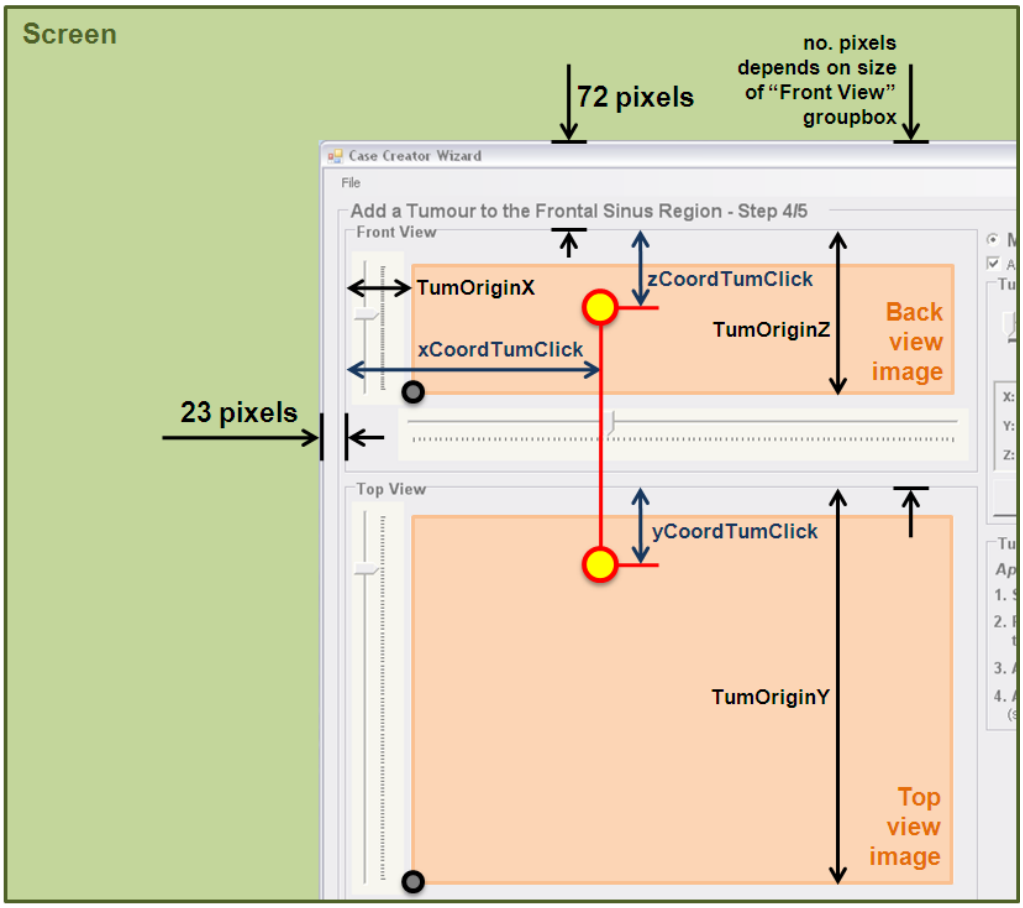

Figure 125: Finding the mouse position within the relevant groupbox

Incorporating the new click-and-place functionality into the tumour positioning system meant updating the values shown on the sliders whenever the mouse was clicked inside an image of the sinus anatomy, which presented a significant coding challenge. Each time the mouse is clicked within either anatomical image to place a tumour, the process described below is run.

For the tumour icon positioned over the top image, showing the back view of the sinus area, the new slider values are calculated as shown in Figure 126. The variables `xCoordTumClick` and `zCoordTumClick` now contain the x- and y-co-ordinates of the mouse click within the "Front View" groupbox and will be used as the tumour icon's co-ordinates when the positioning subroutine is run. The final step is to convert these co-ordinates into sliding scale values, to be passed to the tumour positioning subroutine, which will in turn place the tumour icon at the point of the mouse click. A similar process is used for the positioning of the tumour icon in the second image, with the same x-co-ordinate as calculated here, paired with a new y-co-ordinate.

```
xCoordTumClick = (MousePosition.X - Me.Location.X - 23)
zCoordTumClick = (MousePosition.Y - Me.Location.Y - 72)

TrackBarXTum.Value = (xCoordTumClick - TumOriginX) /
      TBXTumFactor
TrackBarZTum.Value = (TumOriginZ - zCoordTumClick) /
      TBZTumFactor

TumourPosition()
```

Figure 126: Conversion of mouse click form co-ordinates into sliding scale values

The slider values are set by finding the mouse location within the anatomical image from an origin at the bottom left ("TumOriginX/Y/Z" in Figure 125), as this is where the sliders' zero points are set: the image location is subtracted from the mouse position within the groupbox (`xCoordTumClick - TumOriginX`) or the inverse for vertical co-ordinates (`TumOriginZ - zCoordTumClick`). This final mouse position is divided by the sliding scale conversion factor, to convert the pixel value into trackbar points, and find the corresponding slider value out of 100. After having set these

values on the sliders, the tumour positioning subroutine is run, and the tumour icon appears in the location indicated by the user when they first clicked the mouse button.

In order to make the positioning of the tumour icons with a mouse click more intuitive, code was written to allow them to appear to be positioned by their centre, as opposed to the top left corner as described earlier. This involved the inclusion of a shift to the position of the tumour icons and the co-ordinates of the tumour body in NX. All co-ordinates had to be adjusted by the radius of the tumour icon or body, as the corner-origin systems are still in use in VB and NX. As shown in Figure 127, the tumour icon was originally positioned by the top left corner, meaning that its position did not intuitively match the location of the mouse click (scenario 1). In the newly developed system, each time a mouse click event occurs, the icon's position is calculated with the half-size shift included, creating the effect of positioning the icon by its centre (scenario 2).

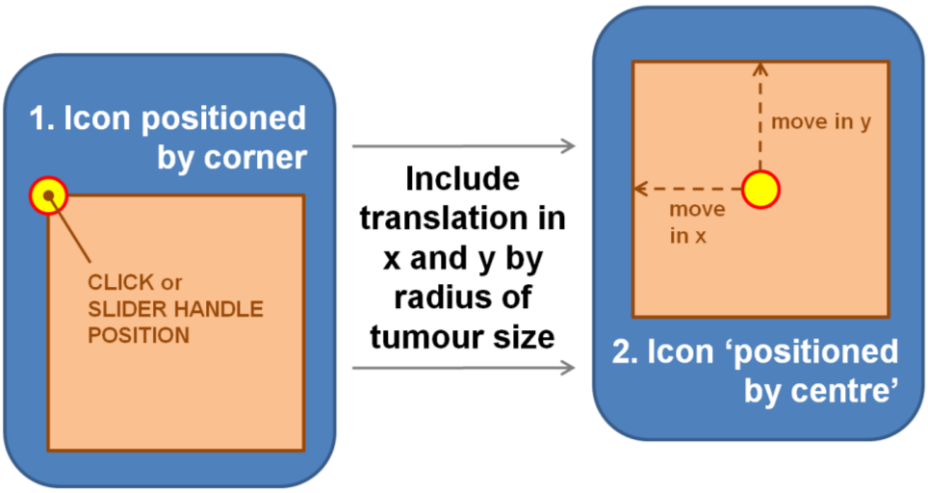

Figure 127: Shift applied to tumour icon to position by centre

9.3 Sizing of Tumour Body

Details of the developmental stages of the tumour sizing system, in which three methods were trialled, are provided in this section.

9.3.1 'Three Sizes' Method

In early incarnations of the GUI, the user was prompted to select from three sizes of tumour at this stage, similarly to the swelling severity options supplied in the developmental stages of the swelling function, described in Section 8.1.1. The controls provided to do so are shown in Figure 128 (multiple tumours are available to the user in this and the subsequent versions of the program; the addition of multiple tumours is described in Section 9.4).

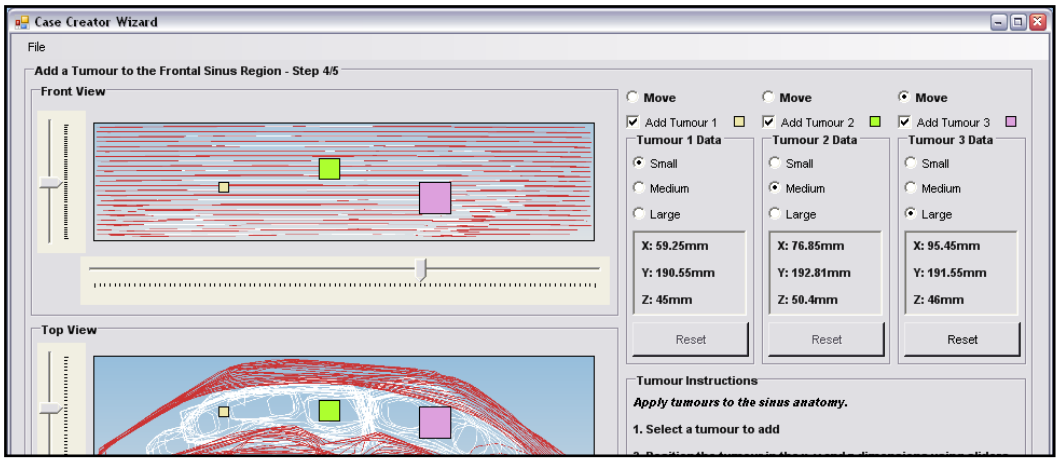

Figure 128: Three sizes available for tumours

Each of the tumours available to the user are sized independently, to give increased design freedom and to allow tumours to be tailored to fit specific training requirements. In this sizing method, each option ("Small", "Medium" and "Large") carried a numerical value, which was used throughout the code as a variable named `TumSize1`, `2` or `3`. The alteration of size by selecting a different radio button would cause the tumour icon on the form to transform to suit the new selection using the relevant size variable; the size of the square was altered to dimensions of, for example: `TumSize1` x `TumSize1` as shown in Figure 129 below. This gives the user an immediate visual representation of their actions, both of the positioning and size of the tumour relative to the anatomy.

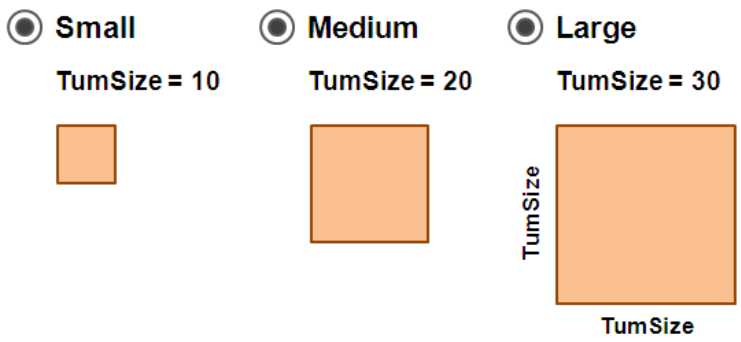

Figure 129: Tumour size variable values in 'three sizes' method

9.3.2 Sliding Scale Method

As with the application of swelling, explained in Section 8.1.1, it was felt that the provision of only three sizes gave the user too little freedom, and would not allow the level of challenge to the surgical trainees to be increased. The same method was used to increase the design freedom of the staff creating the case as in swelling application; sliding scales were implemented for the alteration of each tumour on a finer scale. Figure 130 shows the alteration of tumour size using the sliders; the upper limit of tumour size has also been increased to allow far larger tumours to be created.

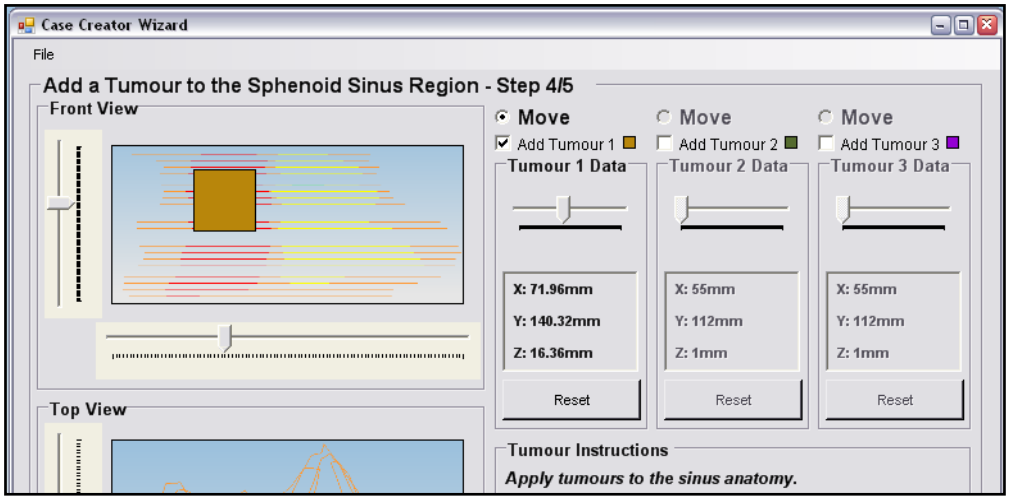

Figure 130: Resizing tumours using sliding scales

The sliders alter the size of the tumour icon in the same way as the radio buttons; the tumour size variables are fed with a numerical value derived from the size slider. This number is then used throughout the code, to adjust the size of the tumour icon and

tumour body in the CAD model, and to give linguistic feedback to the user of the approximate size of the tumours, again using “Small”, “Medium” and “Large” depending on the range that the user’s selection falls into.

9.4 Addition of Multiple Tumours

As seen in the previous section, the option to apply up to three tumours was added to the GUI during the development of the tumour addition system. This is done through the use of a checkbox selection system for each tumour as shown in the top right area of Figure 203, which builds upon the on/off switching system described in Section 9.1. The user may add tumours to the anatomy by checking the one of the checkboxes, at which point the relevant tumour icon will appear. The tumour may then be repositioned and resized as with the single tumour method, however some difficulties are encountered due to the sharing of controls.

The user may switch control between tumours by selecting the relevant radio button above the tumour they wish to reposition, at the top right of the window as shown in Figure 203. When the radio button for tumour 1, 2 or 3 is selected, the tumour icon is highlighted with a black outline, the option to reset the tumour is enabled, the resizing handles are moved to the sides of the activated tumour and the sliding scales are set to match the position of that tumour on the anatomical images of the sinus region.

With the addition of tumour positioning by mouse-click, came a more instinctive method of switching control between tumours; the user was permitted to simply click on the tumour icon they wished to control. This then performed the same actions as if the relevant radio button had been checked.

Intuitive programming was also used to switch control of the sliders automatically when the user adds or removes tumours from the anatomy. When a tumour is turned on, the positioning focus is automatically switched to that tumour. Likewise, as a tumour is turned off, the focus is switched to the lowest numbered (1, 2 or 3) tumour

that is still switched on. If no tumours are left switched on, the positioning sliders are disabled and all tumour icons are made invisible.

Each tumour is positioned and sized individually, which required complex programming for the GUI to function correctly. As the same set of images and sliding scales is used to position all three tumours, a means of switching the subject of the sliders' control was required, depending upon the user's selection. This presented a challenge, related to the retrieval of each tumour's position and sliding scale value properties each time a switch occurred.

The retrieval of a previous tumour's positional information is vital, as the user may wish to reposition the tumours any number of times after their initial placement. Each time the user switches back to relocate a previous tumour they need to be provided with the relevant information and controls to work from where they left off. If the data were not retrieved and reflected on the sliding scales, the repositioning of tumours would have to take place from where the last tumour had been placed, leading to confusion and difficulty in achieving the desired result. The method by which data is retained and displayed again to the user is described in the remainder of this section.

The process to reflect the selected tumour's positional data on the sliding scales begins earlier, when each tumour is initially positioned. Every time the tumour positioning subroutine is run, the slider values are stored in a separate variable. For example, if tumour 1 of the frontal sinus is in use, a line of code in the subroutine appears as shown in Figure 131:

```
SAVEDFrontalTum1XTB = TrackBarXTum.Value
```

Figure 131: Storage of tumour positioning slider value for re-use

This line stores the value on the x-location sliding scale; if focus is switched, and the slider values are reset or changed, `SAVEDFrontalTum1XTB` will remain at the same value, as variables for tumour 2 or 3 are altered instead.

Included in the code run when the tumour radio button selection is changed are lines that set the sliding scales to the 'saved' values, such as `SAVEDFrontalTum1XTB`. Therefore in the example above, when focus is switched back to tumour 1 in the frontal sinus the x-location slider will show the value saved in `SAVEDFrontalTum1XTB`, which will match the x-position of the icon for tumour 1. The 'saved' values are also used when the user chooses to save the case settings, to be applied or altered later. This process is described in Section 10.5.1. In Figure 203, focus was switched to tumour 2, forcing the sliding scales to represent the position of the relevant tumour icon, enabling the tumour reset control, highlighting the icon with a black border and moving the resizing handles to the appropriate locations.

The same approach was taken as the method set out in Section 9.1 to the application of tumour settings in NX, whereby if a tumour is deactivated, the modelling code relating to that tumour is ignored. Furthermore, the tumour body that exists in the CAD model is made invisible (see Section 9.5), to avoid any confusion with the required user-defined tumours produced by Case Creator.

9.5 Simulation of Tumour Body in NX

The first method trialled to produce user-designed tumour bodies in NX involved the creation of 2D splines in the CAD model that subsequently formed the skeleton of a solid body. Sets of three 2D splines were created for each body, forming the top, middle and bottom sections of the tumour and consisting of six nodes each. The use of six nodes on each spline allowed a rounded shape to be achieved on each layer, whilst keeping the number of nodes to a minimum to decrease programming and running time. Using this method, the splines could not be solidified automatically using the 'Through Curves' function in NX, as the VB codenames of the splines were unknown. This meant that the same problems were encountered with spline alteration as with the production of solid swelling bodies, explained earlier in Section 8.5. Furthermore, if the user revisited the tumour settings stage of the wizard and made alterations, this would lead to new splines being created again, leaving superfluous bodies in the model.

This problem was overcome again through the use of 'scaffold splines', pre-existent in the CAD model, awaiting alteration to fit the required geometry. This was implemented into the tumour application functionality of the program after its development for swelling application. In early development, the scaffold splines were left bare, to be combined into a solid body after alteration. This, however lengthened the application time on completing the wizard, and led to some inherent errors with the modelling software. This problem was avoided by pre-solidifying the tumours (as shown in Figure 132), which in turn meant that the VB codename of each tumour solid was known, and could be used in the code. The importance of this was emphasised in the development of the swelling application procedure (Section 8.5.1).

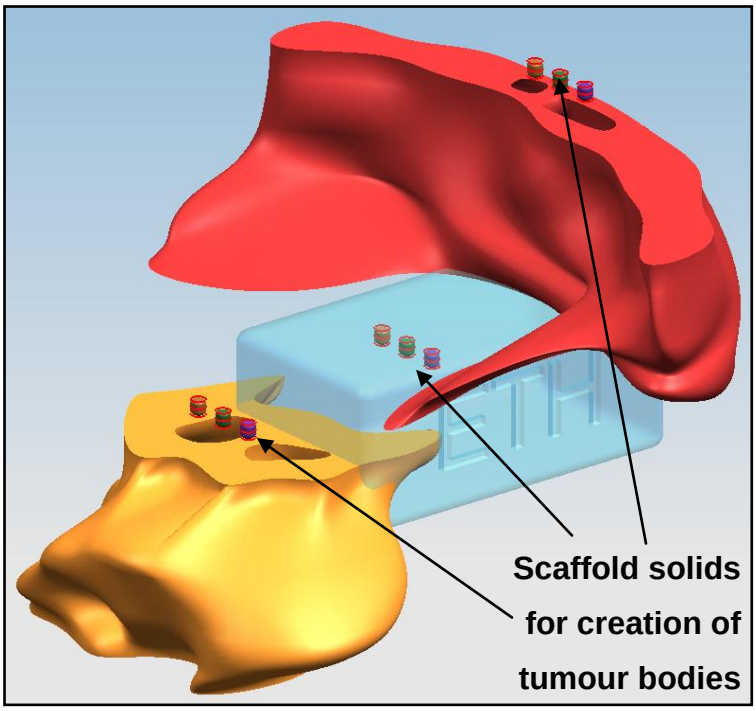

Figure 132: Scaffold solids for tumour simulation

In order to define the position of the tumours in the CAD model, the settings the user made in VB are converted to CAD co-ordinates, as described in Section 9.2. Each time the tumour positioning subroutine is run (when the user clicks to position a tumour, moves the positioning sliders or uses the resizing handles) the new co-ordinates of the tumour body centroid in the CAD model are recalculated. The co-ordinates are stored in three non-sinus area-specific variables, `Tum1CoordNXX`, `Y` and

Z. Once the tumour stage of the wizard is completed, the values are passed on to area-specific variables such as SAVEDFrontalTum1XNX (x-co-ordinate of the centroid of tumour 1 in the frontal sinus CAD model). This use of general variables enables the same tumour positioning subroutine to be used for all areas of the sinuses.

Each CAD co-ordinate is defined in a similar way to the position of the tumour icon on the form in VB. The starting position of the tumour body is set at the position of the relevant sinus model in the CAD model, SinusX/Y/ZPos, while the position relative to this origin is set using the positioning sliders with a conversion factor TBX/Y/ZTumFactorMM. The factor converts the trackbar value into millimetres, just as the icon position was found using a pixel conversion factor. The conversion factor is found by comparing the size of the anatomical image in Case Creator (pixels) with the size of the sinus area in the CAD model (mm) and dividing the result by the number of trackbar divisions on the relevant slider.

To create the tumour body in the correct location, the nodes around the three scaffold splines must be positioned around the centroid according to the tumour size selected. Figure 133 shows how this was done:

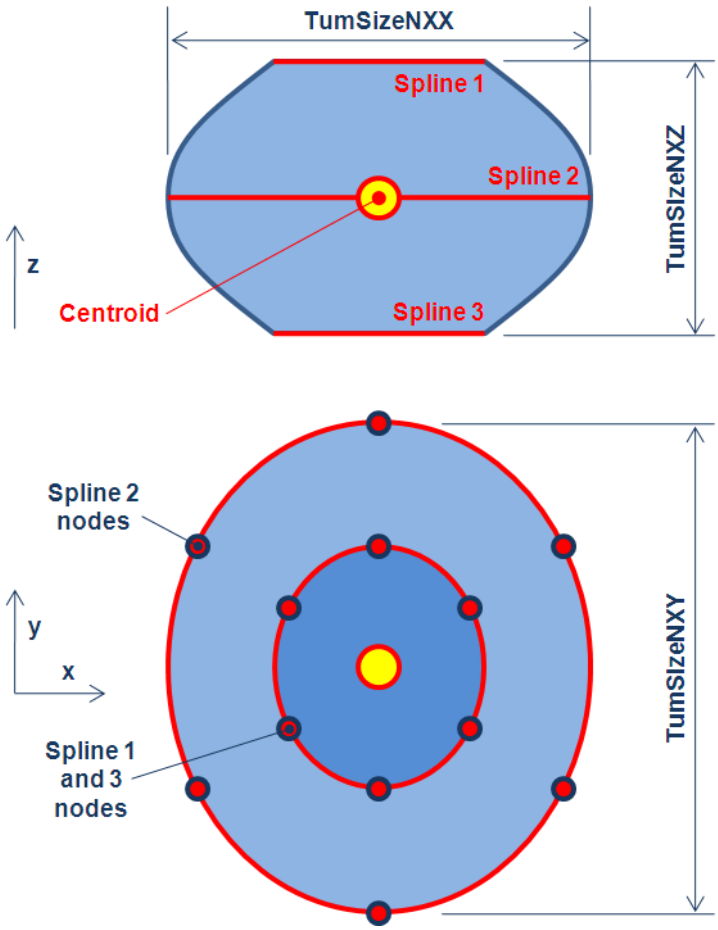

Figure 133: Sizing of tumour bodies in three dimensions

The co-ordinate definition code was developed to incorporate the size in each direction to alter the node x-, y- and z-co-ordinates of the nodes around each scaffold spline, to form the rounded shape shown in Figure 133.

As with the application of swelling, the manner in which the code was written in VB was improved to shorten the duration of the editing process. This was again achieved through the use of subroutines in the VB code, used a number of times throughout the program to perform the same action having been provided with the relevant information each time.

Until the first time settings are applied to a tumour, the relevant body is hidden in the CAD model to avoid confusion. Once the spline alteration code has been run, the

tumour body is made visible to the user within the CAD window. If the user has decided not to apply the tumour, the spline alteration code is ignored and the tumour body is made invisible. This caters for the revision of case settings, where the user may decide to switch off one or more of the tumours after previously applying settings. All of these actions are performed by providing the 'tumour spline settings', 'show body' and 'hide body' subroutines with the VB codename of the tumour body (`TargetName`) prior to their use. This would not be possible if the solid were created after spline alteration, as described at the start of this section. The code to be run when tumour 1 in the frontal sinus is addressed is shown in Figure 134:

```
TargetName = "THRU_CURVE(2)"
If SAVEDFrontalTum1 = 1 Then
   SplineNameTum1 = "HANDLE R-149004"
   SplineNameTum2 = "HANDLE R-149006"
   SplineNameTum3 = "HANDLE R-149005"
   TumCoordNXX = SAVEDFrontalTum1XNX
   TumCoordNXY = SAVEDFrontalTum1YNX
   TumCoordNXZ = SAVEDFrontalTum1ZNX
   TumSizeNXX = SAVEDFrontalTum1SizeXNX
   TumSizeNXY = SAVEDFrontalTum1SizeYNX
   TumSizeNXZ = SAVEDFrontalTum1SizeZNX
   TumourSplines()
   ShowBody()
Else
   HideBody()
End If
```

Figure 134: Code run to apply settings to Tumour 1 in frontal sinus

It can be seen that if the tumour is required (if `SAVEDFrontalTum1` = 1; this variable will be described in further detail in Section 10.5.1) `TumCoordNXX/Y/Z` are provided with the values stored in `SAVEDFrontalTum1X/Y/ZNX` (CAD co-ordinates of the tumour body) and `TumSizeNXX/Y/Z` with the values stored in `SAVEDFrontalTum1SizeX/Y/ZNX` (tumour body size in three dimensions). The names of the splines that the three sets of nodes control are supplied to variables `SplineNameTum1`, `2` and `3`, all of which are then used in the general tumour spline alteration subroutine `TumourSplines`. The subroutine to show the tumour body is then run using the value of `TargetName` supplied earlier. If tumour 1 is not required (`SAVEDFrontalTum1` ≠ `1`) the code skips to the Else statement, which runs the

subroutine to hide the tumour body in the CAD model. This process is repeated for all three tumours in each sinus area, using the same subroutines with updated variable values. The repeated use of the same subroutine allows simple inclusion of the functionality to apply further tumours to the anatomy in future versions of the program.

Both the swelling and tumour application subroutines were grouped together within a larger subroutine for each sinus area, named `Frontal/Sphenoid/EthmoidApply`. This large subroutine may itself be called and used repeatedly, for example in the code run when the user clicks "Apply".

Figure 135 shows six tumours applied throughout the sinuses, with no swelling applied to ease visibility. Three tumours are placed within the frontal sinus, two in the sphenoid sinus cavities and one in the ethmoid sinus placeholder block. It can be seen that the unused tumours do not appear; they have been hidden until involved in the case, as described in Section 9.4.

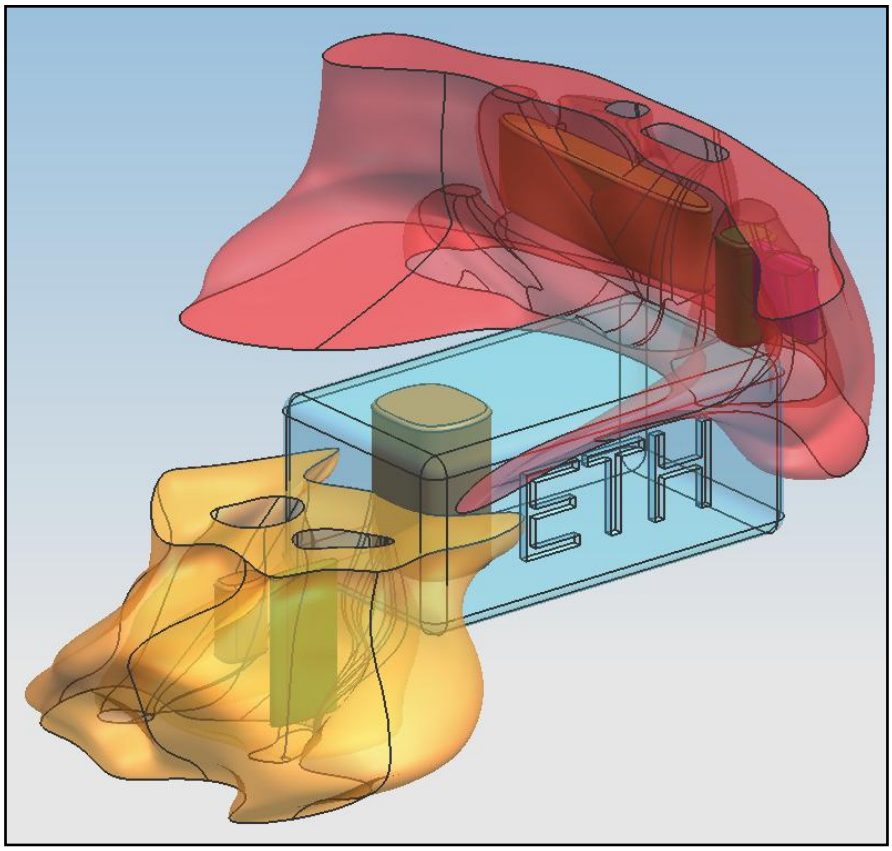

Figure 135: Tumours applied to all sinus areas

It can be seen in Figure 135 that the customised tumours are still of fairly regular size and shape. It is suggested that this issue is addressed in the future, and some work has been done to begin to overcome the unrealistic appearance of the tumour bodies. This work is described in Section 13.4.

Having completed swelling and tumour application, the next step is to export the solid models as an STL file, for production through additive manufacturing.

9.6 Exporting Model from NX

The model shown in Figure 136, containing three tumours in each sinus area and swelling in the frontal and sphenoid sinuses was exported in the STL format from NX.

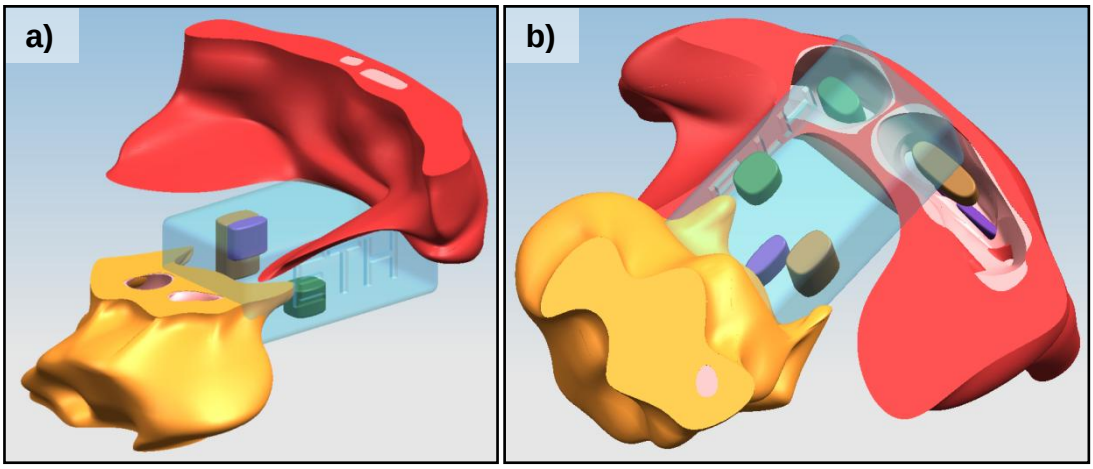

Figure 136: Fully customised sinus anatomy in CAD software *a)* isometric view, *b)* from below

As described in Section 2.3, in order to successfully manufacture the model, each individual body must be represented in the STL file as one 'shell', a surface representation of a 3D model constructed from an approximated tessellation of triangular facets. The quality of the shell faces is then assessed, to determine their suitability for manufacture.

In Figure 137*a)*, the model can be seen to contain 13 separate shells (the placeholder for the exterior of the ethmoid sinus has not been included in the STL to allow clearer visibility of the ethmoid tumours). These shells are the exterior solids and interior cavity solids in the frontal and sphenoid sinuses, and nine tumours. Figure 137*b)* shows the part information for the exterior body of the frontal sinus, including data on the triangle normals and bad edges. The model is sound, as no errors are exhibited in the part information and the part consists of only one shell. No errors were found for any parts of the STL file, meaning that the customised model from NX could be successfully produced through additive manufacturing.

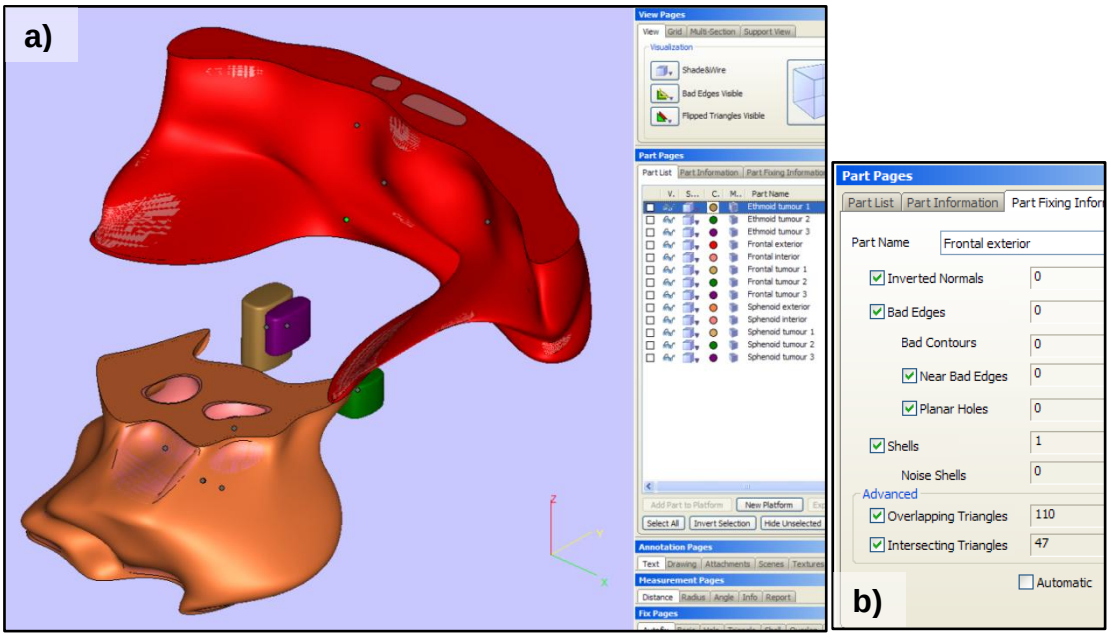

Figure 137: *a)* Model exported as STL file, *b)* part information for exterior frontal anatomy

CHAPTER TEN

DESIGN OF GUI AND PROGRAM TRIAL A

10 Design of GUI and Program Trial A

10.1 Development of 'Wizard' Style User Interface

The project plan in Figure 64 shows that the design and use of the GUI was under development throughout the investigations into the simulation of swelling and tumours in the 3D CAD model. This chapter presents the development of the GUI and the final concept, with reference to some examples already shown in Chapters 8 and 9.

In early versions of the program, when the successful application of the functions was the priority, the user was presented with a series of tasks, arranged onto separate 'tabs' in one window. The order of the tasks was clear, however there was no indication that the user was progressing through a process, towards an end result. This served to allow quick development and testing of the swelling and tumour application functions of the program, but would not be suitable for use by other users. As the tasks being undertaken by the user within 3D CAD would most likely be unfamiliar, their guidance through the tasks was extremely important, to give a sense of being in control and an understanding of the results being created. Potentially, all tasks could be displayed to the user simultaneously, with guidance provided; however this would create a very crowded GUI. The sequential display of tasks avoids this problem and guides the user clearly through the tasks to be performed. The 'wizard' style of user interface allowed this approach to be taken in an applicable and recognisable format.

This type of interface is used commonly in home computing, to allow the user to perform otherwise complex and knowledge-based tasks quickly, with some input into the end result. Examples of the wizard interface include the installation of new software or hardware, the transfer of photographs from a digital camera, or the customised design of documents, and even products and clothing over the internet. In this case, the medical staff who will use Case Creator do not possess specialist knowledge of CAD modelling software; such knowledge would be costly and time-consuming to acquire.

Wizards commonly follow the same basic design:

- Welcome the user to the program, sometimes offering a range of options immediately to determine the path of the process, or the appropriate product or function
- Key information is provided, to ensure that the user is not unaware of any effects of the decisions they will be asked to make
- Division of tasks into simple decisions to be made sequentially, to avoid confusion and decisions being neglected accidentally
- Buttons marked "Next", "Previous" and "Home" to navigate through the series of tasks within the same window
- At the end, a button marked "Finish" or "Apply" to complete the wizard and see the effects of the user's actions

The wizard format consists of one window, the contents of which change depending on selections made by the user. Each step of the task to be completed is shown sequentially to the user, who makes decisions and selections when prompted by the instructions shown. Once they are satisfied with the selections made, the user decides to progress to the next step, or navigate backwards through the steps to change a selection. The user should, ideally, only need to use the wizard window to complete the task, without opening or interacting with any other programs. They may be asked to open files or select the destination for saved items; however these windows are automatically provided to the user for the appropriate action to be taken. At all times, the user's actions are limited to the associated decisions required to complete the current step of the wizard. This ensures quick fulfilment of the task, and reduction of confusion or interruption of the process by the user.

The user is provided with three options for navigation through the steps of the process. The navigation options are displayed on buttons at the bottom of the window, and remain visible for the duration of the process. The user is permitted to move forwards and backwards through the process, either one step at a time (using "Next" and "Previous") or by moving back to the start of the wizard (using "Home").

The steps to produce a completed CAD model with the Case Creator program were defined as follows:

- Sinus area selection
- Swelling application
- Vertical Region definition
- Tumour application
- Verification of settings

These would form the major steps of the wizard, along with navigational and administrative steps:

- Welcome/home page
- Instructions and information for use
- Saving and naming CAD file
- Post-application confirmation

The decisions to be made by the user: swelling application, vertical region definition and tumour application can be easily split into individual decisions and performed in CAD without direct interaction from the user. It is also expected that the format is recognisable and familiar to users; if not, the simple navigation method and progressive nature of the design should be intuitive to use.

The wizard-style approach to Case Creator required the identification, development and implementation of a new coding structure. By using *If-Then-Else* statements throughout the code, the program serves the choice-based nature of the application of pathology to the model. Every eventuality is catered for, so that the program responds appropriately to any user action.

10.2 Navigational Programming

Due to the decision-based nature of the tasks being carried out by the user, programming the behaviour of the wizard at each stage was an extremely complex undertaking. The wizard would not behave in the same way each time it was used, but instead be required to react and adjust to the settings being made at each step of the

process. Each decision made by the user changes the appearance, available options and most importantly, the end result of the wizard. A way to incorporate these decisions into the programming of the wizard was needed, and was found in the use of *If-Then-Else* statements. The first major usage of the *If-Then-Else* construct was to develop the program's navigation system.

Each step of the program was created as a separate pane (known as a "`GroupBox`" in VB) to be displayed in the Case Creator window. Using properties in VB, the visibility of the panes can be adjusted, leaving only the required step of the process visible to the user. This visibility will be controlled by the navigation buttons, and forms the fundamental structure of the coding for this program. In order for these buttons to function correctly, and display the next stage in the process, the code must determine which stage is currently in use. One large *If-Then-Else* statement therefore runs the length of the entire code for each of the three navigation buttons.

This long *If-Then-Else* statement tests, in order, which stage of the process is visible to the user at the point at which the button was pressed. Actions are then performed according to the stage being addressed, and the subsequent required stage is made visible to the user. Some steps of the code for the "Next" button are summarised in the simplified flow chart in Figure 138.

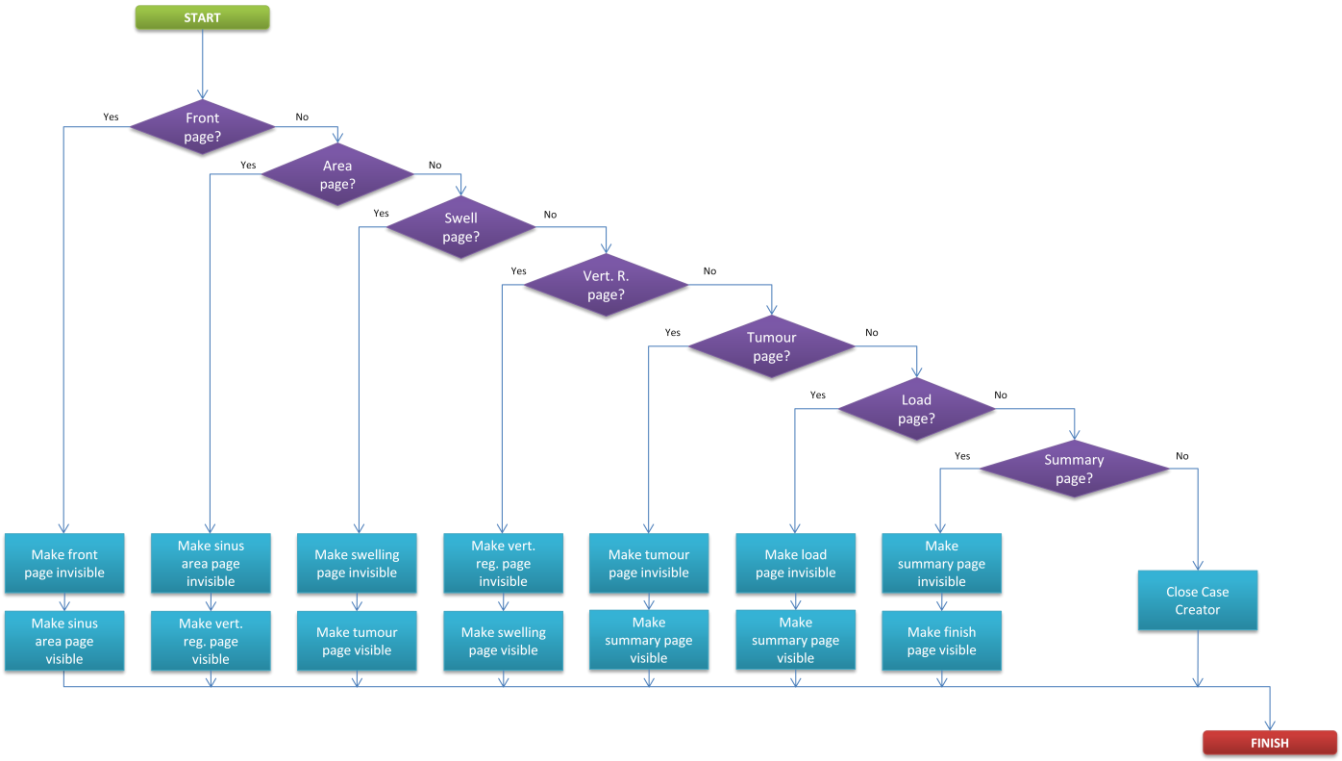

Figure 138: Simplified flow chart of "Next" button process

As shown, the *If* statement initially tests whether the front page is visible when the "Next" button is clicked. If so, the front page is made invisible and page 2 becomes visible. If this is not the case, the code tests the next statement (*ElseIf* page 2 = visible). If this is true, page 2 is made invisible and page 3 becomes visible, and so on.

In this way, the user may progress through the pages of the wizard by clicking the "Next" button. By using similar code, the "Previous" button may be programmed to make the previous page of the wizard visible, allowing the user to revisit stages of the process. The "Home" button was programmed to make the homepage visible and all other panels invisible, allowing the user to restart the process.

The selections that the user made at each stage were determined, utilised and displayed by using further *If* statements. Each time the user progressed through the steps of the wizard, settings were altered to make it behave in the appropriate manner and offer the correct options to the user. Once the page of the wizard in use had been identified, as described above, all the display settings for the next page could be

defined according to the selections made by the user. Again, this was done through the use of *If* statements, this time verifying whether radio buttons or checkboxes are checked, or the value shown on sliding scales.

After finalising the navigation system, the way in which the program would be used to apply the complete set of required settings to each area of the sinuses was developed.

10.3 Cyclical Navigation System

The first wizard concept to be developed relied upon the user being asked to select one of the four sinus areas to affect at the start of the process, before moving through the stages associated with that area and applying the settings to the model. The user selects from the four sinus areas by clicking on one of the radio buttons or images marked with the name of that sinus area, shown in Figure 139.

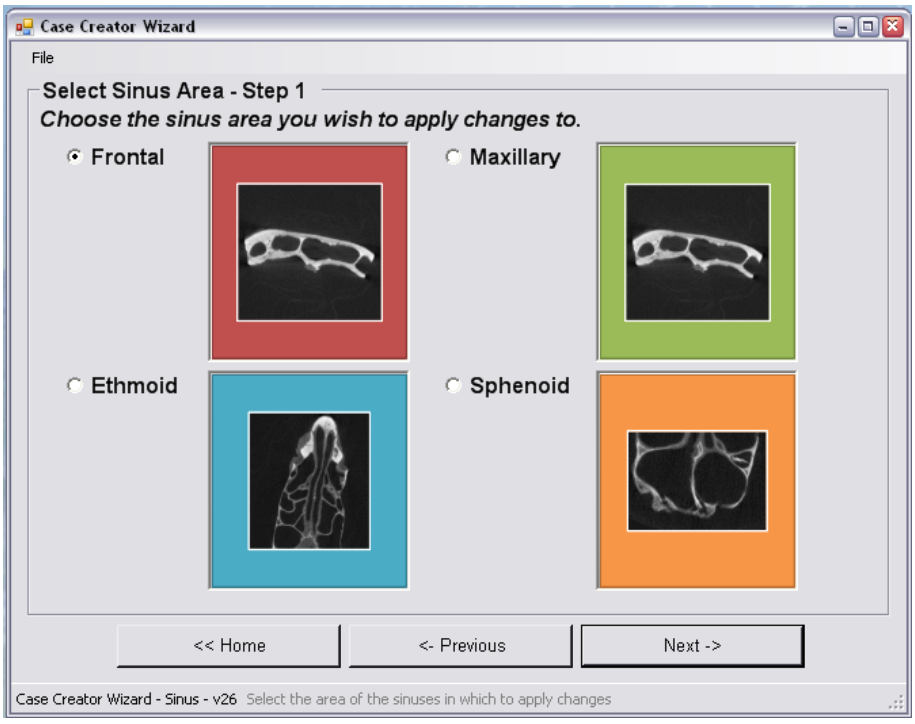

Figure 139: Sinus area selection page of Case Creator wizard

The most influential check performed with *If* statements occurred when the user progressed from this stage of the wizard. The code established which of the four radio buttons had been selected, therefore determining the area of the sinuses that the user

wished to work with. This then set a text variable, "`SinusRegion`" as the name of the sinus area selected, which affected the appearance and behaviour of the entire program from this point forwards. `SinusRegion` was used in each of the upcoming sections of code to set the appropriate controls, window sizes, variables, images and text, and to apply the case settings correctly at the end of the process.

A complex section of code was also created to cater for the possible multi-directional navigation of the user through the wizard. For example, if the user had navigated through the steps of the wizard having selected the frontal sinus for use, used the swelling and tumour settings controls, then decided to change to the sphenoid sinus by navigating back to the sinus area selection page, all settings that were previously applied should be reset to begin from a clear case. This would mean that the sliding scales and information displayed should appear as they were originally, ready for the new case to be defined. However, if the user simply navigated back to the area selection stage, then moved on again without changing their selection, the settings should be retained.

This was done by checking the value of `SinusRegion` as the user progressed from this stage, before it was set to match the radio button selection. If the user had previously visited the sinus area selection page, moved on, then navigated back, `SinusRegion` would contain the name of the area being worked on. If not, and the user was viewing the area selection page for the first time, `SinusRegion` would be blank. The code checks at this stage whether the area selected on the radio buttons is different to the area name stored in `SinusRegion`. If this is the case, all the controls and information displayed throughout the wizard are reset to those appropriate for the new sinus area, and the value of `SinusRegion` is updated. If the value of `SinusRegion` matches the selection on the radio buttons, the user did not change their selection and the section of code to reset controls is ignored. This is shown in the flowchart in Figure 140:

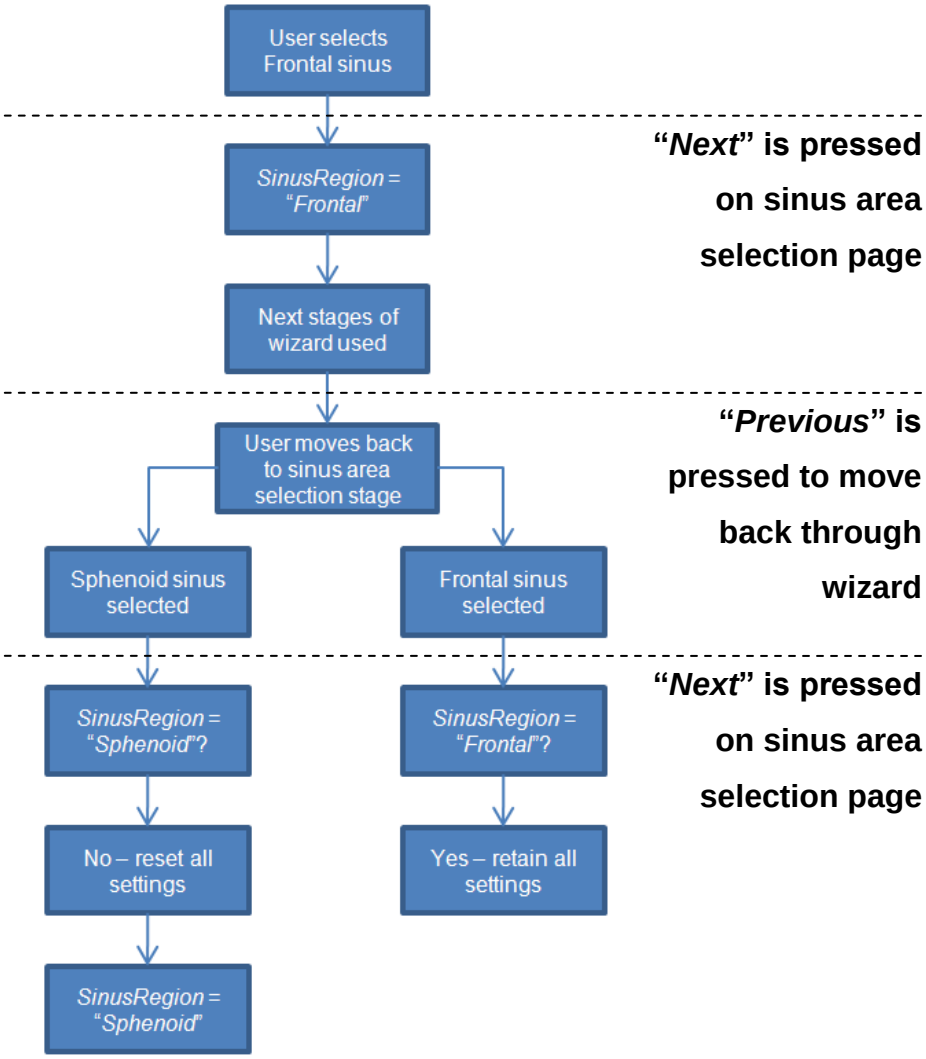

Figure 140: Identification of sinus area change using SinusRegion

This part of the code also checked whether a loaded case settings file was being revised (to be explained in Section 10.5.2) and if so, sets the upcoming controls (such as sliding scales, checkboxes and radio buttons) to the loaded values. If not, the controls are left how they were set as a result of the code described above.

After progressing through the wizard and applying changes to the 3D CAD model, the user is offered the opportunity to add pathology settings to another sinus area; if they choose to do so, they move through the wizard steps in the same way as previously, and may repeat the process until all the sinus areas had been affected. The sinus areas in which pathology has been applied are clearly marked "DONE" and the user is not

permitted to select these sinus areas; this is done by disabling the radio buttons associated with each area, as shown in Figure 141:

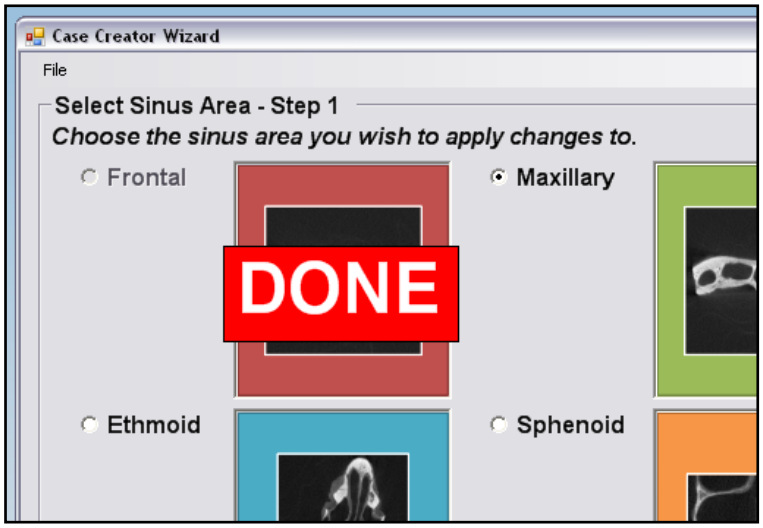

Figure 141: Frontal sinus settings have been applied; option to do so is disabled

The stages of the wizard required for the user to apply changes to the swelling and tumour application settings were designed throughout the development of the application techniques themselves. The initial designs for the stages of the wizard are described in the following section.

10.4 Stages of Case Creator Wizard

The user moves sequentially through these stages, in either direction, to set the swelling and tumour information needed to simulate their case.

10.4.1 Home Page

When Case Creator is started, the user is presented with the home page (Figure 142). The user may return here at any point by clicking the "Home" button, to restart the settings definition process. The option to load previously created case settings is also provided for quick use at this stage, as described in Section 10.5.2.

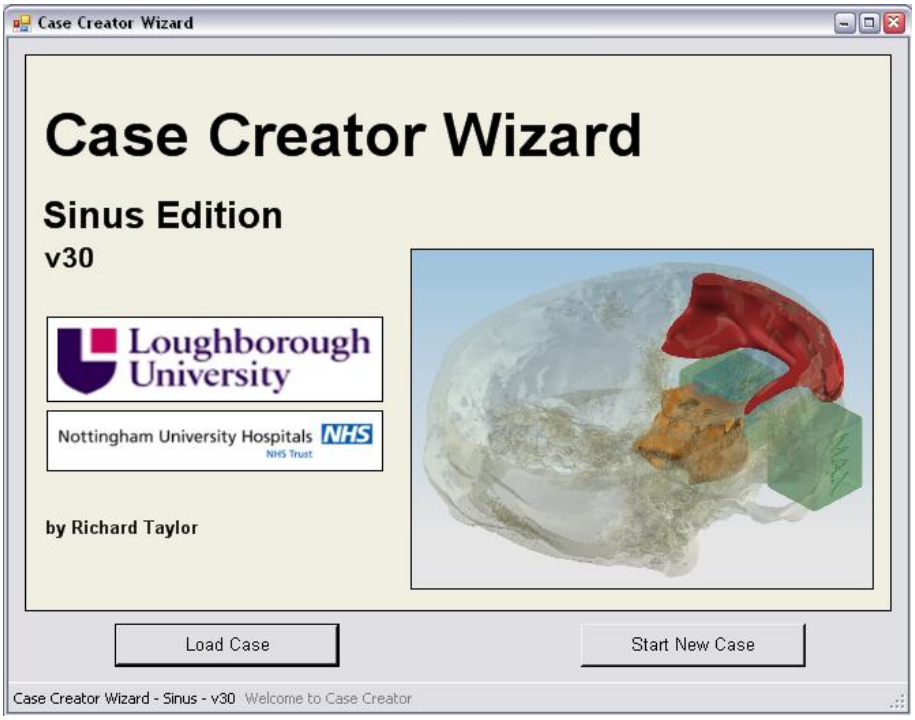

Figure 142: Home page of Case Creator wizard

If the user has navigated back to the homepage after having worked partway through the wizard, a new case is not started; instead the user is automatically guided back to the sinus area selection stage (Figure 139).

10.4.2 Swelling Application Page

As described in Section 8.2, sliding scales are used to define the level of swelling in five directions in the frontal and sphenoid sinuses. In this navigation system, the swelling page of the wizard is used once per cycle, to control different areas of the sinuses. The user is offered the choice at each stage to apply the swelling, as shown in Figure 143 or leave the anatomy unchanged.

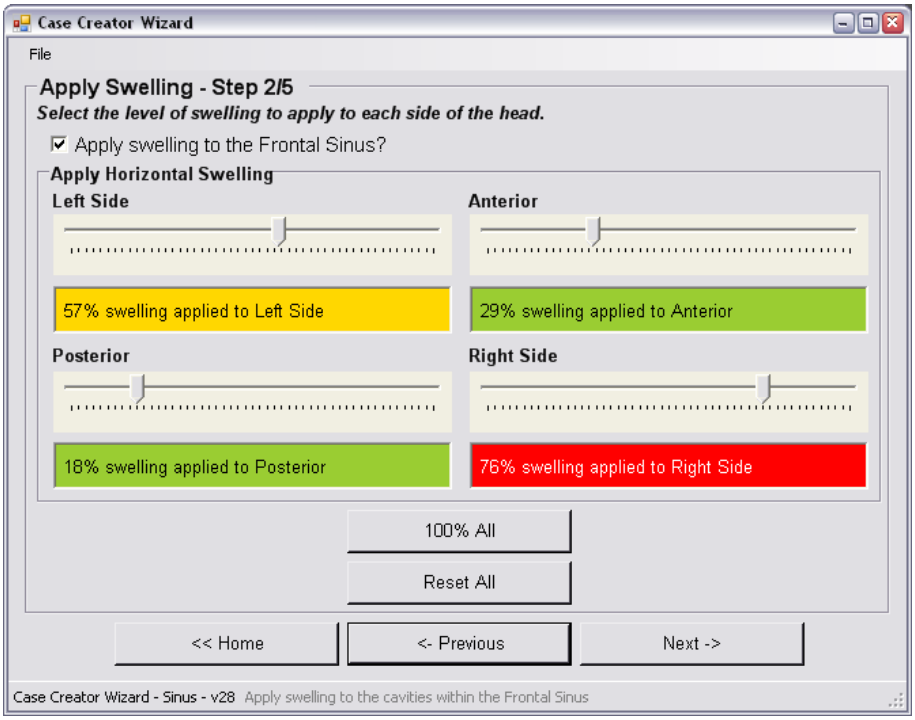

Figure 143: Swelling application page of Case Creator wizard

The user indicates that swelling is not to be applied by unchecking the "Apply swelling?" checkbox, as shown in Figure 144:

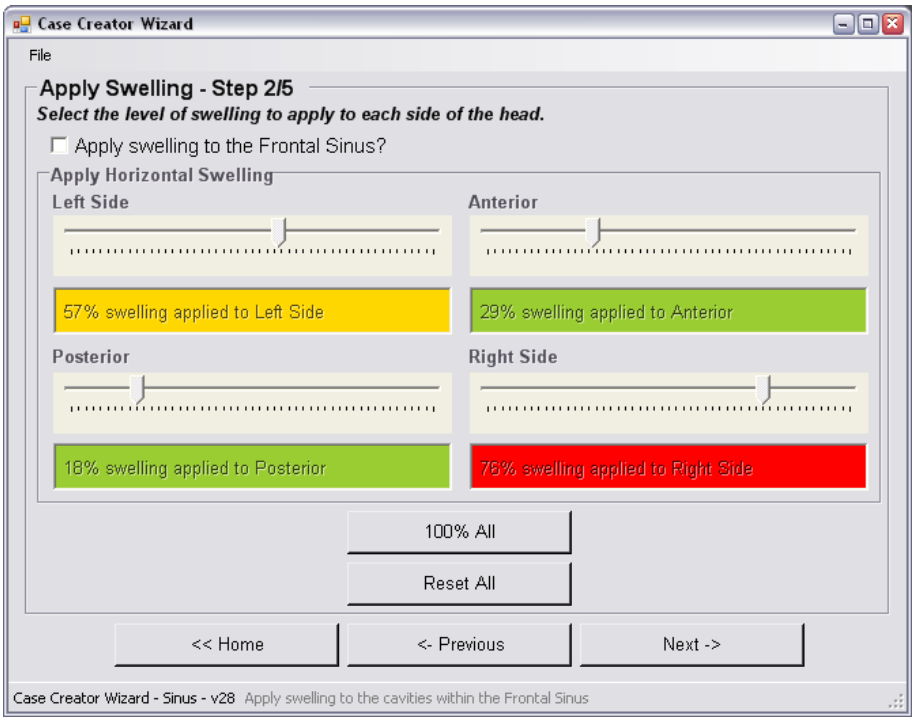

Figure 144: No swelling is to be applied; swelling checkbox has been unchecked

For the sphenoid sinus, two stages were used to separate the left and right cavities for the application of individual swelling. The programming of this functionality was very challenging, as the same 'page' of the wizard was to be kept visible at all times, while the content changed. *If* statements were used again to perform different actions when "Next" is pressed, depending on the window content visible at that moment. If the sphenoid sinus is selected, and the first set of swelling application controls are visible (for the left cavity), then these are made invisible, and the controls for the right cavity are shown. If, when "Next" is pressed, the controls for the right cavity are visible, then the user has completed the application of swelling and the next stage of the wizard must be made visible. At each of these stages, the instructions given to the user must also be updated. The entire "Next" button process for this stage of the wizard is shown schematically in Figure 145.

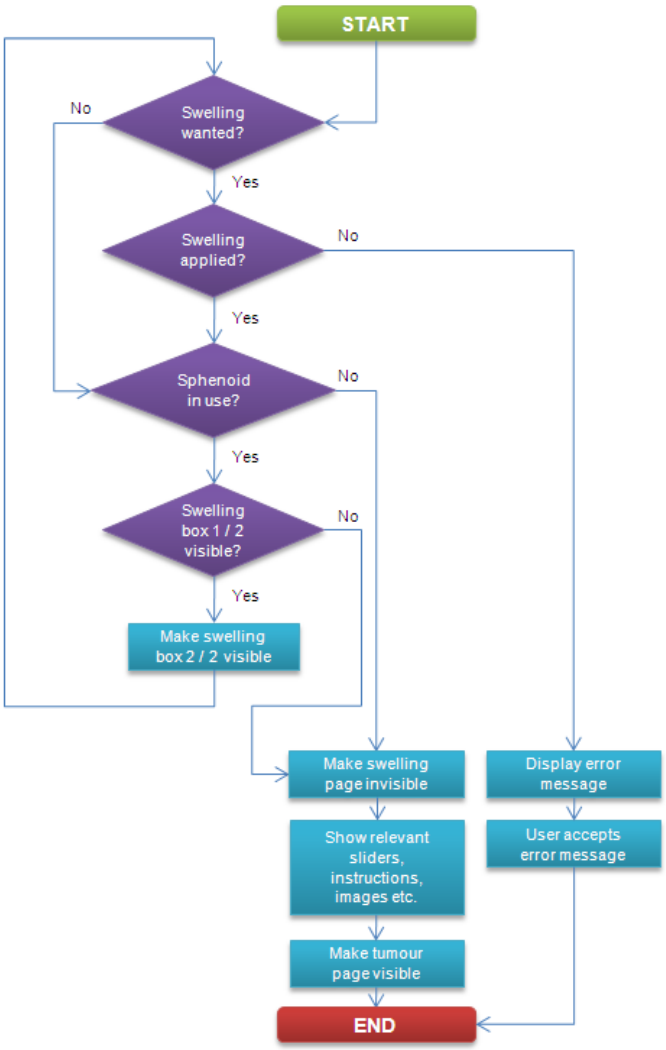

Figure 145: Flowchart of "Next" button actions at swelling application stage

If the checkbox is unchecked, the entire swelling section of the code is skipped in the final application through the use of *If* statements such as:

```
If CheckBoxSwell.Checked = True Then
   (swelling application code)
End If
```

The code will then check the sinus area in use; if the sphenoid sinus is being altered, different actions may be needed concerning the separate sphenoid cavity swelling pages.

As shown in Figure 145, should the user attempt to apply swelling, but not select any values for the swelling on the four sliding scales, they will receive an error message (Figure 146) forcing them to do so, or to uncheck the swelling checkbox.

Figure 146: No swelling applied - error message is prompted

10.4.3 Vertical Region Selection Page

At this stage, the coloured bars give a quick impression of the area that has been selected, and the user is also given a percentage of the sinus area that will be affected, as Figure 147 shows.

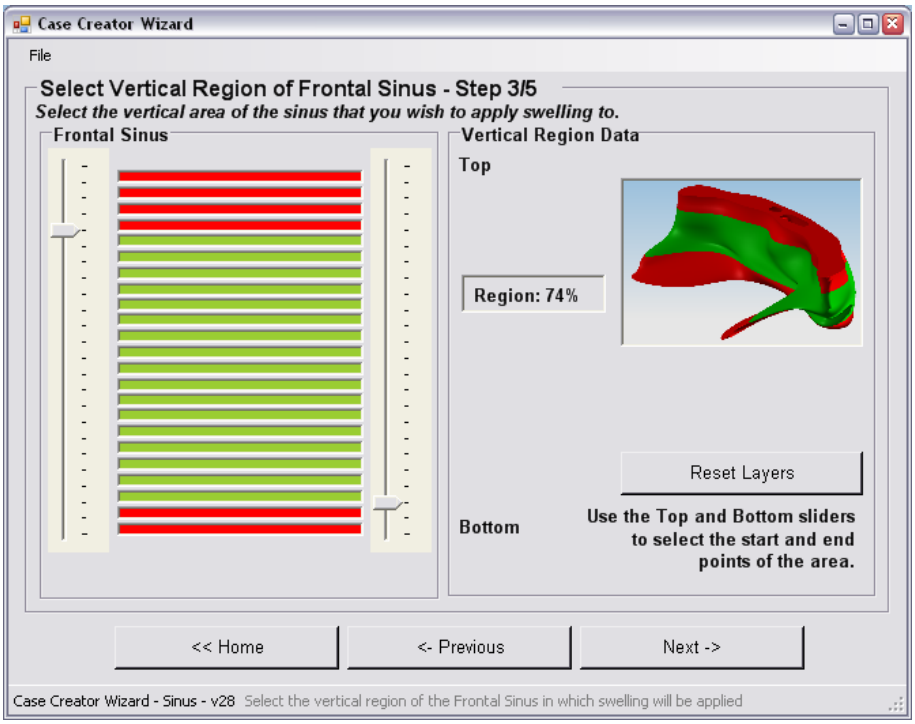

Figure 147: Vertical region selection page of Case Creator wizard

The wizard informs the user of any errors or unusual selections that they may have made while using the vertical region definition stage. The user is not permitted to select a 'negative area', by placing the caudal slider above the cranial slider (Figure 148*a)*). An error message then forces the user to select a valid region (Figure 148*b)*).

a)

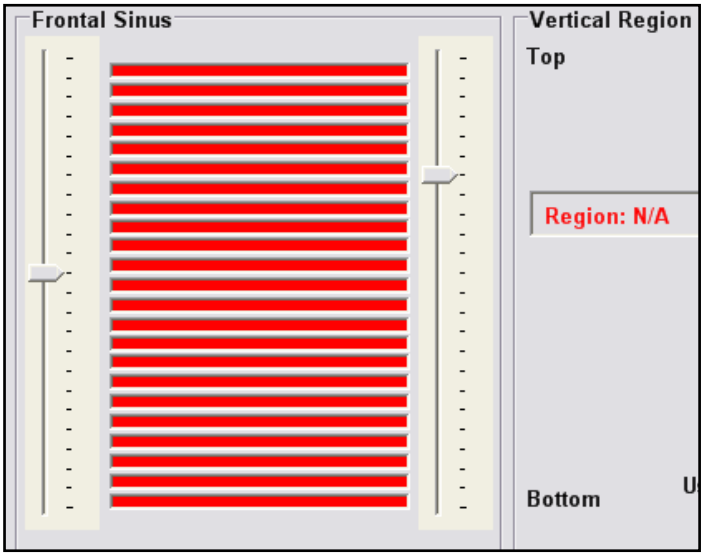

b)

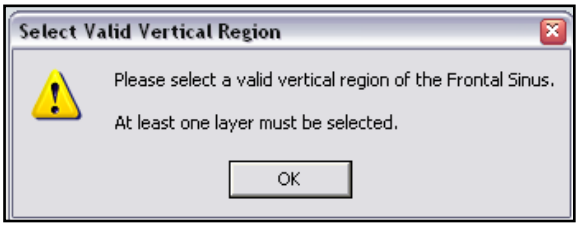

Figure 148: *a)* Vertical region error; bottom layer above top layer, error message (*b)*) is prompted

10.4.4 Tumour Application Page

As described in Chapter 9, the tumour application page displays the anatomy to be addressed in two dimensions, allowing the user to gain a good understanding of the position and size of the tumours to be applied. Figure 149 shows tumours being added to the frontal sinus, by placing the tumour icons over the anatomical images in both dimensions, and resizing using the sliders on the right of the window.

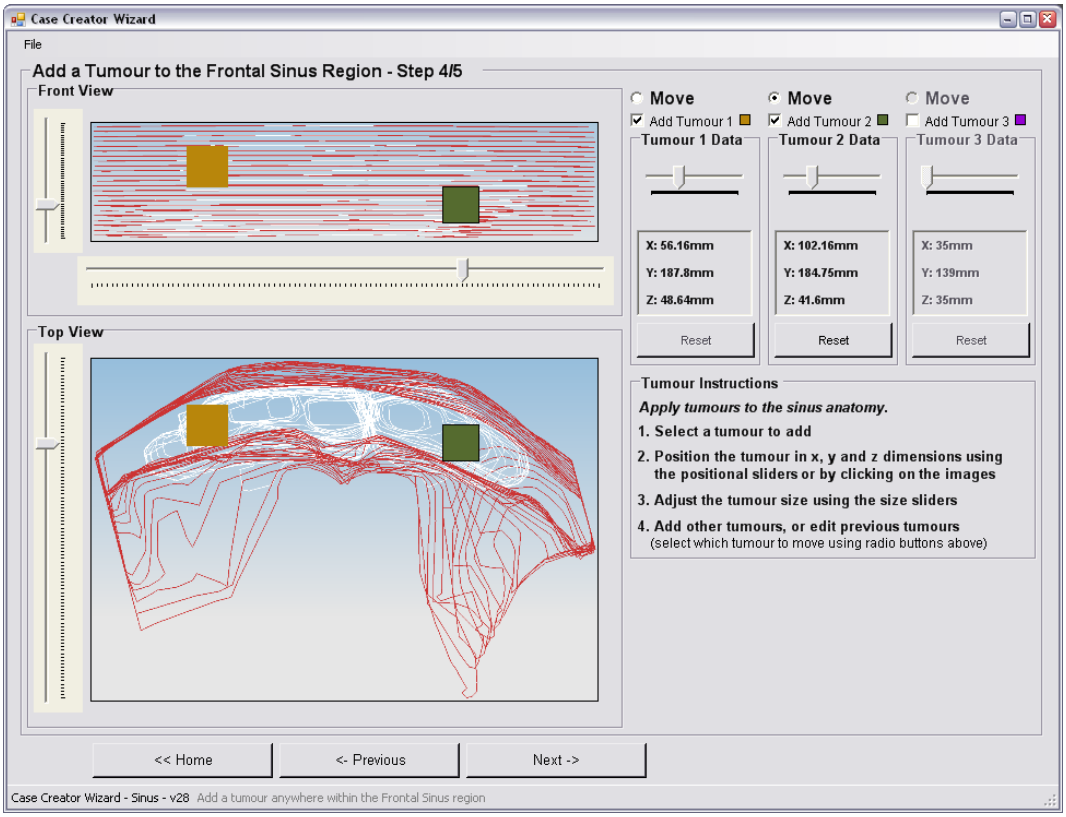

Figure 149: Tumour application page of Case Creator wizard

10.4.5 Summary Page

Prior to displaying the summary, the user is given instruction on which controls to use next, depending on the action they wish to take, as shown in Figure 150:

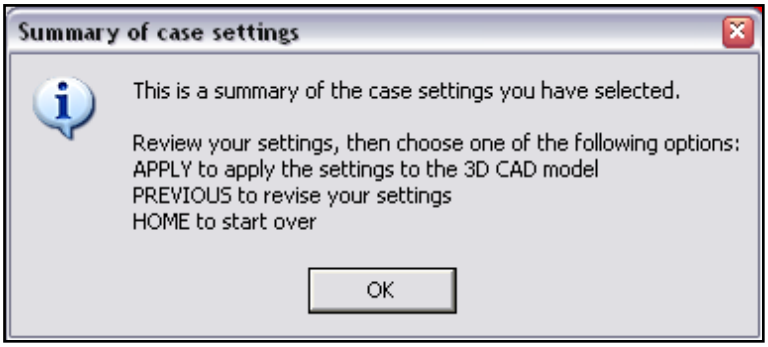

Figure 150: Information provided before summary page is shown

As described in the information message in Figure 150, the user has three options at this point in the wizard. They may accept the settings they have applied and run the application process, simulating the pathology they have defined on the CAD model;

move back through the wizard step by step to alter the settings; or move back to the start of the wizard to work through from the beginning, perhaps redefining the set of original settings they wish to apply. These options are displayed on the buttons at the application stage, shown in Figure 151, along with the vertical region, horizontal swelling and tumour information relating to the case specifications:

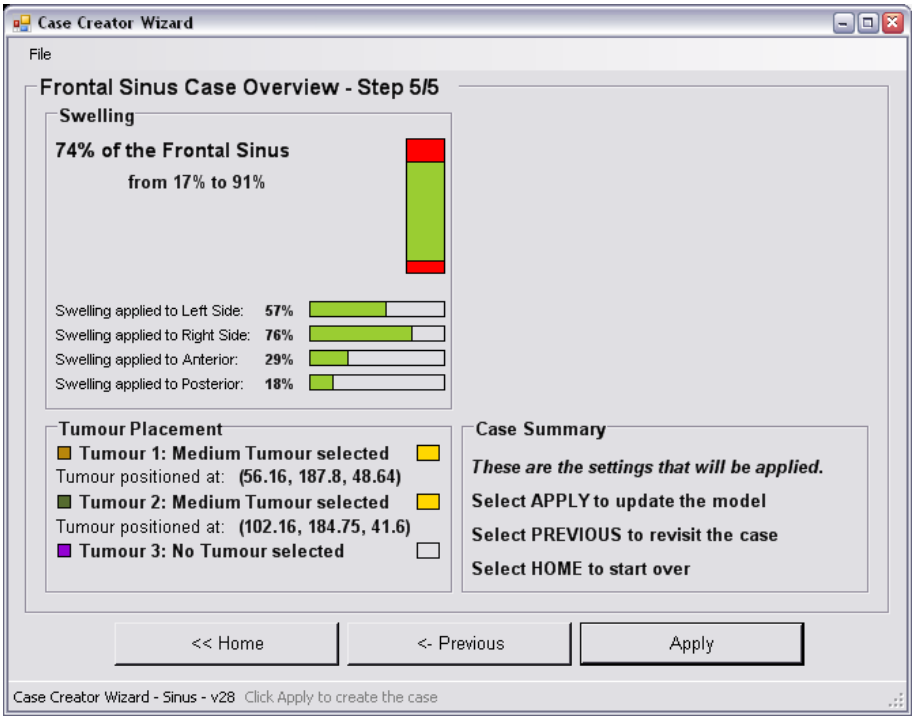

Figure 151: Summary page of Case Creator wizard

10.4.6 End Page

If the user selects to apply the case settings from the summary page, the simulation process begins and the CAD model is updated using the subroutines described in Chapters 8 and 9. After the model is completely updated, the user is provided with further options, confirmation of the successful application of settings and the remaining sinus areas to alter (Figure 152).

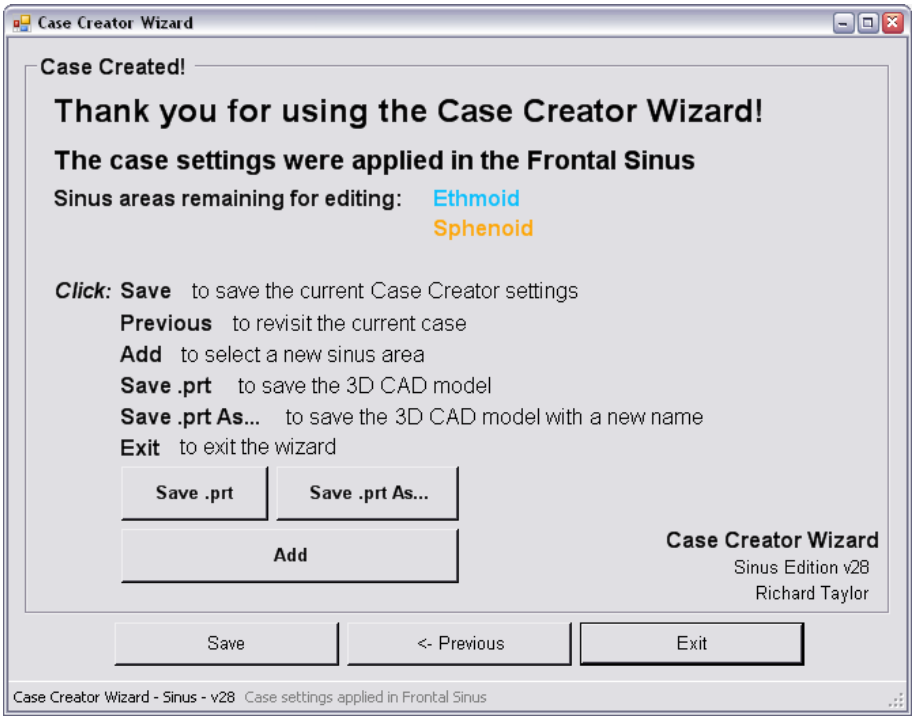

Figure 152: Final options screen and confirmation of case settings application

The user may now save the CAD part file by clicking “Save .prt” or “Save .prt As...”. The first will use the filename provided by the user at the start of the wizard; this step is discussed in Section 10.5.3. The second will display a text box in which the user may enter a new filename for the part, as shown in Figure 153, then click “OK” to save the file:

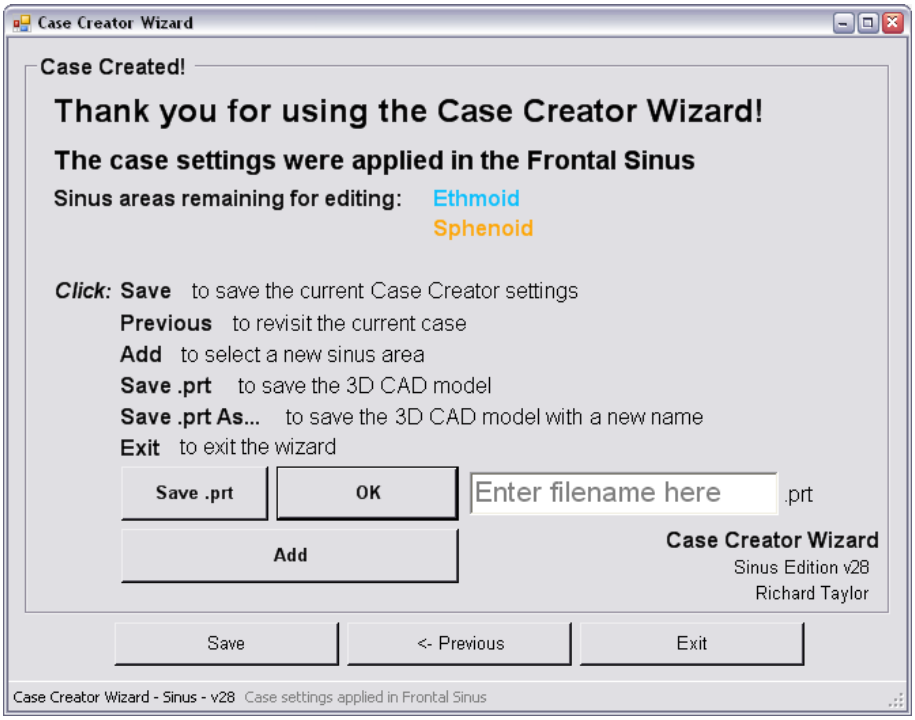

Figure 153: Procedure to save CAD part file with a new filename

The user may also save the pathology settings they have defined through the wizard, for quick future use (described in Section 10.5.1). This is done using the "Save" button (previously used as the "Home" button). After use, the button returns to its original function, allowing the user to return to the wizard home page. If any sinus areas remain available for application to the model, the user may click "Add" to move back to the sinus area selection page and choose further settings to apply. The user is not permitted to select sinus areas that have already been applied, and the "DONE" symbol is shown to make this clear to the user. The whole process of working through the wizard and applying the settings then begins again. Alternatively, the user may move back through the wizard step by step using the "Previous" button, which will undo any changes that were made to the CAD model in the most recent settings application, to allow the user to work with the model as it appeared before these changes were made. This process is described in further detail in Section 10.6, and makes use of the functionalities described in the following section.

10.5 'Save' and 'Load' Functions

Functions that will prove useful for the purposes of training and operation rehearsal are the save and load capabilities of Case Creator. These allow the user to apply a set of case properties by using the wizard, as described in Sections 8 and 9, and save the settings to be reopened for re-use or alteration at a later date. This is especially useful for the production of multiple iterations of the same case for class training or operation rehearsal purposes.

10.5.1 Saving Case Settings

A method was developed in VB to save case settings ready for loading into the wizard at a later date. The approach taken was to digitally store all selections that had been made by the user: radio button selections, checkbox values, sliding scale values and calculated variables in a simple manner. The user would then be permitted to work through the wizard as before, with the loaded values displayed on all controls in order to completely recreate the case that had been in progress.

The user may save the changes they have made to the case settings at any stage, by selecting to do so through the program menu (Figure 154) or at the end of the wizard (see Section 10.4.4):

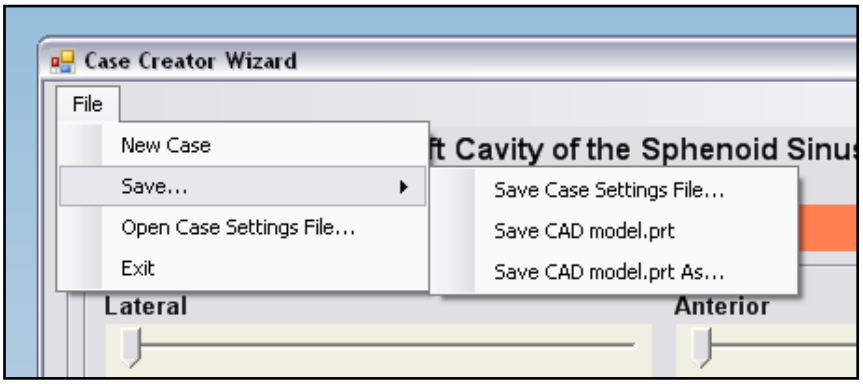

Figure 154: Save and Open functions in Case Creator wizard menu

A range of sinus area-specific storage variables are used to store the settings at each stage of the wizard, as shown in Figure 155 for frontal swelling:

```
SAVEDFrontalSwell
SAVEDFrontalAnt = TrackBarAnt.Value
SAVEDFrontalLeft = TrackBarLeft.Value
SAVEDFrontalPost = TrackBarPost.Value
SAVEDFrontalRight = TrackBarRight.Value
```

Figure 155: Frontal sinus swelling settings stored in area-specific variables

The code in Figure 155 shows the storage variables for swelling in the frontal sinus being set at the levels defined by the user, at the swelling stage of the wizard. Once the user begins work on a different sinus area, the sliding scale (`TrackBar`) values will be altered, but the saved variables will still contain the correct information for the frontal sinus. The first variable, `SAVEDFrontalSwell` is used to record whether swelling was applied by the user, with a binary value of 0 or 1. If the value is 0, the swelling application subroutine will not be run when the case is loaded, to save modelling time. This method was also used for the application of tumours, with variables named `SAVEDFrontalTum1` and so on.

Once the user reaches the end of the wizard, they may forget to save the settings they have applied before exiting the program. In order to prevent the user from losing their work, a prompt is shown if unsaved changes have been made to the case settings. The display of this prompt is controlled by a text variable, "`ChangesAppliedSettings`" which returns a value of "Yes" if unsaved changes have been made. The value is updated every time the user clicks the "Next" button, and is reset each time the save process is run. The option on the prompt window (Figure 156) to save the case settings performs the save subroutine.

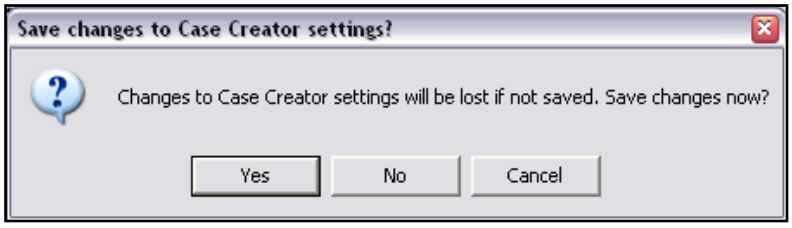

Figure 156: Prompt to save case settings before exiting the wizard

To allow the data stored in the variables to be accessed at a later date, the information has to be written to the computer, as all variables will be reset after the program is closed. The method used writes the information to a text file line by line, employing the VB *WriteLine* function. This function writes the piece of required information to a line of the text file and starts a new line in the file, for the next piece of information to be written. In this way, all variable and setting values are saved, with some annotation at appropriate points to aid, if necessary in studying the text file. A section of the saved file is shown in Figure 157*a)*, along with a description of the stored information in Figure 157*b)*.

a)

```
---FRONTAL---
------LAYERS---
23
19
2
------SWELLING---
1
20
35
38
10
```

b)

```
Total number of layers in frontal region
Swelling Start Layer TrackBar.value
Swelling End Layer TrackBar.value

Swelling to be applied? (0=NO or 1=YES)
Anterior swelling TrackBar.value
Left swelling TrackBar.value
Posterior swelling TrackBar.value
Right swelling TrackBar.value
```

Figure 157: *a)* Saved information in .txt file, *b)* explanation of information

When the save process is run, the user is given conformation in the form of a message box (Figure 158) which displays the areas of the sinus in which settings have been altered, that are now being saved:

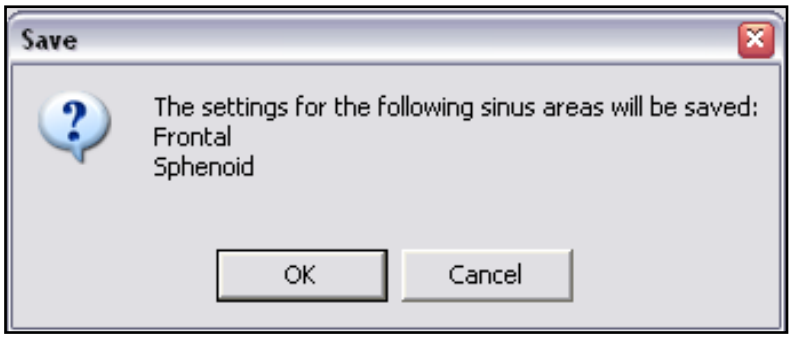

Figure 158: Information provided showing which sinus area settings will be saved

10.5.2 Loading Case Settings

The user may decide to load a previously created set of case settings by selecting the option from the program menu, as seen in Figure 154. When a case is to be loaded, the user is firstly prompted to select a file from an Open File dialog box. Once a settings text file is selected, a new page of the wizard is shown; the Loaded Case page. The appearance of the load page is controlled by the `SetupLoadPage` subroutine, which is based on the `SetupSummaryPage` subroutine described earlier.

This page shows a visual and numerical summary of the settings for each of the four sinus areas in an identical way to the case summary page, which may be immediately and simultaneously applied to the CAD model. The displayed information on this page is drawn directly from the loaded variables as part of the `LoadCaseSettings` subroutine. To read the saved file, all the storage variables that were previously used in the saved file are once again supplied with these values. This is done line by line, setting the variables to the contents of the appropriate line of the saved text file as shown in Figure 159:

```
SAVEDFrontalLayers = filecontents(2)
SAVEDFrontalStartLayerTB = filecontents(3)
SAVEDFrontalEndLayerTB = filecontents(4)
SAVEDFrontalSwell = filecontents(6)
SAVEDFrontalAnt = filecontents(7)
SAVEDFrontalLeft = filecontents(8)
SAVEDFrontalPost = filecontents(9)
SAVEDFrontalRight = filecontents(10)
.....
```

Figure 159: Area-specific variables updated with loaded values

When the user selects to create the case in the CAD software directly from loaded data, the spline manipulation code is run as described earlier, although some preparative code was needed in order for the program to function correctly in this scenario. Naturally, the code must only be run for those sinus areas that were altered before the case was saved, all others must be left in their original state; this is achieved as follows.

As the user makes their selections during the case design phase, the variables to be saved are updated. One variable is used to record whether any changes were made to a sinus area, by storing a binary value in the saved file. When the saved case is to be loaded and run, the code firstly checks if any changes were applied to the frontal sinus. This check is performed on the saved variable "`SAVEDFrontal`", which has a value of 0 if no work was done on the frontal sinus or 1 if settings were applied. If the value is 0, the code skips to the next sinus area and checks whether any changes were applied to the sphenoid, ethmoid and maxillary sinuses in turn. If the stored value is 1, the spline manipulation code is run to simulate the swelling and tumours that were saved. To increase running speed further, more variables were created that record whether swelling, or each of the three available tumours were applied. Again, the settings application code only runs if the value of the variable is found to be 1.

The user is allowed to change the settings of the loaded case, as set out in the aims of this function. To start revision of the case, the user is guided to the settings selection page, where their previous selections are reflected on the list of setting checkboxes. They may add or remove settings from the list, before starting to work through the list as normal. With the previous navigation method, this required complex programming to display the correct information at each stage of the wizard. However, by using the new navigation method, the same page setup subroutines may be used as in regular wizard use, as they are already programmed to display the saved variables (Figure 160). The saved binary variables were included in the checks performed in the page setup subroutines:

```
If FrontalSwelling = "" And SAVEDFrontalSwell = 0 Then
   TrackBarAnt.Value = 0
   TrackBarLeft.Value = 0
   TrackBarPost.Value = 0
   TrackBarRight.Value = 0
Else
   TrackBarAnt.Value = SAVEDFrontalAnt
   TrackBarLeft.Value = SAVEDFrontalLeft
   TrackBarPost.Value = SAVEDFrontalPost
   TrackBarRight.Value = SAVEDFrontalRight
End If
```

Figure 160: Code checks if case has been loaded, to apply saved values to sliders

When the settings are altered on this occasion, the variables to save are once again updated, to allow the new version of the case to overwrite the old, or to save the new case as a separate file for subsequent loading.

10.5.3 Saving NX Part File

No method is currently known by which VB code may be used to automatically export a STL file from NX, which is the ideally required final output. Therefore, as a means of output from the wizard, the user is given the opportunity to save the CAD model as a NX part file (.prt) by only interacting with the Case Creator program. The part file may be subsequently used to produce a STL file for 3DP of a physical model.

To perform this action, the user is initially asked to provide a name for the part file they are creating at the start of the wizard, as shown in Figure 161.

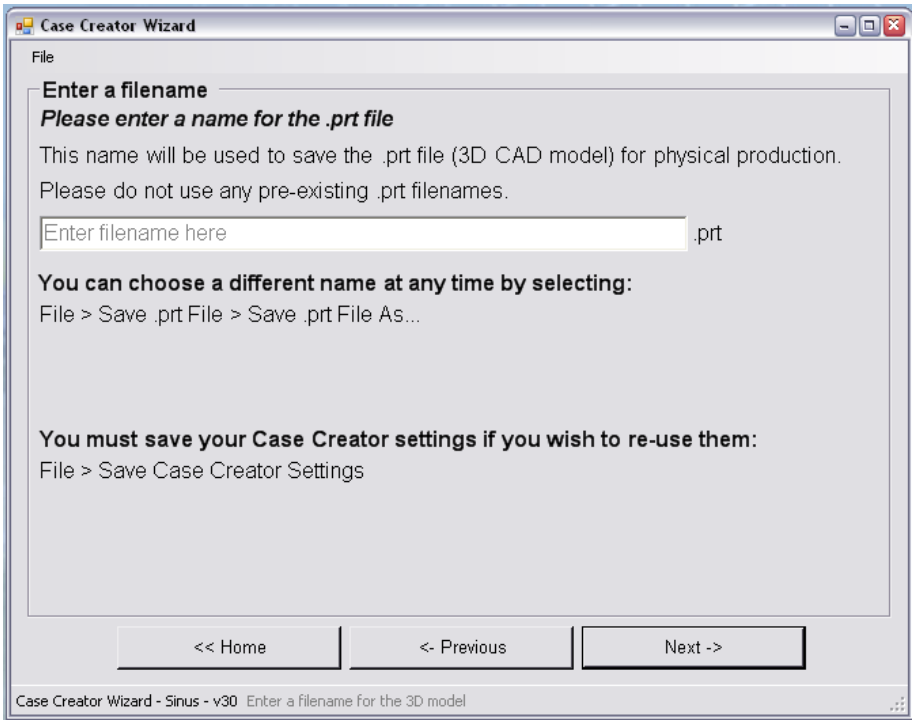

Figure 161: CAD part filename entry page of Case Creator wizard

The user is prompted to supply a filename for the .prt file by typing in the space provided. This name is stored in a variable (`prtSaveName`) until required by the CAD software. The process to save the CAD file is not run until the user decides to do so; the purpose of this stage is to acquire the filename for future use. The name is

displayed in the File menu of subsequent stages to clarify the options available; in Figure 154, the CAD model filename was defined as "CAD model" on the naming page of the wizard.

When the user chooses to save the CAD model, the code that is run actually performs the "Save As" process in NX, automatically using the filename entered by the user as the part file name.

In a similar way to saving the case settings, the user is prompted to save the CAD model on exiting the wizard, if their changes have not been saved (Figure 162). This is controlled by another text variable, "`ChangesAppliedprt`" which returns a value of "Yes" if unsaved changes have been made. This value is then reset on saving the CAD model, and updated to "Yes" each time the settings application code is run.

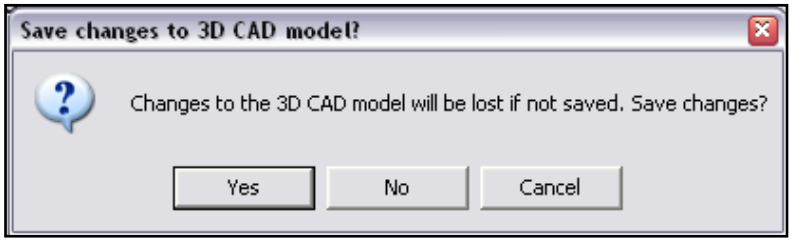

Figure 162: Prompt to save CAD model before exiting the wizard

10.5.4 New Case Settings File

At any point after settings have begun to be defined by the user, they may select to start a new case settings file. This resets the whole wizard and returns the user to the start of the process.

The new case settings file may be started through selecting the option from the program menu. This option is shown greyed out if the user has not yet defined any settings for the case. Once they have done so, the option is made available, as shown in Figure 154.

When the option to start a new settings file is selected, the user is prompted, in the same way as when they exit the wizard, to save the NX part file or the previous case

settings (if unsaved) for future use. The NX part file in use is subsequently closed and the original, unaltered file is opened again.

10.6 'Undo' Function

When the user has applied the case settings to the CAD model, they are presented with a range of options. They may save the case settings for use later, save the CAD model, add further settings to the current case, exit the wizard, or revise the current settings by moving back through the wizard. Should the user select this option, the changes made to the CAD model during the last settings application need to be undone.

This is due to the way in which swelling is simulated, by subtracting scaffold solids from the anatomy to leave the swollen cavity lining in place. If the settings were then changed and the level of swelling was increased without undoing the subtract operation, NX would attempt to subtract the scaffold solids from the already swollen geometry. Errors would be encountered as the new scaffold solids would be likely to fall completely within the previously created cavity space, meaning that they could not be subtracted.

Undoing the previous actions also acts as a confirmation to the user that they will be making changes to the model. By seeing that the swelling and tumour bodies are no longer visible once they begin to work through the wizard once more, the effect of their actions should be made clear. Coding was required to run the undo function in NX automatically, the correct number of times to undo the latest group of settings. The solution to this problem was found by running an 'undo counter' when case application occurred, the value of which would be used to repeatedly run the undo function.

When the settings application code for each sinus area is run, a counter is updated at the application of each setting, as shown in Figure 163:

```
UndoCount = UndoCount + 1
```

Figure 163: UndoCount is updated on application of settings

Once application is complete, `UndoCount` stores the number of separate settings (swelling subtractions and tumours made visible) that have been applied. If 'Previous' is clicked at the end of the wizard to revise the case settings and make alterations, the undo function in NX is run this number of times in an iterative loop (Figure 164):

```
For UndoNumber = 1 To UndoCount
    (Undo function code)
Next
```

Figure 164: Undo subroutine is run the required number of times by using *For-Next* loop

This leaves the model as it appeared before the latest settings were applied, which could include some previously applied settings.

Once the program was robust enough to allow users to navigate fully through the wizard, a finalised system to apply swelling and tumours had been developed, and the user could save, load and undo alterations to the 3D CAD model, the first round of program trials were run. Through these trials, suggestions would be obtained for further development of the program.

10.7 Program Trials

The results acquired from trial testing of the program by fourteen users from relevant areas of expertise are presented and discussed in this section. The program was trialled by users from relevant fields of work, to gain an understanding of users' opinions of the program and the results achieved through its use, the ways in which users may use the program, the program's suitability for the target user and to collect suggestions for improvements to the program. Participants were selected to cover the range of target users of the program; medical staff, ENT surgeons of varying experience, and maxillofacial prosthetists were asked to trial the program and give feedback on their experience. This range of participants also meant that the users had

varying levels of experience in using 3D CAD modelling software and creating surgical training models. The results provided by users of differing experience levels in these, and the performance of sinus surgery, could therefore be compared to analyse how easy the program was to use.

Figure 64 shows the schedule of events for the testing, redevelopment and re-testing of the program. Two trials (trial A – eight users and trial B – seven users including one re-test) were run, giving time for alteration of the program in accordance with suggestions from participants from trial A. This gave the opportunity to compare the results from each trial for the aspects of the program that were altered, to assess the value of the new features that were changed. Ideally, participants who had trialled the original program in trial A would be re-tested using the re-developed program in trial B, however time constraints owing to the demanding nature of the participants' work made this impossible. Difficulties were also encountered when attempting to schedule program trials at ENT seminars, where trials could not be added to the agenda, and meetings with specific participants due to their constantly changing availability. Clinical expert Anshul Sama participated in both studies, allowing some comparison to be drawn between his views of both versions of the program.

The results from each trial are presented separately, with a summary of the changes implemented between the two trials, after acting on suggestions from trial A.

A user questionnaire was designed with reference to [174-176] to assess the quality, usability, appropriateness and effectiveness of the program and its functions, and finally the demographics of the surveyed participants. The questionnaire was administered personally; participants were asked to read and answer questions themselves, with the aim of obtaining realistic and unpressured results. The questionnaire may be viewed in full in Appendix A, and is divided into five sections, to gain detailed feedback about all areas of the wizard's design and information regarding the survey participants:

- General (ease of use, navigation system, order/number of functions)
- Swelling application

- Tumour application
- Results
- Participant information

For each closed question, the users were asked to indicate their individual level of agreement with a statement on an ordinal Likert scale and in some cases, use space on the questionnaire form to provide qualitative responses. By using the Likert scale, the users' responses could be analysed to assist in the subsequent development of the program. The statements were phrased positively, using conventional language to assist the user in accurately judging their level of agreement. Any explanation provided by users was taken into account and considered for use in redeveloping the program either between trials, or in the future. The Likert rating system is summarised in Table 9:

Rating	Level of agreement
1	Strongly disagree
2	Disagree
3	Neutral
4	Agree
5	Completely agree

Table 9: Likert rating system for closed Case Creator trial questions

10.7.1 Results from Case Creator Trial A

The average results for all questions in the first trial that were answered on the Likert scale are shown in Figure 165:

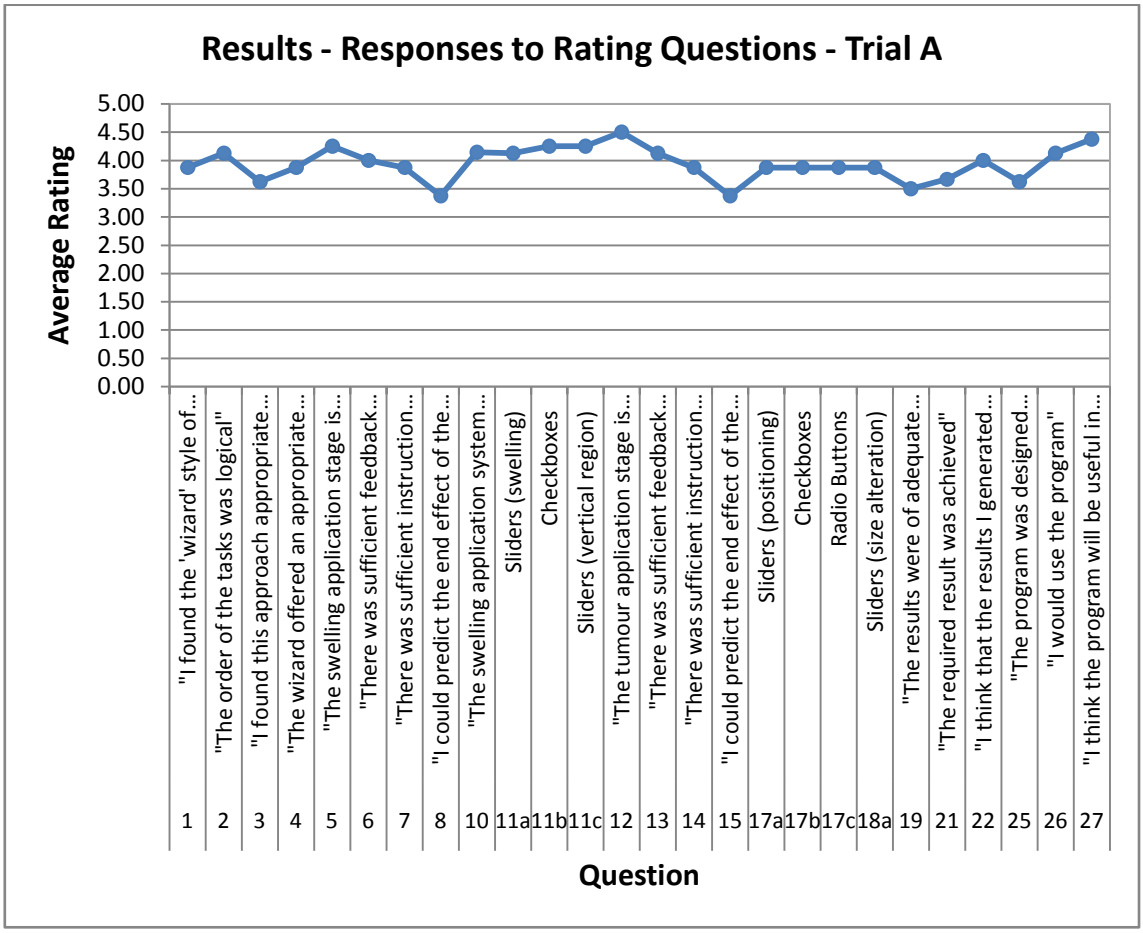

Figure 165: Average ratings for common program features – Trial A

The average ratings from trial A can be seen to centre on a general agreement with the statements; the average rating given was 3.94.

10.7.1.1 Participant Information

The participants were asked to provide an estimate of their level of experience in three relevant areas; performance of sinus surgery, creation of training models for surgical students and the use of 3D CAD modelling software. The experience level was rated on a scale from 0 (no experience) to 5 (very experienced). This information helped the reception of the program by users from different fields to be ascertained, possibly highlighting areas in which the program needed to be made more accessible to a wider range of users.

The experience levels of users from both trials were recorded as shown in Table 10:

		Participant							
		1	2	3	4	5	6	7	8
Skill	Performing sinus surgery	4	5	3	5	2	1	0	0
	Creating training models for surgical students	4	4	0	3	0	0	4	4
	Using 3D CAD modelling software	4	3	0	5	0	0	1	4

Table 10: Experience level of participants in three relevant skill areas – Trial A

Participant 1 is suspected to have entered incorrect information; as a new doctor on rounds on a ward in the Ear Nose and Throat (ENT) department at QMC in Nottingham, the participant is unlikely to have good experience of creating training models for surgical students. The participant also remarked that they had not yet observed sinus surgery, so they cannot have good experience of performing the same surgery. This highlights an inherent problem with the performance of survey-based feedback; participants may answer without fully reading or understanding the question, or carefully considering their answer. With this in mind, the experience level ratings supplied by participant 1 will be omitted from any analysis using this data. Otherwise, participants' responses are considered to be realistic, as their experience level ratings are consistent with their profession and other information provided in conversation.

The experience levels of participants from Trial A in each skill are shown in Figure 166, omitting the information provided by participant 1:

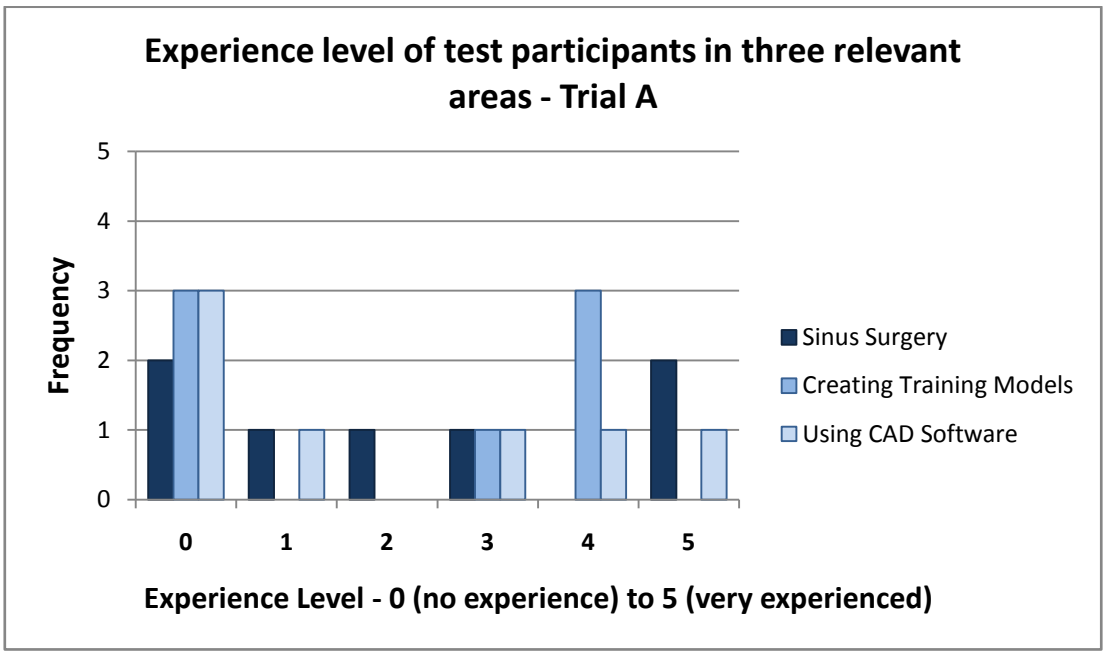

Figure 166: Ratings frequency for experience level in relevant skill areas – Trial A

The level of participant experience in the performance of sinus surgery and creation of training models is spread, and the users participating in the trial were relatively inexperienced in the use of 3D CAD software, as expected and cited in the reasoning for the creation of the program. Users who rated themselves as experienced in the performance of sinus surgery also frequently rated themselves as inexperienced in the use of 3D CAD software. This gave further strength to the argument for the introduction of Case Creator as a means of enabling non-CAD users to easily create and edit custom sinus simulation models.

For the analysis of responses to some questions, particularly those relating to the ease of use of the program, the answers provided by experienced and inexperienced users in each area are studied separately, to gain an understanding of the effectiveness and appropriateness of the program for all types of user.

10.7.1.2 General Ratings

In the first section, the user was asked to rate the ‘wizard’ approach adopted by the program, and the order in which the steps of pathology application were presented. The first question asked the user to rate the ease of use of the ‘wizard’ style program,

with navigation buttons to guide them through the tasks to be performed. The results collected are shown in Figure 167:

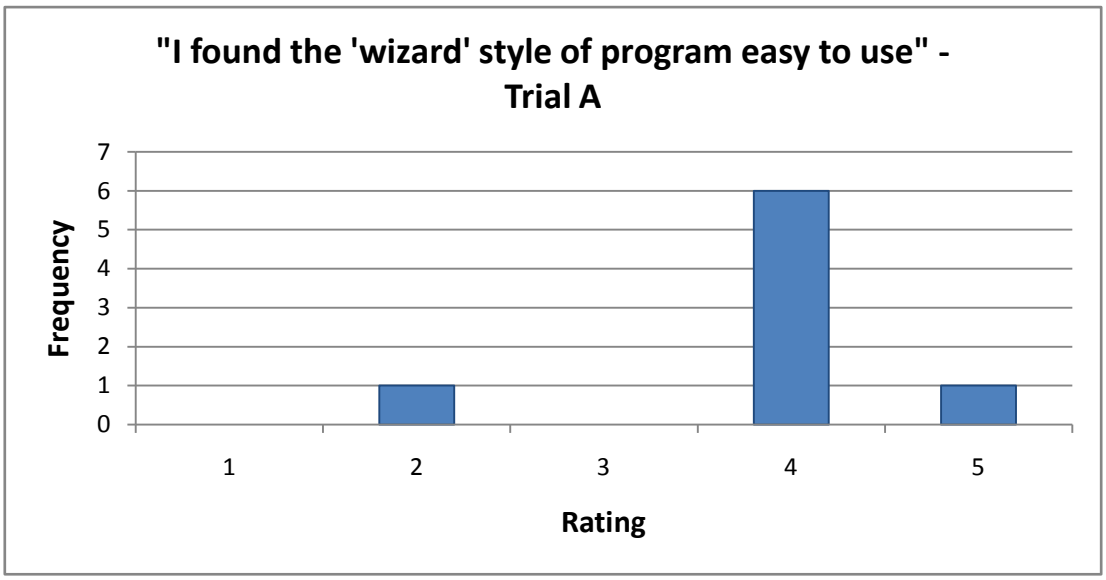

Figure 167: Ratings frequency for ease of use of 'wizard' style program – Trial A

It can be seen that the most common response was an agreement with the statement; the average rating of users' agreement with the statement was 3.88. Users commented that the wizard was very useful for non-CAD users. Indeed, users who rated themselves as inexperienced in the use of CAD modelling software rated the wizard approach highly with an average rating of 4.25 (see Figure 168). Comments were also received that instructions or assistance should be provided during the first usage.

The ratings were also collated to show how users' experience in the relevant skill areas correlated with the ratings given for ease of use. Participants' results were split into 'experienced' and 'inexperienced', then matched with the rating they provided for the ease of use of the wizard style program. Participants were split into these groups by considering an experience rating of 0-2 to signify inexperience, and 3-5 to signify experience in the given field. The results are shown in Figure 168:

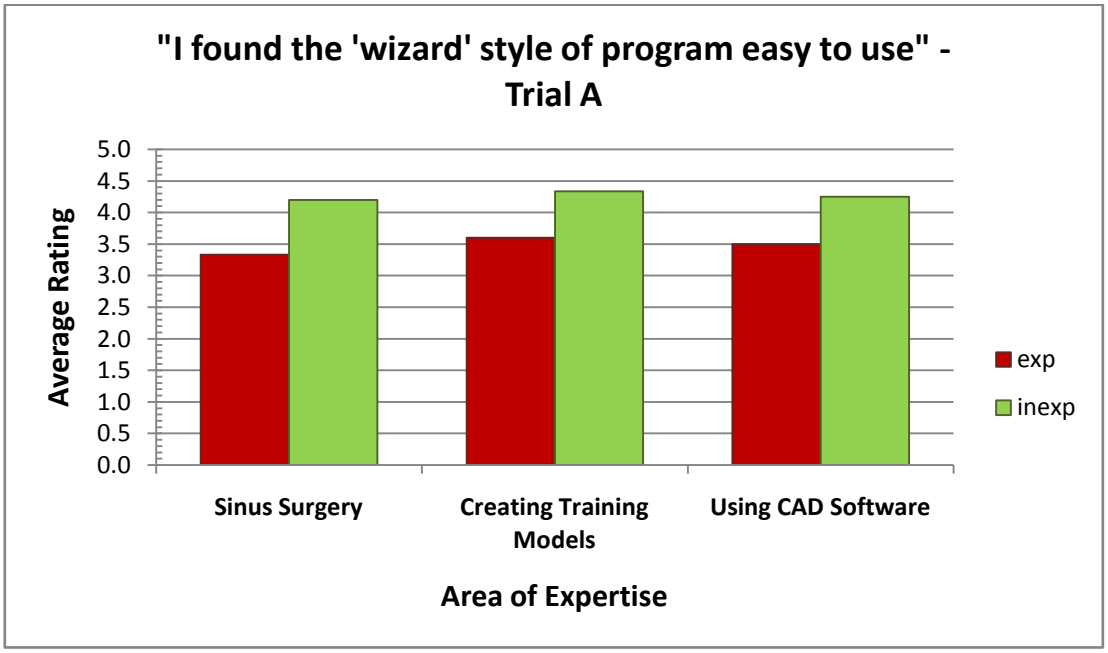

Figure 168: Average ratings for 'wizard' style program vs. experience in relevant skill areas – Trial A

It can be seen that inexperienced users in the three key skills found the wizard easier to use than those experienced in the tasks. Critically, as described earlier, inexperienced CAD users rated the wizard approach well (average rating of 4.25). Case Creator was designed to enable the use of CAD software by all, but most particularly inexperienced CAD users.

Users' opinions of the order of the tasks in the wizard (e.g. swelling, vertical region, tumours, apply settings) were then gauged. The results obtained are shown in Figure 169:

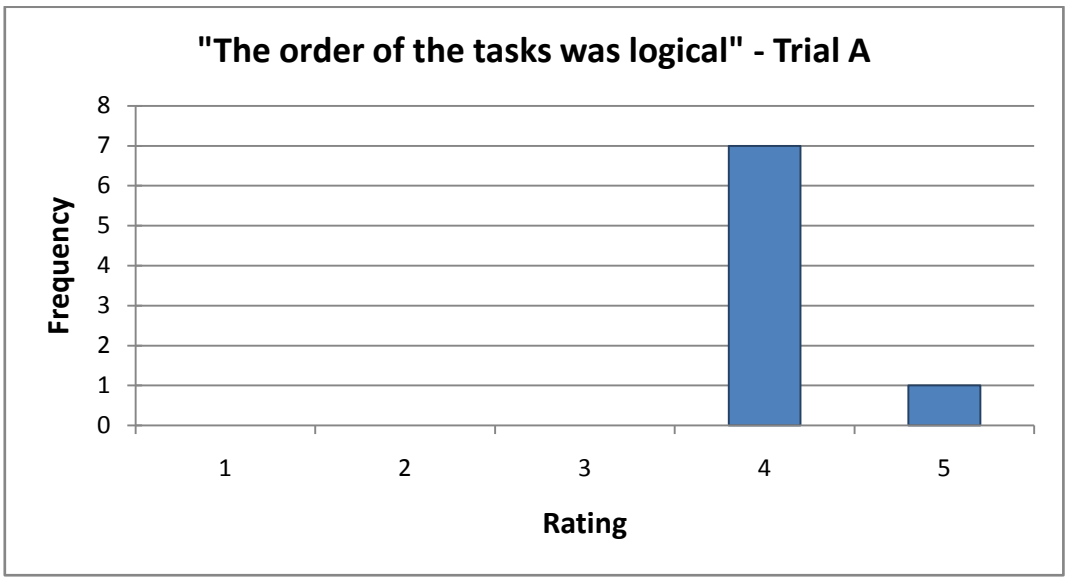

Figure 169: Ratings frequency for task order – Trial A

The results were favourable, showing that users found the order of tasks described above to be logical. The average rating given in response to this statement was 4.13, giving good reason to retain the order of tasks in future versions of the program.

All users were asked to give their opinion on the number of anatomy alteration options provided by the program. The results are shown in Figure 170:

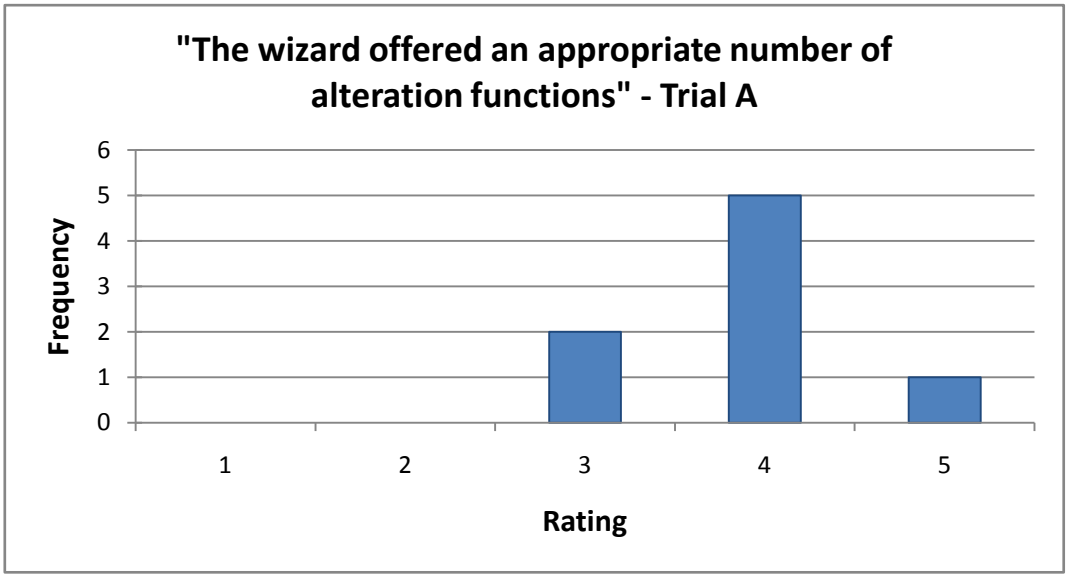

Figure 170: Ratings frequency for number of functions supplied – Trial A

The program performed well in this question, with an average agreement rating of 3.88. The only suggestion made by users for further functions to include in the program was a freehand drawing tool for swelling or tumour definition, the implementation of which will be described in more detail in Sections 13.2 and 13.4.

Users were asked to rate the level of feedback and instruction provided in the swelling and tumour application stages of the wizard. The feedback questions aimed to determine the effectiveness and appropriateness of the percentage values, coloured bars representing the level of swelling or size of tumours and positional data communicated to the user throughout the wizard. The results are shown in Figure 171:

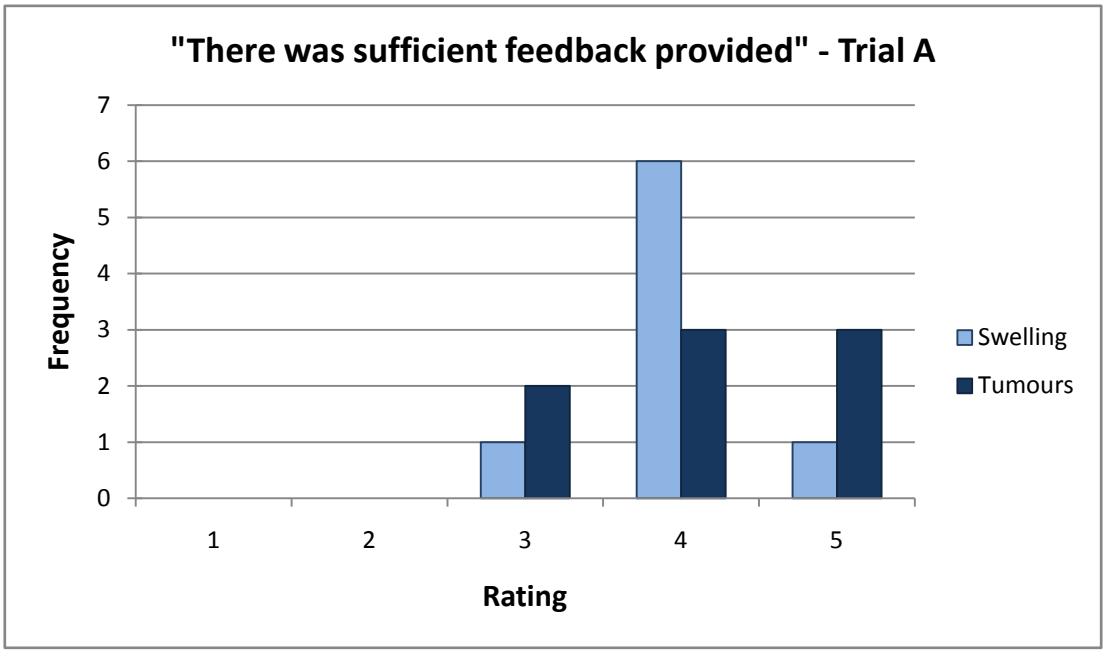

Figure 171: Ratings frequency for feedback given during settings application – Trial A

The level of feedback at the swelling application stage was considered sufficient by most participants. Users praised the feedback, commenting that the percentage levels gave the user the opportunity to correct their actions and that the coloured bars provided a good visualisation of the data. For feedback at the tumour application stage, some users remarked that the use of two planes to position tumours in three dimensions, including the visual feedback of the tumour icon over the anatomical images, was useful.

Participants rated the instruction provided throughout the swelling and tumour application stages of the wizard in the same manner. 'Instruction' was classified as the step-by-step guidance given at each stage and error messages displayed to the user. A summary of the ratings given by the participants is shown in Figure 172:

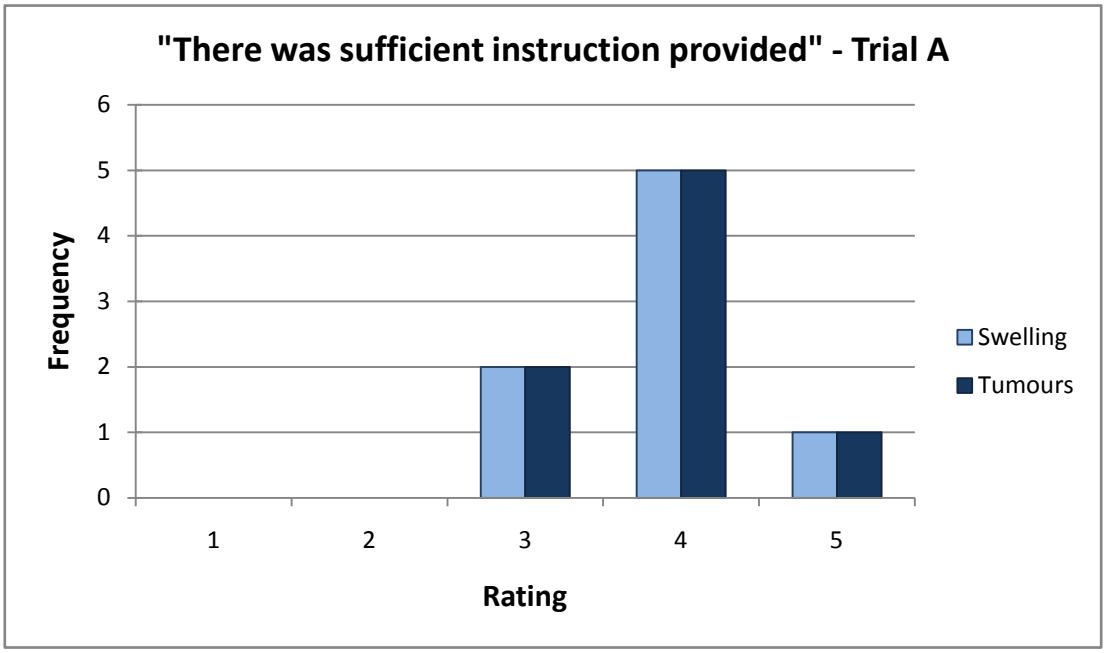

Figure 172: Ratings frequency for instruction given during settings application – Trial A

An average rating of 3.88 was given, and the only criticisms about the level of instruction provided during swelling application were centred around an inexperienced user's first use of the program, which may require further instruction than that given on-screen. However, when observing the use of the program by test participants, the instructions were occasionally ignored. The provision of an instruction manual was suggested by one user; this may not be a suitable solution considering some users' failure to read the instructions already provided. The instruction provided at the tumour application stage of the wizard was also favourably received; users stated that the instructions were easy to follow and allowed the user to make informed decisions to achieve an accurate outcome.

10.7.1.3 Navigation System

Users were then asked to rate the navigation system used in the program as a means of applying pathology to the anatomy. In trial A, the cyclical navigation system was tested.

The cyclical wizard navigation system asked users to select an area of the sinuses to affect with pathology, before applying these changes then moving on to the next area, if necessary. All possible pathologies were displayed to the user for each sinus area, to be switched on or off as required. This meant that the process of moving through the wizard was slower than possible, but that the user was made aware of all pathology options in each area as they progressed through the wizard. The results obtained when the users were asked to rate the appropriateness of the cyclical approach are as follows in Figure 173:

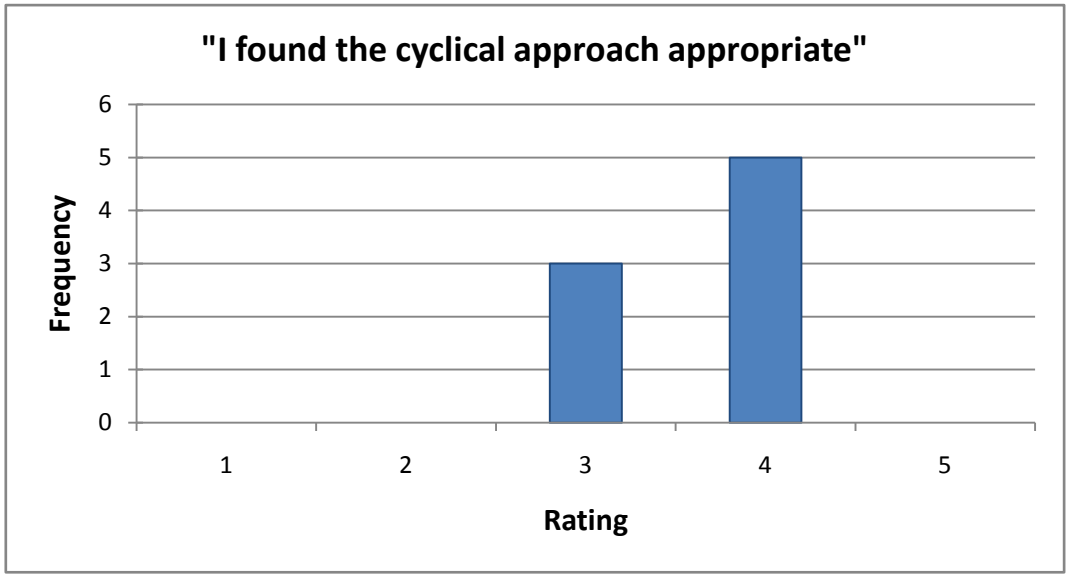

Figure 173: Ratings frequency for appropriateness of cyclical navigation system – Trial A

Opinion of the appropriateness of the cyclical navigation system is split, with an average rating of 3.63; a large proportion of the users rated their agreement as 'neutral', with the other users agreeing with the statement. Anshul Sama suggested the use of a menu of settings to allow the user to choose any of the settings to apply, instead of being guided through the predetermined list. Other users commented that there was a lack of 'flow', and that they struggled to see the end product.

10.7.1.4 Inclusion of Functionalities

Participants were then asked to rate the need for inclusion of the two pathologies that may be applied using the wizard; cavity swelling and tumours. By gauging the users' opinion of these program functions, suggestions were obtained for potential improvements to the program in future versions. Users responded as shown in Figure 174:

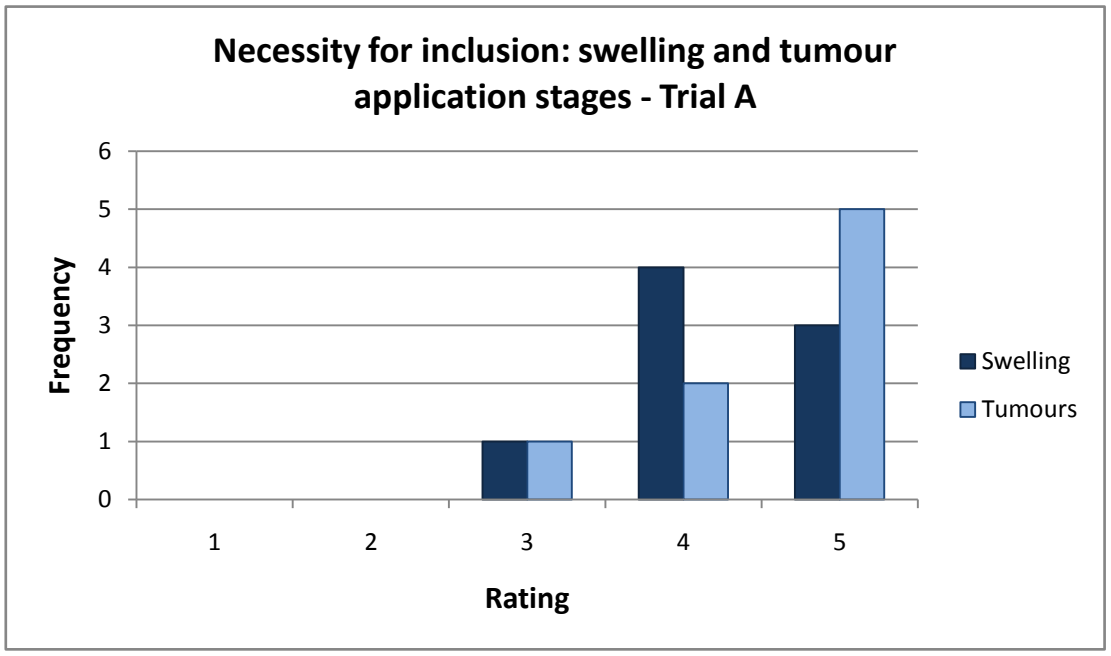

Figure 174: Ratings frequency for inclusion of swelling and tumour application – Trial A

It can be seen that users of the wizard agree strongly with the inclusion of the swelling application function, with an average rating of 4.25. Participants experienced in the performance of sinus surgery voted similarly to those that are not, with average ratings of 4.33 and 4.20 respectively. One participant hoped that this would lead to the inclusion of different material properties within the model, as is being addressed by the related research project.

The average response to the need for inclusion of the tumour application function was 4.50. In this case, users experienced in sinus surgery rated the importance of tumour application slightly less highly than inexperienced users, with average ratings of 4.33

and 4.60 respectively. Again, the average result gives further strength to the argument for continued inclusion of the tumour application function.

10.7.1.5 Swelling Application Controls

After having gained an understanding about the users' opinions of the need for the two pathology application functions, the ease of use of the controls provided in each case was established. The users were questioned on their opinion of sliding scales, radio buttons and checkboxes as means of applying changes to their pathology settings.

In the case of swelling application, users were asked to rate the sliding scales for application of directional swelling and definition of the vertical region of swelling, and checkboxes for toggling the inclusion of swelling in the case. The ease of use of these controls is summarised in Figure 175.

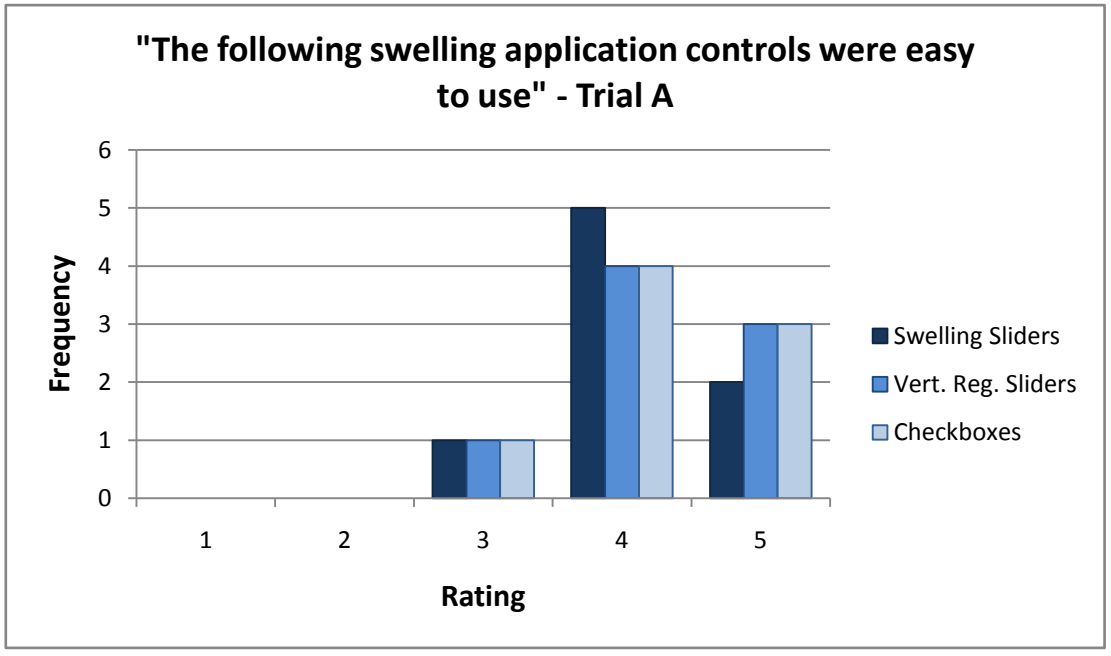

Figure 175: Ratings frequency for ease of use of swelling application controls – Trial A

The graph mirrors the fact that most users had the same opinion of all controls, with only one user voting differently. The results seen here are in favour of the slider system for setting swelling severity from different directions (average rating 4.13) and definition of the vertical region of swelling (average rating 4.25). The only alternative

offered by some participants was the potential inclusion of a freehand drawing tool for the application of swelling, as mentioned earlier, and which will be discussed in Section 13.2. The average rating for the checkboxes was also 4.25, showing that users find this system easy to use to control whether swelling will be applied to the model.

The overall swelling application approach was rated by the users, with the results shown in Figure 176:

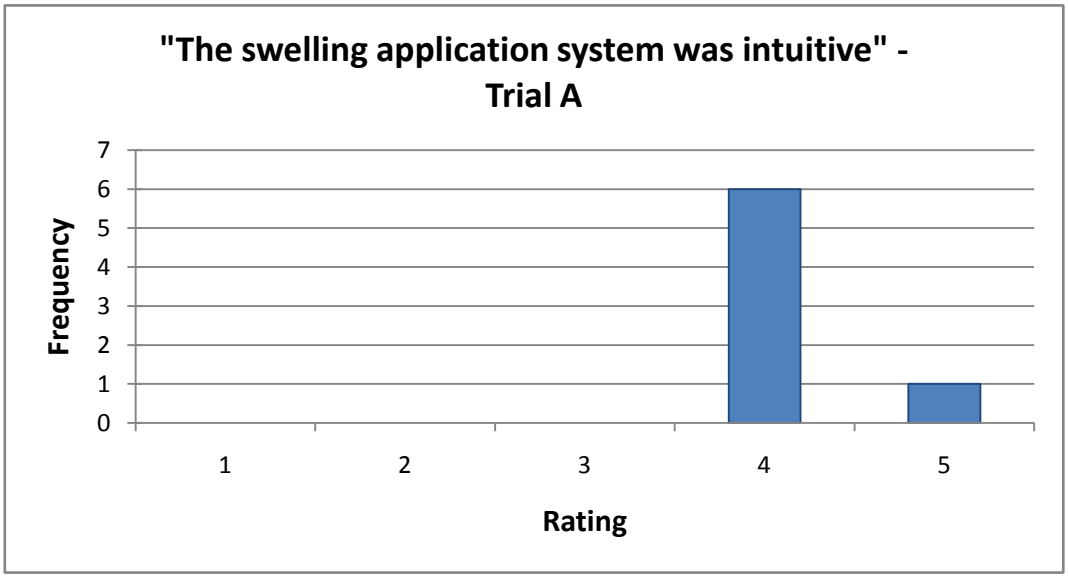

Figure 176: Ratings frequency for intuitiveness of swelling application system – Trial A

Participants rated the intuitiveness of the swelling application system favourably, taking into consideration the directional swelling application method, vertical region definition and separate treatment of the sphenoid cavities to give an average rating of 4.14. One participant failed to answer this question for unknown reasons. The results are encouraging and mean that the swelling application procedure will be retained for future versions.

10.7.1.6 Tumour Application Controls

The ratings received for the tumour application controls (positioning and sizing sliders, tumour activation checkboxes and control radio buttons) are shown in Figure 177:

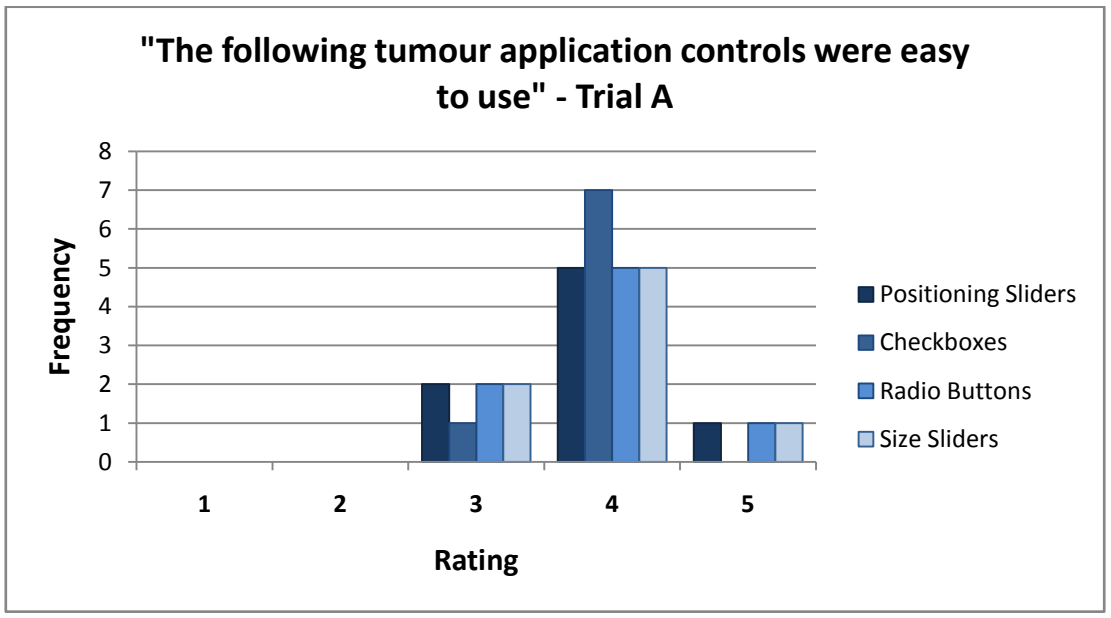

Figure 177: Ratings frequency for ease of use of tumour application controls – Trial A

Users responded positively to the tumour application controls, each receiving an average rating of 3.88. Users found the sliding scales easy to use to resize the tumour icons, but did not approve of the results obtained by using this system.

10.7.1.7 Results Achieved through Case Creator

For both swelling and tumour application, participants were asked to rate the extent to which they could predict the end effect of the changes they were applying to the case settings, before the final application. This rating gives insight into the users' understanding of the functions performed by the program and how successfully the functions were communicated and replicated. The results are shown in Figure 178:

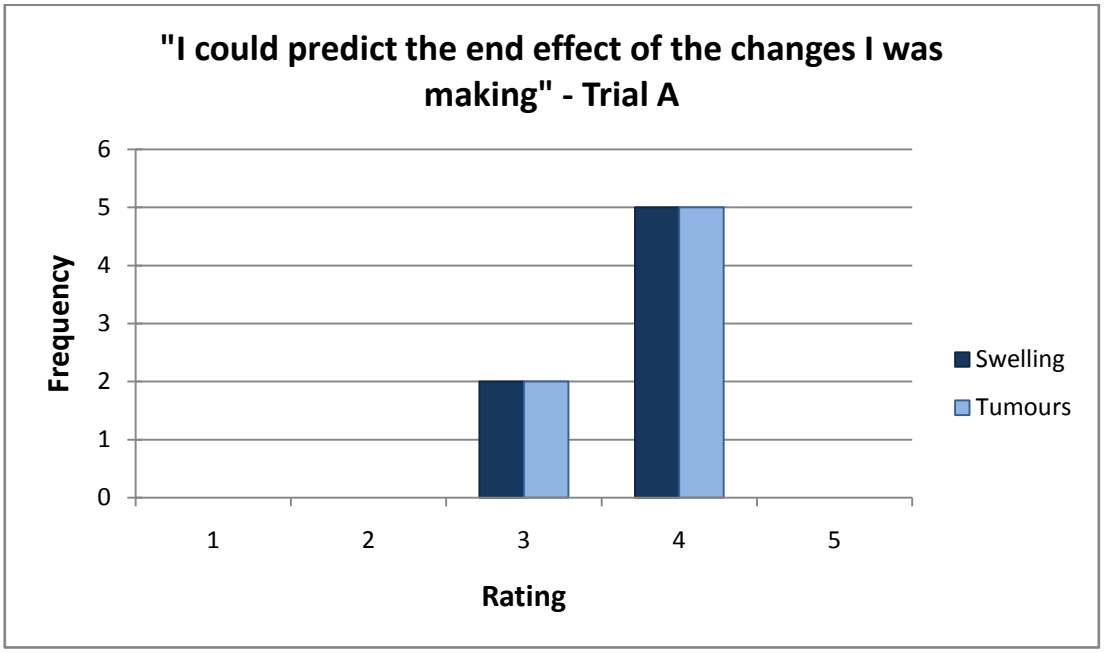

Figure 178: Ratings frequency for predictability of end result – Trial A

The results of this question are spread; users were occasionally unable to predict the result of the settings they were making with Case Creator. The average rating for the predictability of results from swelling and tumour application was 3.71. A good number of participants rated the predictability of results well; one result was skewed by the unavailability of the CAD software during the test and is not included in the results. The user affected by this problem rated the predictability of results poorly because the results could not be shown, but had not followed (as was strongly suggested) the set case creation routine to achieve the results for which a pre-made, viewable 3D CAD model was available.

Participants commented that the graphical nature of tumour application, where the user can visualise the placement and size of the tumour body in three dimensions aids the predictability of results. Criticisms of the results from the tumour application stage of the wizard were centred on the rectangular shape of the tumour icon, and the body that was created in the CAD model as a result. Users therefore found it difficult to predict the areas of the model that would be filled by the tumour body.

When asked to rate and comment on the realism of the results achieved by using the wizard, participants gave the results shown in Figure 179.

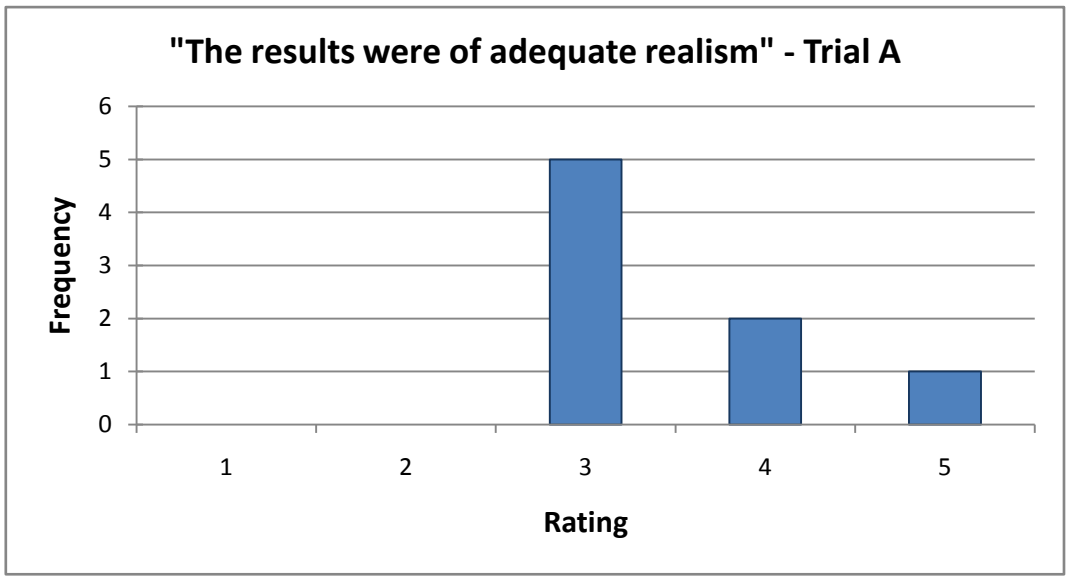

Figure 179: Ratings frequency for realism of wizard results – Trial A

A good number of users agreed that the results achieved by the wizard were of adequate realism, with an average rating of 3.50. However, some commented that the simplified block shape of the tumour in the CAD model was not realistic, drawing the ratings down slightly. No comments were received about the realism of the swelling that was applied to the cavities of the 3D sinus model in CAD.

When asked to rate their agreement with the statement: "I would use the program", users responded as shown in Figure 180. This question was designed to gauge interest for the program, and the range of fields from which future users may come.

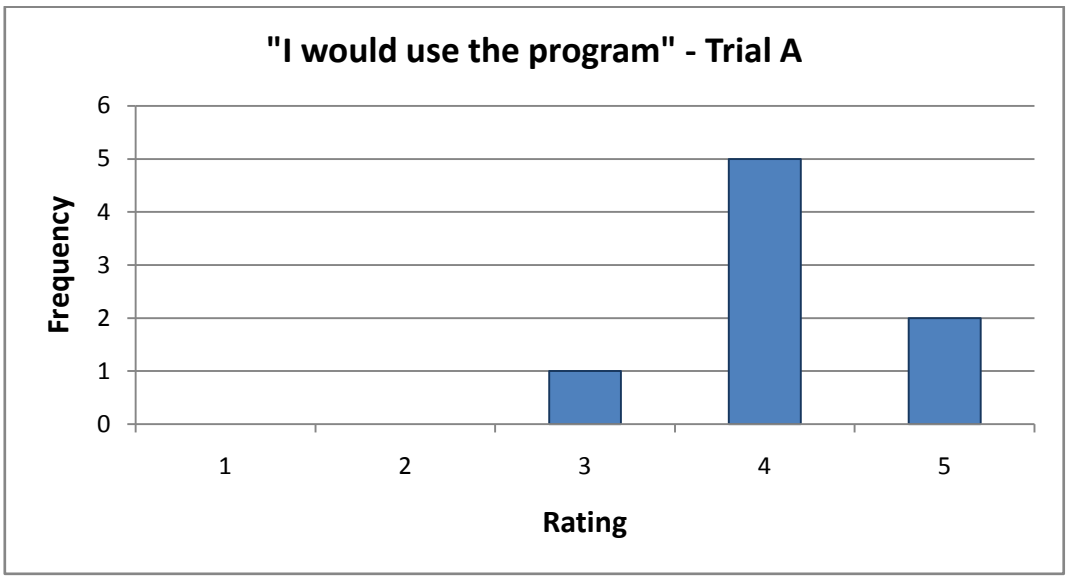

Figure 180: Ratings frequency for use of program – Trial A

Users responded positively to this question, suggesting that the program would be used by a range of medical professionals, with an average rating of 4.13. The participant who responded neutrally to the question was a maxillofacial prosthetist.

When the results of this question are split into the responses from experienced and inexperienced participants in the three related fields as shown in Figure 181, the appropriateness of the program to the intended audience is evident:

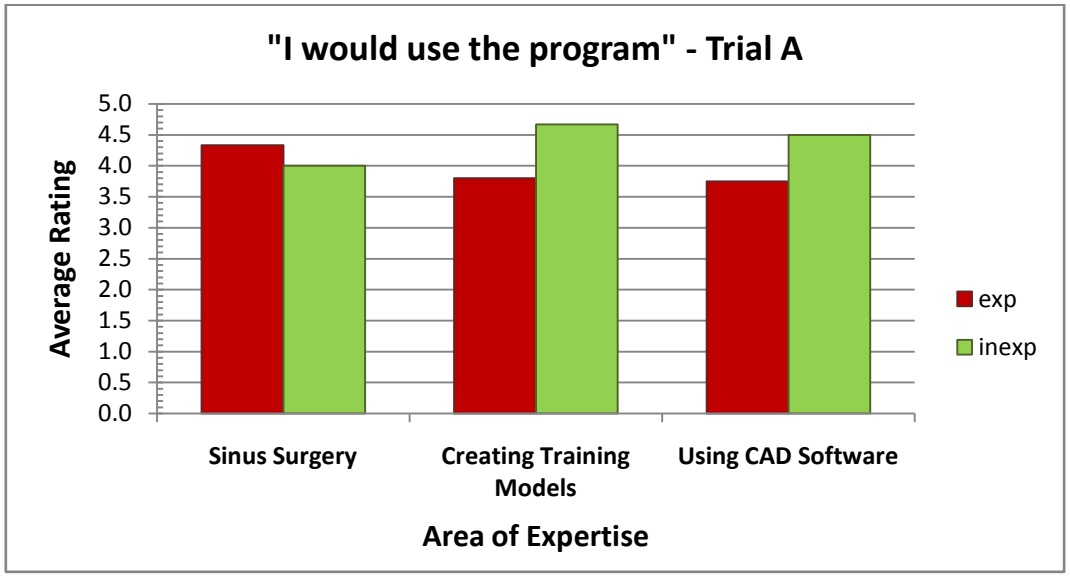

Figure 181: Average ratings for use of program vs. experience in relevant skills – Trial A

Users who rated themselves as experienced in the performance of sinus surgery, and those who rated themselves as inexperienced in the use of CAD software responded well, with average ratings of 4.33 and 4.50 respectively. Inexperienced sinus surgeons also showed that they would use the program, with an average level of agreement of 4.00, confirming that the program has met its aim.

Finally, users were asked to rate the usefulness of the results they had achieved in the training of sinus surgeons. The results obtained are shown in Figure 182:

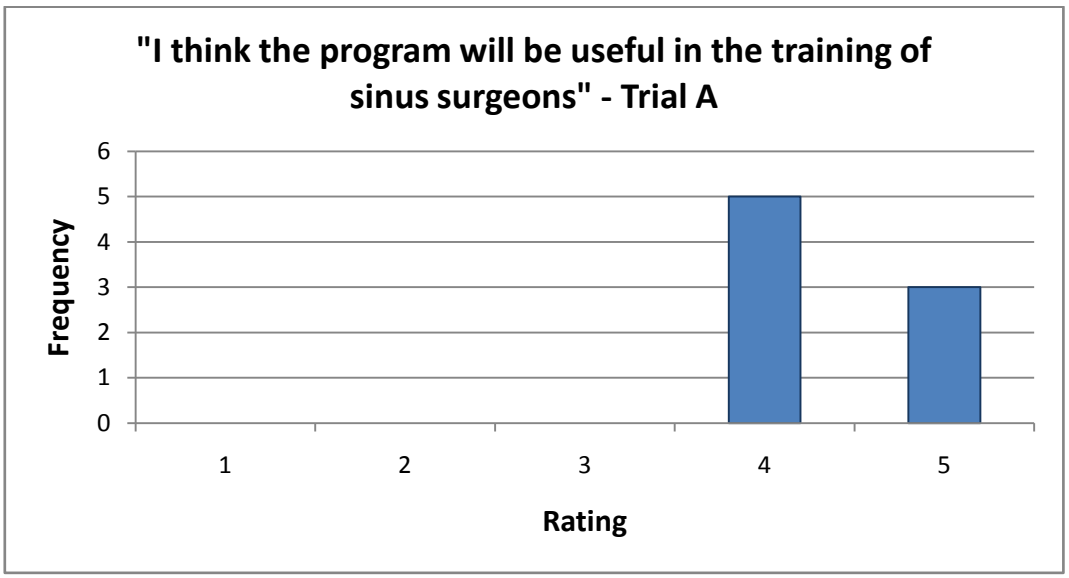

Figure 182: Ratings frequency for use of program in training sinus surgeons – Trial A

It can be seen that all users agreed that the program will be of use in the training of sinus surgeons; the average response was 4.38. Users commented that it is extremely difficult to 'simulate' defects on patients who do not exhibit them, making the ability to alter data to create exactly what is required useful.

When questioned how they might use the program, maxillofacial prosthetists said that the program could be used to adjust CT data to create different scenarios for teaching.

10.7.1.8 Summary

Eight medical professionals from an ENT/sinus surgery background trialled the Case Creator program, providing an insight into their opinions of the program, its functions and possible improvements to be made. A spread of user experience was observed in the performance of sinus surgery, creation of surgical training models and use of 3D CAD modelling software.

The majority of users found the 'wizard' style of program easy to use, especially users who considered themselves inexperienced in the use of 3D CAD software. This was encouraging, as the program therefore catered to the target audience.

The inclusion of swelling and tumour application functionalities were considered necessary, and no suggestions for other functionalities to include were received. The ease of use of the swelling application controls were rated favourably: the sliding scales for definition of severity and vertical region of swelling will therefore be retained for further testing in the second trial. Users also found the swelling application system, where cavities of the sphenoid sinus are treated separately, the vertical region of swelling is defined and swelling severity is set from four horizontal directions intuitive. The tumour positioning controls were rated favourably, all with average agreement ratings of, however some improvement is needed to finalise the system.

Encouraging results were received regarding the number of users who would use the program in their work. Experienced sinus surgeons and inexperienced CAD users would use the program, showing that again, the program was judged to be suitable for use by the intended users. Participants agreed that the results obtained through the use of the program would be of use in the training of sinus surgeons.

CHAPTER ELEVEN

REDEVELOPMENT OF GUI AND PROGRAM TRIAL B

11 Redevelopment of GUI and Program Trial B

Before the second stage of the program trials was undertaken, some changes were made to the program in accordance with suggestions from the participants in trial A. The new concurrent navigation system was implemented, with the aim of decreasing the time needed to produce the required results, increasing ease of use and allowing simultaneous treatment of multiple sinus areas. As a result of suggestions in trial A that instructions or training should be provided, an instruction page was included in the new wizard design (Section 11.2). The way in which tumours are resized was also updated, with the use of resizing handles to allow the user to define the shape of tumours in more detail, again focussing on ease of use. This would address some aspects of the problem of tumour realism highlighted by users in trial A, however suggestions have been made in Section 13.4 for ways in which this realism could be further improved.

11.1 Redeveloped Wizard Navigation System

The cyclical process was seen by some, in the trial use of the program, to be unintuitive and time-consuming, especially if only a small number of settings were required in each area of the sinuses. Anshul Sama suggested the use of an itemised menu at the start of the wizard, to allow the user to select which settings they would alter and apply, before moving through the wizard working with only these settings.

The new, 'concurrent' navigation system relies upon the initial selection of the case settings to be defined and applied instead of addressing each sinus area consecutively. The user selects the settings they wish to apply at the very start of the wizard process, as described in Section 11.2.2. This method was developed and implemented into the coding and settings definition stages of the previous wizard design. The simple introduction of the settings menu and removal of the sinus area selection page caused a large amount of coding issues that had be adapted to fit the new method.

The main issue to overcome was uncertain page order. Previously, the order of the pages was set; when the user clicked "Next" or "Previous", the next page in the

sequence would be displayed. In the new system, the user selects which pages they wish to view at the start of the wizard, meaning that the next page to be shown is not merely the next page in the list, but the next page in the list that has been selected. Secondly, the same page may be viewed two or three times in succession, but related to different areas of the sinuses, causing issues with displaying the correct data and the use of the same controls for each area.

To allow the program to find which page to display to the user next, a subroutine named `GoToNextPage` was created. The code contained within `GoToNextPage` is shown in two parts below. This code is run every time the user clicks the "Next" button, to find the next required page in the list and display the correct information to the user. The first section of code is used to save the settings made on the previous page, found by checking which page is currently visible. The settings are saved to display the correct data on the subsequent wizard pages during navigation and to apply the case settings to the CAD model. The code is shown in Figure 183:

```
If GroupBoxSwelling.Visible = True Then
   SetSwellingSettings()
ElseIf GroupBoxVertReg.Visible = True Then
   SetVertRegSettings()
ElseIf GroupBoxTum.Visible = True Then
   SetTumourSettings()
End If
```

Figure 183: Settings from previous wizard page saved by determining which page is now visible

The values of sliding scales, checkboxes and radio buttons, and the positions of tumour icons are saved into sinus area-specific variables (such as `SAVEDFrontalAnt` for the level of anterior swelling applied in the frontal sinus) in each of the `Set...Settings` subroutines. These subroutines make use of `SinusRegion` once again to determine which set of variables to update.

An *If* statement was then written to find the next selected setting in the list, to display to the user, as shown in Figure 184. In the figure, "`CheckBox`" has been shortened to "`CB`", and some sinus area names have also been abbreviated to allow the code to be displayed clearly.

This subroutine, named `GoToNextPage`, makes use of a new system whereby the progress of the user through the list of settings is monitored in a string variable. In the case of applying swelling to the frontal sinus, the user's progress through the application of this setting is recorded in the variable `FrontalSwelling` as: `""` (nothing – the user has not reached this setting, or the setting is unselected); `"STARTED"` (the user is currently working on this setting) or `"DONE"` (the user has completed and moved past this setting). The value is set to `"DONE"` when the user clicks the "Next" button, prior to `GoToNextPage` being run.

The code in `GoToNextPage` first checks whether the user has selected to apply swelling to the frontal sinus, the first setting in the list. If so, the code also determines whether work on this setting is incomplete, by checking the value of `FrontalSwelling`. If `FrontalSwelling` does not return the value `"DONE"`, the conditions are satisfied and the code enters this section. If not, the code will check whether the conditions for showing the settings page for the vertical region of swelling in the frontal sinus are met, and so on for all pages of the wizard. If no conditions were satisfied, all selected settings were completed by the user and the summary page should be displayed.

```
If CBFrontalSwell.Checked = True And FrontalSwelling <> "DONE" Then
   SettingNo = SettingNo + 1
   SetupFrontalSwell()
ElseIf CBFrontalSwell.Checked = True And FrontalVertReg <> "DONE" Then
   SettingNo = SettingNo + 1
   SetupFrontalVertReg()
ElseIf CBFrontalTumour.Checked = True And FrontalTumour <> "DONE" Then
   SettingNo = SettingNo + 1
   SetupFrontalTumour()
ElseIf CBSphenSwellL.Checked = True And SphenSwellingL <> "DONE" Then
   SettingNo = SettingNo + 1
   SetupSphenoidLSwell()
ElseIf CBSphenSwellR.Checked = True And SphenSwellingR <> "DONE" Then
   SettingNo = SettingNo + 1
   SetupSphenoidRSwell()
ElseIf (CBSphenSwellL.Checked = True Or CBSphenSwellR.Checked = True)
   And SphenoidVertReg <> "DONE" Then
   SettingNo = SettingNo + 1
   SetupSphenoidVertReg()
ElseIf CBSphenTumour.Checked = True And SphenoidTumour <> "DONE" Then
   SettingNo = SettingNo + 1
   SetupSphenoidTumour()
ElseIf CBEthmoidTumour.Checked = True And EthmoidTumour <> "DONE" Then
   SettingNo = SettingNo + 1
   SetupEthmoidTumour()
Else
   SetupSummaryPage()
End If
```

Figure 184: Code to determine settings page to display to user when using "Next" button

If, as stated above, the code finds the next page to be displayed and enters that section of the *If* statement, the following actions are performed. Firstly, a counter is updated to display the step of the wizard currently being addressed. `SettingNo` starts at a value of zero, so if swelling is to be applied in the frontal sinus, `SettingNo` will be incremented to 1. This is then displayed to the user with `SettingsTotal`, which was set when the user's first list of settings were selected. The values are displayed in the format "Step `SettingNo`/`SettingsTotal`". In this example, step 4 of 8 is being performed. Each time a page setup subroutine is run, the value of `SettingNo` is increased by one and the new value displayed on the Case Creator window as shown in Figure 185:

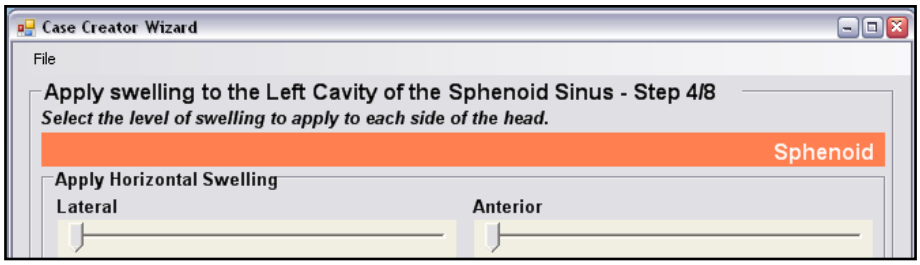

Figure 185: SettingNo and SettingTotal display the step being performed

In the first navigation method, the titles, information displayed and images on each page were set at the point when the user clicked "Next" or "Previous" to move through the steps of the wizard. This method worked as the order of pages was constant; with this new method, the setup of each page had to be run as a separate subroutine, to be called upon at any point in the progress of the wizard. These subroutines are also used to set the appearance and data on pages when moving backwards through the wizard with the "Previous" button, as explained later. After updating the value of `SettingNo`, the relevant page setup subroutine is run.

Within each setup subroutine, the information displayed on the page is either reset, or set to the saved values for that setting. This depends again on the contents of the setting progress variable: if the value is blank, the user has not yet addressed this stage of the wizard and all on-screen information and controls must be reset to clear the settings from the last time the page was used. If the value is `"STARTED"` then the user is revisiting this stage of the wizard and the saved settings are re-applied to the controls and data displays.

A similar approach is taken to finding the next page to display to the user if they navigate backwards through the wizard using the "Previous" button. Again, only those stages that were initially selected will be shown, but the order is unknown; the code designed to solve this problem, the `GoToPreviousPage` subroutine is shown in Figure 186.

```
If CBEthmoidTumour.Checked = True And EthmoidTumour = "DONE" Then
   SettingNo = SettingNo - 1
   SetupEthmoidTumour()
   EthmoidTumour = "STARTED"
ElseIf CBSphenTumour.Checked = True And SphenoidTumour = "DONE" Then
   SettingNo = SettingNo - 1
   SetupSphenoidTumour()
   SphenoidTumour = "STARTED"
ElseIf (CBSphenSwellL.Checked = True Or CBSphenSwellR.Checked = True)
   And SphenoidVertReg = "DONE" Then
   SettingNo = SettingNo - 1
   SetupSphenoidVertReg()
   SphenoidVertReg = "STARTED"
ElseIf CBSphenSwellR.Checked = True And SphenSwellingR = "DONE" Then
   SettingNo = SettingNo - 1
   SetupSphenoidRSwell()
   SphenoidSwellingRight = "STARTED"
ElseIf CBSphenSwellL.Checked = True And SphenSwellingL = "DONE" Then
   SettingNo = SettingNo - 1
   SetupSphenoidLSwell()
   SphenoidSwellingLeft = "STARTED"
ElseIf CBFrontalTumour.Checked = True And FrontalTumour = "DONE" Then
   SettingNo = SettingNo - 1
   SetupFrontalTumour()
   FrontalTumour = "STARTED"
ElseIf CBFrontalSwell.Checked = True And FrontalVertReg = "DONE" Then
   SettingNo = SettingNo - 1
   SetupFrontalVertReg()
   FrontalVertReg = "STARTED"
ElseIf CBFrontalSwell.Checked = True And FrontalSwelling = "DONE" Then
   SettingNo = SettingNo - 1
   SetupFrontalSwell()
   FrontalSwelling = "STARTED"
Else
   SettingNo = 0
   GroupBoxSwelling.Visible = False
   GroupBoxVertReg.Visible = False
   GroupBoxTum.Visible = False
   GroupBoxSummary.Visible = False
   GroupBoxSettingSelect.Visible = True
   Me.Size = New System.Drawing.Size(668, 525)
End If
```

Figure 186: Code to determine settings page to display to user when using "Previous" button

The code in Figure 183 is run prior to this, in order to save the settings made on the page the user has navigated away from. To move back through the wizard, the code checks whether the last setting in the list is required, and whether it has been completed. If both conditions are satisfied, the code reduces the value of `SettingNo` to match the setting being applied and runs the page setup subroutine. Importantly, the

content stored in the progress variable is updated to read "STARTED" so that the setup subroutine will show the previously applied settings. The final part of GoToPreviousPage runs if the user has reached the beginning of their selected list of settings; the settings selection page is therefore shown, at which point the user's selection may be changed. If they alter their choice, new and old settings will be shown together in the correct order and previously applied settings will still be visible, thanks to the programming style used in GoToNextPage and GoToPreviousPage. Of course, the user must be permitted to add further settings to the case after some have been applied. The user is offered this opportunity at the end of the wizard, which was described in Section 10.4.4.

Figure 187 shows the user's progression through the program using the new concurrent navigation system.

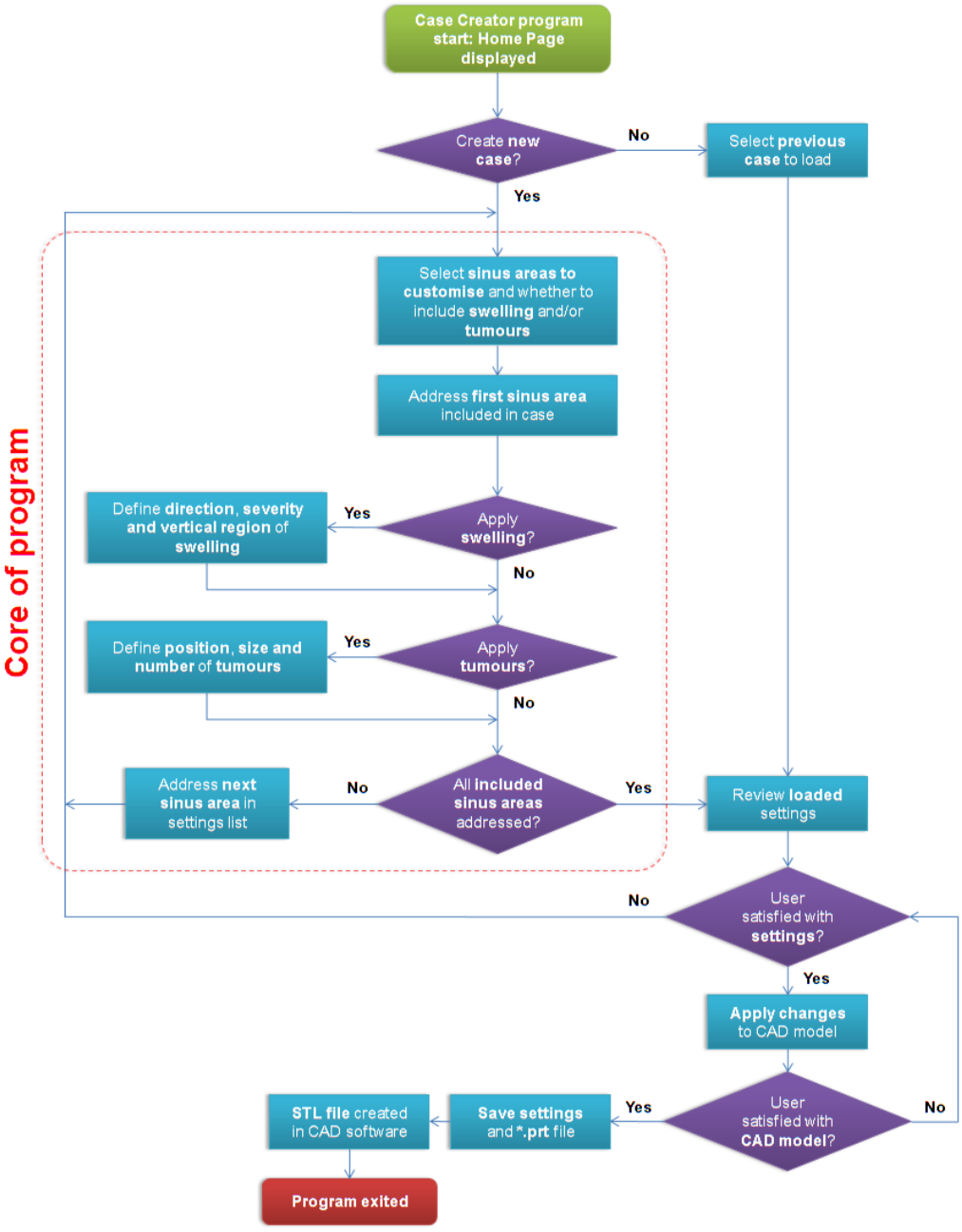

Figure 187: User progression through Case Creator program

The area of the flow chart marked “core of program” is the part of the program which uses the core navigational coding structure of the concurrent system described in this chapter. In the core of the program, the user is guided through the settings they have chosen to apply to the model in each area of the sinuses, in the order they appear on the initial list of available settings (shown in Section 11.2.2).

With the implementation of the new navigation method, some changes were required to the appearance of stages of the wizard and the way in which the final case settings are applied to the CAD model. As the user is now guided through settings application for all areas of the sinus concurrently, the application process had to be altered to accommodate the simultaneous alteration of the CAD model. Previously, the values used to apply the user's settings were taken directly from the controls on the wizard. In the new navigation system each stage of the wizard may be visited a number of times to apply settings to different areas of the sinuses, making this method impossible to use. Instead, the saved values from each sinus area are used to supply the settings application subroutines with the required information prior to their use. This means that the settings for all sinus areas may be applied one after another, and also makes the application of saved and loaded cases a possibility. The new appearance and behaviour of the altered stages of the wizard is described in Section 11.2.

11.2 Stages of Redeveloped Case Creator Wizard

11.2.1 Program Information Page

After viewing the home page for the first time, the user is given some information and instructions about the program and its use. This page of the wizard explains the purpose of the program to the user, and the process they are about to go through. The explanation and information provided are shown in Figure 188:

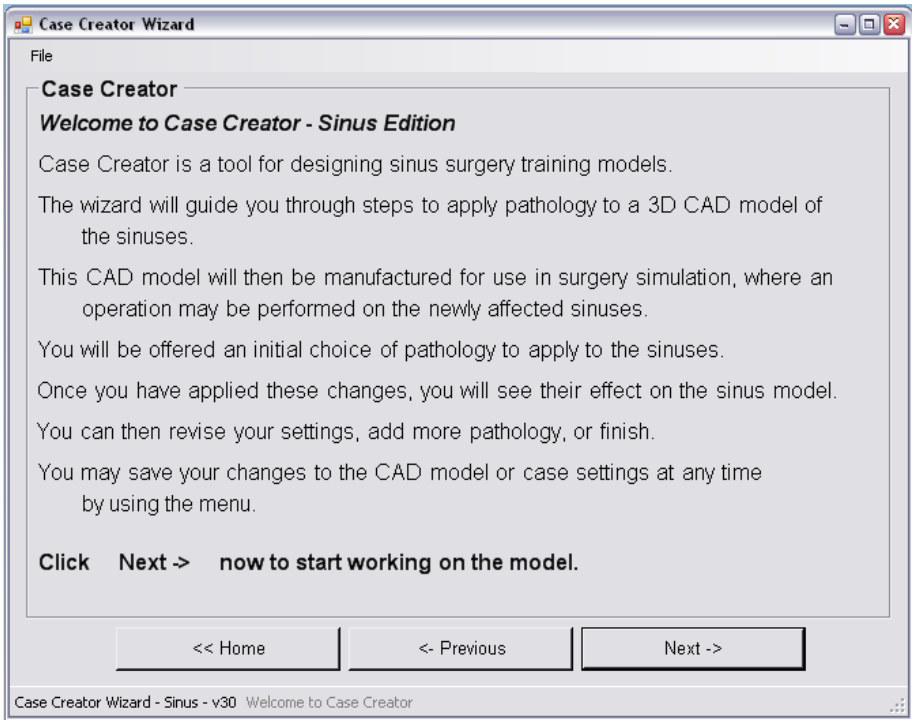

Figure 188: Program information page of Case Creator wizard

After this stage, the user moves into the part of the wizard in which they define the settings that will be applied to the CAD model.

11.2.2 Settings Selection Page

This page replaced the sinus area selection page used in the cyclical navigation system after consultations with Case Creator test users and feedback from surveys. The method described in this section, involving a menu of available settings, was therefore offered as a solution to the problem.

The implementation of the settings menu meant that the user need not navigate through the wizard multiple times to create a full case, once for each area of the sinus to be affected. The new method was developed with the aim of increasing the ease of use and reducing the time taken to produce a finished model, by applying the settings concurrently. The settings offered to the user in a list of checkboxes (Figure 189) are as follows:

- Frontal swelling
- Frontal tumours

- Sphenoid swelling – left
- Sphenoid swelling – right
- Sphenoid tumours
- Ethmoid tumours
- Maxillary tumours (disabled until medical imaging data is made available)

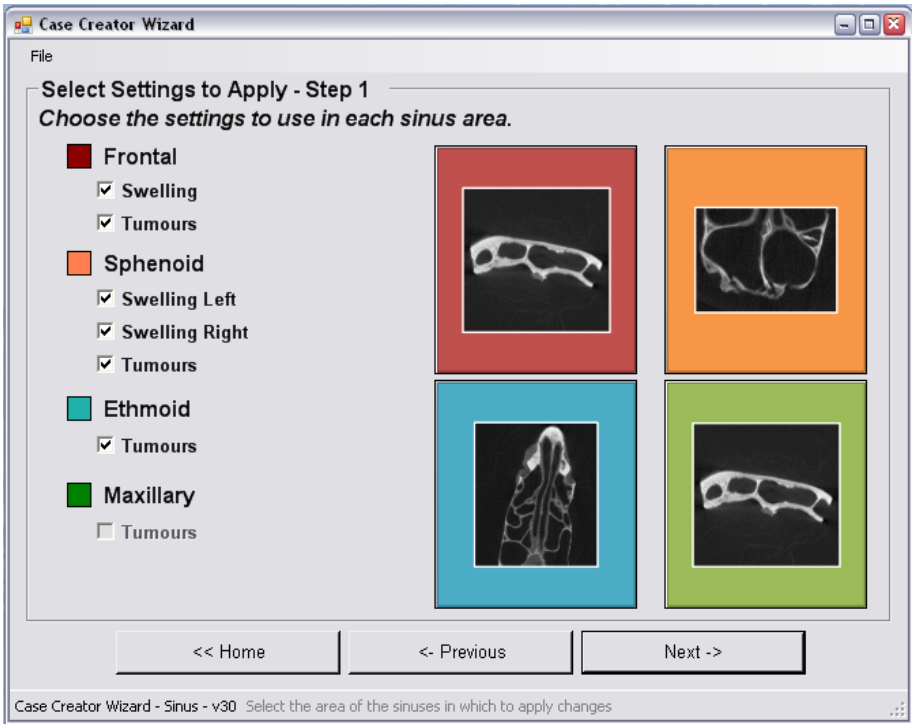

Figure 189: Settings selection page of Case Creator wizard

The selections made from this list determine the stages that will be displayed to the user throughout the rest of the wizard. The total number of settings to be applied is calculated at this stage and stored in the variable `SettingsTotal`, using the code shown in Figure 190. This number is then used to give the user information about their progress through the wizard.

```
SettingsTotal = 0
If CheckBoxFrontalSwell.Checked = True Then
   SettingsTotal = 2
End If
If CheckBoxFrontalTumour.Checked = True Then
   SettingsTotal = SettingsTotal + 1
End If
If CheckBoxSphenoidSwellLeft.Checked = True And
   CheckBoxSphenoidSwellRight.Checked = True Then
   SettingsTotal = SettingsTotal + 3
ElseIf CheckBoxSphenoidSwellLeft.Checked = True Or
   CheckBoxSphenoidSwellRight.Checked = True Then
   SettingsTotal = SettingsTotal + 2
End If
If CheckBoxSphenoidTumour.Checked = True Then
   SettingsTotal = SettingsTotal + 1
End If
If CheckBoxEthmoidTumour.Checked = True Then
   SettingsTotal = SettingsTotal + 1
End If
```

Figure 190: Updating value of SettingsTotal to display at each step of wizard

In this section of code, run as the "Next" button is clicked to move onto the first page of settings definition, firstly returns `SettingsTotal` to zero to ensure that the new total is correct and unaffected by any previous selections that the user may be revising. The code then checks whether each setting has been selected; if so, the total is increased by the appropriate amount, until the final value is found. In some cases, the value is increased by two or three, to account for the vertical region selection stages of the wizard. This total is used with `SettingNo` to display the step of the wizard being addressed at each stage.

If no settings have been selected, the user is shown the error message in Figure 191:

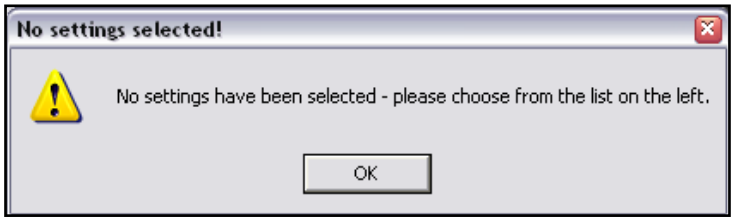

Figure 191: Error message shown when no settings are selected

Otherwise, the user moves on to define the settings for the selections made on the list, as described in the following sections.

11.2.3 Swelling Application Page

With the new navigation system, there is no need for the checkbox system on each of the swelling pages, as the user has already made their selection at the start of the wizard process. Due to the nature of the new navigation system, it is essential that the user is completely clear about which sinus area they are working on at all times. In this, the vertical region definition and tumour application stages of the wizard, the sinus area being addressed is clarified through the continued use of the colour code established on the previous page. The name of the sinus area is also displayed to avoid confusion, should the same page be used in succession for different areas, as shown in Figure 192:

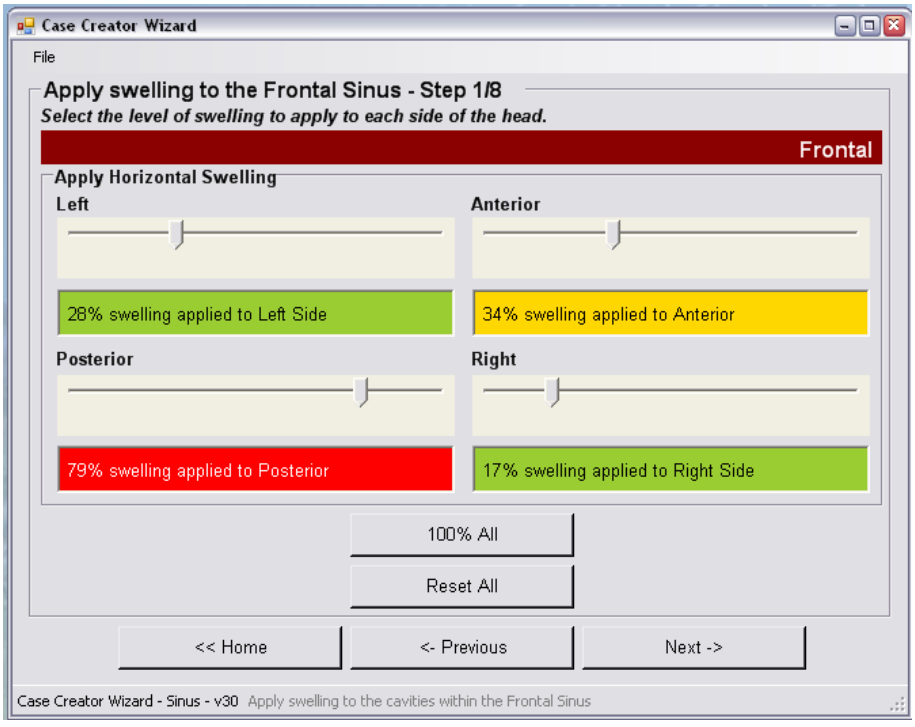

Figure 192: Final version of swelling application page of Case Creator wizard

After consultations with users of the program and feedback from the program surveys, the terminology used to describe the directions in which swelling is to be applied in the sphenoid sinus cavities was altered. Instead of using the words “left” and “right” to describe swelling from the sides of the two cavities, their position within the head

was used as a reference. The terms “medial” (towards the centre of the head) and “lateral” (towards the outside) were used, as shown for the left cavity of the sphenoid sinus in Figure 193. The two terms are reversed for the right cavity of the sphenoid sinus.

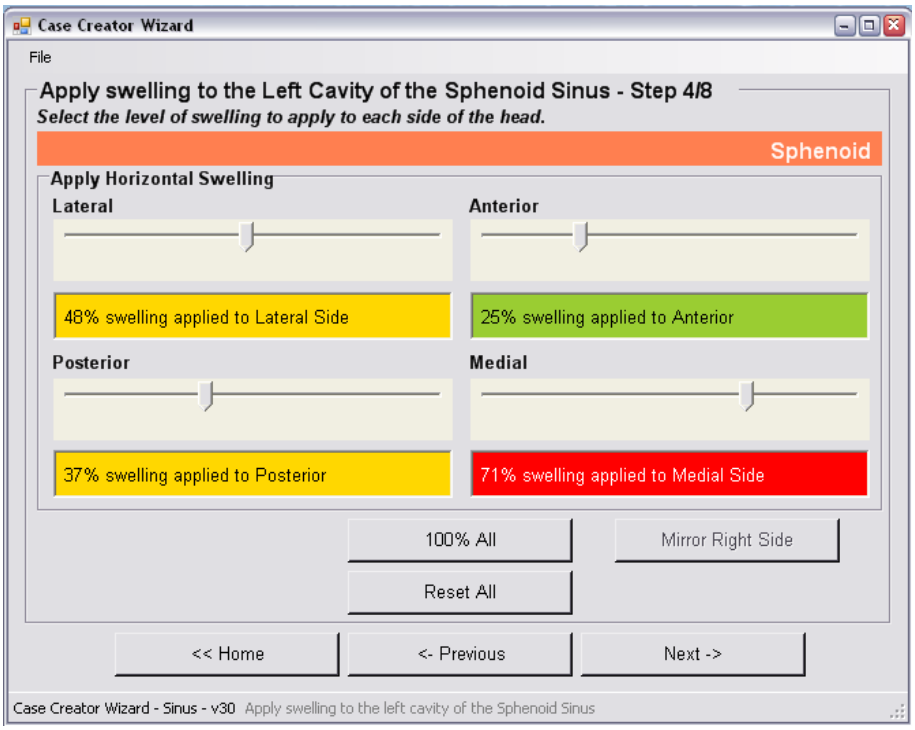

Figure 193: Labelling of swelling directions for left sphenoid cavity

As can be seen in Figure 193, a new functionality was added through feedback from users and the program usability survey. Users indicated that it would be useful to have the option to mirror the swelling applied to the opposite side of the sphenoid sinus, and as a result the button marked “Mirror Right/Left Side” was added to the window. When this button is clicked, the settings from the other side of the sinus are automatically applied to the sliding scales. The button is disabled in Figure 193 as swelling is yet to be applied to the right side of the sphenoid sinus.

Information displayed on the summary page at the end of the wizard is also updated at this stage, to show the amount of swelling applied, if any, in each of the four horizontal directions.

11.2.4 Vertical Region Selection Page

This stage of the wizard is only displayed should the user select to apply horizontal swelling to the frontal or sphenoid sinus. As with the horizontal swelling application page, suggestions from clinicians were taken into account and more technical terminology was used to label the controls within the program window. The term "cranial" was used to label the top of the region, while "caudal" was used to signify the bottom. The layman's terms were retained, to avoid any confusion for non-medically trained users of the program. Figure 194 shows the stage at which the user selects the vertical region of the frontal sinus to which anatomical changes will be applied.

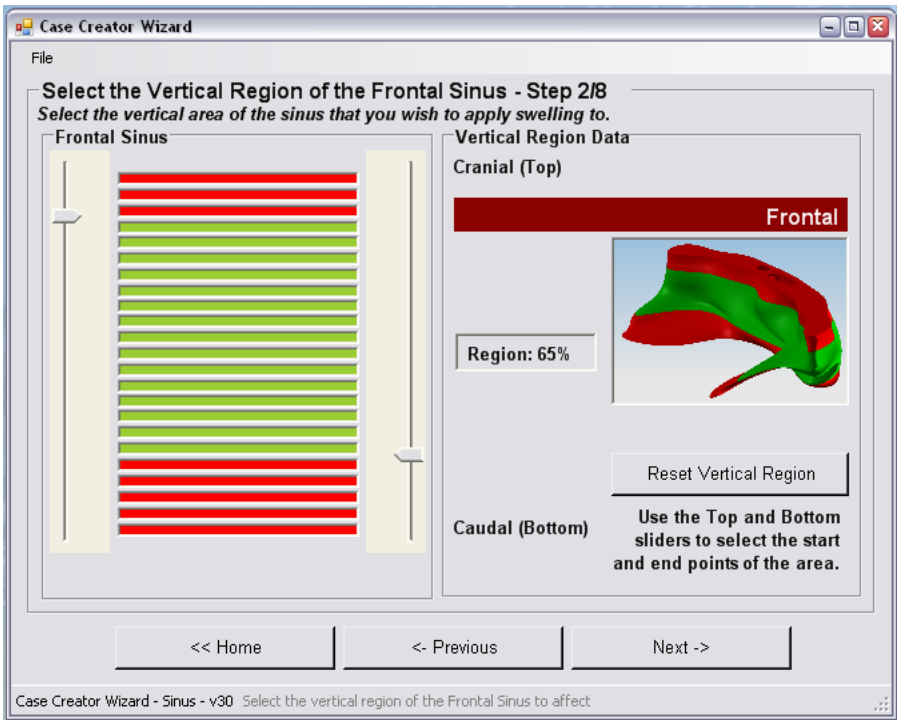

Figure 194: Selection of vertical region of swelling in frontal sinus

Figure 195 shows the vertical region definition window for the sphenoid sinus, where the user may individually control the left and right cavities of the sinus:

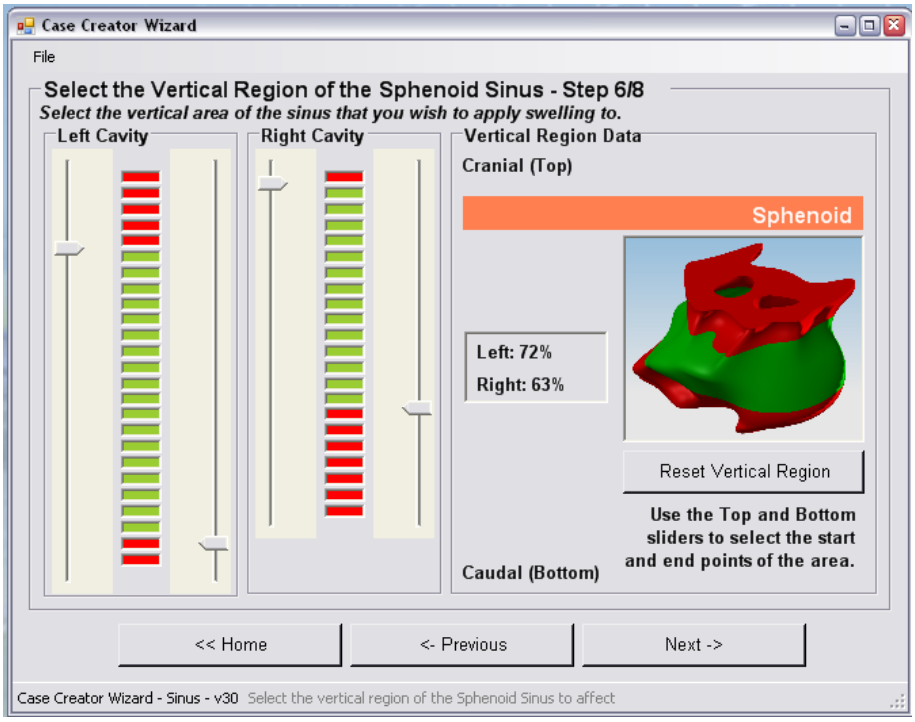

Figure 195: Selection of vertical region of swelling in sphenoid sinus

11.2.5 Tumour Application

Two tumour sizing methods were developed before a final concept was implemented into the program for testing in trial B.

11.2.5.1 Tumour Sizing - Multi-directional Sliding Scale Method

From receiving feedback on the program through questionnaires and suggestions from the users, more freedom was required in the shaping of tumours, to achieve a realistic result. Users commented that in real cases, tumours would not be uniformly shaped, as they must be by using the square sizing method. Users also requested the ability to spread a single tumour manually throughout the anatomy to cover a user-defined area. While the potential of the program to fulfil these requests is limited by the capabilities of VB, they may be provided to some extent. The first redevelopment of the tumour sizing system was based upon a progression of the previous method.

Instead of using a single sliding scale to alter the size of the tumours in all directions simultaneously, three sliding scales were provided for each tumour, to allow the user to alter the three dimensions of the tumour individually. The previous method was

converted to the use of three sliders by linking the width and height of both tumour icons to the values selected on the x, y and z-dimension sliders for that tumour.

However, to replace each of the previous sliders with three new sliders would lead to the right side of the window being crowded. The function of the group of three sliders may also be unclear, especially in the case of the vertical size sliders. It was therefore decided that the sliders would be positioned at the same location as the tumour, overlaid on the anatomical image. This decision considerably increased the complexity of this function's implementation. The sliders could not always be visible, as this would obscure the image and the other tumours, making their positioning and resizing very difficult and inaccurate. Instead, the resizing sliders were programmed to appear only when required. Otherwise, the sliders would be hidden to allow repositioning and alteration of other tumours.

This was achieved by linking the visibility of the sliders for each tumour to the position of the mouse pointer on-screen. Code was written so that when the mouse pointer entered the area bounded by the tumour icon, the slider(s) for that icon would appear, ready for use. The sliders were made invisible once the mouse pointer left the slider, anatomical image or tumour icon area. When repositioning the tumour icons the relevant, invisible sliders match the new position, before next becoming visible to the user. Figure 196 shows the x- and z-dimension sizing sliders appearing for the back view of tumour 1 in the frontal sinus, when the mouse pointer is held over the tumour icon.

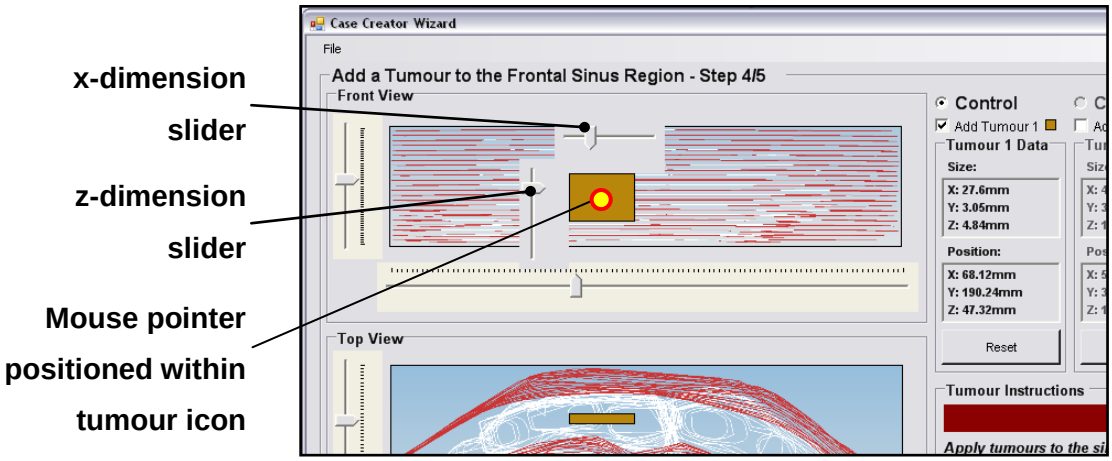

Figure 196: Tumour size sliding scales appearing on demand

Even with the new slider visibility settings, the window became crowded and the image of the sinus anatomy was not clearly visible during resizing. The appearance and disappearance of the sliders was unintuitive at times, and because of the maximum tumour size required, the size and value shown on the sliders appeared unrelated to the size of the tumour icon they controlled.

It became clear, as a result of this attempted development, that if the user was to be provided with the ability to resize tumours in three dimensions individually, a more well-established, recognisable and easy-to-use method should be used.

11.2.5.2 Tumour Sizing - Resize Handles Method

One of the most widely used and easily recognised methods for resizing objects on-screen is a set of resizing handles. Novice computer users are regularly exposed to this method as it is used extensively in word processing and the production of graphics at all levels of complexity. To resize an object, the user first selects the object to resize, which prompts ‘handles’ – small blocks around the perimeter of the object – to become visible. There are often eight handles visible to the user, positioned at the corners and mid-points of the lines of the bounding box, as shown in Figure 197:

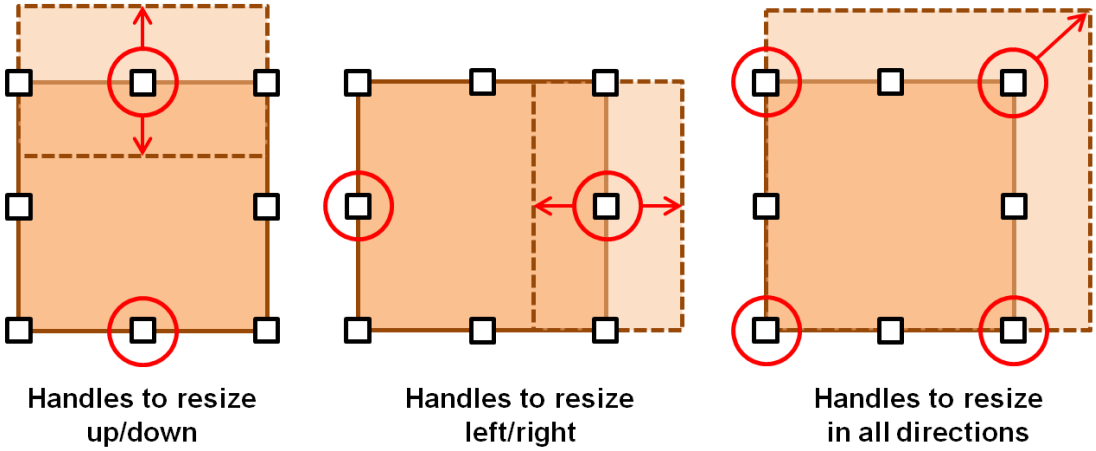

Figure 197: Functions and positions of resize handles

Figure 197 shows that there are three functions performed by the group of eight resize handles: resizing horizontally, vertically and in all directions simultaneously. This function is suitable for incorporation into the current system as the tumour icons in VB are limited to a rectangular shape. The code for the first two of these functions was written from scratch and implemented into the Case Creator program; the third was omitted but may be added as a future development for reasons to be discussed later in this section.

Four resize handles would therefore be shown to the user, in order to resize the tumour horizontally and vertically. For the resizing of the tumour icons, the same four white blocks are used repeatedly as the resizing handles. Each time the selected tumour changes, the resize handles move to the appropriate locations on-screen, at the mid-points of the four sides of the icon, as shown in Figure 198.

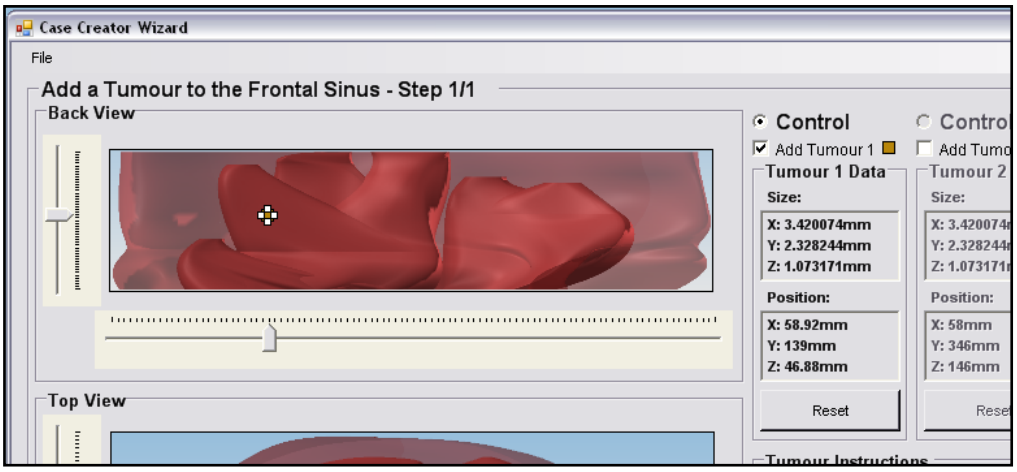

Figure 198: Resizing handles move to match position of tumour icon

It can be seen in Figure 198 that with the smallest tumour size, the four resize handles are positioned in very close proximity to one another. It is for this reason that the decision was made to omit the diagonal resizing handles on the icon corners, as the tumour icon would be almost completely obscured at this size, and the selection of the required sizing handle could be made difficult. To overcome this problem, the handle size could be reduced, or the minimum size of the tumour icon increased. At this stage, it was decided that greater freedom for the user would be provided, as the same results may still be achieved with the four resizing handles provided. Indeed, in word processing applications, when the object to be resized reaches a small enough size, some of the handles are hidden from the user to enable clearer vision of the object in question. This function may be implemented at a later date (see Section 13.4).

Once the change to the location of the resizing handles to match the position of the newly selected tumour icon had been successfully programmed into the code, the function of the handles was tackled. The handles work by the user clicking the mouse button and then dragging the mouse pointer, with the button held down, to the required location of that side of the tumour icon. When the mouse button is released, the newly resized tumour icon is displayed, and the resizing handles change position to match the new tumour icon size. This process is divided into two events for the purpose of programming, as illustrated in Figure 199:

Event 1: User clicks mouse button within resize handle area

Event 2: User releases mouse button (must be after previous event occurred)

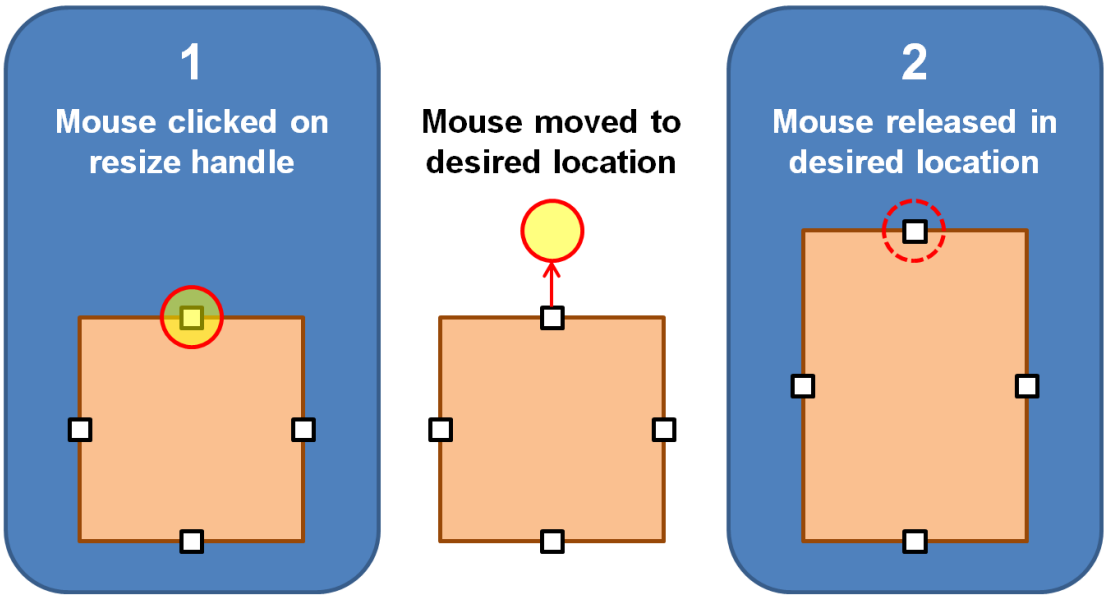

Figure 199: Resizing tumour icon using handles - events for programming

The code run when the mouse is clicked over the top resizing handle is shown in Figure 200:

```
OldSize = MousePosition.Y
```

Figure 200: Mouse y-co-ordinate stored when top resizing handle is clicked

This is the only line of code needed when the `MouseDown` (mouse button clicked) event occurs over the handle (Figure 199 Event 1). This line updates the `OldSize` variable to store the y-co-ordinate of the mouse pointer within the screen when the button is clicked, to be used in calculations when the button is released.

When the mouse button is released (Figure 199 Event 2), the new y-co-ordinates of the mouse pointer are stored in the `NewSize` variable. The previous and current mouse positions are then compared to find the amount of size change applied by the user. Next, the code checks which tumour is being adjusted by the user by determining the status of the tumour selection radio buttons (to be described in Section 9.4).

Having identified the tumour being adjusted, the program then alters the height of the tumour icon, as the vertical size is being altered. The difference between the old and new mouse pointer y-co-ordinates is added to the current height of the icon to create the resized panel (tumour icon).

Each handle performs in a different manner when used, but those positioned on the top and left sides of the icon must alter the position of the tumour in addition to the size, due to the top-left positioning system employed in VB. When either the top or left handle is in use, the location of the top left corner of the icon must change on resizing. If this were not done, the size would only appear to be altered downwards, as the icon would remain in the same position, as shown in Figure 201:

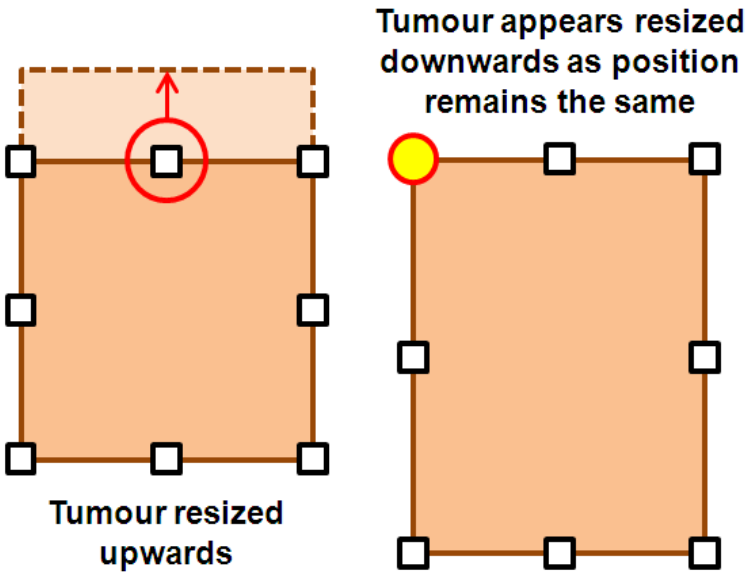

Figure 201: Resizing tumour icon - repositioning required

In this case, the new location of the icon is set at the previous x-co-ordinate, paired with a new y-co-ordinate. The y-co-ordinate is calculated by subtracting the difference between the new and old mouse locations. This achieves immediate movement of the icon to its new position, creating the effect of resizing the icon upwards from its previous location, as shown in Figure 202:

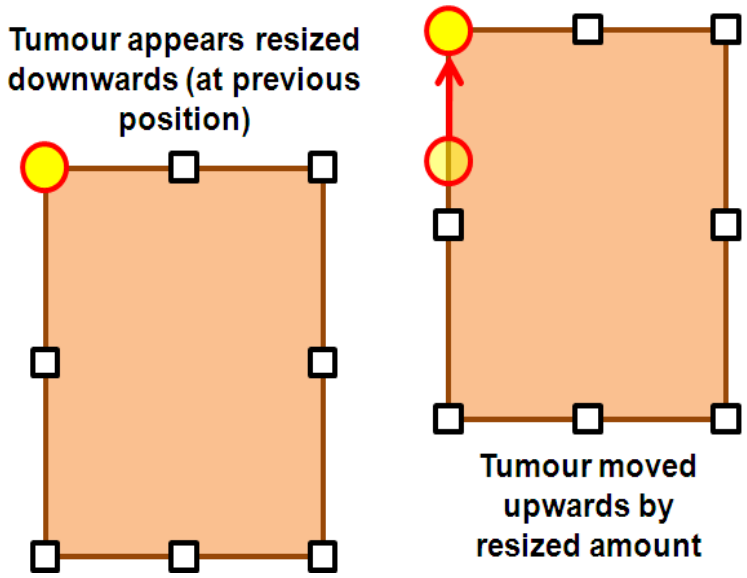

Figure 202: Resized tumour icon is repositioned upwards

Now, to feed the required information into `TumourPosition`, the tumour repositioning subroutine, the slider value is updated. The subroutine will save the location for use when the tumour selection is altered or the settings are saved, calculate the position of the tumour body in the CAD model and update all displayed information about the tumour location. The correct slider value is also therefore shown to the user, to allow immediate repositioning of the resized tumour. The position of the vertical centre of the tumour icon within the groupbox is found by adding half of the panel height to the panel location. The slider value is then calculated by converting this position from pixels to trackbar points. The position of the tumours, resize handles and trackbar values are shown in Figure 203:

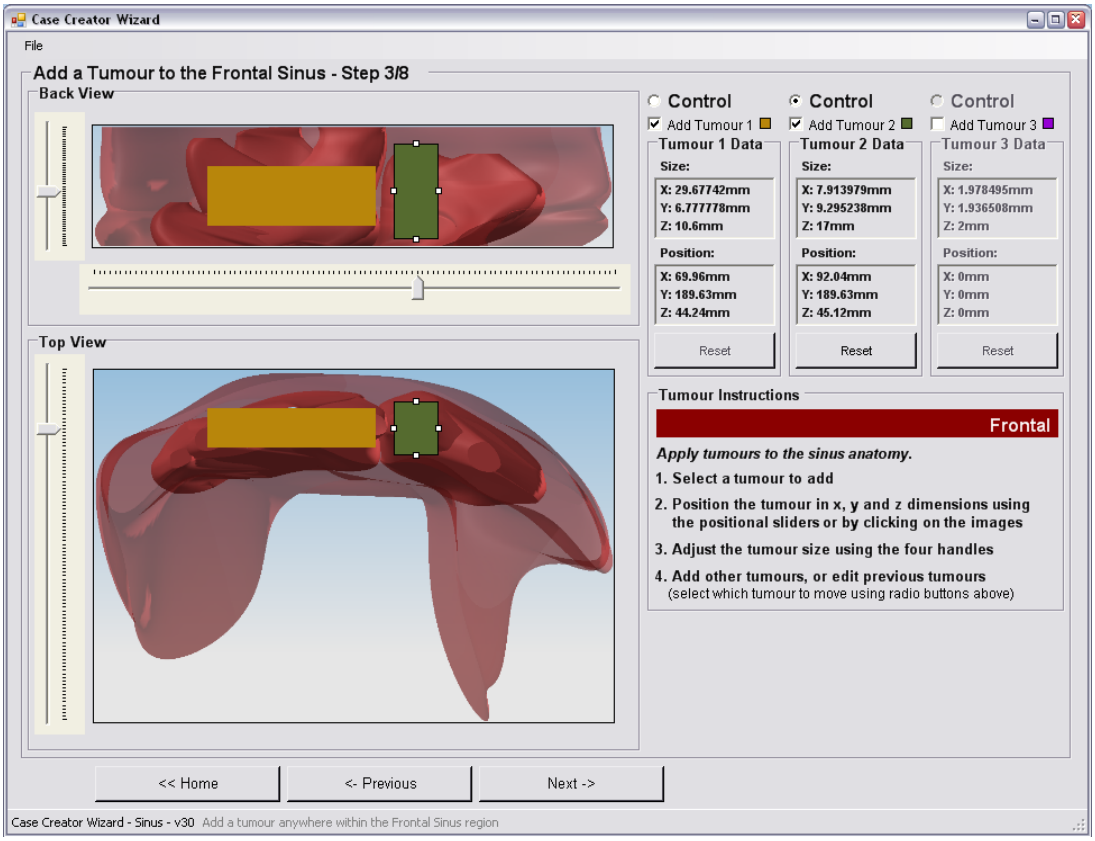

Figure 203: Tumour application stage in frontal sinus

A second subroutine, `TumourResize` is used to perform all tasks related to the size of the tumour icon and body in NX. The subroutine updates the required sizes of the tumour bodies in NX by converting the tumour icon sizes into millimetres. The feedback to the user is then updated with this information, and the size of the tumour icon is stored in sinus area-specific variables for use when loading cases or moving back through the wizard to review previously applied settings.

A similar process is used to resize the tumours using the left handle, which must also reposition the icon. The handles on the bottom and right sides of the icon do not reposition the tumour, but must nevertheless update the slider value. To ensure that the function of the resizing handles is known to the user, prompts are given at the tumour addition stage of the wizard, and the cursor changes to a recognisable resizing arrow when the mouse pointer is positioned over the resize handle.

This development to the resizing of tumours is considered to be the best method available. The handles are easy and intuitive to use, and the method and results perform as expected. Some users, when trialling the program, attempted to resize the tumours in this way even though the functionality was not yet in place, showing that this method was expected to be used.

This alteration to the program means that customisability level 5+ has been achieved (referring to Table 8), as the sizing and positioning of the tumours may now be performed without limits using the resizing handles and mouse click or sliding scale positioning systems.

11.2.5.3 Tumour Application Page

The appearance of the tumour application page in the sphenoid sinus is shown in Figure 204. The behaviour of the wizard at this stage, including the positioning, resizing and controlling of the tumours within the anatomy was explained earlier in Chapter 9. Three tumours have been positioned and resized within the sphenoid sinus in the figure below. Tumour three is currently under the control of the positioning sliders and resizing handles.

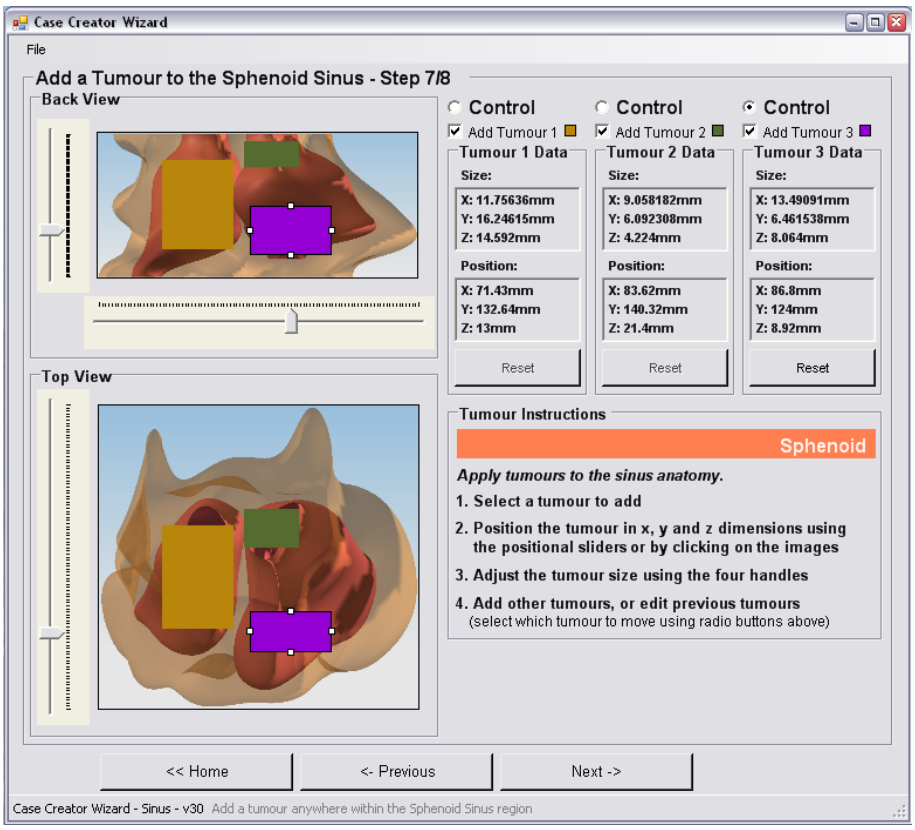

Figure 204: Tumour application stage in sphenoid sinus

After working through all the selected settings, the user is provided with a summary of the pathology to be applied to the 3D CAD model.

11.2.6 Summary Page

The new navigation system meant that a different approach needed to be taken to the display of the user's settings at the end of the process. Previously, only one sinus area was addressed at a time, leading to a simple summary page showing the settings made. Now, far more information is displayed simultaneously, requiring a clear layout and easily understandable information (Figure 205). The same window is displayed to the user if they decide to load a previous case, as described in 10.5.2. The text and percentage bars are set to match the variables set in each sinus area, depending on whether that setting was originally applied. If not, the relevant section of the summary page is greyed out, making it clear to the user which areas have been addressed to this point. In Figure 205, only two tumours were applied in the frontal sinus, leaving the data for the third tumour blank and greyed out, as with tumour 2 in the ethmoid sinus.

As the settings for horizontal swelling in the sphenoid sinus were mirrored, the two cavities can be seen to have equal swelling.

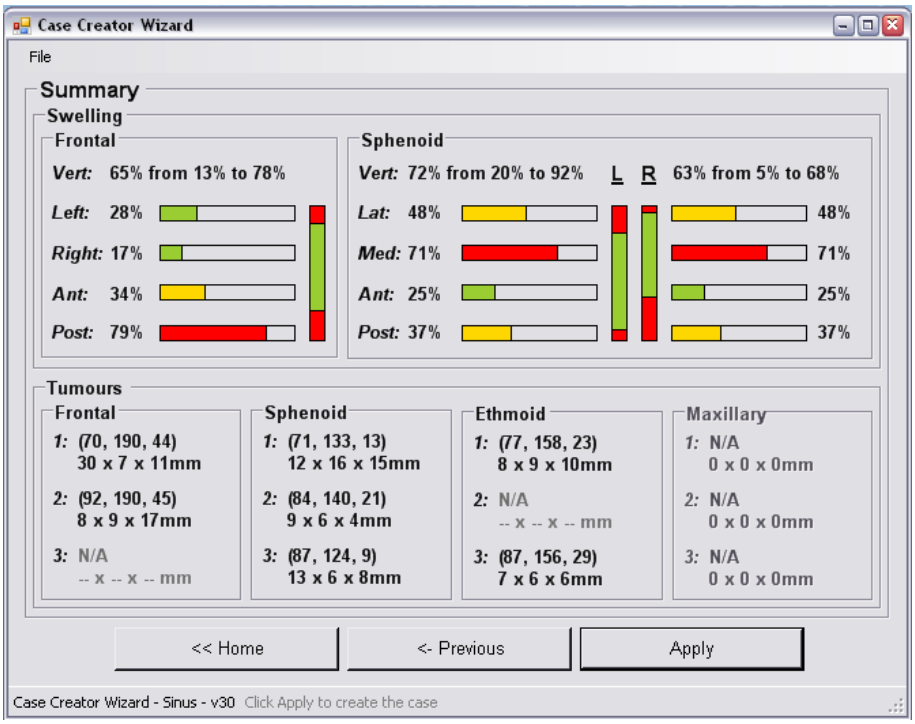

Figure 205: Settings summary page of Case Creator wizard

If the user chooses to apply these settings, the model begins to update. While the update is taking place, the user is kept informed of the progress with a window, shown in Figure 206:

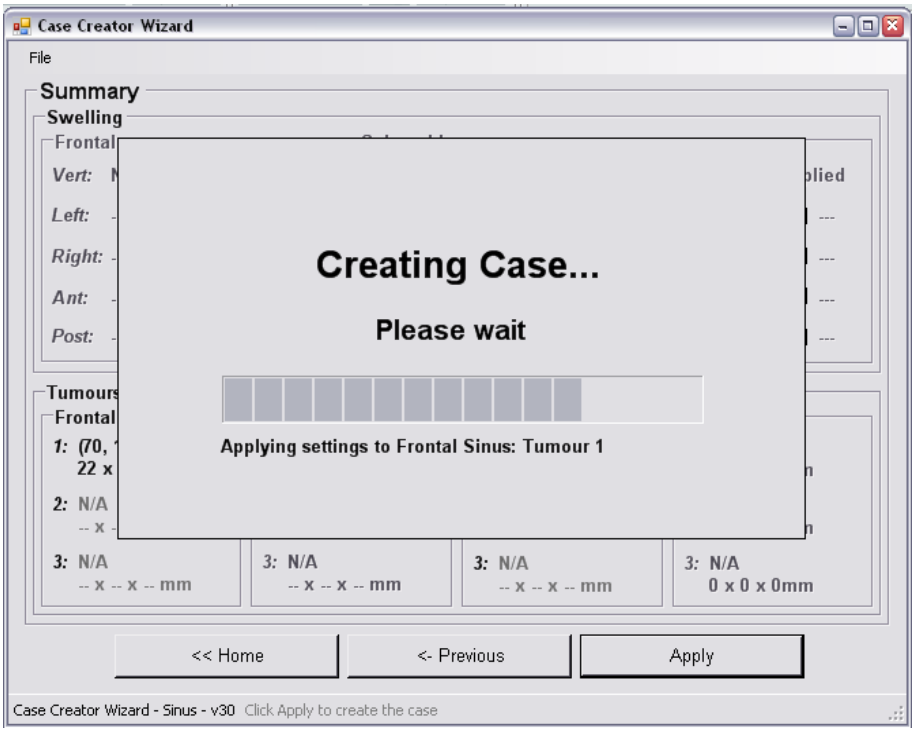

Figure 206: Progress window displayed during update of CAD model

The progress window shows the program working through each step of the application process, and which action is currently being performed.

11.2.7 End Page

In a similar way to the first design of the end page, described in Section 10.4.6, the user is presented with a range of navigation options after having applied the settings to the 3D CAD model, or they may save their settings or .prt file. If the user chooses to add further pathology to the case, they are returned to the settings selection page to restart the process.

After these alterations to the program had been made, in response to the results and suggestions from users in the first trial, the second trial was carried out.

11.3 Results from Case Creator Trial B

The aim of the second trial was to gain an impression of the success of the new program features, whilst also gaining further understanding of the way in which the original aspects of the program are perceived. Six new participants were tested, and

Anshul Sama was re-tested, to allow him to draw comparisons between the two versions of the program.

Figure 207 shows the average results for all questions answered on the Likert scale of agreement set out in Table 9:

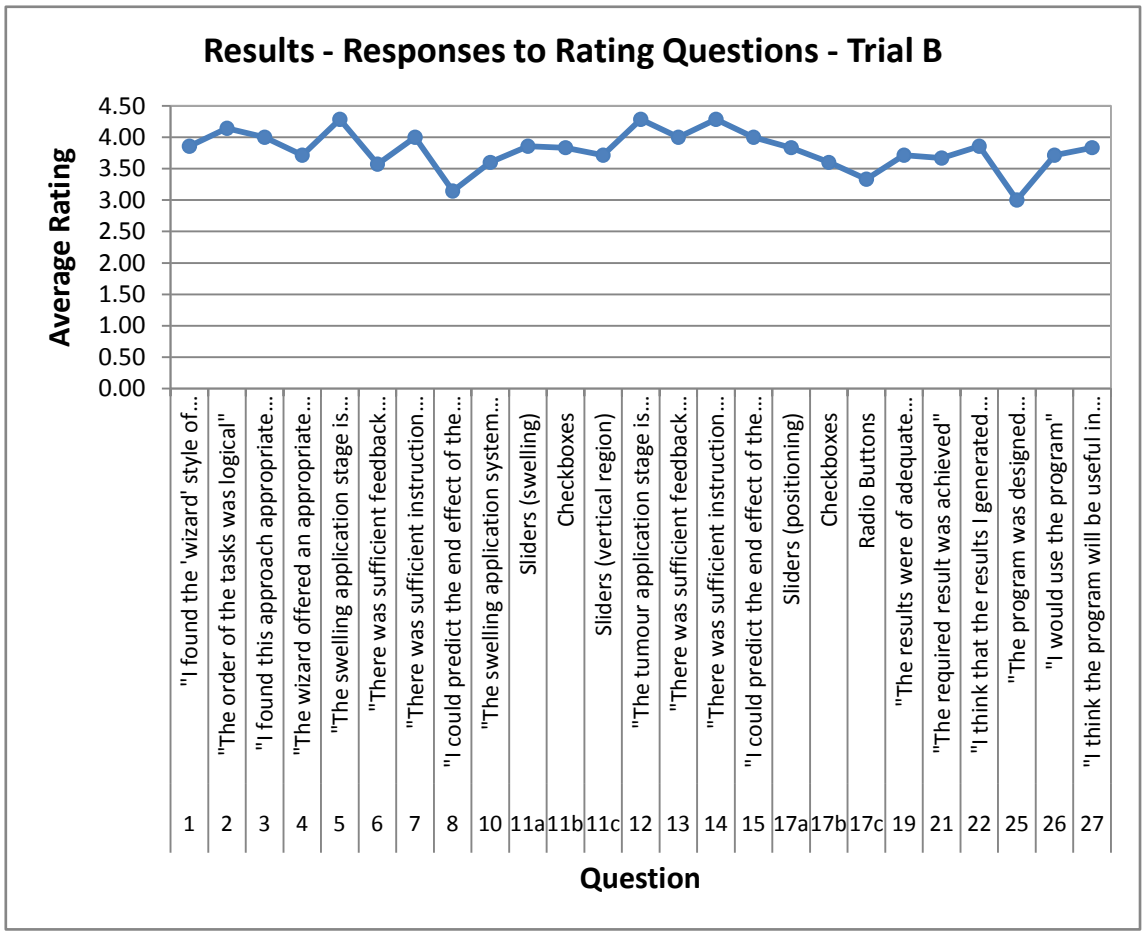

Figure 207: Average ratings for common program features – Trial B

The average ratings from trial B are more widely spread than those from the previous trial, however the average result of 3.78 was still favourable.

11.3.1 Participant Information

Table 11 shows the experience levels of the six new participants in trial B, as rated by participants themselves on the scale of 0-5 in each of the three key areas.

		Participant					
		9	10	11	12	13	14
Skill	Performing sinus surgery	1	3	4	3	3	3
	Creating training models for surgical students	0	3	3	0	0	2
	Using 3D CAD modelling software	0	1	2	0	0	2

Table 11: Experience level of participants in three relevant skill areas – Trial B

It can be seen that in this trial, only participant 9 rated themselves with an experience level of below 3 in the performance of sinus surgery. In comparison with the previous trial, this group of participants is therefore, on the whole, more experienced in this skill. As only one participant would be counted as "inexperienced" in this skill, no comparison can be realistically drawn between the ratings provided by experienced and inexperienced sinus surgeons. Conversely, this trial contains participants that rate themselves as being less experienced in the creation of training models and the use of 3D CAD modelling software. The experience levels of Trial B participants are shown in Figure 208:

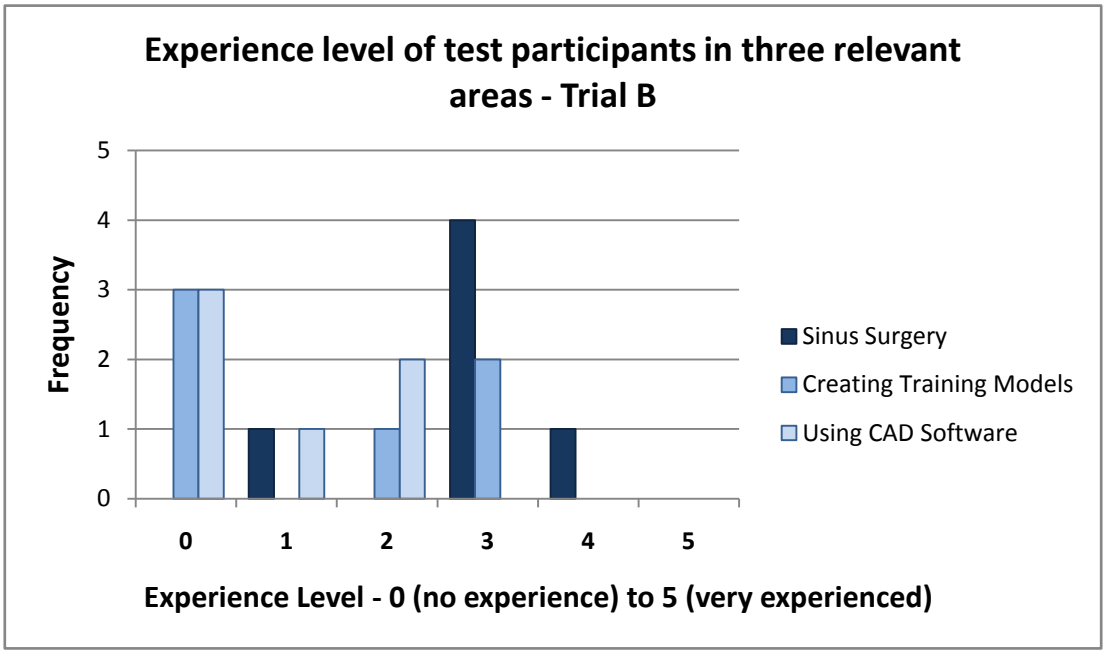

Figure 208: Ratings frequency for experience level in relevant skill areas – Trial B

Again, similarly to trial A, there is a spread of experience in each of the three skill areas; a higher concentration of moderately experienced surgeons was found in the

second trial, however on the whole participants were still found to be inexperienced in the use of 3D CAD software.

11.3.2 General Ratings

Participants rated the ease of use of the guided, step-by-step wizard approach as shown in Figure 209:

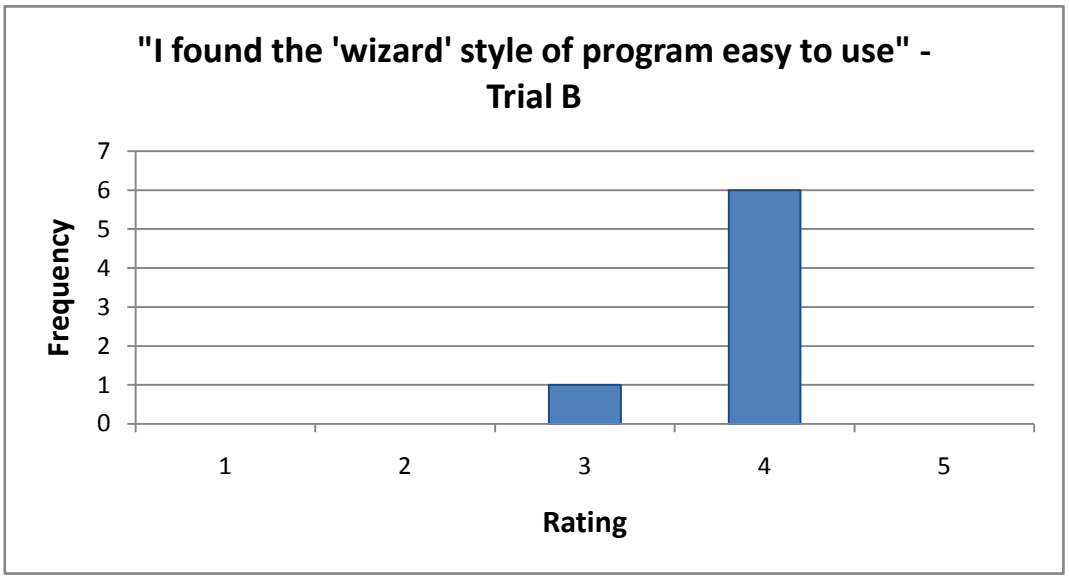

Figure 209: Ratings frequency for ease of use of 'wizard' style program – Trial B

This question was met with positive responses by the users, with an average response of 3.86, and no further comments received about the ease of use of the wizard style of program.

The order of the tasks was then assessed, with the results obtained as shown in Figure 210:

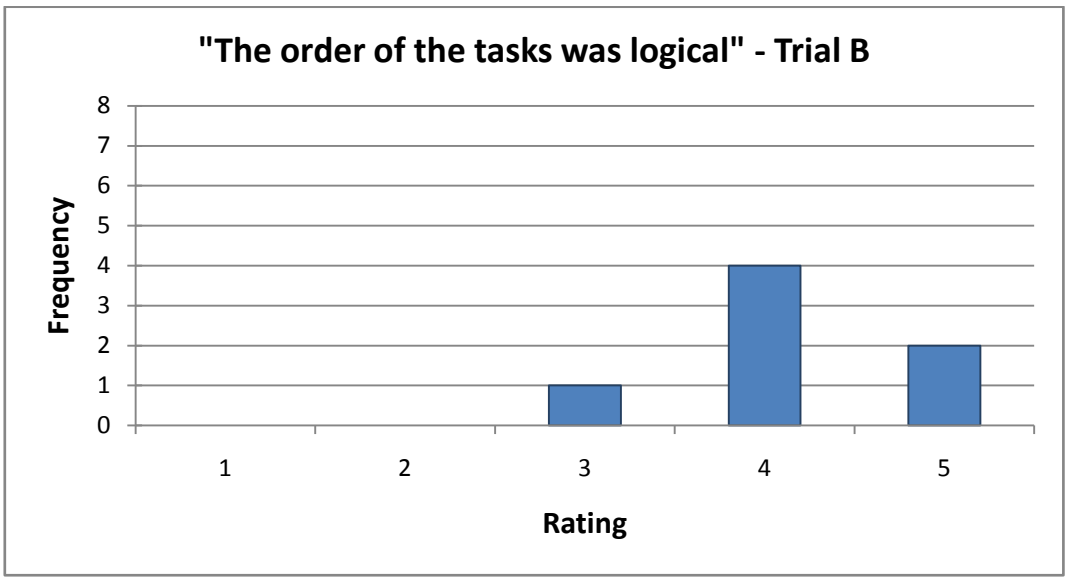

Figure 210: Ratings frequency for task order – Trial B

Again, the results were favourable, mirroring users' positive opinion of the order of tasks. The average rating given in response to this statement was 4.14; the order of tasks will therefore be retained for future versions of the program.

When asked to rate the number of functionalities available, the users in the second trial responded as shown in Figure 211:

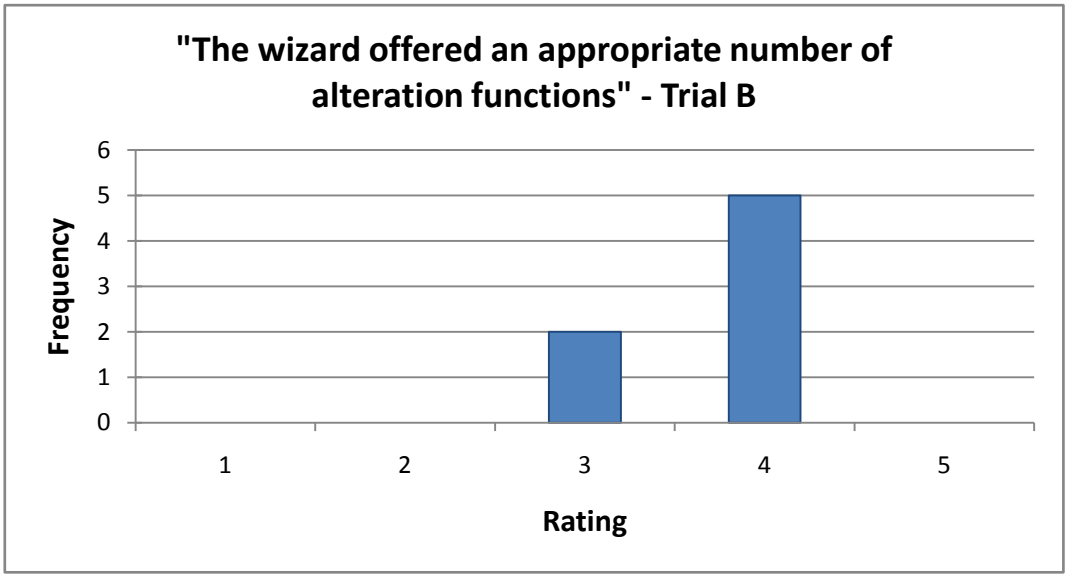

Figure 211: Ratings frequency for number of functions supplied – Trial B

Again, the program performed well in this question, with an average rating of 3.71. A suggestion was received to simulate swelling in the maxillary and ethmoid sinus areas, which is included in the suggestions for further work in Section 13.2.

The results from users' ratings of the feedback provided throughout the wizard are shown in Figure 212:

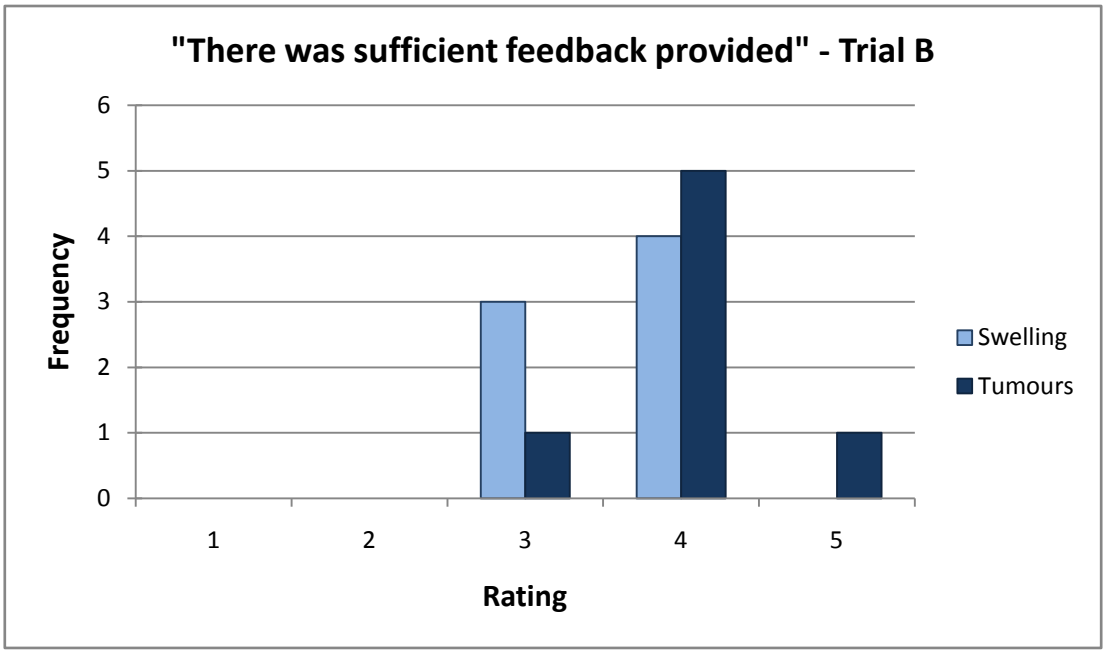

Figure 212: Ratings frequency for feedback given during settings application – Trial B

Some commented that the inclusion of a model updating with their settings in real time would be beneficial. The possibility of this function is discussed in Section 13.2. Users responded positively to the feedback given at the tumour application stages of the wizard. Figure 213 shows a summary of the ratings given by the participants for the instructions provided:

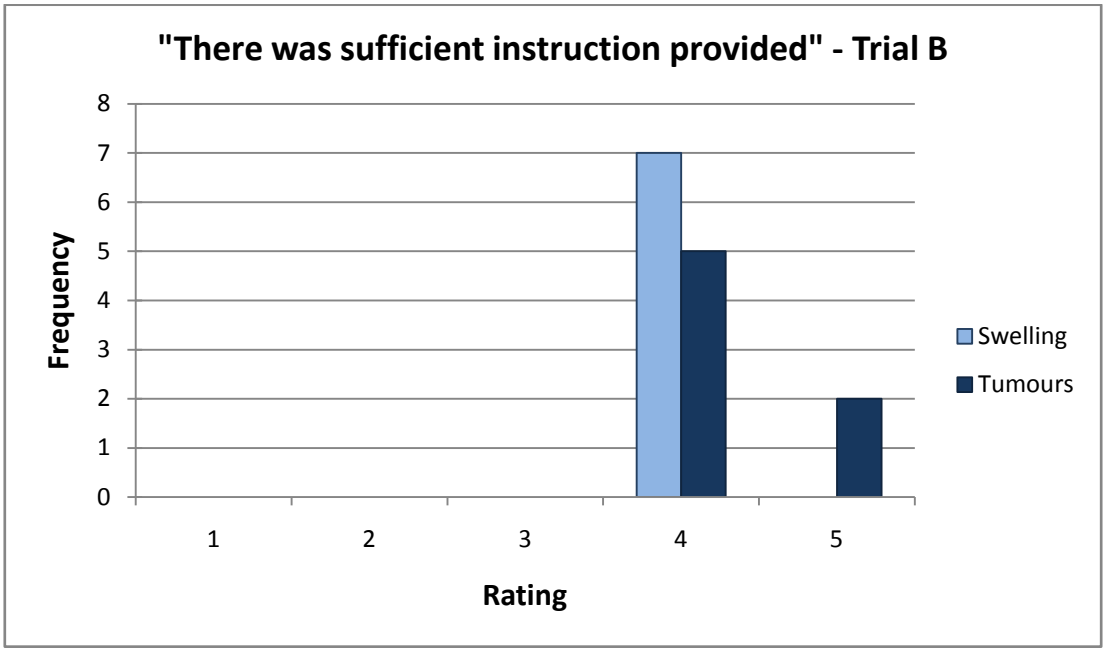

Figure 213: Ratings frequency for instruction given during settings application – Trial B

It can be concluded that the new instruction stage of the wizard has had the desired effect, and that users now agree that there is sufficient instruction provided throughout the wizard in both the swelling and tumour application stages.

11.3.3 Navigation System

In trial B, the concurrent navigation system was tested, where the pathology to be applied is selected at the start of the process, as opposed to cycling through the process for each sinus area. This system was developed at the suggestion of Anshul Sama after the first trial, and aimed to reduce the amount of time taken to apply case settings, while allowing the user to treat different areas of the sins complex simultaneously. The appropriateness of this approach was rated as shown in Figure 214:

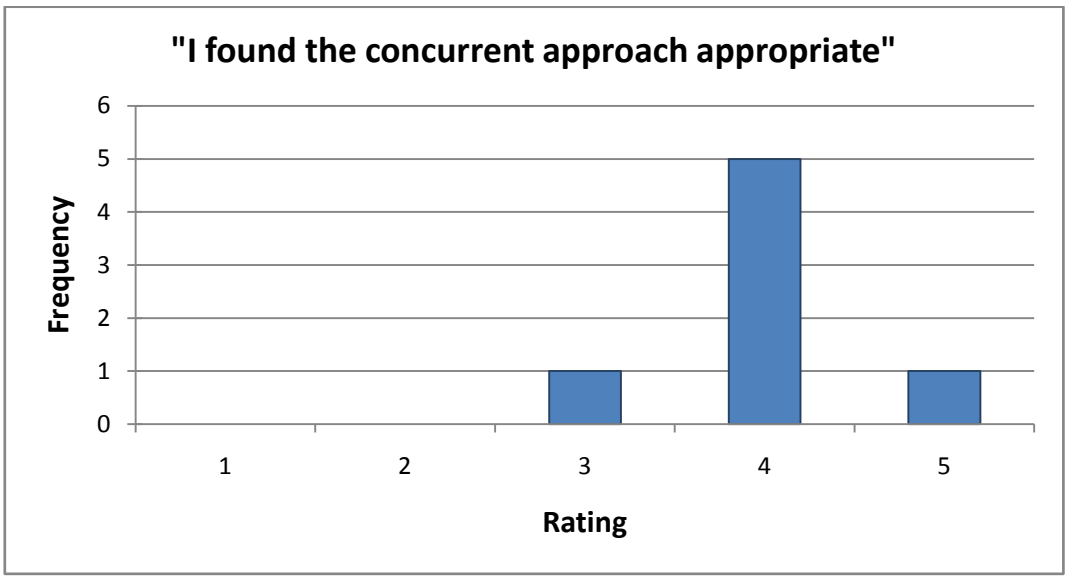

Figure 214: Ratings frequency for appropriateness of concurrent navigation system – Trial B

The new navigation system was met with approval by users in trial B, giving the appropriateness of the system an average rating of 4.00. This is an improvement upon the previous result, although the sample is small. In a consultation after the implementation of his suggested navigation system, Anshul Sama commented that the program was far easier to use, more intuitive and allowed results to be obtained faster than with the previous system.

11.3.4 Inclusion of Functionalities

As in the previous trial, users were asked to rate the importance of including the swelling and tumour application functionalities in the program. The results obtained are shown in Figure 215:

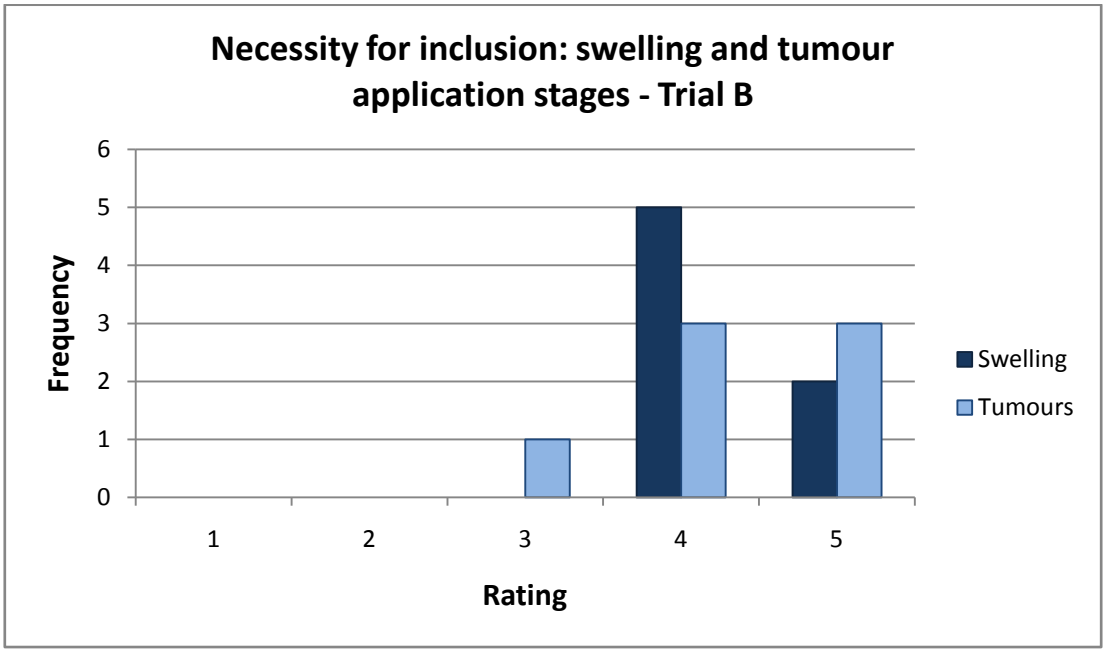

Figure 215: Ratings frequency for inclusion of swelling and tumour application – Trial B

Users responded positively to the inclusion of the swelling and tumour functionalities, with average agreement ratings of 4.29. Users commented that most patients with disease in the sinuses will exhibit swelling and that this function allows the user to show varying types of nasal disease. The response to the inclusion of these functionalities confirms that they should be retained in future developments of the program.

11.3.5 Swelling Application Controls

Participants were then asked to rate the ease of use of the swelling application controls, with the results shown in Figure 216. Users were not questioned on the use of the checkboxes in trial B; this system is maintained to some degree in the new program, with the decision to toggle swelling on or off at the start of the wizard (see Section 11.2.2, Figure 189) but not as part of the swelling application system.

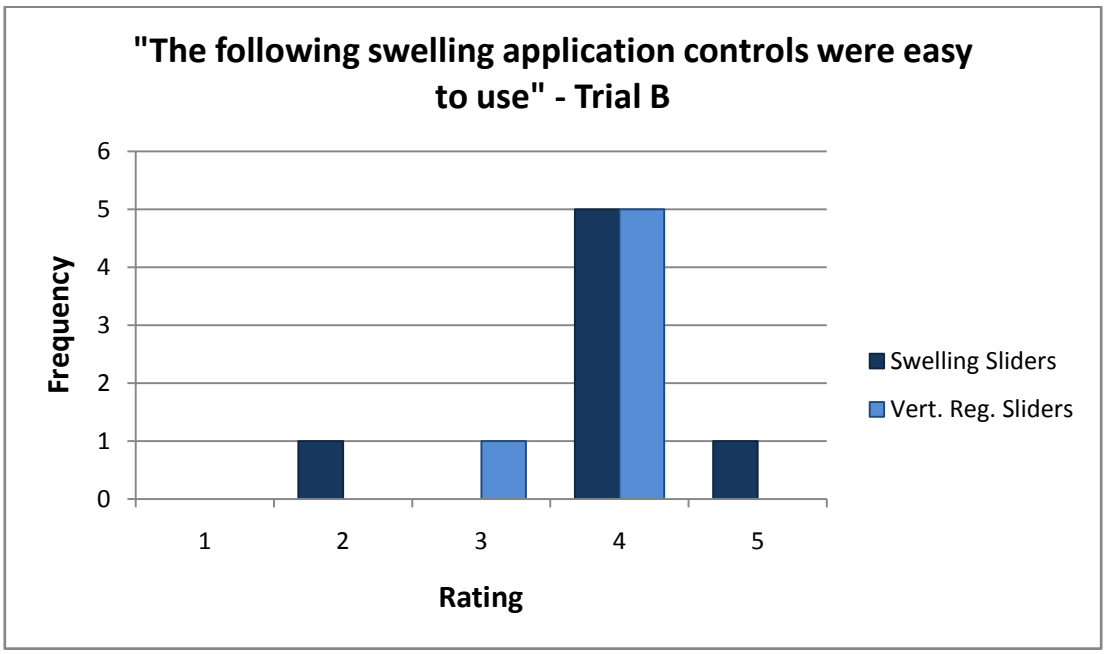

Figure 216: Ratings frequency for ease of use of swelling application sliders – Trial B

Again, all users except one rated the controls equally, with average ratings of 3.86 for swelling application sliders, and 3.71 for vertical region definition sliders. The user who responded with negative ratings for both controls was observed to have difficulty using the controls, but after some instruction gained a better understanding of the sliders and their function. The overall approach taken to the application of swelling was rated by users as shown in Figure 217:

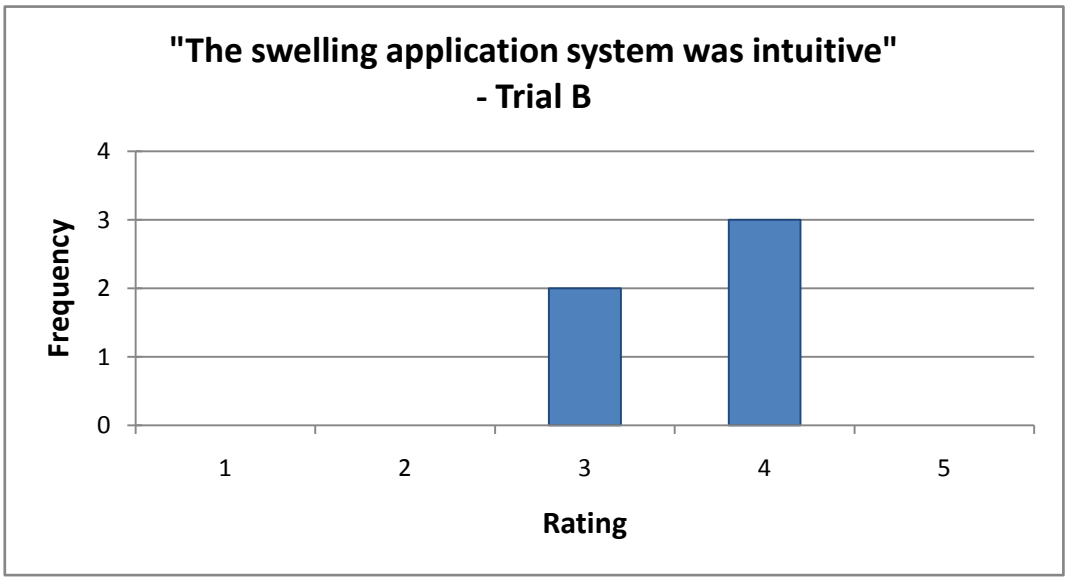

Figure 217: Ratings frequency for intuitiveness of swelling application system – Trial B

Two users failed to answer this question, leading to only five results being collected. The participants that did provide a response gave an average rating of 3.60, and provided some suggestions of ways to improve the intuitiveness of the swelling application system. One user proposed that the shape of swelling may be controlled more directly, in a similar manner to the freehand drawing tool suggested previously. No criticisms of the approach whereby swelling is applied in horizontal directions, before being restricted to a defined vertical region, were received.

11.3.6 Tumour Application Controls

The ratings provided for the ease of use of the tumour application controls are shown in Figure 218. In addition to being questioned on the use of the tumour addition and positioning controls, users were asked to rate the ease of use of the new sizing system (using sizing handles). Users of the new sizing system responded favourably to the resizing handles, with similar results to those shown in Figure 218; however two users failed to provide a rating, possibly producing skewed (and only five) results. Further participants are required to test the new tumour sizing system to build a significant population. Encouragingly, participants were seen to use the sizing handles without instruction, moving the mouse cursor over the handle and waiting until the resizing cursor was shown before performing the alteration. This shows that the system is intuitive and recognisable to users of the program. One user gave a rating of 2, after struggling to position the mouse pointer correctly over the resizing handle, potentially signifying that the handles are too small for easy use. This issue may be addressed in future versions of the program (see Section 13.4).

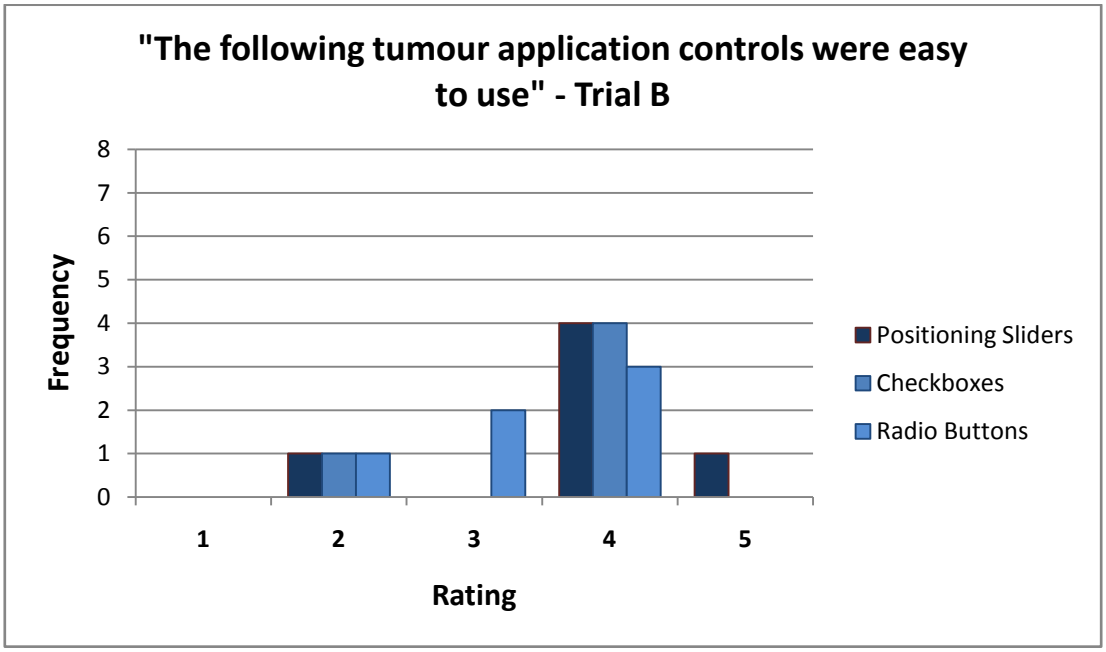

Figure 218: Ratings frequency for ease of use of tumour application controls – Trial B

One user failed to provide ratings for all three controls, and a further user did not give a rating for the use of checkboxes. Participants rated the positioning sliders at an average of 3.83, and further testing or development could be necessary to gauge users' opinions of the mouse-click positioning system. The average rating provided by the five users who rated the tumour activation checkboxes was 3.60. The tumour control radio buttons were given an average rating of 3.33, which is lower than desired. The three averages were again drawn down by the same user who had difficulty using the swelling application controls, after they experienced similar difficulty at this stage.

11.3.7 Results Achieved through Case Creator

Users' understanding of the tasks they had performed with the wizard were analysed by asking them to rate the predictability of results. The results obtained are shown in Figure 219:

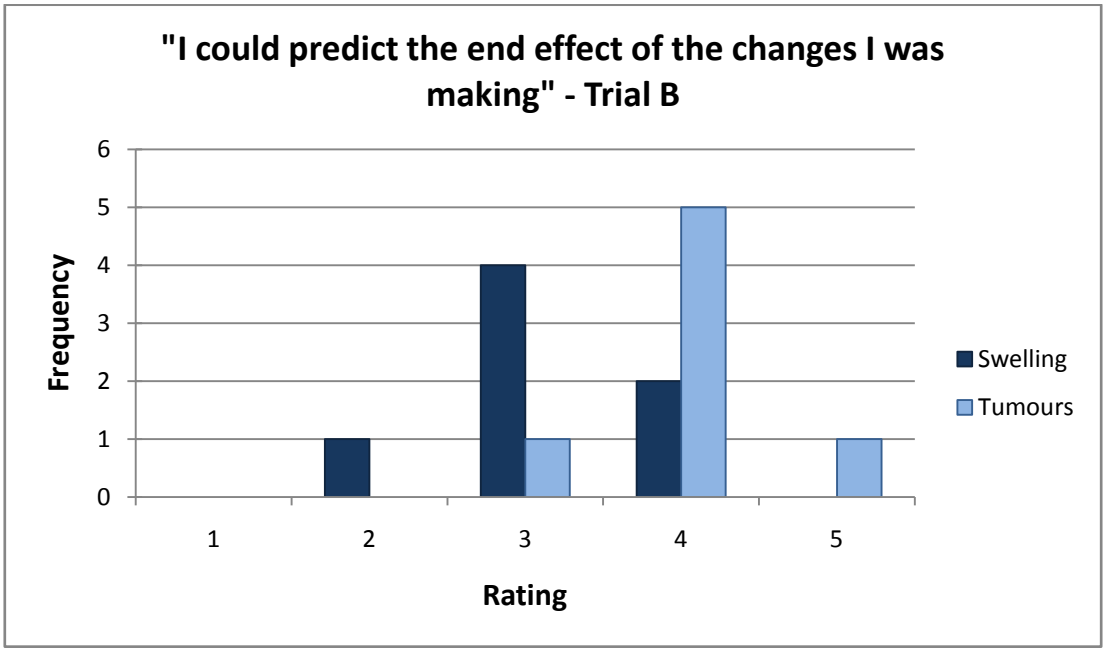

Figure 219: Ratings frequency for predictability of end result – Trial B

Users rated the predictability of results from the swelling function of the program with an average rating of 3.14. This is an issue to address, potentially with the introduction of a simulation of the final result of swelling at the application stage, before the CAD model is updated. The end effects of tumour application were found to be more predictable by the participants, who gave an average rating of 4.00. Users commented that it was difficult to predict where to place tumours in relation to the swelling that had been previously set, but not yet applied to the 3D CAD model. This is discussed in Section 13.2.

The realism of the results achieved by using Case Creator was again rated by participants, who provided the ratings shown in Figure 220.

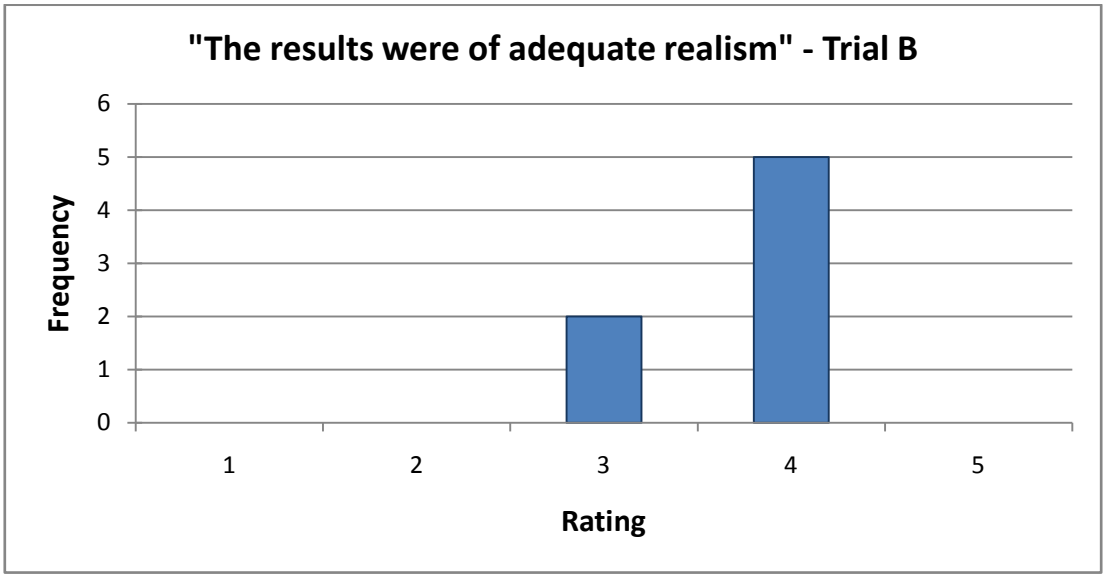

Figure 220: Ratings frequency for realism of wizard results – Trial B

Users again found the results to be of adequate realism, indeed with a higher average rating than in the previous trial (3.71). No comments were received as to how realism may be improved, however some further work on tumour simulation has been suggested following results in the first trial (see Section 13.4).

Participants in trial B rated their agreement with the statement "I would use the program" as shown in Figure 221:

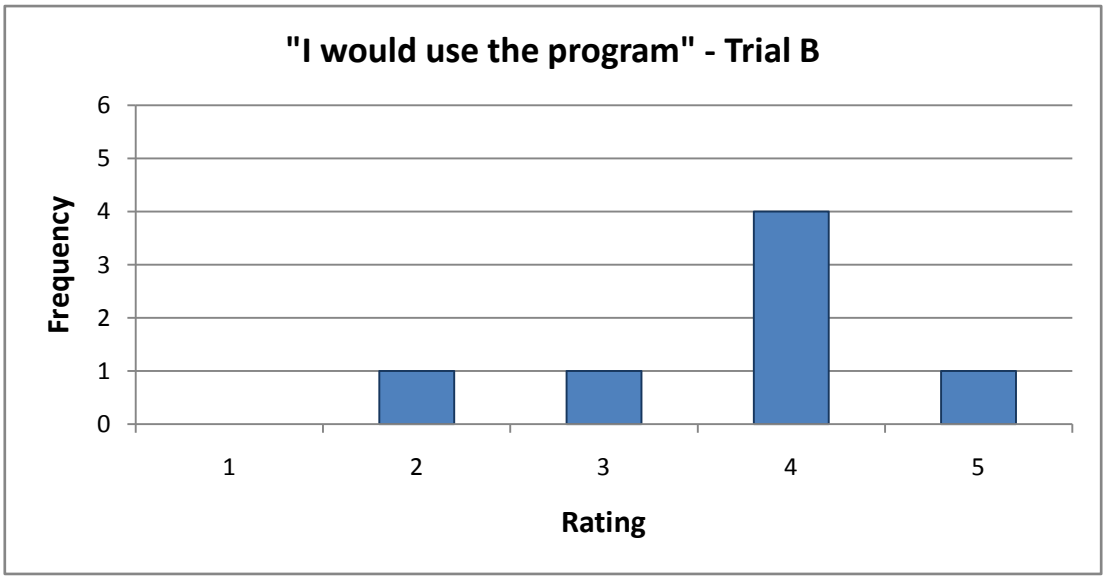

Figure 221: Ratings frequency for use of program – Trial B

There was a spread of responses to this question, with the majority of users stating that they would use the program and an average response rating of 3.71. As a wide enough range of participant experience in the performance of sinus surgery and use of 3D CAD modelling software were not obtained for this trial, the results of this question from experienced and inexperienced users cannot realistically be compared. However, experienced sinus surgeons in trial B rated their agreement with this statement with an average of 3.83, and inexperienced 3D CAD users with an average of 3.67. Although these results are slightly lower than those achieved in the first trial, the users still responded positively, and the lower result could be due to the participating users' own area of expertise; some users were ENT surgeons who specialise in thyroid surgery.

The user who responded negatively (trainee ENT/thyroid surgeon) suggested nonetheless that the program should be used for teaching, implying that although they may not use the program personally, they consider the program to be worth using. Other users commented that the program is a good tool for learning and studying the difficult and complex anatomy of the sinuses. Trainee surgeons said that the program would be used in teaching, to understand and fully evaluate the extent and effects of pathology in the sinuses. Qualified surgeons commented that the program could be used for planning surgical procedures a short time prior to the scheduled operation time.

Finally, the usefulness of the results obtained through the use of the program in the training of sinus surgeons were rated by the users, providing the ratings shown in Figure 222:

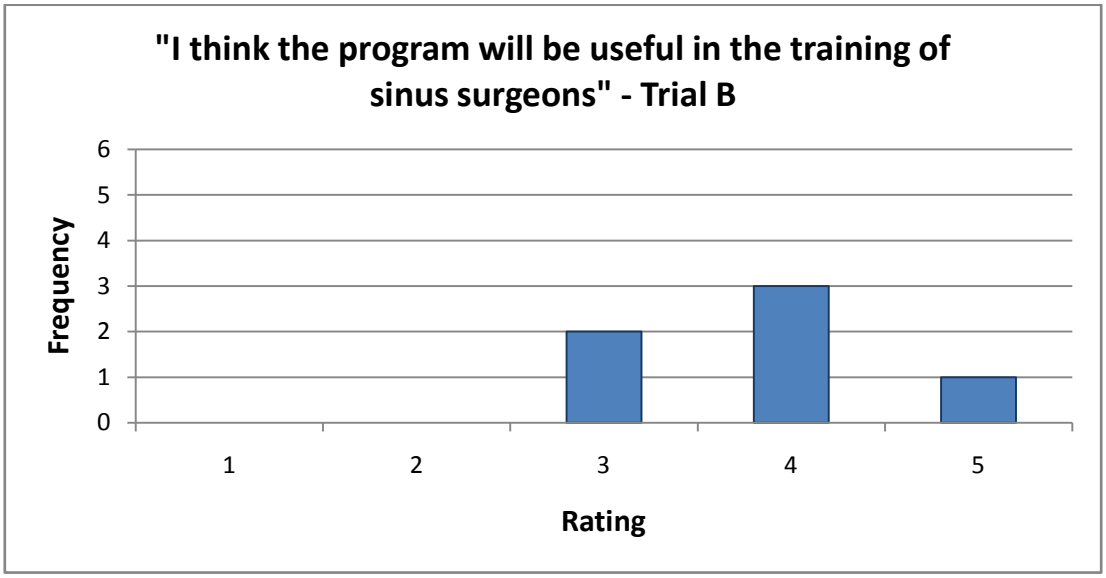

Figure 222: Ratings frequency for use of program in training sinus surgeons – Trial B

Results were not as positive as in the first trial, with an average rating of 3.83, however there was promising feedback from the users. The program was described as a "very novel idea" and "useful", and users said that they could "see a future in training for it" and that it would "greatly alter training when completed".

11.3.8 Summary

Seven further trials of the program were run, after alterations had been made. One user was re-tested to allow comments and comparisons to be drawn between the two versions of the program. The experience of the users, all from an ENT/sinus/thyroid surgery background, in the three key areas was not as spread in this trial, meaning that comparisons of responses from experienced and inexperienced users could not realistically be made.

Similarly to the first trial, users found the wizard style of program easy to use, as they were guided through the steps to be performed to achieve a customised 3D CAD model. The inclusion of the swelling and tumour application functions was also considered necessary, as in the first trial.

The ease of use of all swelling and tumour application controls were rated slightly less positively than in the first trial, and some suggestions were received for potential

alternatives, however these are complex and may not be feasible, as discussed in Sections 13.2 and 13.4. Too few results were obtained regarding the ease of use of the new resizing handles to form any conclusions, however participants were seen to recognise the function of the handles and use them instinctively to achieve the results they required, which is promising and more successful than the previous version of the program, which made use of sliding scales to produce square tumour blocks.

There was a slightly lower level of agreement that participants would use the program than in the first trial, however this may be due to the participants' different field of expertise. Most participants agreed that the program would be of use in the training of sinus surgeons; even if a rating of "3 - neutral" was given, participants provided positive comments about the potential of the program to assist training in this way.

The newest development of the navigation system, where selected pathology is set in all areas of the sinus concurrently, was found appropriate to the alteration of anatomy (4.00), and easier, quicker and more intuitive to use than the previous system.

11.4 Conclusions from Program Trials

Professionals from a wide range of medical backgrounds: sinus surgery, ENT, thyroid surgery and medical modelling trialled two versions of the Case Creator program. Certain aspects of the program have been highlighted for further development after analysing the results obtained in the two trials: swelling severity setting; tumour shaping in 3D CAD model; communication of end result before application to 3D CAD model.

Users in both trials found the 'wizard' approach appropriate to the customisation of the 3D CAD model. The new concurrent navigation and simultaneous pathology application system was received well by users, and will be retained for future versions of the program. The resizing handles that were implemented into the tumour application system may need further trialling to ascertain their success and suitability, however users did instinctively use the handles to achieve the required shape of tumour. It is proposed that this system is also retained for future versions, although

further testing may be beneficial to gain more feedback from users and develop the system.

The favourable results obtained through the trial concluded the work in this research on the creation of a design tool for the customisation of sinus anatomy for the production of simulation models for surgical training.

CHAPTER TWELVE

DISCUSSION AND CONCLUSIONS

12 Discussion and Conclusions

The conclusions drawn from this research are as follows:

The 3DP process, on the Spectrum Z510 3D printer used in this research, was found to be incapable of reproducing the required RGB value on printed parts without some compensation being applied. However, after investigation, no straightforward compensation rules could be determined. In the investigation into the mapping of textured images onto the model of the sinuses to achieve a realistic appearance when manufactured by 3DP, the process' accompanying software (ZEdit) was not found to be capable of achieving a realistic or usable result. It was subsequently concluded in consultation with a clinical expert that in-vivo images would not be required for realistic simulation of the anatomy, and that a suitable range of anatomically representative colours should be used. Two shades were found which, when printed and infiltrated with wax, match the colours selected for simulation of the internal soft tissue anatomy of the sinuses. These had the RGB values: 223,136,160 and 250,184,185. These will achieve a realistic shade when printed and infiltrated for the final simulation model, however the shades are not patient-specific; it is foreseeable that this may be required in some instances.

The investigation into the internal colouring of 3DP parts showed that the printing equipment, at present, negates any colour applied to the interior of the virtual part model, even when the STL data has internal colour. The 'proximity nesting' internal colouring induction trial showed that the Spectrum Z510 3D printer will not produce two parts vertically adjacent to one another, inserting blank layers between the parts, which eliminates the possibility of achieving internal colouring through the sandwiching of external colour between the two parts. This benchmarking exercise was designed to determine the limitations of the printing process, enforced by the programming created by the machine manufacturers. This method could not be used to create a complete model of the sinuses, however further investigation must be performed before this becomes possible to implement internal colouring in 3DP parts.

The investigation into customisable anatomical models exported directly from medical imaging data showed that the IGES file format offered a suitable level of customisability for this research, due to the construction of the file as a series of 2D splines offset vertically from one another, with the geometry of each spline controlled by movable nodes along its length. This was an important discovery, as the rest of the work on the customisation tool was then enabled. The implementation of swelling with this process is lengthy, as the original and swollen positions of the nodes must be recorded. Further automation of the geometry acquisition process may be required for simpler implementation to a range of datasets.

In the same investigation, Microsoft Visual Basic was found to be a suitable means of controlling the spline geometry without the need for direct interaction with the 3D CAD software. Additionally, the journaling feature in Unigraphics NX5 was found to be the most efficient method of generating VB code to control the functions of the CAD software, saving large amounts of coding time and providing an initial insight into the interaction between NX and VB. These two, vital conclusions prompted the development of the customisation tool, named "Case Creator Wizard", to be used by inexperienced CAD users to control the functions of the CAD software. Importantly, by linking with Microsoft Excel, the VB script will not need to be altered for future versions of the program.

Swelling and tumours were concluded to be the two most beneficial types of pathology to simulate using the customisation tool through consultations with clinicians. Swelling in three dimensions was found to be made more clinically realistic and cause less modelling errors when the horizontal and vertical aspects of swelling were combined, to gradually alter the splines' geometry and vertical position. Each spline node was moved towards its '100% swollen' position, defined by the creation of a shrunken version of the cavity. Through the development of swelling in three dimensions it was concluded that the most efficient method of simulating swelling in the vertical direction was to gradually collapse all cavity-defining layers closer to the layer of convergence (the cavity opening). This effectively shrinks the cavity vertically inwards and when combined with horizontal movement of spline nodes, achieves the effect of increasing swelling to the cavity in three dimensions.

This was the most effective method found to be possible whilst maintaining the required levels of customisability. At present, the amount by which each layer of the model moves is calculated and entered manually, which hinders the application of the program to different datasets. This would be improved through automation, by entering the shift factor of each layer into the same Excel spreadsheet used for horizontal swelling.

The Case Creator trials showed that users of the program who judged themselves to be inexperienced in the use of CAD software agreed that the wizard style of program was easy to use. Between the two stages of the trials, the personal approach to the testing of the program allowed users to provide verbal and written feedback, to be taken into account in the alteration stage. Of the two wizard styles trialled, users in the second trial rated the appropriateness of the 'concurrent' navigation system to anatomy alteration more highly than the 'cyclical' approach. This system used an initial list of settings that could be selected and applied by the user, offering the advantage of faster creation of results, simultaneously throughout different areas of the sinuses.

Users of the program concluded that it would be of use in the training of sinus surgeons, and noted potential uses of the end product: enhancing the understanding of anatomy and pathology; performing surgical procedures in a training environment on varying cases; planning and practicing surgery prior to the actual procedure; altering CT scan data to project the development of pathology to assist in planning of treatment.

On the whole, the project has succeeded in meeting the aims and objectives set out initially. The colour reproduction accuracy of the 3DP process on the Spectrum Z510 3D printer was assessed, and found to be incapable of directly reproducing the required shade, however shades were identified that could be used to represent the anatomy of the sinuses.

The program developed through this research makes possible the customisation of an anatomical model prior to its manufacture for use in surgical simulation for training of

procedures in the sinuses. Furthermore, this may be performed by users who are inexperienced in the use of 3D CAD modelling software, such as surgeons, students and training staff. Swelling of the mucosa, of user-defined severity in four directions, may be simulated in the frontal and sphenoid sinuses as well as tumours (or polyps) within the frontal, sphenoid and ethmoid sinus regions. The program removes any need for the user to directly interact with the CAD software, and offers a far more tailored approach to be taken to the design of surgical training programmes. The use of this program could help to avoid the problems experienced with current methods of training: the ethical issues encountered with the use of animals or cadavers; the risk to patient safety when students are involved in their treatment; and the lack of repeatability of realistic training cases for the acquisition and practice of new skills.

However, there remain several significant limitations to the current system which are described in more detail and related to possible further work in the next chapter.

CHAPTER THIRTEEN

LIMITATIONS AND RECOMMENDATIONS FOR FURTHER WORK

13 Limitations and Recommendations for Further Work

These recommendations take the form of suggestions to improve the usability or scope for Case Creator, based largely on feedback from users of the program.

Due to the use of VB to construct the program, certain limitations have been placed upon the functions available to the user. The issues resulting from these limitations were raised by most of the participants in the testing of the program. The issues are discussed here as recommendations for further work on Case Creator, however some may require transfer to an alternative design platform or the development of fundamental changes to the VB system.

13.1 General Improvements to Case Creator

One of the shortcomings of the current program is the limitation of customisation to a single CT scan dataset. In the future, and to make the program more viable as a teaching aid, more datasets should be included in the program. Ideally, the program should be expanded and developed to function with any CT scan dataset, allowing a vast range of cases to be simulated.

The layout of the 3D CAD model should be revised to exactly represent the anatomy, with all sinus areas interconnected and positioned realistically in relation to one another.

At present, no means of coding the automatic export of STL files from NX is known. The inclusion of this feature in the program would greatly increase its usability and would allow the same member of staff to perform all steps of the process from initial design to final manufacture. The ability to export STL files automatically from NX should therefore be implemented into the program, should the coding required become available.

13.2 Swelling Application

A consideration during development of the swelling definition and application system, which was mirrored by the participants of the program trial, was to implement

automatic updating of the CAD model while the swelling definition sliding scales were in use. With this function in place, the user would be able to see the effects of their settings as they were adjusted, instead of waiting until the final application to see the results.

The most significant problem with the implementation of this feature is the time taken to simulate swelling in the CAD model. The process of altering the scaffold splines, updating the solid formed through the splines, then subtracting this solid from the cavity lining solid can last up to twenty seconds. This procedure would have to be run every time the swelling sliders were adjusted, leading to an extremely long process. However, the user may then avoid the need to move back through the wizard after having applied the settings, to adjust their selection.

A possible alternative to the full simulation of the changes being made is to provide a wireframe visualisation. By altering the scaffold splines to show the settings being applied, but not performing any of the Boolean operations related to the solids in the model, the procedure could be accelerated and a good view of the new anatomy could be achieved.

During trials, one user attempted to adjust the swelling applied to the model by dragging the summary percentage bars at the final stage of the wizard. This functionality could be implemented simply, however its introduction could cause confusion among users and would negate the ability to navigate back through the wizard to the swelling application stage.

Some participants, including Anshul Sama, expressed interest in the ability to slice through the 3D model at any point to view a cross-section of the anatomy they had altered, or ‘peel away’ the model to show selected bodies. While the slicing of the model is technically possible in NX, the parameters of the solid would be lost, leading to errors in future modelling or manufacturing, and would mean that no further alterations could be made to the model. The visibility of individual bodies in the CAD model may be controlled to ease visibility as described earlier. However in this case,

visibility may not be improved from any direction by blanking out parts of the model, as the solids involved completely surround the sinus cavities.

One user suggested the implementation of a freehand drawing tool to define the swelling within the cavities of the sinus area, however if this were found to be possible with the tools currently used, this would be a very complex function to program and may confuse some users. This function is described in more detail in Section 13.4.

Of course, swelling should also be made possible in the maxillary and ethmoid sinuses. As explained in Chapter 8, the geometry of the ethmoid sinus and sheer number of cavities make the simulation of swelling an extremely complex task. The inclusion of these sinus areas will therefore depend on the acquisition of good quality, clear medical image sets, and in the case of the ethmoid sinus, the development of a new swelling simulation method.

13.3 Vertical Region Definition

Test users commonly asked whether the image of the CAD model shown on the vertical region definition page, split into red and green sections, updated continually to match their selection. This is not currently the case, as to perform this operation with the 3D CAD model would take time, as explained above, and the resulting model cannot be shown in the Case Creator window as a live-updating image.

A similar effect could be achieved with an image of the anatomy, over which a simulation of the vertical region to be affected is shown. This simulation could take the form of a simple pair of horizontal lines, overlaid on the image, that are moved upwards or downwards by the region sliders to represent the extents of the vertical region.

13.4 Tumour Application

When using the program in the test situation, five users commented that the shape of the tumours were not realistic, as the shapes shown in the GUI and produced in the CAD model were not organic. As explained in Section 11.2.5.2, the capabilities of VB

mean that only rectangular panels may be displayed in the program window as a tumour icon. Alternatively, rectangular or elliptical shapes may be drawn within the window using code commands; these were not considered suitable due to the difficulty involved in resizing or repositioning the drawn shapes. Newly drawn replacements would need to be produced each time an action was taken, requiring the name of the previous shape to be known, and increasing the complexity of the program considerably.

However, the suggestions for improving the shape of tumours offered by trial users were often far too complex to integrate into a VB-designed program. A suggestion from one trial user involved the inclusion of a freehand drawing tool, with which the user would be able to clearly mark the area to be filled by tumour on the medical images displayed. This function is available in software such as Materialise's Mimics but would be extremely difficult to reproduce on a VB platform and use to create results of any degree of quality or accuracy.

Other suggestions from trial program users were more applicable with the current range of software and design tools in use. One participant suggested the implementation of an "auto-fill" tool, to automatically adjoin tumours to the nearest face of the swollen cavity lining in the CAD model; this issue was identified during program development. This feature must be added to the program, otherwise the attachment of tumours to the side wall of the sinus cavities cannot be guaranteed. The combined, simultaneous addition of swelling and tumour settings, without viewing an updated model or image can make the positioning of tumours in relation to the recently defined swelling settings difficult.

This could be achieved through limitation of permitted tumour positions within the anatomy, only allowing tumours to be placed in locations adjacent to the cavity wall. Equally, operations could be performed in NX to adjust the tumour shapes from VB to attach the tumour bodies to the nearest cavity wall. Alternatively, the images used at the tumour stage to represent the anatomy into which the tumours will be placed could be updated with the information defined by the user at the swelling stage. This

would give the user a more accurate impression of the new anatomical geometry they have to work with.

A further development of this functionality (as suggested by a trial participant) is to allow the user to view all layers of the model at the tumour application stage, by scrolling through the layer stack in the vertical and horizontal directions. This is the method used in Mimics to set threshold levels and monitor region growing, and also in medical software to allow viewing of MRI or CT images. This would permit the user to view the extent of the tumour throughout the anatomy in greater detail than is currently achieved. If the shape of the tumour could be altered at each layer of the anatomy, the user would be provided with the greatest level of customisability. This is, as mentioned before, a similar approach to that taken by Mimics, and begins to move away from the simple approach taken by Case Creator, which was based on the fundamental aim of usability by all.

A simple means of achieving tumours with more organic shapes is to program the shape into the tumour creation code, achieving a more realistic effect by programming the tumour scaffold splines to take on less regular cross sections than those currently used. The co-ordinates of the nodes around the scaffold splines could be set at the locations used currently, but made to include an adjustment based upon the size of the tumour. With the correct adjustments included in the co-ordinate definition code, tumours with less regular surfaces would be produced, especially if the number of layers used to produce the tumours was increased.

Code was created to trial this new tumour creation procedure. The results achieved are shown in Figure 223, which may be compared to those produced by the program in Figure 135:

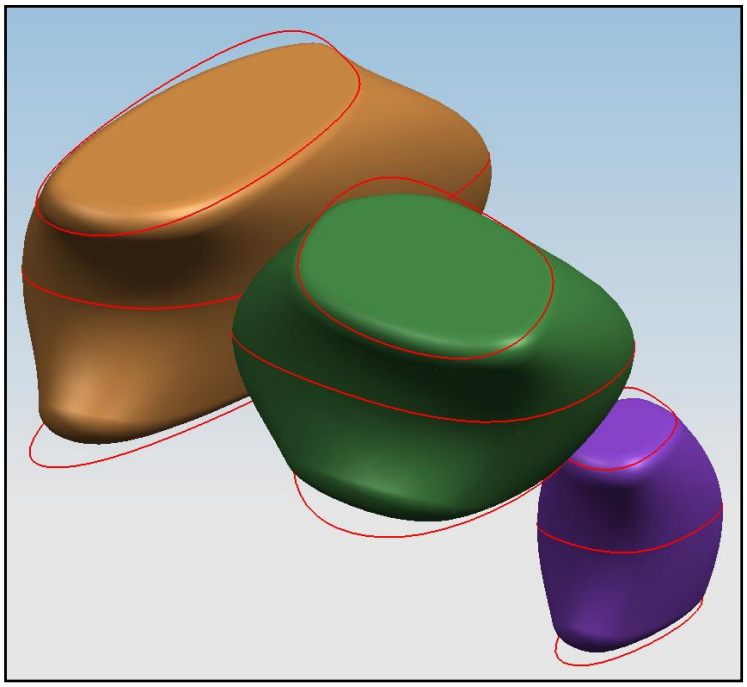

Figure 223: Organically-shaped tumours

Three tumours are shown in Figure 223, using the new code to create more organically-shaped tumour bodies. The code adjusts the co-ordinates of each spline node by a differing amount, depending on the overall size of the tumour as set by the user:

```
coordinates1 = (TumCoordNXX,
                TumCoordNXY + (TumSizeNXY * 0.3),
                TumCoordNXZ + (TumSizeNXZ * 0.5))
```

Figure 224: Code used to create more 'organic' shapes in tumour bodies

In this case, the x-co-ordinate of node 1 on the top layer is kept at its original value. The y-co-ordinate is adjusted to increase by the tumour size, multiplied by a factor of 0.3, resulting in a bulge at the back of the tumour body on the top level. In this example, all tumours draw on the same subroutine for their creation, leading to basically similar shapes; for example an indent can be seen in the front face of all three tumours above. For true variance, separate code should be used for each tumour. Additionally, the number of splines used to model each tumour body could be increased, leading to greater variation of geometry being made possible.

While this method offers a solution, it fails to address the input of the user into the tumour shape, in a similar way to the prescribed swelling simulation achieved in Section 8.1.1. A means to completely shape the tumour, beyond the overall size in three dimensions, would be a valuable and well-received addition to the program.

Through further testing, the suitability of the mouse-click positioning and tumour selection systems should be determined, potentially leading to simplification of the wizard with the removal of positioning sliders and selection radio buttons.

The representation of realistic colours and textures on the surfaces of the pathology in the physical model should be considered, involving the acquisition of in-vivo images and automatic application of textures to the 3D CAD model prior to manufacturing.

The addition of tumours in the maxillary sinus should also be included in future versions of the program.

13.4.1 Silicone

Investigation is ongoing into the possibility of using silicone as a coating to the 3DP parts in order to simulate the skin that covers all features within the sinuses. Work is still being done into the validity of this concept, and the method by which the effect would be achieved; however some trials have been performed to assess the effect that silicone coating and infiltration has on the perceived colour of printed samples. Silicone was also the material chosen to coat the AM model of the sinus anatomy in Yamauchi's training model [158].

Work has been done with the prosthetics staff at QMC in Nottingham to experiment with the coating and infiltration of 3D-printed parts, and the appearance of the resulting sample. Silicone was used to infiltrate sample 4, and by eye, the silicone appears to alter the perceived colour in almost exactly the same way as the wax infiltrant. The silicone sample also offers slightly more clarity than wax to improve visibility of the colour of the part beneath. There is a wide range of silicones which may be used, and each may be altered in viscosity through the use of thinners in order to allow the part to be more easily immersed, and removed from the liquid and for the

silicone to successfully spread throughout the part. Different application methods may also be investigated, and this is the subject of extensive work in the accompanying research to this.

A second line of investigation is into the possible use of coloured silicone to replicate the appearance of the skin layer surrounding all features in the sinuses. Through the use of a coloured silicone in conjunction with coloured 3DP parts, a 3D effect could be achieved. Further development is made possible with the introduction of paper flocking into the silicone substance, which gives a realistic appearance to the coating layer, giving the impression of variations in skin tone and the presence of blood vessels. It is in this application that the full range of colours obtained in Section 5.3.1 may be used.

A third alternative is to use coloured silicone only, coated over plain 3D-printed material. If the silicone were produced to replicate the colours that have been studied in this section, a good outer appearance may be achieved, with bone-coloured material underneath.

References

1. Di Lorenzo, N., and Dankelman, J., 2005, "**Surgical Training and Simulation**," Minimally Invasive Therapy and Allied Technologies, **14**(4 & 5) pp. 211-213.
2. Fried, M. P., Satava, R., Weghorst, S., 2004, "**Identifying and Reducing Errors with Surgical Simulation,**" Quality and Safety in Health Care, **13**(suppl 1) pp. i19.
3. Charap, M., 2004, "**Reducing Resident Work Hours: Unproven Assumptions and Unforeseen Outcomes,**" Annals of Internal Medicine, **140**(10) pp. 814.
4. Kohn, L.T., Corrigan, J.M., and Donaldson, M.S., 1999, "**To Err is Human: Building a Safer Health System**," National Academy Press, Washington, DC.
5. Penton Media, I., 2010, "**Prototypes for Tools and for Patients**," **2010**(September).
6. Kühnapfel, U. G., Kuhn, C., Hübner, M., 1997, "**The Karlsruhe Endoscopic Surgery Trainer as an Example for Virtual Reality in Medical Education,**" Minimally Invasive Therapy & Allied Technologies, **6**(2) pp. 122-125.
7. Manestar, D., Manestar, M., and Groscurth, P., 2006, "**3D-Model of the Nose and Paranasal Sinuses - Anatomy in Coronal Sections and Corresponding CT-Images**," Endo-Press, Tuttlingen, Germany.
8. Hart, G. W., 2005, "**Rapid Prototyping Models - George W. Hart**," **2010**(9/1) http://www.georgehart.com/rp/rp.html.
9. Bibb, R., Eggbeer, D., and Williams, R., 2006, "**Rapid Manufacture of Removable Partial Denture Frameworks,**" Rapid Prototyping Journal, **12**(2) pp. 95-99.
10. Lopes Dos Santos, J. R., 2009, "**Rapid Prototyped Model of Conjoined Twins for Separation Planning**,".
11. Noorani, R., 2006, "**Rapid Prototyping: Principles and Applications**," John Wiley & Sons, Inc., Hoboken, New Jersey, USA.

12. Patirupanusara, P., Suwanpreuk, W., Rubkumintara, T., 2007, "**Properties Improvement of Three-Dimensionally Printed Polymethyl Methacrylate by Bis-GMA-Based Resin Infiltration**," Polymer Testing, **26**(4) pp. 519-525.
13. Yeong, W. Y., Chua, C. K., Leong, K. F., 2004, "**Rapid Prototyping in Tissue Engineering: Challenges and Potential**," Trends in Biotechnology, **22**(12) pp. 643-652.
14. Jee, H. J., and Sachs, E., 2000, "**A Visual Simulation Technique for 3D Printing**," Advances in Engineering Software, **31**(2) pp. 97-106.
15. Creehan, K.D., and Bidanda, B., 2006, "**Rapid Prototyping: Theory and Practice**,"Springer Science+Business Media, Inc., New York, NY, USA, pp. 87-106.
16. Wei, S., and Lal, P., 2002, "**Recent Development on Computer Aided Tissue Engineering**," Computer Methods and Programs in Biomedicine, **67**(2) pp. 85-103.
17. Kermer, C., Lindner, A., Friede, I., 1998, "**Preoperative Stereolithographic Model Planning for Primary Reconstruction in Cranio-Maxillofacial Trauma Surgery**," Journal of Cranio-Maxillofacial Surgery, **26**(3) pp. 136-139.
18. Eggbeer, D., Evans, P. L., and Bibb, R., 2006, "**A Pilot Study in the Application of Texture Relief for Digitally Designed Facial Prostheses,**" Proceedings of the Institution of Mechanical Engineers, Part H: Journal of Engineering in Medicine, **220**(6) pp. 705-714.
19. Chua, C.K., Leong, K.F., and Lim, C.S., 2003, "**Rapid Prototyping: Principles and Applications**," World Scientific Publishing Co. Pte. Ltd., Singapore.
20. Dimitrov, D., Schreve, K., and de Beer, N., 2006, "**Advances in Three Dimensional Printing - State of the Art and Future Perspectives**," Rapid Prototyping Journal, **12**(3) pp. 136-147.
21. Dimitrov, D., van Wijck, W., Schreve, K., 2006, "**Investigating the Achievable Accuracy of Three Dimensional Printing**," Rapid Prototyping Journal, **12**(1) pp. 42-52.
22. Hague, R.J.M., and Reeves, P.E., 2000, "**Rapid Prototyping, Tooling and Manufacture**," RAPRA Review Reports, 117.

23. Bak, D., 2003, "**Rapid Prototyping Or Rapid Production? 3D Printing Processes Move Industry Towards the Latter**," Assembly Automation, **23**(4) pp. 340-345.
24. Choi, J. -., Choi, J. -., Kim, N. -., 2002, "**Analysis of Errors in Medical Rapid Prototyping Models**," International Journal of Oral and Maxillofacial Surgery, **31**(1) pp. 23-32.
25. Massachusetts Institute of Technology (MIT), 2008, "**MIT OpenCourseWare - Nuclear Science and Engineering**," **2008**(April).
26. Mori, S., Endo, M., Nishizawa, K., 2006, "**Comparison of Patient Doses in 256-Slice CT and 16-Slice CT Scanners,**" British Journal of Radiology, **79**(937) pp. 56.
27. La Rivière, P.J., 2005, "**Medical Imaging Systems Technology - Modalities**,"World Scientific Publishing Co. Pte. Ltd., Singapore, pp. 1-36.
28. Koc, B., Ma, Y., and Lee, Y. -., 2000, "**Smoothing STL Files by Max-Fit Biarc Curves for Rapid Prototyping**," Rapid Prototyping Journal, **6**(3) pp. 186-205.
29. Sachs, E., Cima, M., Williams, P., 1992, "**Three-Dimensional Printing: Rapid Tooling and Prototypes Directly from a CAD Model**," Journal of Engineering for Industry, **114**(4) pp. 481-488.
30. Z Corporation, 2008, "**Z Corp.**," **2008**(1/15) http://www.zcorp.com/.
31. Gibson, I., 2001, "**Colour RP**," Rapid Prototyping Journal, **7**(4) pp. 212-216.
32. Nadeau, D. R., 1999, "**Building Virtual Worlds with VRML**," Computer Graphics and Applications, **19**(2) pp. 18-29.
33. Yang, S., Leong, K. F., Du, Z., 2002, "**The Design of Scaffolds for use in Tissue Engineering: Part II - Rapid Prototyping Techniques**," Tissue Engineering, **8**(1) pp. 1-11.
34. Khalyfa, A., Vogt, S., Weisser, J., 2007, "**Development of a New Calcium Phosphate Powder-Binder System for the 3D Printing of Patient Specific Implants,**" Journal of Materials Science: Materials in Medicine, **18**(5) pp. 909-916.
35. Lanzetta, M., and Sachs, E., 2003, "**Improved Surface Finish in 3D Printing using Bimodal Powder Distribution**," Rapid Prototyping Journal, **9**(3) pp. 157-166.

36. Dimitrov, D., van Wijck, W., Schreve, K., 2003, "**An Investigation of the Capability Profile of the Three Dimensional Printing Process with an Emphasis on the Achievable Accuracy,**" CIRP Annals - Manufacturing Technology, **52**(1) pp. 189-192.

37. Jones, N., 2001, "**The Nose and Paranasal Sinuses Physiology and Anatomy**," Advanced Drug Delivery Reviews, **51**(1-3) pp. 5-19.

38. Walsh, W.E., and Kern, R.C., 2006, "**Head and Neck Surgery - Otolaryngology**,"Lippincott, Williams and Wilkins, Philadelphia, pp. 307-318.

39. Nilsson, M., 2007, "**Fitting Hearing Aids in Three Domains**," The Hearing Journal, **60**(10) pp. 28.

40. Grossan, M., 2003, "**Sinus Disease and Problems Explained**," **2008**(2/19) http://www.ent-consult.com/sinus_lay.html.

41. American Academy of Allergy Asthma and Immunology (AAAAI), 2008, "**Sinusitis: What are Sinuses?**" **2008**(4/1) http://www.aaaai.org/patients/publicedmat/sinusitis/whataresinuses.stm.

42. Ozturk, A., Alataş, N., Ozturk, E., 2004, "**First Secondary Middle Turbinate**," European Journal of Radiology Extra, **52**(3) pp. 93-95.

43. Coding News, 2008, "**Spot Sinus Landmarks on Your Road to Flawless FESS Coding**," **2010**(11/12) pp. 1. http://codingnews.inhealthcare.com/toolkit/spot-sinus-landmarks-on-your-road-to-flawless-fess-coding/.

44. Arslan, H., Aydinlioglu, A. I., Bozkurt, M., 1999, "**Anatomic Variations of the Paranasal Sinuses: CT Examination for Endoscopic Sinus Surgery,**" Auris Nasus Larynx, **26**(1) pp. 39-48.

45. Haluck, R. S., and Krummel, T. M., 2000, "**Computers and Virtual Reality for Surgical Education in the 21st Century**," Archives of Surgery, **135**pp. 786-792.

46. Ecke, U., Klimek, L., Müller, W., 1998, "**Virtual Reality: Preparation and Execution of Sinus Surgery**," Computer Aided Surgery, **3**(1) pp. 45-50.

47. Stammberger, H., and Wolf, G., 1988, "**Headaches and Sinus Disease: The Endoscopic Approach,**" The Annals of Otology, Rhinology & Laryngology - Supplement, **134**pp. 3-23.

48. Yamashita, J., 2004, "**The World's First Precise Model of the Human Paranasal Sinus for ESS Training**," **2008**(19th February).

49. Yamashita, J., Yamauchi, Y., Mochimaru, M., 2002, "**A Training System for Endoscopic Sinus Surgery with Mixed Reality**," **Virtual Reality Society of Japan Annual Conference**, Anonymous pp. 261-264.

50. O'Brien, K. L., Dowell, S. F., Schwartz, B., 1998, "**Acute Sinusitis: Principles of Judicious use of Antimicrobial Agents,**" Pediatrics, **101**(1) pp. 174.

51. Settipane, G. A., 1996, "**Epidemiology of Nasal Polyps,**" Allergy and Asthma Proceedings, Anonymous OceanSide Publications, Inc, **17,** pp. 231-236.

52. Ironside, P., and Matthews, J., 1975, "**Adenocarcinoma of the Nose and Paranasal Sinuses in Woodworkers in the State of Victoria, Australia,**" Cancer, **36**(3) pp. 1115-1121.

53. Elwood, J. M., 1981, "**Wood Exposure and Smoking: Association with Cancer of the Nasal Cavity and Paranasal Sinuses in British Columbia,**" Canadian Medical Association Journal, **124**(12) pp. 1573.

54. Stammberger, H., and Posawetz, W., 1990, "**Functional Endoscopic Sinus Surgery,**" European Archives of Otorhinolaryngology, **247**(2) pp. 63-76.

55. Kennedy, D. W., 2008, "**Endoscopic Sinus Surgery,**" Rhinosinusitis, pp. 1-14.

56. Doble, P., 2004, "**Sinus Surgery: Endoscopic and Microscopic Approaches**,"Thieme, pp. 207-218.

57. Klein, L. W., 2000, "**Computerized Patient Simulation to Train the Next Generation of Interventional Cardiologists: Can Virtual Reality Take the Place of Real Life?**" Catheterization and Cardiovascular Interventions, **51**(4) pp. 528.

58. Edmond, C. V. J., Wiet, G. J., and Bolger, B., 1998, "**Virtual Environments: Surgical Simulation in Otolaryngology**," Otolaryngologic Clinics of North America, **31**(2) pp. 369-381.

59. Marks, S. C., 1999, "**Learning Curve in Endoscopic Sinus Surgery**," Otolaryngology - Head and Neck Surgery, **120**(2) pp. 215-218.

60. Darzi, A. W., Smith, S. G. T., and Taffinder, N., 1999, "**Assessing Operative Skill**," British Medical Journal, **318**(7188) pp. 887.

61. Moorthy, K., Munz, Y., Sarker, S. K., 2003, "**Objective Assessment of Technical Skills in Surgery**," British Medical Journal, **327**pp. 1032-1037.

62. Wigton, R. S., 1992, "**See One, do One, Teach One**," Academic Medicine, **67**pp. 743-743.

63. Powers, L. R., and Draeger, S. K., 1992, "**using Workshops to Teach Residents Primary Care Procedures,**" Academic Medicine, **67**(11) pp. 743.

64. DeMaria, S. J., Levine, A. I., and Cohen, L. B., 2008, "**Human Patient Simulation and its Role in Endoscopic Sedation Training,**" Gastrointestinal Endoscopy Clinics of North America, **18**(4) pp. 801-813.

65. Ericsson, K. A., 2008, "**Deliberate Practice and Acquisition of Expert Performance: A General Overview**," Academic Emergency Medicine, **15**(11) pp. 988-994.

66. Lehmann, K. S., Ritz, J. P., Maaß, H., 2005, "**A Prospective Randomized Study to Test the Transfer of Basic Psychomotor Skills from Virtual Reality to Physical Reality in a Comparable Training Setting**," Annals of Surgery, **241**(3) pp. 442-449.

67. Spencer, F. C., 1978, "**Teaching and Measuring Surgical Techniques - the Technical Evaluation of Competence**," Bulletin of the American College of Surgeons, **63**pp. 9-12.

68. Barnes, R. W., 1987, "**Surgical Handicraft: Teaching and Learning Surgical Skills**," The American Journal of Surgery, **153**(5) pp. 422-427.

69. Sackier, J. M., 1998, "**Evaluation of Technical Surgical Skills. Lessons from Minimal Access Surgery**," Surgical Endoscopy, **12**(9) pp. 1109-1110.

70. Aggarwal, R., Black, S. A., Hance, J. R., 2006, "**Virtual Reality Simulation Training can Improve Inexperienced Surgeons' Endovascular Skills**," European Journal of Vascular and Endovascular Surgery, **31**(6) pp. 588-593.

71. Reznick, R. K., and MacRae, H., 2006, "**Teaching Surgical Skills - Changes in the Wind**," The New England Journal of Medicine, **355**pp. 2664-2669.

72. Torkington, J., Smith, S. G. T., Rees, B. I., 2000, "**The Role of Simulation in Surgical Training**," Annals of the Royal College of Surgeons of England, **82**(2) pp. 88.

73. Ericsson, K. A., 2006, "**The Influence of Experience and Deliberate Practice on the Development of Superior Expert Performance,**" The Cambridge Handbook of Expertise and Expert Performance, pp. 683-703.

74. Ziv, A., Wolpe, P. R., Small, S. D., 2006, "**Simulation-Based Medical Education: An Ethical Imperative**," Simulation in Healthcare, **1**(4) pp. 252-256.

75. Vozenilek, J., Huff, J. S., Reznek, M., 2008, "**See One, do One, Teach One: Advanced Technology in Medical Education**," Academic Emergency Medicine, **11**(11) pp. 1149-1154.

76. Okuda, Y., Bryson, E. O., DeMaria, S. J., 2009, "**The Utility of Simulation in Medical Education: What is the Evidence?**" Mount Sinai Journal of Medicine: A Journal of Translational and Personalized Medicine, **76**(4) pp. 330-343.

77. Torkington, J., Smith, S. G. T., Rees, B. I., 2001, "**The Role of the Basic Surgical Skills Course in the Acquisition and Retention of Laparoscopic Skill,**" Surgical Endoscopy, **15**(10) pp. 1071-1075.

78. Dumay, A. C. M., and Jense, G. J., 1995, "**Endoscopic Surgery Simulation in a Virtual Environment,**" Computers in Biology and Medicine, **25**(2) pp. 139-148.

79. Zinreich, S. J., Kennedy, D. W., Rosenbaum, A. E., 1987, "**Paranasal Sinuses: CT Imaging Requirements for Endoscopic Surgery,**" Radiology, **163**(3) pp. 769.

80. Cotin, S., Delingette, H., and Ayache, N., 2000, "**A Hybrid Elastic Model for Real-Time Cutting, Deformations, and Force Feedback for Surgery Training and Simulation,**" The Visual Computer, **16**(8) pp. 437-452.

81. Cundiff, G. W., 1997, "**Analysis of the Effectiveness of an Endoscopy Education Program in Improving Residents' Laparoscopic Skills,**" Obstetrics & Gynecology, **90**(5) pp. 854.

82. Kühnapfel, U. G., Çakmak, H. K., and Maaß, H., 2000, "**Endoscopic Surgery Training using Virtual Reality and Deformable Tissue Simulation**," Computers & Graphics, **24**(5) pp. 671-682.

83. Ericsson, K. A., 2004, "**Deliberate Practice and the Acquisition and Maintenance of Expert Performance in Medicine and Related Domains,**" Academic Medicine, **79**(10) pp. S70.

84. Ayache, N., Cotin, S., Delingette, H., 1998, "**Simulation of Endoscopic Surgery**," Minimally Invasive Therapy and Allied Technologies, **7**(2) pp. 71-77.

85. Munz, Y., Kumar, B. D., Moorthy, K., 2004, "**Laparoscopic Virtual Reality and Box Trainers: Is One Superior to the Other?**" Surgical Endoscopy, **18**(3) pp. 485-494.

86. Chaudhry, A., Sutton, C., Wood, J., 1999, "**Learning Rate for Laparoscopic Surgical Skills on MIST-VR, a Virtual Reality Simulator: Quality of Human-Computer Interface,**" Annals of the Royal College of Surgeons of England, **81**(4) pp. 281.

87. Avis, N.J., Briggs, N.M., Kleinermann, F., 1999, "**Medicine Meets Virtual Reality: The Convergence of Physical & Informational Technologies: Options for a New Era in Healthcare**,"IOS Press Inc., pp. 23-29.

88. Madan, A. K., Frantzides, C. T., Shervin, N., 2003, "**Assessment of Individual Hand Performance in Box Trainers Compared to Virtual Reality Trainers,**" The American Surgeon, **69**(12) pp. 1112-1114.

89. Madan, A. K., Harper, J. L., Frantzides, C. T., 2008, "**Nonsurgical Skills do Not Predict Baseline Scores in Inanimate Box Or Virtual-Reality Trainers,**" Surgical Endoscopy, **22**(7) pp. 1686-1689.

90. Laguna, M., Wijkstra, H., and Rosette, J., 2005, "**Training in Laparoscopy,**" Laparoscopic Urologic Surgery in Malignancies, pp. 253-269.

91. Fuchs, K. H., 2002, "**Minimally Invasive Surgery**," Endoscopy, **34**(2) pp. 154-159.

92. Tafra, L., 2001, "**The Learning Curve and Sentinel Node Biopsy,**" The American Journal of Surgery, **182**(4) pp. 347-350.

93. Keshtgar, M. R. S., Chicken, D. W., Waddington, W. A., 2005, "**A Training Simulator for Sentinel Node Biopsy in Breast Cancer: A New Standard**," European Journal of Surgical Oncology, **31**(2) pp. 134-140.

94. Munz, Y., Almoudaris, A. M., Moorthy, K., 2007, "**Curriculum-Based Solo Virtual Reality Training for Laparoscopic Intracorporeal Knot Tying:**

Objective Assessment of the Transfer of Skill from Virtual Reality to Reality," The American Journal of Surgery, **193**(6) pp. 774-783.

95. Sarker, S. K., and Patel, B., 2007, "**Simulation and Surgical Training**," International Journal of Clinical Practice, **61**(12) pp. 2120-2125.
96. Reznick, R. K., 1993, "**Teaching and Testing Technical Skills**," The American Journal of Surgery, **165**(3) pp. 358-361.
97. Gaba, D. M., 2004, "**The Future Vision of Simulation in Health Care,**" Quality and Safety in Health Care, **13**(suppl 1) pp. i2.
98. Krummel, T. M., 1998, "**Surgical Simulation and Virtual Reality: The Coming Revolution**," Annals of Surgery, **228**(5) pp. 635-637.
99. Roberts, K. E., Bell, R. L., and Duffy, A. J., 2006, "**Evolution of Surgical Skills Training,**" World Journal of Gastroenterology, **12**(20) pp. 3219.
100. Fichera, A., Prachand, V., Kives, S., 2005, "**Physical Reality Simulation for Training of Laparoscopists in the 21st Century: A Multi-Specialty, Multi-Institutional Study,**" Journal of the Society of Laparoendoscopic Surgeons, **9**(2) pp. 125-129.
101. Gaba, D. M., 1999, "**Improving Anaesthesiologists' Performance by Simulating Reality**," Anesthesiology, **76**(4) pp. 491-494.
102. Cheung, L. K., Wong, M. C. M., and Wong, L. L. S., 2001, "**The Applications of Stereolithography in Facial Reconstructive Surgery**," **Medical Imaging and Augmented Reality**, Anonymous pp. 10-15.
103. Buyukmihci, N.C., 1989, "Alternatives to the Harmful use of Nonhuman Animals in Veterinary Medical Education,"Association of Veterinarians for Animal Rights, California, pp. 14-16.
104. Taylor, S. J., and Wilson, D. J., 2007, "**The Human Tissue Act (2004), Anatomical Examination and the Importance of Body Donation in Northern Ireland**," The Ulster Medical Journal, **76**(3) pp. 124-126.
105. Parker, S.P., 2003, "**McGraw-Hill Dictionary of Scientific and Technical Terms**," McGraw-Hill, New York.
106. Nebot-Cegarra, J., and Macarulla-Sanz, E., 2004, "**Improving Laparoscopy in Embalmed Cadavers: A New Method with a Lateral Abdominal Wall Muscle Section**," Surgical Endoscopy, **18**(7) pp. 1058-1062.

107. Wolfe, B. M., Szabo, Z., Moran, M. E., 1993, "**Training for Minimally Invasive Surgery - Need for Surgical Skills**," Surgical Endoscopy, **7**(2) pp. 93-95.

108. Aboud, E., 2005, "**Making Cadavers Live for Laboratory Surgical Training. An Alternative Model for Surgical Training (a Cadaver Based Model)**," **ALTEX 5th World Congress**, Anonymous pp. 8.

109. Jones, J. W., McCullough, L. B., and Richman, B. W., 2004, "**Training on Newly Deceased Patients**," Surgery, **135**(1) pp. 108-109.

110. Yamashita, J., Morikawa, O., Hashimoto, R., 2004, "**Manikin and Method of Manufacturing the Same**,".

111. Lossing, A. G., Hatswell, E. M., Gilas, T., 1992, "**A Technical Skills Course for First-Year Residents in General Surgery: A Descriptive Study**," Canadian Journal of Surgery, **35**(5) pp. 536-540.

112. Liu, Q., Leu, M. C., and Schmitt, S. M., 2006, "**Rapid Prototyping in Dentistry: Technology and Application**," The International Journal of Advanced Manufacturing Technology, **29**(3-4) pp. 317-335.

113. Chamberlain, P. B., 2000, "**Thick Layer Rapid Prototyping of Bones from Computed Tomography Images**,".

114. Kelley, D. J., Farhoud, M., Meyerand, M. E., 2007, "**Creating Physical 3D Stereolithograph Models of Brain and Skull**," PLoS ONE, **2**(10).

115. Sanghera, B., Naique, S., Papaharilaou, Y., 2001, "**Preliminary Study of Rapid Prototype Medical Models**," Rapid Prototyping Journal, **7**(5) pp. 275-284.

116. Wu, D., Hu, Q., Lu, Q., 2008, "**Study on the Application of Rapid Prototyping in Assistant Surgical Planning,**" 7th Asian-Pacific Conference on Medical and Biological Engineering, Anonymous Springer, pp. 729-732.

117. Coleman, J., Nduka, C. C., and Darzi, A. W., 1994, "**Virtual Reality and Laparoscopic Surgery**," British Journal of Surgery, **81**(12) pp. 1709-1711.

118. Ahlberg, G., Heikkinen, L., Iselius, L., 2001, "**does Training in a Virtual Reality Simulator Improve Surgical Performance?**" Surgical Endoscopy, **16**(1) pp. 126-129.

119. Virtual Airline Pilot, 2006, "**Virtual Airline Pilot Flight Simulator Home Page**," **2008**(4/1) http://www.virtualairlinepilot.co.uk/.

120. Kirk, R. M., 1998, "**Surgical Excellence - Threats and Opportunities,**" Annals of the Royal College of Surgeons of England, **80**(6 Suppl) pp. 256-259.

121. Kühnapfel, U. G., Neisius, B., Krumm, H. G., 1995, "**CAD-Based Simulation and Modelling for Endoscopic Surgery,**" Minimally Invasive Therapy, **4**pp. 336-339.

122. Derossis, A. M., Fried, G. M., Abrahamowicz, M., 1998, "**Development of a Model for Training and Evaluation of Laparoscopic Skills,**" The American Journal of Surgery, **175**(6) pp. 482-487.

123. Neubauer, A., Wolfsberger, S., Forster, M. -., 2005, "**Advanced Virtual Endoscopic Pituitary Surgery**," IEEE Transactions on Visualisation and Computer Graphics, **11**(5) pp. 497-507.

124. Jackson, B.G., and Rosenberg, L.B., 1995, "**Interactive Technology and the New Paradigm for Healthcare**,"IOS Press, pp. 147-151.

125. Petersik, A., Pflesser, B., Tiede, U., 2003, "**Realistic Haptic Interaction in Volume Sculpting for Surgery Simulation,**" Surgery Simulation and Soft Tissue Modeling, **2673**pp. 1001.

126. Ström, P., Hedman, L., Särnå, L., 2006, "**Early Exposure to Haptic Feedback Enhances Performance in Surgical Simulator Training: A Prospective Randomized Crossover Study in Surgical Residents**," Surgical Endoscopy, **20**(9) pp. 1383-1388.

127. Park, J., MacRae, H., Musselman, L. J., 2007, "**Randomized Controlled Trial of Virtual Reality Simulator Training: Transfer to Live Patients**," The American Journal of Surgery, **194**(2) pp. 205-211.

128. Ahlberg, G., Enochsson, L., Gallagher, A. G., 2007, "**Proficiency-Based Virtual Reality Training significantly Reduces the Error Rate for Residents during their First 10 Laparoscopic Cholecystectomies**," The American Journal of Surgery, **193**(6) pp. 797-804.

129. Grantcharov, T. P., Bardram, L., Funch-Jensen, P., 2003, "**Learning Curves and Impact of Previous Experience on Performance on a Virtual Reality Simulator to Test Laparoscopic Surgical Skills**," The American Journal of Surgery, **185**(2) pp. 146-149.

130. Bann, S. D., Khan, M. S., and Darzi, A. W., 2003, "**Measurement of Surgical Dexterity using Motion Analysis of Simple Bench Tasks**," World Journal of Surgery, **27**(4) pp. 390-394.

131. Neequaye, S. K., Aggarwal, R., van Herzeele, I., 2007, "**Endovascular Skills Training and Assessment**," Journal of Vascular Surgery, **46**(5) pp. 1055-1064.

132. Arora, H., Uribe, J., Ralph, W., 2005, "**Assessment of Construct Validity of the Endoscopic Sinus Surgery Simulator**," Archives of Otolaryngology - Head and Neck Surgery, **131**(3) pp. 217.

133. Cotin, S., Delingette, H., and Ayache, N., 1999, "**Real-Time Elastic Deformations of Soft Tissues for Surgery Simulation,**" IEEE Transactions on Visualization and Computer Graphics, **5**(1) pp. 62-73.

134. Marescaux, J., Clément, J. M., Tassetti, V., 1998, "**Virtual Reality Applied to Hepatic Surgery Simulation: The Next Revolution**," Annals of Surgery, **228**(5) pp. 627.

135. Christensen, A. M., Humphries, S. M., Goh, K. Y. C., 2004, "**Advanced "Tactile" Medical Imaging for Separation Surgeries of Conjoined Twins**," Child's Nervous System, **20**(8-9) pp. 547-553.

136. Lempp, H. K., 2005, "**Perceptions of Dissection by Students in One Medical School: Beyond Learning about Anatomy. A Qualitative Study**," Medical Education, **39**(3) pp. 318-325.

137. Newmark, J., Dandolu, V., Milner, R., 2007, "**Correlating Virtual Reality and Box Trainer Tasks in the Assessment of Laparoscopic Surgical Skills,**" American Journal of Obstetrics and Gynecology, **197**(5) pp. 546.

138. D'Urso, P. S., Barker, T. M., Earwaker, W. J., 1999, "**Stereolithographic Biomodelling in Cranio-Maxillofacial Surgery: A Prospective Trial**," Journal of Cranio-Maxillofacial Surgery, **27**(1) pp. 30-37.

139. Lermusiaux, P., Leroux, C., Tasse, J. C., 2001, "**Aortic Aneurysm: Construction of a Life-Size Model by Rapid Prototyping**," Annals of Vascular Surgery, **15**(2) pp. 131-135.

140. Hieu, L. C., Zlatov, N., Vander Sloten, J., 2005, "**Medical Rapid Prototyping Applications and Methods**," Assembly Automation, **25**(4) pp. 284-292.

141. Chua, C. K., Chou, S. M., Lin, S. C., 1998, "**Rapid Prototyping Assisted Surgery Planning**," The International Journal of Advanced Manufacturing Technology, **14**(9) pp. 624-630.

142. Petzold, R., Zeilhofer, H. F., and Kalender, W. A., 1999, "**Rapid Prototyping Technology in Medicine: Basics and Applications**," Computerized Medical Imaging and Graphics, **23**(5) pp. 277-284.

143. Poukens, J., Haex, J., and Riediger, D., 2003, "**The use of Rapid Prototyping in the Preoperative Planning of Distraction Osteogenesis of the Cranio-Maxillofacial Skeleton**," Computer Aided Surgery, **8**(3) pp. 146-154.

144. Chim, H., and Schantz, J. -., 2005, "**New Frontiers in Calvarial Reconstruction: Integrating Computer-Assisted Design and Tissue Engineering in Cranioplasty**," Plastic and Reconstructive Surgery, **116**(6) pp. 1726-1741.

145. Abe, M., Tabuchi, K., Goto, M., 1998, "**Model-Based Surgical Planning and Simulation of Cranial Base Surgery,**" Neurologia Medico-Chirurgica, **38**(11) pp. 746-751.

146. Potamianos, P., Amis, A. A., Forester, A. J., 1998, "**Rapid Prototyping for Orthopaedic Surgery**," Journal of Engineering in Medicine, **212**(5) pp. 383-393.

147. Sailer, H. F., Haers, P. E., Zollikofer, C. P. E., 1998, "**The Value of Stereolithographic Models for Preoperative Diagnosis of Craniofacial Deformities and Planning of Surgical Corrections**," International Journal of Oral and Maxillofacial Surgery, **27**(5) pp. 327-333.

148. Singare, S., Yaxiong, L., Dichen, L., 2006, "**Fabrication of Customised Maxillofacial Prosthesis using Computer-Aided Design and Rapid Prototyping Techniques,**" Rapid Prototyping Journal, **12**(4) pp. 206-213.

149. D'Urso, P. S., Askin, G., Earwaker, W. J., 1999, "**Spinal Biomodeling**," Spine, **24**(12) pp. 1247-1251.

150. Allard, T. T., 2006, "**The Role of 3D Printing in Biological Anthropology**".

151. Muller, A., Krishnan, K. G., Uhl, E., 2003, "**The Application of Rapid Prototyping Techniques in Cranial Reconstruction and Preoperative Planning in Neurosurgery**," Journal of Craniofacial Surgery, **14**(6) pp. 899-914.

152. Wan Harun, W., Devadass, V., and Aziz, I., 2007, "**Digital Approach in Reconstruction of Craniofacial Defect,**" pp. 2632-2635.

153. Girod, S., Teschner, M., Schrell, U., 2001, "**Computer-Aided 3D Simulation and Prediction of Craniofacial Surgery: A New Approach**," Journal of Cranio-Maxillofacial Surgery, **29**(3) pp. 156-158.

154. Gibson, I., Cheung, L. K., Chow, S. P., 2006, "**The use of Rapid Prototyping to Assist Medical Applications**," Rapid Prototyping Journal, **12**(1) pp. 53-58.

155. Santler, G., Kärcher, H., and Ruda, C., 1998, "**Indications and Limitations of Three-Dimensional Models in Cranio-Maxillofacial Surgery**," Journal of Cranio-Maxillofacial Surgery, **26**(1) pp. 11-16.

156. Hieu, L. C., Bohez, E., Vander Sloten, J., 2003, "**Design for Medical Rapid Prototyping of Cranioplasty Implants**," Rapid Prototyping Journal, **9**(3) pp. 175-186.

157. Dalgarno, K. W., Pallari, J. H., Woodburn, J., 2006, "**Mass Customization of Medical Devices and Implants: State of the Art and Future Directions**," Virtual and Physical Prototyping, **1**(3) pp. 137-145.

158. Yamauchi, Y., Yamashita, J., Morikawa, O., 2004, "**an Endoscopic Sinus Surgery Training System for Assessment of Surgical Skill,**" Medicine Meets Virtual Reality 12: Building a Better You: The Next Tools for Medical Education, Diagnosis, and Care, pp. 416.

159. Suzuki, M., Ogawa, Y., Kawano, A., 2004, "**Rapid Prototyping of Temporal Bone for Surgical Training and Medical Education**," Acta Otolaryngology, **124**(4) pp. 400-402.

160. Lohfeld, S., Barron, V., and McHugh, P. E., 2005, "**Biomodels of Bone: A Review**," Annals of Biomedical Engineering, **33**(10) pp. 1295-1311.

161. Lin, C. C., Lo, L. J., Lee, M. Y., 2001, "**Craniofacial Surgical Simulation: Application of Three-Dimensional Medical Imaging and Rapid Prototyping Models**," Chang Gung Medical Journal, **24**(4) pp. 229-238.

162. Pößneck, A., Nowatius, E., Trantakis, C., 2005, "**A Virtual Training System in Endoscopic Sinus Surgery**," International Congress Series, **1281**pp. 527-530.

163. Edmond, C. V. J., 2002, "**The Impact of the Endoscopic Sinus Surgery Simulator on Operating Room Performance**," The Journal of the American

Laryngological, Rhinological and Otological Society, Inc., **112**(7) pp. 1148-1158.

164. McDonnell, D., Esposito, M., and Todd, M. E., 1992, "**A Teaching Model to Illustrate the Variation in Size and Shape of the Maxillary Sinus**," Journal of Anatomy, **181**(2) pp. 377-380.
165. Yamauchi, Y., Suzuki, M., Mochimaru, M., 2001, "**A Training System for Endoscopic Sinus Surgery with Skill Evaluation**," CARS 2001, Anonymous.
166. Lloyd, G. A. S., Lund, V. J., and Scadding, G. K., 2007, "**CT of the Paranasal Sinuses and Functional Endoscopic Surgery: A Critical Analysis of 100 Symptomatic Patients,**" The Journal of Laryngology and Otology, **105**(03) pp. 181-185.
167. Davidson, T. M., Brahme, F. J., and Gallagher, M. E., 1989, "**Radiographic Evaluation for Nasal Dysfunction: Computed Tomography Versus Plain Films,**" Head and Neck, **11**(5) pp. 405-409.
168. Schievano, S., Migliavacca, F., Coats, L., 2007, "**Percutaneous Pulmonary Valve Implantation Based on Rapid Prototyping of Right Ventricular Outflow Tract and Pulmonary Trunk from MR Data,**" Radiology, **242**(2) pp. 490.
169. Irsen, S.H., Leukers, B., Tille, C., 2007, "**Advances in Medical Engineering**,"Springer, Berlin, pp. 121-126.
170. Webb, P. A., 2000, "**A Review of Rapid Prototyping (RP) Techniques in the Medical and Biomedical Sector**," Journal of Medical Engineering and Technology, **24**(4) pp. 149-153.
171. Alfidi, R. J., MacIntyre, W. J., and Haaga, J. R., 1976, "**The Effects of Biological Motion on CT Resolution,**" American Journal of Roentgenology, **127**(1) pp. 11-15.
172. Winder, J., and Bibb, R., 2005, "**Medical Rapid Prototyping Technologies: State of the Art and Current Limitations**," Journal of Oral and Maxillofacial Surgery, **63**(7) pp. 1006-1015.
173. Lim, J., and Zein, R., 2006, "**Rapid Prototyping: Theory and Practice**,"Springer, New York, pp. 63-86.

174. Fink, A., 1995, "**The Survey Handbook,**" Sage Publications, Inc, California, USA.

175. Fink, A., 1995, "**How to Report on Surveys,**" Sage Publications, Inc, California, USA.

176. Frazer, L., and Lawley, M., 2000, "**Questionnaire Design & Administration: A Practical Guide,**" John Wiley & Sons Australia, Ltd.

APPENDIX

Appendix A - Case Creator Questionnaire

Thank you for trialling the Case Creator program. Your feedback is extremely important, and will ensure that the program will provide real benefit to the people who will use it, and their patients.
Please indicate your level of agreement with each statement by circling the relevant number (as described below), and write your answers clearly within the space provided.

Scoring system: **1 = Strongly Disagree** **2 = Disagree** **3 = Neutral** **4 = Agree** **5 = Completely Agree**

OVERALL APPROACH

'Wizard' style program

(Next/Previous/Home buttons)

1. "I found the 'wizard' style of program easy to use."

1 **2** **3** **4** **5**

Do you have any suggestions for a more appropriate approach?

2. "The order of tasks was logical."

1 **2** **3** **4** **5**

If you disagree, which tasks were not logically ordered?

Cyclical Approach

(Selection of sinus area to alter, move through wizard, apply, move on to next area, repeat)

3. "I found this approach appropriate to anatomy alteration."

1 **2** **3** **4** **5**

Do you have any suggestions for a more appropriate approach?

4. "The wizard offered an appropriate number of alteration functions."

1 **2** **3** **4** **5**

Do you have any suggestions for more appropriate functions?

SWELLING APPLICATION

5. "The swelling application stage is necessary for inclusion in the program."

1 **2** **3** **4** **5**

Why?

6. "There was sufficient **feedback** provided at the swelling application stage."

1 **2** **3** **4** **5**

Why was the feedback good/bad?

7. "There was sufficient **instruction** provided at the swelling application stage."

1 **2** **3** **4** **5**

Why were the instructions good/bad?

8. "I could predict the end effect of the changes I was making."

1 **2** **3** **4** **5**

If not, what made the effect of your actions unclear?

9. Can you suggest any further improvements to the swelling application stage?

10. "The swelling application system (applying swelling from four directions, switching swelling on/off, separating swelling in right/left cavities, selecting vertical region) was intuitive."

1 **2** **3** **4** **5**

11. "The following swelling application controls were easy to use."

Sliders – apply swelling from four directions: **1 2 3 4 5**
Checkboxes – turn swelling on/off: **1 2 3 4 5**
Sliders – select start/end of (vertical) affected region: **1 2 3 4 5**

TUMOUR APPLICATION

12. "The tumour application stage is necessary for inclusion in the program."

1 **2** **3** **4** **5**

Why?

13. "There was sufficient **feedback** provided at the tumour application stage."

1 **2** **3** **4** **5**

Why was the feedback good/bad?

14. "There was sufficient **instruction** provided at the tumour application stage."

1 **2** **3** **4** **5**

Why were the instructions good/bad?

15. "I could predict the end effect of the changes I was making."

1 **2** **3** **4** **5**

If not, what made the effect of your actions unclear?

16. Can you suggest any further improvements to the tumour application stage?

17. "The following tumour positioning controls were easy to use."

Sliders – position tumour over two 2D images: **1 2 3 4 5**
Click – position tumour over two 2D images: **1 2 3 4 5**
Checkboxes – turn individual tumours on/off: **1 2 3 4 5**
Radio buttons – switch control between tumours: **1 2 3 4 5**

18. "The sizing system was easy to use."

Sliders – size alteration (later, *resize handles*): **1 2 3 4 5**

RESULTS

19. "The results were of adequate realism."

1 **2** **3** **4** **5**

If not, how was realism lacking?

20. Did you alter the results after you initially applied the settings?

Yes / **No**

21. "The required result was achieved."

1 **2** **3** **4** **5**

If not, what difficulty did you experience?

22. "I think that the results I generated will be of use later."

1 **2** **3** **4** **5**

Can you explain your answer?

USER INFORMATION

23. Please give your level of experience in each area below.
(0 = none, 5 = very experienced):

Performing sinus surgery:	**0 1 2 3 4 5**
Creating training models for surgical students:	**0 1 2 3 4 5**
Using 3D CAD Modelling software:	**0 1 2 3 4 5**

24. What is your area of expertise?

25. "The program was designed appropriately for my area of expertise."

1 **2** **3** **4** **5**

If not, which parts of the program were inappropriate for your area of expertise – and why?

26. "I would use the program."

1 **2** **3** **4** **5**

If so, please describe how you would use the program:

27. "I think the program will be useful in the training of sinus surgeons."

1 **2** **3** **4** **5**

Please explain your answer further:

28. Do you have any other comments?

Thank you very much for completing the questionnaire and assisting in the development of what we hope will be a beneficial tool in the training of future sinus surgeons.

Richard Taylor
Additive Manufacturing Research Group, Loughborough University

(Contact details)